IL
NUOVO CIMENTO
ORGANO DELLA SOCIETÀ ITALIANA DI FISICA
SOTTO GLI AUSPICI DEL CONSIGLIO NAZIONALE DELLE RICERCHE

VOL. IX, N. 1 *Serie decima* 1° Luglio 1958

The Charge Spectrum of the Cosmic Radiation at 41° N (*).

M. KOSHIBA, G. SCHULTZ and MARCEL SCHEIN

Department of Physics and Enrico Fermi Institute for Nuclear Studies
University of Chicago

(ricevuto il 22 Giugno 1957)

Summary. — From a large stack of G-5 emulsions flown at Texas, 41° N geomagnetic latitude, the charge spectrum of the cosmic radiation at 104 000 feet was obtained. Special emphasis is given to the observation of the detailed shape of the spectrum in the region $Z \geqslant 9$. The gap-counting is extensively used even at these high Z values after very careful calibration with break-up events and δ-ray countings. The charge spectrum thus obtained was extrapolated to the top of the atmosphere by making use of the fragmentation probabilities in air which were obtained from the analysis of a total of 209 interactions in the same stack. This extrapolation gives for the ratio of the light nuclei, L, ($Z=3$, 4 and 5) and the heavy nuclei, H, ($Z \geqslant 9$), to the medium ones, M, ($Z=6$, 7 and 8) the values 0.32 ± 0.07 and 0.48 ± 0.10, respectively, at the top of the atmosphere. The fragmentation probabilities in hydrogen, the main constituent of interstellar matter, were also obtained from the careful study of the interactions in the stack and allowed to make a further extrapolation of the charge spectrum from the top of the atmosphere to the one at the source region of the cosmic radiation. The ratio of the heavy nuclei to the medium ones was found to be 0.66 ± 1.6 at the source. This charge spectrum at the source region is compared with the average chemical abundances of the elements in the universe as well as with those in certain types of stars. The results seem to indicate a close similarity of the chemical abundance curve of the cosmic radiation with that of certain types of young stars.

(*) Supported in part by the Office of Naval Research, U. S. Atomic Energy Commission and the International Geophysical Year.

Presented at the Varenna Cosmic Ray Conference - June 1957.

1. – Introduction.

One recalls that the discovery of the existence of the heavier elements [1] in the primary radiation represents a serious difficulty for some of the theories of the origin of cosmic rays. During the last years, the problem of the Li, Be and B flux in the primary radiation has been attacked by several groups [1-6] yielding results somewhat contradicting each other. The purpose of these studies was, of course, to obtain reliable information regarding the age of the cosmic radiation. This seems possible since the cosmic abundances of these light nuclei from astrophysical data are extremely small so that one can ascribe the observed cosmic ray fluxes to the break-up of the heavier elements due to collisions with interstellar matter.

However, if one aims at something more than an order of magnitude estimate of the age of the cosmic radiation, various difficulties arise even if definite values of the light nuclei fluxes can be obtained at some atmospheric depth. That is, in converting the charge spectrum observed at some finite atmospheric depth to that at the top of the atmosphere, one has to solve the diffusion equations containing parameters specifying the interaction mean free paths of various heavy nuclei and their fragmentation probabilities. The determination of the fragmentation probabilities has been attempted by various groups [2,7,8] and here again the results differ appreciably. Now suppose this difficulty were avoided by obtaining precise data regarding fragmentation probabilities in air nuclei or by getting to such a high altitude that one can neglect the change in the spectrum due to collisions with air nuclei, one still must obtain the fragmentation probabilities in interstellar matter, which is mainly hydrogen, in order to get reliable information regarding the age of the cosmic radiation based on the fluxes of light nuclei (Li, Be and B). These fragmentation probabilities in air and in hydrogen can, in principle, be separately obtained from observations of break-up events in the emulsion by grouping these events according to the number of slow particles in the event, since a small number of slow particles means, generally, that a small number of nucleons in the target nucleus participated in the interaction.

---

(1) P. FREIER *et al.*: *Phys. Rev.*, **74**, 213 (1948); H. L. BRADT and B. PETERS: *Phys. Rev.*, **80**, 943 (1950).

(2) A. D. DAINTON, P. H. FOWLER and D. W. KENT: *Phil. Mag.*, **43**, 729 (1952).

(3) M. F. KAPLON *et al.*: *Phys. Rev.*, **85**, 295 (1952).

(4) M. F. KAPLON *et al.*: *Phys. Rev.*, **93**, 914 (1953).

(5) T. H. STIX: *Phys. Rev.*, **95**, 782 (1954).

(6) R. E. DANIELSON *et al.*: *Phys. Rev.*, **103**, 1075 (1956).

(7) J. H. NOON *et al.*: *Phys. Rev.*, **92**, 1585 (1953).

(8) P. E. HODGESON: *Phil. Mag.*, **42**, 955 (1951).

One can look upon the problem of the charge spectrum in a still more general way. It seems that some of the important aspects of the problem other than that of the abundances of the light nuclei have not been duly considered for several years. B. PETERS ([9]) discussed the abundances of noble gases and other heavy elements. However, in view of recent developments regarding studies of thermonuclear reactions and their relation to stellar evolution, both theoretical and experimental, the possibility exists of obtaining more specific information on the origin of the cosmic radiation. The existence of rather strong peaks in the cosmic ray abundance curve at, for example, Fe, suggests that the source might be located in stars where the process of the synthesis of elements has progressed considerably.

Let us now very briefly review the information regarding the source, or the ejector of the cosmic radiation as deduced from a study of the charge spectrum. First of all, we assume that the flux values of the light nuclei Li, Be and B are practically zero at the place of ejection. There has been some discussion of the problem that there may be a small finite flux of these light nuclei at the source region. However, the results presented here, especially those referring to the considerable amount of Ne found (ionization potential 21.5 eV) strongly indicate a very high temperature of at least 10^8 degrees absolute at the source. This temperature is high enough to destroy practically all the light nuclei Li, Be and B by $(p\gamma)$ reactions and subsequent α-decays.

Depending on the extent to which the thermonuclear reactions proceeded in the star, the relative abundances of the various medium and heavy nuclei should be different. The following reactions were considered:

1) proton proton cycle;
2) α captures leading to ^{12}C, ^{16}O and ^{20}Ne, etc.;
3) CN cycle, NeNa cycle, etc.;
4) inter-connection of different cycles by (αn) reactions and shift towards higher Z up to around Ca;
5) building up of still heavier elements by neutron capture;
6) other processes such as proton reactions in magnetic stars, etc.

Naturally, two or more of these reactions can occur at the same time depending on the temperature and the chemical composition of the material. The results of these reactions can, in principle, be calculated and, in fact, such calculations have been made in order to compare the theory with the observed chemical abundances of elements on certain stars. They already yielded valuable information concerning certain properties of these stars ([10]). For this reason,

([9]) *Progress in Cosmic Ray Physics* (1951), p. 238.
([10]) *Synthesis of the Elements in Stars* (1957), prepublication print, E. M. BURBIDGE *et al.*

it seems worthwhile to try to obtain a more accurate charge spectrum of the cosmic radiation. The detailed comparison of such a spectrum with astronomical observations may reveal a great deal about the properties of the source. The classification of nuclei into three general groups, L, M and H, is not sufficient for a detailed discussion of the problem. Instead, we may try to obtain at least the following quantities: 1) C to N ratio, Ne to Na ratio which may tell us something about thermonuclear cycles, 2) the relative abundances of C, O, Ne, Mg, etc., which would give us information about the intermixing of various cycles at the source, and 3) the relative abundance of Fe with respect to light nuclei which may give us some information about the extent to which the neutron capture has proceeded to build up heavier elements. Information of this kind should be valuable to possibly locate the source region of cosmic rays in certain types of stars in our galaxy.

2. – Methods of charge determination in nuclear emulsion.

For determination of the charge of each individual heavy nucleus, including those of Z higher than 10, the following methods were used:

1) typical break-up events;
2) δ-ray counting;
3) photometric opacity measurement;
4) the slope of gap-length distribution;
5) blob counting.

These are the methods applicable to relativistic particles as found close to the top of the atmosphere at 41° N. It is preferable first to determine the charge spectrum at relativistic energies not only because it is experimentally simpler than at non-relativistic energies but also because there may exist a considerable variation of the heavy nuclei flux from day to day in the low energy region ([11]).

2·1. *Typical break-up events.* – This method is essentially the basis for the other charge determinations since in any other type of measurement one must have a few definite calibration points. It is true that for δ-ray countings, the knowledge of the δ-ray densities of relativistic protons and α-particles is, in

([11]) M. KOSHIBA and M. SCHEIN: *Phys. Rev.*, **103**, 1820 (1956). Even in the relativistic energy range, different results regarding the relative abundances, for example, of nitrogen or of different groups of elements measured at different times might signify such a variation. However, it is more probable that some of the disagreements are due to insufficient accuracy in the charge determination of Z sione in the relativistic range, actual variation of the heavy nuclei flux could have been observed by the neutron detectors at lower altitudes.

principle, sufficient for calibration purposes. However, the straight-forward extrapolation using the Z-dependence of δ-ray density (constant $\times Z^2$ + background) into the higher Z range ($Z > 6$) is very difficult because of the background so that the genuine δ-ray density is obtained as a small difference of two large quantities. Hence, one must have at least a calibration point around $Z = 6$, 7 or 8.

Some precaution must be taken in choosing the break-up events for the purpose of the calibration of charge determination. One usually accepts those cases where neither evaporation tracks nor grey tracks are observed and then assumes that these events are due to hydrogen targets. This is not quite true since a neutron on the periphery of a heavy nucleus can give rise to the same type of break-up events with a primary nucleus of a Z greater by 1 unit. (The observation of a β-ray at the point of break-up does not help in distinguishing a proton from a neutron target since the β-ray in general could be due to a high energy δ-ray). There is an additional difficulty due to the fact that in the energy region above 1 GeV, for example, there is a good chance of creating π-mesons among the secondaries, which are hard to distinguish from protons. Therefore, if possible, one should use only break-ups where no singly charged particles are observed among the secondaries like, for example Be $\rightarrow 2\alpha$, C $\rightarrow 3\alpha$, etc. The possibility that these cases are due to having proton targets is very small at relativistic energies. (In the frame of reference of the incident particle at rest, this would mean that a proton suffers charge exchange scattering and is subsequently trapped by the residual nucleus which in turn decays by α-particle emission.)

2·2. *δ-ray counting.* – This is the method used by most groups. The reason is that we know the Z-dependence (background subtracted) of δ-ray density. The method is described and discussed in a number of papers so we may merely add a few brief remarks. In addition to the extrapolation to higher Z as mentioned before, one encounters, in general, serious difficulties in applying this method to particles of Z greater than 8. Due to the high density of δ-rays twisted and entangled, one cannot make a very reliable estimate of their number. The usual criterion is to accept δ-rays consisting of minimum 4-grains. It seems more preferable to use a criterion which is related to the range of δ-rays rather than to their ionization, especially in case the emulsion stacks are not evenly developed. One can choose, for example, δ-rays which stop in a specified range from the parent track, for example between 10 μm to 30 μm. This selection reduces the number of δ-rays to be counted considerably; however, the background becomes almost negligible and the unevenness of the development affects the results very little. The reason for this is that one can make use of the observation of the characteristic ending of δ-rays, the increase in the grain density and the scattering, the Z^2-dependence of

δ-ray density is applicable to this method, even though only a part of the total energy spectrum of δ-ray electrons is used. Furthermore, by omitting the short range δ-rays, the δ-ray count of heavier tracks ($Z \gtrsim 8$) becomes more objective and reliable.

2·3. *Photometric opacity measurement* (VON FRIESEN). – In principle, this is the most objective way of determining the primary plus secondary ionization of a heavy nucleus. Careful corrections are necessary for uneven development. One way of taking into account this effect is to take the ratio of the transmitted light through the track to that of the neighboring area. A further effect of importance is the dependence on depth as already noticed by several workers. This, however, can be avoided if one is dealing with a stack consisting of a considerable number of emulsions, since by following the track, one can always measure the opacity at the same depth. The integral effect on the transmission of the other tracks above or below the track under consideration must also be accounted for. This can be done by using a condenser of high numerical aperture, reducing the contribution of the tracks above and below the focused illuminated region. There is an additional effect one has to be aware of. It is the effect of stray light coming from outside the area which is being measured. This effect is called by the astronomers the Schwartzshild-Villigar effect. In order to reduce this effect, the total illuminated area was made as small as possible. A photometric opacity measuring device which satisfies the above conditions has been built and used in this laboratory.

2·4. *The slope of the gap length distribution.* – This method was described in detail by FOWLER and PERKINS ([12]). They found an almost complete saturation effect at Z of about 8 or higher, while the method was found well applicable up to about thirty times minimum ionization with results almost independent of the processing of the plate. The serious difficulty in trying to use this method for ionization measurements of particles with Z greater than 8 is, aside from the above-mentioned saturation effect, that the density of gaps becomes so small that the statistical accuracy of the results for tracks of the usual length of a few millimeters per plate, becomes poor in particular for longer gaps. One needs at least two sets of gap density measurements for each track corresponding to two chosen values of gap lengths in order to determine the slope of the gap length distribution.

2·5. *Blob-counting.* – As was shown by FOWLER and PERKINS ([12]), the gap length distribution is well represented by the formula,

$$G_l = g \exp\left[-g(\alpha + l)\right], \tag{1}$$

([12]) P. H. FOWLER and D. H. PERKINS: *Suppl. Nuovo Cimento*, **2**, 238 (1956).

where G_l is the density of gaps with length greater than l, α is the average diameter of developed grains, g is a characteristic parameter specifying the ionization and can be obtained by the formula,

$$g = \frac{1}{l_2 - l_1} \log \left(\frac{G_{l_1}}{G_{l_2}} \right) .$$

It was shown that it is proportional to Z^2 up to about $Z \sim 3$ and then begins to show saturation before reaching almost complete saturation at $Z \sim 8$ ([12]). However, there still exists a possibility that g further increases with Z beyond $Z \sim 8$ since there are factors other than the primary ionization which affect the gap density. For example, even if the primary ionization saturates completely, a further reduction of gap density due to increased secondary ionization (δ-rays of low energies) may become noticeable. This effect would be rather difficult to observe by method 4 as discussed in the last paragraph since it is very hard to obtain good statistics on larger gaps and since it is difficult to measure very small gap lengths with high accuracy.

Let us now consider the expression

$$G_0 = g \exp [-g\alpha] . \tag{1'}$$

This is the formula for $l = 0$; i.e. for the density distribution of all resolvable gaps; in other words, the blob density. One has to realize, however, that the use of this single expression for the estimation of g necessarily involves the effect of the variation of α, the average grain diameter, on the results. That means the method requires a separate calibration for plates of different degree of development. Note also that the expression as a function of g has a maximum at $g = 1/\alpha$ which is 170 grains per 100 μm for ordinary plates, so that for a given value of G_0 there are two values of g which satisfy the above equation. This is one of the reasons why this method was not applied to tracks of ionization higher than that of relativistic α-particles (4 times minimum) while it was in common use in the low ionization range. Provided the calibration is properly done, one can extend this method beyond the maximum of G_0. In the vicinity of the maximum itself, G_0 is insensitive to the change of g. In using this method, a number of factors had to be considered: the resolvability of a gap depends on *a*) the magnification and the resolving power of the microscope, *b*) the illumination, *c*) the development of the plate, *d*) the subjectivity of the resolvibility, and *e*) the dip-angle of the track.

The use of the same apparatus, microscope and illuminating unit under the same working conditions eliminates factors *a*) and *b*). Careful calibration in the same plate reduces effect *c*) to a value well within the statistical error of the results, provided that the edge of the plate is not included and that

surface effects are taken into account. In this work, all gap-countings were done in the lower half thickness of the emulsion, on the glass side. In order to get effect *d*) under control, the results of one and the same person were used for calibration of the charge after he obtained a stable criterion of resolvability with a precision of less than 3% error. (Reproducibility of these results was checked by letting the same person count the same track over and over again. It was found that a certain practising period was necessary in order to obtain a stable criterion of resolvability.) Effect *e*) results from two causes: first, the obvious problem one encounters in grain counting, i.e. the correction by a factor of $1/\cos\theta$ where θ is the dip angle of the track before processing. The second cause is the change of the minimum gap length from α to $\alpha/\cos\theta$. The correction factor $C = G_0(\theta)/G_0(0)$ can easily be obtained from the equation (1′) as follows:

$$C = \frac{1}{\cos\theta} \exp\left[-\frac{g\alpha}{\cos\theta}(1-\cos\theta)\right]. \tag{2}$$

The variation of G_0 as a function of the dip angle θ, therefore, also gives the corresponding value of g.

Some parts of the emulsion stack used for this work were found to have been warped at the time of exposure, so that there are cases where a high energy particle passes through one plate with a certain dip angle and then enters the same plate later with a different dip angle. Using these cases, the compatibility of the two estimates of g, one from the equation (1′) and the other from the equation (2), have been checked. The latter essentially is equivalent to the use of (1).

The results of the G_0-countings are shown in Fig. 1*a* and Fig. 1*b*. In Fig. 1*a*, the logarithm of $G_0(\theta = 0)$ is plotted as a function of Z. Open circles indicate those tracks which have been calibrated by other methods, such as break-ups or δ-ray counting as described in the previous paragraphs. Actually, it is necessary to know the dip angle dependence of $G_0(\theta)$ in order to evaluate the plot of Fig. 1*a*. Equation (2) can be written for small θ as follows:

$$\log\frac{G_0(\theta)}{G_0(0)} = a - g\alpha\ (1-\cos\theta)\,. \tag{2′}$$

In Fig. 1*b*, the logarithm of $G_0(\theta)$ is plotted as a function of $(1-\cos\theta)$. The dotted lines connecting two points indicate a few of the cases of observing the same track twice with different dip angles in the same plate. The approximate determination of the slope of the lines in Fig. 1*b* is sufficient for the purpose of making the dip angle corrections to the data in Fig. 1*a* since the correction itself is small for small dip angles. The results of Fig. 1*a*, i.e. the

1920

g value, give a much better estimate of the slope of the lines in Fig. 1*b* by using equation (2) or (2′). One can see the consistency of the results yielded by the two methods from the comparison of Fig. 1*a* and Fig. 1*b*. The solid lines in Fig. 1*b* were directly obtained from the g values of Fig. 1*a* and equation (1′).

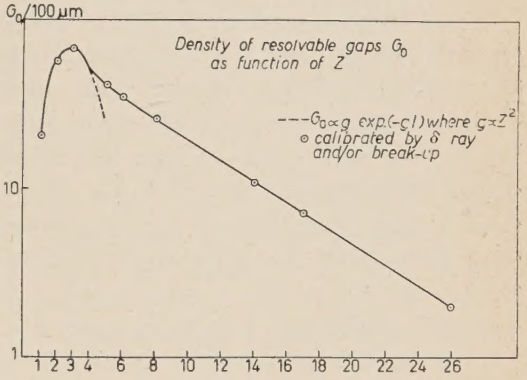

Fig. 1*a*. – G_0 ($\theta = 0$), the blob density, as a function of Z. The dotted line is the curve one expects if there were no saturation of ionization.

The determination of Z of heavy nuclei in this work was done to a large extent by the above described method of G_0-counting, after calibrating Z by break-ups and δ-ray countings. Once calibrated in one plate, it was easy to extend the calibration to other plates by following through the identified tracks. At $Z > 12$, special care had to be exercised. One can expect here that only a small percentage of the break-up events will contain α-particles and heavier fragments only, since heavier nuclei cannot be considered as α-particle structures, as in the case of the lighter nuclei up to about Ne. The calibration in this work for Z around 26 was achieved by the careful study of an event

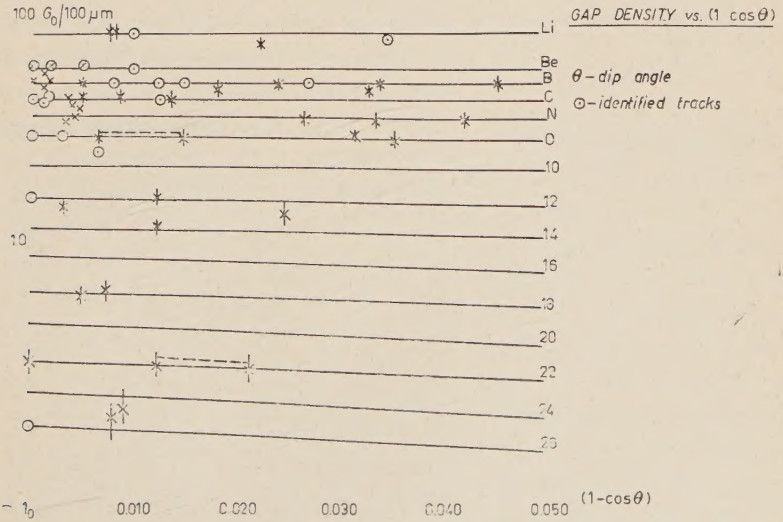

Fig. 1*b*. – $G_0(\theta)$ as a function of $(1 - \cos\theta)$, θ being the dip angle of the track. The lines corresponding to each Z value are drawn by using g-values obtained from Fig. 1*a*. For a fuller explanation of Fig. 1*a* and Fig. 1*b*, see the text.

that was found to be an Fe nucleus of energy (11.8 ± 1.3) GeV per nucleon which collided with a proton and broke up into a Mg nucleus, 3 α-particles and 8 protons. The δ-ray counting as described previously gave the primary charge of 24 ± 3 and the extrapolation of the G_0-counting from the already calibrated region of $Z > 12$ gives 26 ± 1 for the primary charge. The charge of this primary particle was set to 26 and during the course of G_0-counting, the results of charge determination on heavier particles were checked with δ-ray countings and/or with the sum of the charges of the secondaries of good break-up events. Not a single inconsistency in the determination of Z was observed throughout the whole analysis of the data on more than 50 tracks of Z heavier than 12, and good confirmation was obtained that the method of calibration of the charge by G_0-counting was reliable. In fact, there were three cases where the accurate charge determination by G_0-counting in two different plates has led to locating the correct break-up process such as $O \rightarrow B$ and $N \rightarrow C$, which were missed in the first scanning and tracing with a $10\times$ dry objective. After having had this experience the tracks were traced again with a higher magnification plus oil immersion, and several additional interactions were located.

3. – Experimental procedures.

The emulsion stack used in this work consisted of 100 pellicles of 600 μm thick G-5 emulsion, 6 in. $\times$ 12 in., and was exposed in a Skyhood balloon flight over Texas, 41° N geomagnetic latitude, at an altitude of 104 000 feet for 8 hours.

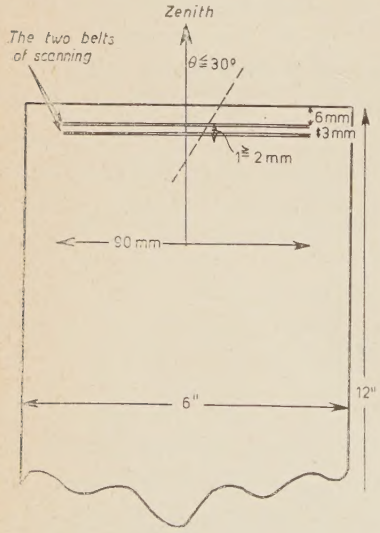

Fig. 2. – The geometrical requirement for the acceptance of a track.

The top edges of the middle 50 plates were scanned for tracks of ionization greater than 7 times minimum ionization (21 grains per 100 μm). The geometrical restrictions were such as to select those tracks entering the plate in the middle 9 cm of its top side with zenith angle, projected on the plate of the emulsion, less than 30 degrees and with track length per plate, projected to the zenith direction, 2 mm or more. This geometrical requirement which is shown in Fig. 2 was set in order to insure 1) a minimum of 5 cm track length inside the sensitive volume in order to obtain better charge determinations and 2) a better extrapolation to the top of the atmosphere. Each emulsion was scanned at two distances

(6 mm and 9 mm) from the top side. Every individual track thus located in one place was traced to the other location in the next plate to see whether the track was also recorded there. Furthermore, several plates were scanned by two people independently and compared with each other. It is believed that a scanning efficiency of better than 98% was obtained for particles of charge $Z \geqslant 4$. However, for Li nuclei the efficiency could have been as low as 60% because of surface corrosion by hypo in some of the scanned plates. In the case of Li nuclei, there is another ambiguity: if an interaction occurs near the top edge of the plate causing a star of many prongs it is sometimes difficult to distinguish primary Li nuclei from α-particles since at the edge of the emulsion it is hard to determine the scattering in the presence of edge distortions and since a Li interaction with a heavy nucleus may not exhibit a narrow forward cone of break-up products. Therefore, in some cases one can mistake α-particles for Li nuclei and vice versa.

Each single heavy nucleus track found in scanning was traced through the stack until either it interacted or left the stack. During the course of this tracing, which was done first by $10\times$ dry objectives and then by $53\times$ oil immersion objectives, we found that the stack was warped, at the time of exposure. The tracks which were shorter than 2 mm per plate, projected to the zenith in the middle of the plate, were omitted from the analysis.

The over-all precision of the charge determination, judging from the internal consistency of the various methods applied here, was such that in more than 95% of the cases a correct Z could be assigned for a track of Z up to 8 and that in more than 80% of the cases a charge could be assigned within one charge unit to tracks of charge around 26.

4. – Results and discussion.

The charge spectrum obtained is shown in Fig. 3*a*. It can be noticed that there are pronounced peaks corresponding to Li, Be, B, C, O, F, Ne, Na, Mg, Si and Fe. In order to show the resolution in Z to each particle of charge greater than 12 a triangle was assigned which had the same area over a base corresponding to the statistical uncertainty of the G_0-counting (Fig. 3*b*).

In order to determine the charge spectrum at the top of the atmosphere, one needs the interaction mean free paths in air of various groups of nuclei groups as well as the fragmentation probabilities in air. Because of the corrosion at the surfaces of some of the scanned plates, we used the interaction mean free paths given by the Rochester group ([13]). As to the fragmentation probabilities, we have chosen interactions occurring in the well-developed region of the plates. A total of 209 interactions were grouped according to

([13]) M. F. KAPLON, J. H. NOON and G. W. RACETTE: *Phys. Rev.*, **96**, 1408 (1954).

the charge of the primary nucleus, according to the size of the target nucleus. The size of the target nucleus was estimated from the number of slow particles emitted in the interaction. The group classified as interactions with targets of medium heavy nuclei had six or less slow particles; they should include some of the collisions at the periphery of Ag or Br nuclei. This, however, may not modify the fragmentation probability seriously, since a small number of slow particles in the interaction means in general that a small number of nucleons participated in the interaction. The results regarding the fragmentation probabilities are shown in Table I. In the table, collisions with neutrons on the periphery of the nucleus without slow prongs were included in the first group referring to single nucleon targets. This requires some justification. First of all, we note that if an incoming nucleus is self-conjugate, having the same number of protons and neutrons, the fragmentation probability of giving a fragment of charge Z_1 and of the number of neutron N_1 fragment (Z_1, N_1) from a proton target is equal to that of giving a fragment $Z_2 = N_1$, $N_2 = Z_1$, from a neutron target. Therefore, if the secondary fragment and its mirror nucleus belong to the same group, L, M or H, as in the case of ^{7}Li and ^{7}Be or ^{13}C and ^{13}N, it is justified to include collisions with neutron targets provided the primary is self-conjugate. These cases in which the secondary and its mirror nucleus belong to different groups, as in the case of ^{10}Be and ^{10}C, ^{11}B and ^{11}C, ^{12}B and ^{12}N, and ^{17}O and ^{17}F require further consideration. The prerequisite that the primary should be a self-conjugate nucleus is well satisfied for incoming M-nuclei and for H-nuclei of even charges, which are more

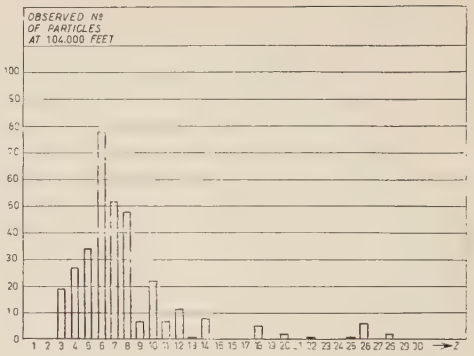

Fig. 3*a*. – The observed numbers of particles of various charge at 104 000 feet.

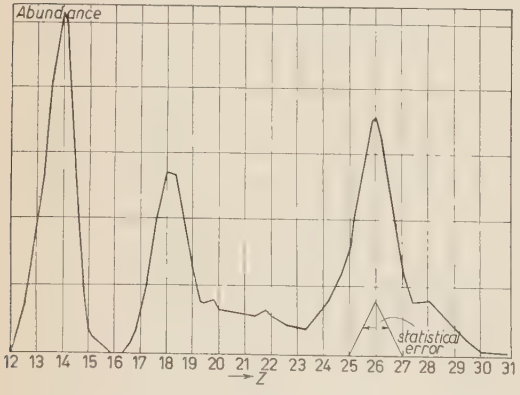

Fig. 3*b*. – The resolution of Z in the charge spectrum shown for Z greater than 12; each track is given a triangle of the same area with the base equal to twice the statistical error in the G_0-counting.

TABLE I. – *Fragmentation Probabilities.*

Single Nucleon Target (43 *Interactions*):

			$P_{H\alpha} = 9/8 = 1.12 \pm .38$
$P_{L\alpha} = 10/8 = 1.25 \pm .40$	$P_{M\alpha} = 45/27 = 1.67 \pm .25$		$P_{HL} = 3/8 = 0.38 \pm .22$
	$P_{ML} = 7/27 = 0.26 \pm .10$		$(.08 \pm 0.5)$
$P_{LL} = 0/8 = 0$	(0.83 ± 0.5)		$P_{HM} = 3/8 = 0.38 \pm .22$
	$P_{MM} = 2/27 = 0.07 \pm .05$		$P_{HH} = 2/8 = 0.25 \pm .18$

(Numbers in parentheses refer to Rochester data)

Medium Nuclei Target; *number of slow particles* 6 (54 *Interactions*):

$P_{L\alpha} = 8/17 = 0.47 \pm .16$	$P_{M\alpha} = 20/23 = 0.87 \pm .20$	$P_{H\alpha} = 22/14 = 1.57 \pm 3.4$
	$P_{ML} = 4/23 = 0.17 \pm .09$	$P_{HL} = 4/14 = 0.29 \pm .14$
$P_{LL} = 1/17 = 0.06 \pm .06$	$P_{MM} = 3/23 = 0.13 \pm .08$	$P_{HM} = 3/14 = 0.21 \pm .12$

Heavy Nuclei Target (112 *Interactions*):

$P_{L\alpha} = 21/33 = 0.64 \pm 0.14$	$P_{M\alpha} = 36/54 = 0.67 \pm .11$	$P_{H\alpha} = 26/25 = 1.04 \pm .20$
	$P_{ML} = 7/54 = 0.12 \pm .05$	$P_{HL} = 12/25 = 0.48 \pm .14$
$P_{LL} = 1/33 = 0.03 \pm 0.03$	$P_{MM} = 3/54 = 0.06 \pm 0.3$	$P_{HM} = 2/25 = 0.08 \pm .06$
		$P_{HH} = 2/25 = 0.08 \pm .06$

Total of 209 Interactions

Rochester Data [KAPLON, NOON, RACETTE: *Phys. Rev.*, **96**, 1408 (1954)].
In air:

$P_{LL} = 0.13$	$P_{ML} = 0.42$ (0.56 ± 0.18)	$P_{HL} = 0.48$ (0.48 ± 0.17)
	$P_{MM} = 0.13$	$P_{HM} = 0.27$
		$P_{HH} = 0.25$

Total of 87 Interactions
BRADT PETERS, $P_{ML} = P_{HL} = 0.23$

$\lambda_L = 31.5$ g/cm²
$\lambda_H = 26.5$ g/cm²
$\lambda_M = 18$ g/cm²

abundant than those of odd charge in the primary cosmic radiation as can be seen from Fig. 3, and it is only approximately satisfied for incoming L-nuclei or for H-nuclei of odd charges. The number of cases found corresponding to L-nuclei and odd H-nuclei was 5 and 3, respectively. Among 15 cases of neutron collisions in the M group there are two cases where the mirror nucleus of the secondary may belong ot a different group. These are the reactions: $^{16}O + n \rightarrow B + \alpha p$ and $^{16}O + n \rightarrow B + 3p$. In these reactions

one may have ^{11}B rather than ^{10}B so that a proton target would yield as a secondary ^{11}C. Fortunately, even if this were the case, ^{11}C would decay into ^{11}B with a half life of 20.4 minutes which is negligible compared with the age of the cosmic radiation. Therefore, these cases were both counted as giving secondary light nuclei. The same applies to one case in the H group, $Mg+n \rightarrow \rightarrow B+7p$. There are three reaction in the H group which do not allow this type of conversion; they are the (1) $F+n \rightarrow \alpha+N$, 2) $Na+n \rightarrow 0+3p$ and 3) $Na+n \rightarrow 2\alpha-N$. Such break-ups were counted as reactions giving M-nuclei even though there exists the possibility that the secondary fragments might belong to a different group if the target nucleus were protons rather than neutrons. The same is true for L-nuclei collisions with neutrons. In this case, however, it is unlikely that the probability of having L-nuclei among the secondaries is higher in the reaction $^{11}B+p$ than in the reaction $^{11}C+p$ which is the mirror reaction of $^{11}B+n$. (There is no problem of getting mixed up in case of $Z=2$ and $Z=3$ in the process of taking reactions of mirror nuclei since ^5He and ^5Li are both unstable with extremely short half lives). To include neutron collisions would, therefore, not lead to an underestimate of P_{LL}. At any rate, P_{LL} is believed to be very small since ^8Li and ^8B both decay with half lives less than a second into ^8Be which then immediately decays into 2α-particles.

The charge spectrum obtained at 104000 feet has been transformed into that of the primary radiation before entering the atmosphere. The results of Table I were used in solving the diffusion equations. (Because of our zenith angle requirement $\theta \leqslant 30°$, the spread of residual air mass around its avergae is only 8%.)

The charge spectrum thus obtained at the top of the atmosphere is plotted in Fig. 4, curve *A*.

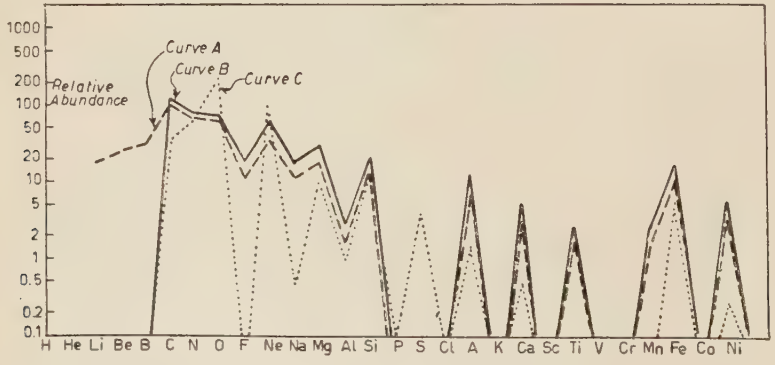

Fig. 4. – Curve *A* gives the results of the extrapolation of Fig. 3*a* to the top of the atmosphere. Curve *B* shows the charge spectrum at the source region obtained by further extrapolation of Curve *A*. Curve *C* gives the average chemical abundances of the elements in the universe as given by UREY and SUESS.

1050

By making use of the fragmentation probabilities in hydrogen as given in Table I, we can reconstruct the charge spectrum of the cosmic radiation at the source. At the time of injection, the amount of L-nuclei, Li, Be, Be is believed to be negligible compared with M-nuclei C, N, O. This requirement determines the amount of M-nuclei and H-nuclei as well as the age of the cosmic radiation. The result of this conversion into a charge spectrum at the source is also shown in Fig. 4, as curve *B*. The amount of interstellar matter traversed by cosmic rays was found to correspond to 60% of the interaction mean free path in hydrogen of the H group $Z \geqslant 9$, which corresponds to $5.3 \cdot 10^6$ years for an average density of 1 proton/cm^3 in interstellar space. The recently revised data of the chemical abundances of elements from spectroscopic measurements and from the analysis of meteorites is also given in Fig. 4, curve *C*. This curve was obtained by UREY and SUESS (14), hereafter referred to as the U-S curve.

By comparing curves *A*, *B* and *C* of Fig. 4 one can easily see the following:

1) The ratio of H-nuclei to M-nuclei is quite different in the two data; 0.66 fr0m curve *B* and 0.38 fron U-S.

2) The relative abundance of metallic elements Mg, Si and Fe seems to run parallel in both data. These non-volatile elements are reliably determined in the U-S curve from the analysis of meteorites.

3) Pronounced peaks at the elements of even *Z*, Ne, Mg and Si are seen in both data. The relatively higher abundances in the cosmic ray data of elements of odd *Z* such as F, Na and Al can easily be explained as due to the break-up of the still heavier elements, remembering that P_{III} in Table I is 0.25. (In our conversion to the source region the elements from $Z \geqslant 9$ are treated as a group. Hence the actual abundances at the source are still slightly higher in the Fe-region than in the F and Ne-region.)

4) The abundance ratios of C, N, O in our data are 1.6:1.1:1.0 which is quite different from the ones in the data of U-S namely, 0.16:0.31:1.00.

It is to be remembered that the U-S curve given in Fig. 4 represents an average chemical abundance, in contrast to the cosmic rays which are presumably due to the emission of particles from certain types of stars. According to astronomical data, young stars, generally with low space velocity and of Population I, are richer in heavier elements while old stars frequently show lower abundances of heavier elements (*). More specifically, the types of stars rich

---

(14) H. E. SUESS and C. H. UREY: *Rev. Mod. Phys.*, **28**, 53 (1956).

(*) It is a pleasure to thank Professor CHANDRASEKHAR for very stimulating discussions.

in heavier elements according to BURBIDGE and others ([16]) are:

1) supernovae;

2) the S stars;

3) the BaII stars;

4) the Carbon stars;

5) the Magnetic stars (the Peculiar A stars).

It is interesting to note that in some of the stars 2), 3) and 4) the carbon abundance was measured and found to be higher than in the U-S data; however, it is in accord with our cosmic ray measurements.

It should also be noted that the age of the cosmic radiation of about $5 \cdot 10^6$ years requires, on the average, a regeneration of the radiation in every such period. Therefore, the results presented here which indicate that there is some similarity in the chemical abundances of elements in cosmic rays and in some of the young stars of an age of a few million years seem quite suggestive.

RIASSUNTO (*)

Da un grosso pacco di emulsioni G-5 fatto ascendere nel Texas, latitudine geomagnetica 41° N, si è ottenuto lo spettro della carica della radiazione cosmica a 104 000 piedi. Si dà special importanza alla forma dettagliata dello spettro nella regione $Z \geqslant 9$. Si ricorre largamente al conteggio dei gap anche a questi elevati valori di Z dopo accuratissima taratura con eventi di frammentazione e conteggi di raggi δ. Lo spettro della carica così ottenuto è stato estrapolato alla sommità dell'atmosfera servendosi delle probabilità di frammentazione nell'aria ottenute dall'analisi di un totale di 209 interazioni nello stesso pacco. Tale estrapolazione dà per il rapporto dei nuclei leggeri L ($Z=3$, 4 e 5) e dei nuclei pesanti, H, ($Z \geqslant 9$), ai medi M ($Z=6$, 7 e 8) rispettivamente i valori 0.32 ± 0.07 e 0.48 ± 0.10 alla sommità dell'atmosfera. Dallo studio accurato delle interazioni nel pacco si sono ottenute anche le probabilità di frammentazione in idrogeno; il principale costituente della materia interstellare, che hanno permesso un'ulteriore estrapolazione dello spettro della carica dalla sommità dell'atmosfera alla sommità della regione di origine della radiazione cosmica. Il rapporto dei nuclei pesanti ai medi fu trovato essere 0.66 ± 1.6 alla sorgente. Tale spettro della carica alla regione di sorgente si confronta sia con le abbondanze chimiche medie degli elementi nell'universo che con quelle incontrate in alcuni tipi di stelle. I risultati sembrano indicare una stretta rassomiglianza della curva delle abbondanze chimiche della radiazione cosmica con quella di certi tipi di stelle giovani.

(*) *Traduzione a cura della Redazione.*

(γ, n) and $(\gamma, 2n)$ Reactions in ^{93}Nb.

E. Silva, J. Goldemberg, P. B. Smith

Departamento de Física, Faculdade de Filosofia, Ciências e Letras da Universidade de São Paulo, Brasil

and

L. Marquez

Centro Brasileiro de Pesquisas Físicas - Rio de Janeiro, Brasil

(ricevuto il 21 Ottobre 1957)

Summary. — The (γ, n) cross-section of ^{93}Nb was measured by the residual activity method. Combining this result with the total neutron yield curve it was possible to separate the contributions of the (γ, n) and $(\gamma, 2n)$ reactions. The ratio of these cross-sections was then compared with special attention to the 2.35 isomeric state ($T_{\frac{1}{2}} = 13$ hs) reported by James; this activity was not found and we determined an upper limit for it as 0.02% of the 0.93 MeV line. An activity of 3.2% abundance due probably to γ rays of annihilation of positrons was found.

1. Introduction.

The yield of the neutrons emitted by ^{93}Nb as a function of the energy of the incident γ rays was measured by Montalbetti, Katz and Goldemberg [1] using a BF_3 counter; in the measurements are included the contributions of the (γ, n) and $(\gamma, 2n)$ reactions. For a comparison of the experimental data with the theory it is necessary to distinguish between these processes; very few investigations have been made in this direction due to

[1] R. Montalbetti, L. Katz and J. Goldemberg: *Phys. Rev.*, **19**, 659 (1953).

experimental difficulties; in general one uses the method of subtracting the yield of the (γ, n) reaction from the total neutron yield; in order to do that the investigated nucleus must have a 100% abundance and the residual nucleus for the (γ, n) reaction must have a convenient half-life and radioactivity; there are not many of these cases in the Periodic Table: Tantalum was investigated by several authors ([2-4]) and an attempt was made in the case of Arsenic by MONTALBETTI *et al.* ([1]).

We followed the same general method for the case of ^{93}Nb; the excitation function of the reaction ^{93}Nb (γ, n) ^{92}Nb was obtained measuring the radioactivity of ^{92}Nb and subtracting it from the total neutron yield curve.

R. A. JAMES ([5]) reported the existence of an isomeric state in ^{92}Nb, with a 13 hour half-life produced by the reaction ^{93}Nb (p, pn) ^{92}Nb. If this state exists one should expect to form it by the (γ, n) reaction in ^{93}Nb; special attention was given to this point and an investigation of the spectrum of ^{92}Nb was made using a crystal spectrometer.

The cross-sections obtained in this paper are compared with the results expected from LEVINGER and BETHE's ([6]) computations and from the statistical theory of nuclear reactions ([7]).

2. – Experimental procedure and results.

2·1. *Exposure and counting of the samples.* – Samples of metallic ^{93}Nb were exposed to the X-ray beam of the 22 MeV Betatron of the University of São Paulo; the distance from the sample to the X-ray target was 30 cm and the irradiation time was 10 minutes; in a typical run at 20 MeV about 9 000 roentgens were delivered to each sample; the yield was measured by an ionization chamber calibrated in roentgens, according to the usual procedure.

After irradiation the samples were taken to a scintillation spectrometer with a 1 in. $\times$ 1 in. NaI(Tl) crystal with discrimination chosen properly. The radioactivity of the samples was followed for several days, a pure 10 days half-life being obtained. Data taken at different energies gave an excitation function (Fig. 1); absolute values were obtained by normalization with the

([2]) J. HALPERN, R. NATHANS and A. K. MANN: *Phys. Rev.*, **88**, 679 (1952).
([3]) E. A. WHALIN and A. O. HANSON: *Phys. Rev.*, **89**, 324 (1953).
([4]) J. H. CARVER, R. D. EDGE and D. H. WILKINSON: *Phil. Mag.*, **44**, 404 (1953)
([5]) R. A. JAMES: *Phys. Rev.*, **93**, 288 (1955).
([6]) J. S. LEVINGER and H. A. BETHE: *Phys. Rev.*, **78**, 115 (1950).
([7]) B. T. FELD, H. FESHBACH, M. L. GOLDBERGER, H. GOLDSTEIN and V. F. WEISSKOPF: *Final Report on the Fast Neutron Project USAEC NYO-636* (1951).

curve of MONTALBETTI *et al.* ([1]) below the threshold for the reaction ^{93}Nb(γ, 2n) ^{91}Nb.

Our results could be modified if the isomeric state reported by JAMES really existed. A preliminary test was made measuring the decay very carefully and the 13 hours activity was not found. Great care was then taken in a search for this isomeric state.

2·2. *Isomeric state.* – The radioactivity of ^{92}Nb was investigated by several authors ([8]) and the results are reproduced in Fig. 1: the ground state desintegrates by K capture with an half-life of 10 days to excited states of ^{92}Zr of 1.83 MeV (3.5 %) and 0.93 MeV (96.5 %); the 1.83 MeV state decays directly to the ground state of ^{92}Zr (2.2 %) or it goes to a state at 0.93 MeV (1.3 %).

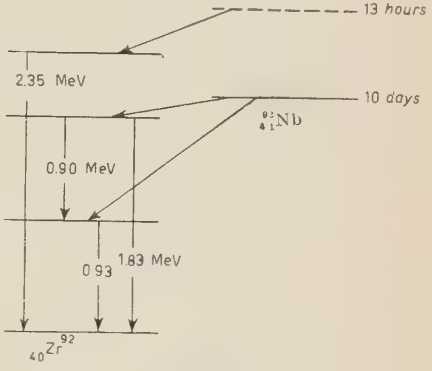

Fig. 1.

JAMES found a line of 2.35 MeV in the irradiation of ^{93}Nb by protons and attributed it to the reaction ^{93}Nb(p, pn) ^{92}Nb with a half-life of 13 hours; this line was attributed to a state in ^{92}Nb which decays by K capture to a state of ^{92}Zr of 2.35 MeV excitation.

It should be possible to reach the same state by a (γ, n) reaction in ^{93}Nb; a special irradiation was then made of a sample of metallic Nb to which a dose of 50 000 roentgens at 22 MeV was delivered. The sample was then transferred to a γ-ray spectrometer with a NaI(Tl) crystal of the well type; a one channel pulse-height analyser was used in the measurements.

The data concerning the 10 days half-life activity was confirmed but the 2.35 MeV γ line was not found. An upper limit of the abundance of this line was established as smaller than 0.02 % of the abundance of the 0.93 MeV line. No activity with an half-life of 13 hours was found. At 500 keV there was found a weak activity with an half-life of approximately 3 days and with an abundance of 3.2 % of the 0.93 MeV line; this is probably due to annihilation radiation of unreported positrons present in the decay scheme of ^{92}Nb.

2·2. *Excitation function and cross-section.* – In Fig. 2 are plotted the excitation functions of MONTALBETTI *et al.* ([1]) for the total neutron yield (curve *a*)

([8]) *Nuclear Level Schemes* - TID 530, USAEC (June 1955).

and the one obtained in this work (curve *b*). The difference is attributed to the reaction $^{93}Nb(\gamma, 2n)\,^{91}Nb$; one must divide this difference by 2 in order to obtain the excitation function for this process; the results are in curve *c* of Fig. 2.

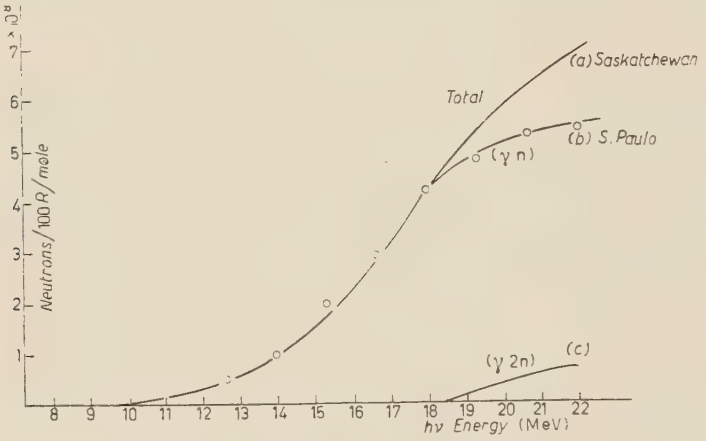

Fig. 2.

Using the photon difference method ([9]) in curves *b* and *c* of Fig. 2 the cross-sections of Fig. 3, curves II and III are obtained.

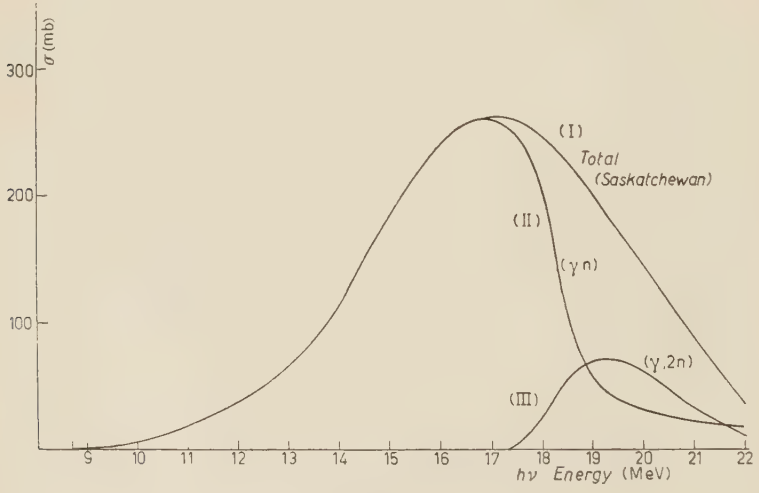

Fig. 3.

([9]) L. KATZ and A. G. W. CAMERON: *Can. Journ. Phys.*, **29**, 518 (1951).

3. – Conclusions.

An expression for the integrated cross-section for dipole absorption of photons was obtained by LEVINGER and BETHE ([6])

$$\sigma_{\text{int}} = \int_0^\infty \sigma_{\text{abs}}(E)\,\mathrm{d}E = 0.015\,A(1 + 0.8x)\,, \tag{1}$$

x is the fraction of nuclear forces of exchange character. This formula has been exaustively compared with experiments ([1, 10-12]); the small discrepancies found are due to the fact that it is impossible to obtain σ_{abs} at all energies. For the heavy elements the (γ, n) process is predominant; although $(\gamma, 2n)$ processes give an appreciable contribution it is not taken in account generally because it is difficult to obtain information on them.

In the case of Nb our results for the (γ, n) process give 1.25 MeV-barns for the integrated cross-section; one obtains 0.2 MeV-barns for the $(\gamma, 2n)$ process. HALPERN and MANN ([13]) measured the cross-section as function of the energy for the reaction $^{93}Nb(\gamma, p)^{92}Zr$ and obtained 0.12 MeV-barn for the integrated cross-section. Summing all these contributions one gets 1.57 MeV-barns. Expression (1) with $x = 0.55$ gives 1.97 MeV-barns; one can there conclude that the cross-sections for the processes not measured (γ, γ). (γ, γ'), $(\gamma, 3n)$, (γ, np) etc., plus the contributions of all the processes above 22 MeV do not amount to more than 0.4 MeV-barns.

Another result of the theory is the energy where the maximum of the cross-section occurs (E_m) and a strong correlation between this value and the threshold for the $(\gamma, 2n)$ process was predicted by EYGES ([11]); as into the case of Tantalum ([3]) this correlation was found in ^{93}Nb; it does not seem however to affect E_m significantly.

The competition between the emission of different kinds of particles can be predicted by the statistical theory of nuclear reactions ([7]); since the emission of protons is strongly suppressed by the Coulomb barrier the only other process to compete with (γ, n) in the energy range studied is $(\gamma, 2n)$. We can then use as good approximation the expression for the ratio of cross-sections of FELD *et al.* ([7]).

$$\frac{\sigma(\gamma, 2n)}{\sigma(\gamma, n) + \sigma(\gamma, 2n)} = 1 - \left[1 + \left(\frac{a}{E}\right)^{\frac{1}{2}} (E - E_b)\right] \cdot \exp\left[-\left(\frac{a}{E}\right)^{\frac{1}{2}} (E - E_b)\right],$$

([10]) J. S. LEVINGER and H. A. BETHE: *Phys. Rev.*, **85**, 577 (1952).
([11]) L. EYGES: *Phys. Rev.*, **86**, 325 (1952).
([12]) R. NATHANS and J. HALPERN: *Phys. Rev.*, **93**, 427 (1955).
([13]) J. HALPERN and A. K. MANN: *Phys. Rev.*, **83**, 370 (1952).

1933

where a is a constant dependent on A, $E_b = 17.1$ MeV is the threshold for the $(\gamma, 2n)$ process and E is the energy of excitation. Comparison of the results of expression 2 (curve a) above and the experiment (curve b) is made in Fig. 4.

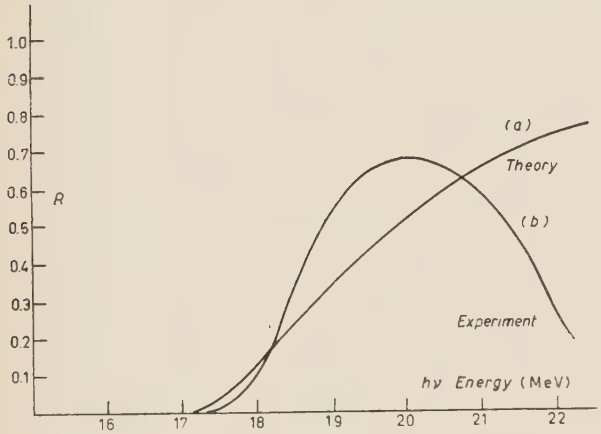

Fig. 4.

An analysis of this figure shows that there is good agreement with statistical theory up to 200 MeV; the small discrepancies found up to this energy are not significant since the cross-sections are not very precise there.

Above 20 MeV, however the experimental curve drops considerably below the expected value; this can be interpreted as due to the presence of neutrons emitted by a direct photo-effect ([14]). As can be seen in curve II of Fig. 3 the (γ, n) cross-section is approximately constant above 20 MeV; one can assume that these neutrons are all emitted by a direct process and compare the value of the cross-section with the results predicted by Courant's theory ([14]). Experimentally one finds 20 mb at 22 MeV and the theoretical value is 4.4 mb; considering the uncertainties involved in this value, it can be interpreted as meaning that a considerable amount of the neutrons above 20 MeV are emitted by a direct photo-effect.

* * *

This work was supported in part by the Conselho Nacional de Pesquisas.

([14]) E. D. Courant: *Phys. Rev.*, **82**, 703 (1951).

RIASSUNTO (*)

Si è misurata la sezione d'urto (γ, n) del ^{93}Nb col metodo dell'attività residua. Combinando questo risultato con la curva del rendimento totale in neutroni è stato possibile separare i contributi delle reazioni (γ, n) e $(\gamma, 2n)$. Si è confrontato con speciale attenzione il rapporto di queste due sezioni d'urto con lo stato isomerico 2.35 ($T_{\frac{1}{2}} = 13$ h) descritto da James; non si è trovata tale attività e se ne è determinato un limite superiore a 0.02% della riga di 0.93 MeV. Si è trovata un'attività col 3.2% di abbondanza dovuta probabilmente a raggi γ da annichilamento di positroni.

(*) *Traduzione a cura della Redazione.*

IL NUOVO CIMENTO Vol. IX, N. 1 1° Luglio 1958

Two-Nucleon Potential From Chew-Low Theory.

R. T. Sharp (*)

Department of Mathematics, Imperial College - London

(ricevuto il 13 Gennaio 1958)

Summary. — The two-nucleon potential is derived within the framework of the static cut-off pion theory of Chew and Low. Except for approximations implicit in the original Hamiltonian, the one-meson-exchange potential is exact and agrees, for example, with that of Brueckner and Watson. In the two-meson-exchange potential scattering effects are treated by the one-meson approximation of Chew and Low. The result is expressed in terms of integrals over the solution of the Low equation. The procedure is indicated for applying the method to certain non-adiabatic effects in the two-nucleon potential, to the Λ-nucleon potential, and to the three-nucleon force.

1. – Introduction.

Nuclear forces have been treated by Gartenhaus (1), and the Λ-nucleon force by Dallaporta and Ferrari (2) and by Lichtenberg and Ross (3), using Chew's value of the renormalized coupling constant and, in Gartenhaus' case, Chew's momentum cut-off. But these treatments are based, not on Chew-Low theory, but rather on the approach of Brueckner and Watson (4). Their theoretical justification is that the potential leads to low energy baryon-baryon scattering in agreement with that predicted by the field-theoretical scattering matrix; this agreement is approximate, however, because of neglect of multiple scattering corrections.

(*) Nuffield Fellow on leave of absence from Department of Mathematics, McGill University, Montreal, Canada.

(1) S. Gartenhaus: *Phys. Rev.*, **100**, 900 (1955).

(2) N. Dallaporta and F. Ferrari: *Nuovo Cimento*, **5**, 111 (1957).

(3) D. Lichtenberg and M. Ross: *Phys. Rev.*, **103**, 1131 (1956).

(4) K. A. Brueckner and K. M. Watson: *Phys. Rev.*, **90**, 699 (1953).

1935

In his review article WICK ([5]) suggests that nuclear forces can probably be treated within the framework of the Chew-Low theory. This suggestion can in fact be carried through consistently and the details, applied to the case of two nucleons, form the subject matter of this paper. The potential is calculated directly as the change in energy of the two fixed nucleons due to their being close enough to exchange mesons. Multiple scattering is taken into account in the « one-meson » approximation of Chew and Low.

2. – The Hamiltonian.

We start with the same Hamiltonian as WICK, generalized to the case of two fixed nucleons. It is

$$H = H_M + \mathcal{H}^1 + \mathcal{H}^2 , \tag{2.1}$$

where $\mathcal{H}^1$ and $\mathcal{H}^2$ are given by the Fourier expansions

$$\mathcal{H}^1 = f \sum_p (V_p^1 a_p + V_p^{1*} a_p^*) , \tag{2.2a}$$

$$\mathcal{H}^2 = f \sum_p (V_p^2 a_p \exp [i\boldsymbol{p}\cdot\boldsymbol{r}] + V_p^{2*} a_p \exp [-i\boldsymbol{p}\cdot\boldsymbol{r}]) , \tag{2.2b}$$

$$V_p^\alpha = Ni(4\pi)^{\frac{1}{2}}(1/\mu)v(p)(2\omega_p)^{-\frac{1}{2}}\tau_\lambda^\alpha \boldsymbol{\sigma}^\alpha\cdot\boldsymbol{p} ; \qquad \alpha = 1, 2. \tag{2.3}$$

The notation is fairly standard. H_M is the sum of the energies of the mesons present; $\mathcal{H}^\alpha$ is the interaction between nucleon α and the meson field; f is the unrenormalized coupling constant; a_p is the annihilation operator for a meson of type p, i.e., of momentum $\boldsymbol{p}$ and charge type λ; $\boldsymbol{r}$ is the position of nucleon 2 relative to nucleon 1; μ is the meson rest mass; $\omega_p = (\mu^2 + p^2)^{\frac{1}{2}}$ is the energy of a meson of type p; N is the normalization factor; $\boldsymbol{\sigma}^\alpha$ and τ_λ^α are the spin and isotopic spin operators for nucleon α; $v(p)$ is the momentum cut-off factor.

The potential energy V is the difference between the lowest eigenvalue of (2.1) and the self-energies of the two nucleons; the expression « lowest eigenvalue » is used loosely here to denote the value of (2.1) for a state in which no free mesons are present. V is in fact a matrix linking the different spin and isotopic spin states of the two nucleons. Before proceeding we will replace (2.1) by a new Hamiltonian (2.4). The object of this replacement is to separate those terms which represent an interaction between the nucleons. If these terms are regarded as a perturbation, the nucleons are uncoupled from each other in zero order while the interaction of each with the meson field is taken

([5]) G. C. WICK: *Rev. Mod. Phys.*, **27**, 339 (1955).

completely into account. The justification for this substitution is, as will be shown in Appendix A, that the two Hamiltonians have the same lowest eigenvalue.

The new Hamiltonian is

$$H = H^1 + H^2 + \mathcal{H}\,, \tag{2.4}$$

where

$$H^\alpha = H^\alpha_M + \mathcal{H}^\alpha_\alpha\,; \qquad \alpha = 1, 2; \tag{2.5}$$

$$\mathcal{H} = \mathcal{H}^1_2 + \mathcal{H}^2_1\,. \tag{2.6}$$

As a device for distinguishing formally the mesons emitted by the two nucleons, we assume that there are two types of mesons, 1 and 2; the superscripts in (2.4), (2.5), (2.6) refer to these two fields. H^1_M is the energy of the 1 mesons; $\mathcal{H}^1_1$ couples the 1 mesons to nucleon 1; $\mathcal{H}^1_2$ allows nucleon 2 to absorb 1 mesons; the other terms in (2.5) and (2.6) are defined analogously. Specifically,

$$\mathcal{H}^1_1 = f \sum_p (V^1_p a^1_p + V^{1*}_p a^{1*}_p)\,; \qquad \mathcal{H}^2_2 = f \sum_p (V^2_p a^2_p + V^{2*}_p a^{2*}_p)\,; \tag{2.7}$$

$$\mathcal{H}^1_2 = f \sum_p V^1_p a^1_p \exp[i\boldsymbol{p}\cdot\boldsymbol{r}]\,; \qquad \mathcal{H}^2_1 = f \sum_p V^1_p a^2_p \exp[-i\boldsymbol{p}\cdot\boldsymbol{r}]\,. \tag{2.8}$$

a^1_p and a^2_p are annihilation operators for meson of type 1 and 2 respectively. We will treat $\mathcal{H}$ as a perturbation; in the unperturbed Hamiltonian $H^1 + H^2$ the nucleons are uncoupled. Although (214) is not Hermitian, its unperturbed part is Hermitian, and affords a complete set of orthonormal states so that conventional perturbation theory is applicable.

To proceed we need the solution of the one-nucleon problem, i.e. the eigenstates and eigenvalues of the one-nucleon Hamiltonian (2.5). This problem is discussed by Wick. We follow him in representing real nucleon states by $|\rangle$, states with one real meson p by $|p\rangle$ and so on. A general one-nucleon state with mesons in definite states of charge and momentum will be denoted by $|n\rangle$. For simplicity the nucleon spin and isotopic spin quantum numbers are suppressed. Also we will not as a rule label one-nucleon states 1 or 2; there will usually be labelled operators as V^1_p or a^1_p acting on them which tell us to which nucleon they refer.

The unperturbed eigenstates of the two-nucleon Hamiltonian are $|n_1, n_2\rangle$ i.e., the direct products of the general one-nucleon states $|n_1\rangle$ and $|n_2\rangle$ for the respective nucleons; $|,\rangle$ is the state with two real nucleons.

The potential energy matrix V is given by ordinary perturbation theory. The first and second order potentials are respectively

$$V^{(1)} = \langle, |\mathcal{H}|, \rangle \tag{2.9}$$

and

$$V^{(2)} = \sum_{n_1, n_2}{}' \frac{\langle, |\mathcal{H}| n_1, n_2\rangle\langle n_1, n_2 |\mathcal{H}|,\rangle}{-(E_{n_1} + E_{n_2})} . \tag{2.10}$$

In (2.10) the prime on $\sum'$ means that n_1 and n_2 must not both be real nucleon states. In the denominator the energies E_{n_1} and E_{n_2} are those of the free mesons and do not include the nucleon self-energies.

The first order potential (2.9) contains all effects due to the exchange of a single meson; the second order potential contains all effects due to exchange of two mesons, and so on. The terminology here is not the standard one. Most authors mean by « order » not the number of mesons exchanged but the degree in the coupling constant.

3. – The potential.

The first order potential is

$$V^{(1)} = V_1^{(1)} + V_2^{(1)} , \tag{3.1}$$

with

$$V_1^{(1)} = \langle, |\mathcal{H}_2^1|,\rangle . \tag{3.2}$$

$V_1^{(1)}$ contains all effects due to transfer of a single meson from 1 to 2. $V_2^{(1)}$ is obtained from $V_1^{(1)}$ by interchanging the two nucleons; it turns out to be the Hermitian conjugate of $V_1^{(1)}$. Substituting the Fourier expansion (2.8) for $\mathcal{H}_2^1$ in (3.2),

$$V_1^{(1)} = f \sum_p \langle |a_p^1|\rangle\langle |V_p^2|\rangle \exp [i\boldsymbol{p}\cdot\boldsymbol{r}] . \tag{3.3}$$

Now according to Wick, Eq. (2.15),

$$f\langle |V_p^2|\rangle = f_r V_p^2 , \tag{3.4}$$

where f_r is the renormalized coupling constant. And using Wick's (5.37) and (2.15) we get

$$\langle |a_p^1|\rangle = \langle |(\omega_p - H^1)^{-1} f V_p^{1*}|\rangle = -f_r \omega_p^{-1} V_p^{1*} . \tag{3.5}$$

We have departed here from Wick's notation by adjusting the zero of H^1 so that it does not include the self energy E_s, and by including in ω_p the infinitesimal imaginary energy $-i\varepsilon$ which picks out states with incoming scattered waves. Substituting (3.4) and (3.5) in (3.3) gives $V_1^{(1)}$. Adding the Her-

mitian conjugate $V_2^{(1)}$ according to (3.1) we find for the first order potential

$$V^{(1)} = -f_r^2 \sum_p \frac{V_p^1 V_p^{2*}}{\omega_p} \exp[i\boldsymbol{p}\cdot\boldsymbol{r}] + \text{Hermitian conjugate.} \tag{3.6}$$

The second order potential is

$$V^{(2)} = V_{11}^{(2)} + V_{12}^{(2)} + V_{22}^{(2)} + V_{21}^{(2)} \tag{3.7}$$

with

$$V_{11}^{(2)} = -\sum_{n_1,n_2}{}' \frac{\langle , | \mathcal{H}_2^1 | n_1, n_2 \rangle \langle n_1, n_2 | \mathcal{H}_2^1 | , \rangle}{E_{n_1} + E_{n_2}}, \tag{3.8}$$

$$V_{12}^{(2)} = -\sum_{n_1,n_2}{}' \frac{\langle , | \mathcal{H}_2^1 | n_1, n_2 \rangle \langle n_1, n_2 | \mathcal{H}_1^2 | , \rangle}{E_{n_1} + E_{n_2}}. \tag{3.9}$$

$V_{22}^{(2)}$ and $V_{21}^{(2)}$ are obtained from $V_{11}^{(2)}$ and $V_{12}^{(2)}$ respectively by interchanging the nucleons; they turn out to be their Hermitian conjugates. Substituting the Fourier expansions (2.8) for $\mathcal{H}_2^1$ and $\mathcal{H}_1^2$ in (3.8) and (3.9) gives

$$V_{11}^{(2)} = -f^2 \sum_{n_1,n_2}{}' \sum_{pq} \frac{\langle | a_p^1 | n_1 \rangle \langle n_1 | a_q^1 | \rangle \langle | V_p^2 | n_2 \rangle \langle n_2 | V_q^2 | \rangle}{E_{n_1} + E_{n_2}} \exp[i(\boldsymbol{p}+\boldsymbol{q})\cdot\boldsymbol{r}], \tag{3.10}$$

$$V_{12}^{(2)} = -f^2 \sum_{n_1,n_2}{}' \sum_{pq} \frac{\langle | a_p^1 | n_1 \rangle \langle n_1 | V_q^1 | \rangle \langle | V_p^2 | n_2 \rangle \langle n_2 | a_q^2 | \rangle}{E_{n_1} + E_{n_2}} \exp[i(\boldsymbol{p}+\boldsymbol{q})\cdot\boldsymbol{r}]. \tag{3.11}$$

In the spirit of the one-meson approximation of Chew and Low, we now retain in $V_{11}^{(2)}$ and $V_{12}^{(2)}$ only intermediate states $|n_1, n_2\rangle$ for which $|n_1\rangle$ or $|n_2\rangle$ is a one-meson state $|s\rangle$ and the other is the real nucleon state $|\rangle$. We get

$$V_{11}^{(2)} = U_{11}^{(2)} + W_{11}^{(2)}, \tag{3.12}$$

$$V_{12}^{(2)} = U_{12}^{(2)} + W_{12}^{(2)}, \tag{3.13}$$

where

$$U_{11}^{(2)} = -f_r^2 \sum_{pqs} \frac{\langle | a_p^1 | s \rangle \langle s | a_q^1 | \rangle V_p^2 V_q^2}{\omega_s} \exp[i(\boldsymbol{p}+\boldsymbol{q})\cdot\boldsymbol{r}], \tag{3.14}$$

$$W_{11}^{(2)} = -f_r^2 \sum_{pqs} \frac{V_p^{1*} V_q^{1*} \langle | f V_p^2 | s \rangle \langle s | f V_q^2 | \rangle}{\omega_p \omega_q \omega_s} \exp[i(\boldsymbol{p}+\boldsymbol{q})\cdot\boldsymbol{r}], \tag{3.15}$$

$$U_{12}^{(2)} = f_r^2 \sum_{pqs} \frac{\langle | a_p^1 | s \rangle \langle s | f V_q^1 | \rangle V_p^2 V_q^{2*}}{\omega_q \omega_s} \exp[i(\boldsymbol{p}-\boldsymbol{q})\cdot\boldsymbol{r}], \tag{3.16}$$

$$W_{12}^{(2)} = f_r^2 \sum_{pqs} \frac{V_p^{1*} V_q^1 \langle | f V_p^2 | s \rangle \langle s | a_q^2 | \rangle}{\omega_p \omega_s} \exp[i(\boldsymbol{p}-\boldsymbol{q})\cdot\boldsymbol{r}]. \tag{3.17}$$

(3.4) and (3.5) were used to simplify these formulas. We transform $\langle s|a_q^1|\rangle$ and $\langle s|a_q^2|\rangle$ by using Wick's (5.37). The result, for $\langle s|a_q^1|\rangle$, is

$$\langle s|a_q^1|\rangle = -\frac{\langle s|fV_q^{1*}|\rangle}{\omega_s+\omega_q}. \tag{3.18}$$

Similarly we transform $\langle|a_p^1|s\rangle$ by using

$$\langle|a_p^1 = \langle p| - \langle|fV_p^{1*}(\omega_p^*-H^1)^{-1}, \tag{3.19}$$

which is a slight rearrangement of Wick's (5.32). The result is

$$\langle|a_p^1|s\rangle = \delta_{ps} - \frac{\langle|fV_p^{1*}|s\rangle}{\omega_p^*-\omega_s}. \tag{3.20}$$

When (3.18) and (3.20) are substituted in (3.14), (3.16) and (3.17), we have the second order potential $V^{(2)}$ expressed in terms of $\langle s|fV_q^1|\rangle$ and equivalent quantities, i.e., in terms of Wick's plane wave $R_s(q)$.

The next step is to express these in terms of Wick's spherical wave $R_s(q)$ and hence relate them to the solution $g_u(\omega)$ of the Low equation. For brevity we deal in detail with $U_{11}^{(2)}$ only. The treatment of $W_{11}^{(2)}$, $U_{12}^{(2)}$, $W_{12}^{(2)}$ is similar.

From (3.14), (3.18), (3.20),

$$U_{11}^{(2)} = U_{11}' + U_{11}'', \tag{3.21}$$

where

$$U_{11}' = f_r^2 \sum_{pq} \frac{\langle p|fV_q^{1*}|\rangle V_p^2 V_q^2}{(\omega_p+\omega_q)\omega_p} \exp[i(\boldsymbol{p}+\boldsymbol{q})\cdot\boldsymbol{r}], \tag{3.22}$$

$$U_{11}'' = -f_r^2 \sum_{pqs} \frac{\langle|fV_p^{1*}|s\rangle\langle s|fV_q^{1*}|\rangle V_p^2 V_q^2}{(\omega_p^*-\omega_s)(\omega_s+\omega_q)\omega_s} \exp[i(\boldsymbol{p}+\boldsymbol{q})\cdot\boldsymbol{r}]. \tag{3.23}$$

Consider U_{11}' first. We write the plane wave states $|p\rangle$ as $|\boldsymbol{p}\lambda\rangle$ exhibiting all the meson variables. In terms of spherical waves

$$|\boldsymbol{p}\lambda\rangle = i(N/N')(12\pi)^{\frac{1}{2}} \sum_i P_i |p_i\lambda\rangle. \tag{3.24}$$

Here N' is Wick's normalization factor for the spherical wave $|pi\lambda\rangle$; P_i is the i'th component of the unit vector $\boldsymbol{P}=\boldsymbol{p}/p$; only the $l=1$ part of $|\boldsymbol{p}\lambda\rangle$ is retained on the right side of (3.24) since it is the only part which contributes to $\langle p|fV_q^{1*}|\rangle$. Similarly

$$V_{\boldsymbol{q}\mu}^1 = i(N/N')(12\pi)^{\frac{1}{2}} \sum_j Q_j V_{qj\mu}. \tag{3.25}$$

We also need the explicit form of V_p^2, V_q^2:

$$V_{p\lambda}^2 = iN(4\pi)^{\frac{1}{2}}(2\omega_p)^{-\frac{1}{2}}\mu^{-1}v(p)p\tau_\lambda^2\sum_h \sigma_h^2 P_h\,. \tag{3.26}$$

We can relate $\langle pi\lambda|fV_q^{1*}|\rangle$ to the solution g_u of the Low equation:

$$\langle pi\lambda|fV_q^{1*}|\rangle = -\tfrac{1}{2}N'^2[qv(p)v(q)/p^2(\omega_p\omega_q)^{\frac{1}{2}}]\sum_{u=1}^{3} g_u(\omega_p)(\Lambda_u')_{i\lambda,j\mu}\,. \tag{3.27}$$

This follows from Wick's (5.35), (6.6) and (6.13). Our $(\Lambda_u')_{i\lambda,j\mu}$ is the same as Wick's. The following formulas for it are found by inverting Wick's (6.12):

$$\Lambda_1 = \varepsilon/9\,; \qquad \Lambda_2 = \tfrac{2}{3} - (\varepsilon/18) - (\zeta/6)\,; \qquad \Lambda_3 = \tfrac{1}{3} - (\varepsilon/18) + (\zeta/6)\,; \tag{3.28}$$

ε and ζ are defined by Wick's (6.11). The superscripts on Λ_u' and below on ε^2 show on which nucleon they operate.

Substituting (3.24-26) and then (3.27) in (3.22), we find for U_{11}'

$$U_{11}' = -\frac{3f_r^2}{16\pi^4\mu^2}\int \mathrm{d}p\,\frac{pv^2(p)g_u(\omega_p)}{\omega_p^2}\int \mathrm{d}q\,\frac{q^4v^2(q)}{\omega_q}\cdot\frac{1}{\omega_p+\omega_q}\cdot \tag{3.29}$$

$$\cdot\sum(\Lambda_u^1)_{i\lambda,j\mu}\varepsilon_{h\lambda,l\mu}^2\int \mathrm{d}\Omega_p P_i P_h\exp[i\boldsymbol{p}\cdot\boldsymbol{r}]\int \mathrm{d}\Omega_q Q_j Q_l\exp[i\boldsymbol{q}\cdot\boldsymbol{r}]\,.$$

The angular integrals can be done immediately:

$$\int \mathrm{d}\Omega_p P_i P_h\exp[i\boldsymbol{p}\cdot\boldsymbol{r}] = 4\pi\{\psi(pr)\delta_{ih} + \varphi(pr)R_iR_h\}\,, \tag{3.30}$$

where $\boldsymbol{R} = \boldsymbol{r}/r$ and

$$\psi(x) = x^{-3}\sin x - x^{-2}\cos x\,; \qquad \varphi(x) = x^{-1}\sin x - 3\psi(x)\,. \tag{3.31}$$

Finally we substitute the values (3.28) for Λ_u' and express the nucleon spin and isotopic spin operators in terms of the conventional two-nucleon operators $\boldsymbol{\sigma}_1\cdot\boldsymbol{\sigma}_2$, $\boldsymbol{\tau}_1\cdot\boldsymbol{\tau}_2$, S_{12}. The result is

$$U_{11}' = -3f_r^2\pi^{-2}\mu^{-2}\sum_u\sum_x A_u^x(r)\xi_u^x\,. \tag{3.32}$$

The integrals A_u^x and the spin and isotopic spin operators ξ_u^x are written out in Appendix B.

The only feature of U_{11}' not present in U_{11}'' is the product $\langle|fV_r^{1*}|s\rangle\langle s|V_q^{1*}|\rangle$; but its presence causes no difficulty formally because of Wick's relation

$\Lambda = \Lambda^{\dagger} = \Lambda^2$. The result for U''_{11} is

$$U''_{11} = -3f_r^2\pi^{-3}\mu^{-2}\sum_{x,u} B_u^x \xi_u^x . \tag{3.33}$$

The value of $W_{11}^{(2)}$ is

$$W_{11}^{(2)} = -3f_r^2\pi^{-3}\mu^{-2}\sum_{u,x} C_u^x \xi_u^x . \tag{3.34}$$

It is convenient to break $U_{12}^{(2)}$ into two parts

$$U_{12}^{(2)} = U'_{12} + U''_{12} \tag{3.35}$$

arising respectively from the parts δ_{ps} and $-(\omega_p^* - \omega_s)^{-1}\langle |fV_p^{1*}|s\rangle$ of $\langle |a_p^1|s\rangle$. Their values are

$$U'_{12} = -3f_r^2\pi^{-2}\mu^{-2}\sum_{u\,x} D_u^x \xi_u^x , \tag{3.36}$$

$$U''_{12} = -3f_r^2\pi^{-3}\mu^{-2}\sum_{u\,x} E_u^x \xi_u^x . \tag{3.37}$$

Finally the value of $W_{12}^{(2)}$ is

$$W_{12}^{(2)} = -3f_r^2\pi^{-3}\mu^{-2}\sum_{u\,x} F_u^x \xi_u^x . \tag{3.38}$$

The integrals B_u^x, C_u^x, D_u^x, E_u^x, F_u^x are given in Appendix B.

The second order potential is obtained by collecting its parts according to Eqs. (3.7), (3.12), (3.13), (3.21), (3.32-38). The result is

$$V^{(2)} = -3f_r^2\pi^{-3}\mu^{-2}\sum_{u\,x}(\pi A_u^x + B_u^x + C_u^x + \pi D_u^x + E_u^x + F_u^x)\xi_u^x + \text{H. c.} \tag{3.39}$$

4. – Remarks.

At the time of writing the integrals A_u^x etc., which appear in the second order potential, have not been evaluated numerically, and the potential cannot therefore be compared with experiment. In this evaluation, considerable simplification is effected by the use of the effective range approximation. This is valid, because as long as the nucleon separation is large compared to the extension of each nucleon, the exchanged mesons which contribute significantly to the potential have energies low compared to the cut-off energy. This means that in the factors $(\omega_p^* - \omega_s)$ etc., in the denominators of B_u^x, E_u^x, F_u^x, Eqs. (B.2), (B.5), (B.6), the dependence on the exchanged mesons p and q can be neglected compared to the dependence on the meson s which is not exchanged. Then these triple integrals each factors into three simple integrals. In A_u^x and D_u^x,

Eqs. (B.1) and (B.4), one can replace g_u by its effective range value [6],

$$[g_u(\omega_q)]_{EF} = \lambda_u q^3/\mu^2\omega_q(1 - \omega_q/\omega_u - i\lambda_u q^3\mu^{-2}\omega_q^{-1}) , \tag{4.1}$$

where ω_u is the resonance energy. The λ_u are given by WICK.

With a view to comparing our « Chew-Low » potential more readily with others we examine it in the Born approximation. We drop the scattered parts $(\omega_p - H)^{-1} f V_p |\rangle$ of the one-meson-one-nucleon states $p\rangle = \{a^* + (\omega_p - H)^{-1} f V_p\} |\rangle$. The first order, one-meson-exchange, potential $V^{(1)}$ is unaffected. In the second order potential $V^{(2)}$ the surviving terms are

$$V_B^{(2)} = U'_{11} + U'_{12} + \text{H. c.} \tag{4.2}$$

In these terms g_u is replaced by its Born approximation value (WICK, (6.8′))

$$[(g_u(\omega_q)]_B = \lambda_u q^3/\mu^2\omega_q . \tag{4.3}$$

However for our purpose it is simpler to take the Born approximation of U'_{11} and U'_{12} before transforming to spherical co-ordinates, e.g. in Eq. (3.22) in the case of U'_{11}. We find

$$\begin{aligned} V_B^{(2)} = f_r^4 \sum_{pq} \left[- \frac{V_q^{1*} V_p^{1*} V_p^2 V_q^2}{\omega_p^2(\omega_p + \omega_q)} + \frac{V_p^{1*} V_q^{1*} V_p^2 V_q^2}{\omega_p^2(\omega_p + \omega_q)} \right] \exp[i(\boldsymbol{p} + \boldsymbol{q})\cdot\boldsymbol{r}] + \\ + f_r^4 \sum_{pq} \left[- \frac{V_q^{1*} V_p^1 V_p^2 V_q^{2*}}{\omega_p^2 \omega_q} + \frac{V_p^{1*} V_q^1 V_p^2 V_q^{2*}}{\omega_p^2 \omega_q} \right] \exp[i(\boldsymbol{p} - \boldsymbol{q})\cdot\boldsymbol{r}] + \text{H.c.} \end{aligned} \tag{4.4}$$

This should be compared with the second order Brueckner-Watson terms

$$\begin{aligned} V_{BW}^{(2)} = f_r^4 \sum_{pq} \left[- \frac{V_q^{1*} V_p^{1*} V_p^2 V_q^2}{\omega_p^2(\omega_p + \omega_q)} - \frac{V_p^{1*} V_q^{1*} V_p^2 V_q^2}{\omega_p \omega_q(\omega_p + \omega_q)} \right] \exp[i(\boldsymbol{p} + \boldsymbol{q})\cdot\boldsymbol{r}] + \\ + f_r^4 \sum_{pq} \left[- \frac{V_q^1 V_p^{1*} V_p^2 V_q^{2*}}{\omega_p^2(\omega_p + \omega_q)} - \frac{V_q^1 V_p^{1*} V_p^2 V_q^{2*}}{\omega_p \omega_q(\omega_p + \omega_q)} \right] \exp[i(\boldsymbol{p} - \boldsymbol{q})\cdot\boldsymbol{r}] + \text{H.c.} \end{aligned} \tag{4.5}$$

Between the terms of $V_B^{(2)}$ and $V_{BW}^{(2)}$ there are discrepancies of signs, denominators, and ordering of the V factors.

In resolving this disagreement let us consider a naive perturbation calculation in which $\mathcal{H} = \mathcal{H}^1 + \mathcal{H}^2$ of (2.1) is the perturbation, but using the renormalized coupling constant. To terms of fourth degree ordinary per-

(6) G. CHEW, M. GOLDBERGER, F. LOW and Y. NAMBU: *Phys. Rev.*, **106**, 1337 (1957).

turbation theory gives for the lowest energy eigenvalue

$$E = -\sum_n{}' \frac{\mathcal{H}_{0n}\mathcal{H}_{n0}}{E_n} - \sum_{nml}{}' \frac{\mathcal{H}_{0n}\mathcal{H}_{nm}\mathcal{H}_{ml}\mathcal{H}_{l0}}{E_n E_m E_l} + \sum_{nm}{}' \frac{\mathcal{H}_{0n}\mathcal{H}_{n0}\mathcal{H}_{0m}\mathcal{H}_{m0}}{E_n^2 E_m}. \tag{4.6}$$

The even terms only are retained in the expansion, since the perturbation changes the number of mesons by 1, an odd number. We now drop terms in which a meson is emitted or absorbed by the same nucleon; such terms either contribute to the self energy or else are higher degree corrections to a lower order potential, and presumably taken into account by the use of f^r in place of f. The first term on the right of (4.6) then gives the standard first order potential. The second term gives the Brueckner-Watson second order potential $V_{BW}^{(2)}$. The third term is

$$V_P^{(2)} = f_r^4 \sum_{pq} \frac{V_p^{1*} V_q^{1*} V_p^2 V_q^2}{\omega_p^2 \omega_q} \exp[i(\boldsymbol{p}+\boldsymbol{q})\cdot\boldsymbol{r}] + f_r^4 \sum_{pq} \frac{V_p^{1*} V_q^1 V_p^2 V_q^{2*}}{\omega_p^2 \omega_q} + \text{H.c.}\,. \tag{4.7}$$

This term $V_P^{(2)}$ is just what must be added to $V_{BW}^{(2)}$ to give our Born approximation potential $V_B^{(2)}$.

The fact that in the Born approximation our result reduces to the perturbation result rather than to the Brueckner-Watson formula is perhaps gratifying in the light of the analysis of FELDMAN (7). Using a Tamm-Dancoff type approximation he found that the neglect by BRUECKNER and WATSON of $V_P^{(2)}$ is unjustified.

The success of the two-nucleon potential of GARTENHAUS (1) now seems to be fortuituous. Apart from this neglect of $V_p^{(2)}$, he uses the Born approximation $[g_u]_B$ for g_u, following BRUECKNER and WATSON; comparison with the more accurate $[g_u]_{EF}$ shows that in the $u = 3$, or (3,3), state he neglects altogether the well-known resonance which dominates the picture at low energies. Similar remarks can be made about the Brueckner-Watson type calculations of the Λ-nucleon potential by DALLAPORTA and FERRARI (2) and by LICHTENBERG and ROSS (3), and about the estimate of three-nucleon forces by BRUECKNER, LEVINSON and MAHMOUD (8).

When this work was completed, the author's attention was drawn to a footnote in a paper by MIYAZAWA (9) to the effect that the Wick-Chew-Low method has been applied to the nuclear force problem by S. Sato.

---

(7) D. FELDMAN: *Phys. Rev.*, **98**, 1456 (1955).
(8) K. BRUECKNER, C. LEVINSON and H. MAHMOUD: *Phys. Rev.*, **95**, 217 (1954).
(9) H. MIYAZAWA: *Phys. Rev.*, **104**, 1741 (1956).

5. – Other applications.

The static approximation, used in this paper, can be regarded as the zero-order Born-Oppenheimer approximation, in which the meson field replaces the electron as the « light particles ». The first order correction then gives a velocity dependent « potential » ([10])

$$-M^{-1}\varphi^*(\nabla_r\varphi)\cdot\nabla_r\,. \tag{5.1}$$

Here M is the nucleon mass and r the nucleon co-ordinates. φ is the state of the meson field and depends parametrically on r. Care must be taken in applying the methods of this paper to the evaluation of (5.1), since we have not shown that it leads to the correct meson state φ. However the following prescription is correct: use ordinary perturbation theory with $\mathcal{H}$, Eq. (2.6) as the perturbation to determine the state φ; but for φ^* use the Hermitian conjugate of the state constructed using as the perturbation instead of $\mathcal{H}$ its Hermitian conjugate $\mathcal{H}^*$ in which each nucleon can emit rather than absorb the mesons of the other. The proof is similar to that employed in Appendix A in connection with the static potential. The author is investigating (5.1) for a possible spin-orbit force.

The present method is immediately applicable to three-nucleon forces. One simply couples each nucleon to its own meson field and allows each to absorb the meson emitted by the others.

The methods of this paper can be applied to the Λ-nucleon potential. For convenience regard the Λ-particle and $\Sigma^{+,0}$-particles as four states of the same hyperon. Define a Hermitian operator $\boldsymbol{\nu}$, a vector in isotopic spin space, which links Λ and Σ-states as follows:

$$(\nu_1 \pm i\nu_2)\Lambda = \mp\, 2^{\frac{1}{2}}\,\Sigma^{\pm}; \qquad \nu_3\Lambda = \Sigma^0\,. \tag{5.2}$$

Then the Λ-pion coupling Hamiltonian takes the same form as that for nucleon pion coupling, except that $\boldsymbol{\nu}$ replaces $\boldsymbol{\tau}$. The whole development then proceeds as before. It is necessary to neglect the Σ-Λ mass difference in order that the analogue of the Low equation for the energy dependence of the transition matrix element separate from the equation for the dependence on internal hyperon variables, etc. The Σ^--Λ mass difference should be retained, however, in the zero-order potential matrix. This procedure amounts to neglecting the nass difference compared to the pion mass, but not compared to the potential itself. At the end a second degree secular equation must be solved to deter-

([10]) L. I. Schiff: *Quantum Mechanics.*

mine, for a given Λ-nucleon state, the amount of admixture of the Σ-nucleon state of the same spin and isotopic spin.

* * *

The author expresses his appreciation to P. T. Matthews for helpful discussions, and to Prof. Salam and others for the hospitality extended to him at Imperial College. His thanks are due to the Nuffield Foundation for the grant of a Dominion Travelling Fellowship.

Appendix A

We wish to show that the Hamiltonians (2.1) and (2.4) lead to the same potential. For this purpose consider $\mathcal{H} = \mathcal{H}^1 + \mathcal{H}^2$ in (2.1) as a perturbation. Then using the Brillouin-Wigner form of perturbation theory, the perturbed energy eigenvalue is given by the implicit equation

$$E = \sum_n{}' \frac{\mathcal{H}_{0n}\mathcal{H}_{n0}}{E - E_n} + \sum_{nml}{}' \frac{\mathcal{H}_{0n}\mathcal{H}_{nm}\mathcal{H}_{ml}\mathcal{H}_{l0}}{(E - E_n)(E - E_m)(E - E_l)} + \cdots . \tag{A.1}$$

See for example Wick's similar discussion of the one-nucleon self-energy. Only even degree terms contribute to the expansion. The terms of degree $2s$, which correspond to the creation and annihilation of s mesons, can be written

$$\sum_{p,\alpha,\beta} \sum_P \frac{V^{\alpha_s}_{p_s} V^{\beta_s *}_{p_s} \cdots V^{\alpha_1}_{p_1} V^{\beta_1 *}_{p_1}}{\prod_i (E - E_i)} \exp\left[i \sum_j \varepsilon_{\beta_j \alpha_j \gamma} \boldsymbol{p}_j \cdot \boldsymbol{r}_j \right] . \tag{A.2}$$

$\sum_P$ is a sum over all permutations of the operators $V^{\alpha_s}_{p_s} \cdots V^{\beta_1 *}_{p_1}$ in which each emission operator stands on the right of the corresponding absorption operator, and in which each intermediate state contains at least one meson. α_1, β_1, etc. are simply 1 or 2; $\prod_i (E - E_i)$ is the usual product over the $2s - 1$ intermediate states; ε is the Levi-Civita permutation symbol.

In (2.4) we may similarly consider $\mathcal{H}' = \mathcal{H}'^1_1 + \mathcal{H}'^2_2 + \mathcal{H}'^1_2 + \mathcal{H}'^2_1$ as a perturbation. The equation for E again takes the form (A.1) with the individual terms again given by (A.2). Hence the two Hamiltonians lead to the same potential.

A minor difference in the two cases is that different numerical factors arise whenever there are more than one meson with the same charge and momentum; but the relative amplitude of such states is negligible when the normalization volume tends to infinity.

Appendix B

These are the integrals which appear in the formulas in the text for the second order potential:

$$A_u^x(r) = \int \mathrm{d}p\,\mathrm{d}q\,\frac{\Psi^x v^2(p)v^2(q)pq^4 g_u(\omega_p)}{\omega_p^2\omega_q(\omega_p+\omega_q)}\,, \tag{B.1}$$

$$B_u^x(r) = \int \mathrm{d}p\,\mathrm{d}q\,\mathrm{d}s\,\frac{\Psi^x v^2(p)v^2(q)p^4q^4v^2(s)\,|\,g_u(\omega_s)\,|^2}{s^2\omega_s^2\omega_q(\omega_p^*-\omega_s)(\omega_s+\omega_q)\omega_p}\,, \tag{B.2}$$

$$C_u^x(r) = \int \mathrm{d}p\,\mathrm{d}q\,\mathrm{d}s\,\frac{\Psi^x v^2(p)v^2(q)p^4q^4v^2(s)\,|\,g_u(\omega_s)\,|^2}{s^2\omega_s^2\omega_p^2\omega_q^2}\,, \tag{B.3}$$

$$D_u^x(r) = \int \mathrm{d}p\,\mathrm{d}q\,\frac{\Psi^x v^2(p)v^2(q)pq^4 g_u(\omega_p)}{\omega_p^2\omega_q^2}\,, \tag{B.4}$$

$$E_u^x(r) = \int \mathrm{d}p\,\mathrm{d}q\,\mathrm{d}s\,\frac{\Psi^x v^2(p)v^2(q)p^4q^4v^2(s)\,|\,g_u(\omega_s)\,|^2}{s^2\omega_s^2\omega_p\omega_q^2(\omega_p^*-\omega_s)}\,, \tag{B.5}$$

$$F_u^x(r) = \int \mathrm{d}p\,\mathrm{d}q\,\mathrm{d}s\,\frac{\Psi^x v^2(p)v^2(q)p^4q^4v^2(s)\,|\,g_u(\omega_s)\,|^2}{s^2\omega_s^2\omega_p^2\omega_q(\omega_q+\omega_s)}\,. \tag{B.6}$$

$\Psi^x \equiv \Psi^x(pr, qr)$ stands for

$$\Psi^1 = \psi(pr)\psi(qr)\,, \tag{B.7}$$

$$\Psi^2 = \psi(pr)\varphi(qr) + \varphi(pr)\psi(qr)\,, \tag{B.8}$$

$$\Psi^3 = \varphi(pr)\psi(qr)\,. \tag{B.9}$$

The spin and isotopic spin operators ξ_u^x in the second order potential are given by

$$\xi_1^1 = 1 - \tfrac{2}{3}\boldsymbol{\tau}_1\cdot\boldsymbol{\tau}_2 + \boldsymbol{\sigma}_1\cdot\boldsymbol{\sigma}_2\{-\tfrac{2}{3} + (4/9)\boldsymbol{\tau}_1\cdot\boldsymbol{\tau}_2\}\,, \tag{B.10}$$

$$\xi_2^1 = 4 - \tfrac{2}{3}\boldsymbol{\tau}_1\cdot\boldsymbol{\tau}_2 + \boldsymbol{\sigma}_1\cdot\boldsymbol{\sigma}_2\{-\tfrac{2}{3} - (8/9)\boldsymbol{\tau}_1\cdot\boldsymbol{\tau}_2\}\,, \tag{B.11}$$

$$\xi_3^1 = 4 + (4/3)\boldsymbol{\tau}_1\cdot\boldsymbol{\tau}_2 + \boldsymbol{\sigma}_1\cdot\boldsymbol{\sigma}_2\{(4/3) + (4/9)\boldsymbol{\tau}_1\cdot\boldsymbol{\tau}_2\}\,, \tag{B.12}$$

$$\xi_1^2 = \tfrac{1}{3} - (2/9)\boldsymbol{\tau}_1\cdot\boldsymbol{\tau}_2 + \boldsymbol{\sigma}_1\cdot\boldsymbol{\sigma}_2\{(-2/9) + (4/27)\tau_1\cdot\tau_2\} + \\ + S_{12}\{(1/9) - (2/27)\boldsymbol{\tau}_1\cdot\boldsymbol{\tau}_2\}\,, \tag{B.13}$$

$$\xi_2^2 = (4/3) - (2/9)\boldsymbol{\tau}_1\cdot\boldsymbol{\tau}_2 + \boldsymbol{\sigma}_1\cdot\boldsymbol{\sigma}_2\{(-2/9) - (8/27)\tau_1\cdot\tau_2\} + \\ + S_{12}\{(1/9) + (4/27)\boldsymbol{\tau}_1\cdot\boldsymbol{\tau}_2\}\,, \tag{B.14}$$

$$\xi_3^2 = (4/3) + (4/9)\boldsymbol{\tau}_1\cdot\boldsymbol{\tau}_2 + \boldsymbol{\sigma}_1\cdot\boldsymbol{\sigma}_2\{(4/9) + (4/27)\tau_1\cdot\tau_2\} + \\ + S_{12}\{(-2/9) - (2/27)\boldsymbol{\tau}_1\cdot\boldsymbol{\tau}_2\}\,, \tag{B.15}$$

$$\xi_1^3 = \tfrac{1}{3} - (2/9)\boldsymbol{\tau}_1\cdot\boldsymbol{\tau}_2\,, \tag{B.16}$$

$$\xi_2^3 = (4/3) - (2/9)\boldsymbol{\tau}_1\cdot\boldsymbol{\tau}_2\,, \tag{B.17}$$

$$\xi_3^3 = (4/3) + (4/9)\boldsymbol{\tau}_1\cdot\boldsymbol{\tau}_2\,. \tag{B.18}$$

RIASSUNTO (*)

Si deriva il potenziale fra due nucleoni nel quadro della teoria del cut-off statico del pione di Chew e Low. A meno di approssimazioni implicite nell'hamiltoniana originale il potenziale di scambio per un mesone è esatto e si accorda, per esempio, con quello di Brueckner e Watson. Nel potenziale di scambio fra due mesoni gli effetti di scattering si trattano con l'approssimazione di un mesone di Chew e Low. Il risultato si esprime in termini di integrali della soluzione dell'equazione di Low. Questo procedimento è indicato per l'applicazione del metodo ad alcuni effetti non adiabatici sul potenziale fra due nucleoni, al potenziale del nucleone Λ, e alla forza agente fra tre nucleoni.

(*) *Traduzione a cura della Redazione.*

The Zenithal Distribution of the Cosmic Ray Neutrons in the High Energy Range.

M. Cervasi Fidecaro (*), G. Fidecaro (*), G. Marini and L. Mezzetti

Istituto di Fisica dell'Università - Roma
Istituto Nazionale di Fisica Nucleare - Sezione di Roma

(ricevuto il 28 Gennaio 1958)

Summary. — The zenith angle distribution of cosmic ray neutrons in the energy range $\gtrsim 10$ GeV has been measured at an altitude of 3500 m above sea level (679 g cm^{-2}) by means of a penetrating shower detector associated with a large area Geiger counter hodoscope. The penetrating showers were generated in thin layers of paraffin and graphite. The instrumental bias and the sistematic errors in the determination of the angles are discussed, and corrections applied whenever possible. The corrected distribution is well approximated with a law of the type $\exp[-m/\cos\theta]$ with $m = 7.1 \pm 1.3$, in agreement with the results of Walker. The discussion shows that this value has to be considered as a lower limit for the true m and is therefore difficult to reconcile with the assumption that the zenithal distribution is due solely to the absorption of the particles of the nuclear cascade in the atmosphere, with a mean free path $\lambda_a = 130$ g cm^{-2} as determined by several authors. From the hodoscope information the angular distribution of ionizing secondaries around the direction of the primary neutron in also calculated. The distributions obtained for penetrating showers produced in carbon and in hydrogen are very similar. The analysis in terms of an isotropic distribution in the center of mass system of the incident neutron and a target nucleon yields an average energy of the observed events $\overline{E} = 24$ GeV. The experimental results on the zenithal distribution are compared with the distributions calculated with the theory of the nuclear cascade in the atmosphere, as developed by Budini and Molière. It is shown that the finite lifetime of some of the particles belonging to the N component can not account for the « anomalous » zenithal effect indicated by the measurements. It is suggested that the discrepancy may be removed with the choice of a value of the anelasticity parameter much greater than that assumed by Budini and Molière.

(*) Now at CERN, Geneva.

1949

1. – Introduction.

It is well known that the zenithal distribution of the different cosmic ray components can be related to the vertical absorption in the atmosphere. In the particular case of the nucleonic component, if the intensity at the angle θ and depth h, $I(\theta, h)$, has to satisfy the relation

$$I(\theta, h) = I(0, h/\cos\theta)\,, \tag{1}$$

the following assumptions must be true:

a) the primary radiation at the top of the atmosphere is isotropic;

b) the direction of the primary particles is retained through the processes of propagation of the nucleonic cascade;

c) the development of the cascade depends only on the quantity of matter traversed.

If the absorption is exponential, with a mean free path (m.f.p.) λ_a, the zenithal distribution is given by:

$$I(\theta, h) = \exp\left[-m/\cos\theta\right] \qquad \text{with } m = h/\lambda_a. \tag{2}$$

For small angles:

$$I(\theta, h) \cong \exp\left[-m\right] \cos^m\theta\,. \tag{2a}$$

A zenithal distribution in agreement with (1) will be called here « normal » or « by pure absorption ».

Several experiments have been reported to check the validity of (1) in the case of the nucleonic component. The results can be roughly divided in two groups, according to the energy, and therefore to the extent to which the hypothesis *b*) and *c*) are fulfilled.

At low energy ($\lesssim 1$ GeV) the measurements show a tendency towards zenithal distributions broader than that given by (1) because of the non-negligible angular spread in the propagation of the nucleonic cascade through the atmosphere ([1-4]).

On the other hand, at higher energies, where the conservation of the primary direction is more fully respected, hypothesis *c*) is expected to break down

([1]) M. Conversi and P. Rothwell: *Nuovo Cimento*, **12**, 191 (1954).
([2]) C. Baccalin, P. Bassi and C. Manduchi: *Nuovo Cimento*, **1**, 657 (1955).
([3]) E. Lohrmann: *Nuovo Cimento*, **1**, 1126 (1955).
([4]) K. W. Ogilvie: *Can. Journ. Phys.*, **34**, 1081 (1956).

because of the presence of unstable particles in the nucleonic cascade. Particles having strong interaction and finite lifetime do not contribute anymore, after decaying, to the development of the nucleon shower, if their decay products have a negligible nuclear interaction. As a consequence, the apparent absorption m.f.p. becomes shorter in comparison to the case where all the particles have an infinite lifetime. This is the case with pions and some of the K-mesons. This effect is relatively more important at larger zenithal angles, where for the same geometrical length travelled by the particle before decaying, the quantity of matter traversed is smaller because of the atmospheric density being an increasing function of the depth.

One can therefore expect an « anomalous » zenithal effect, consisting in a zenithal distribution steeper than the one corresponding to (1). The « anomalous » zenithal effect depends in a complicated way on the development of the cascade. Qualitatively one expects it to be negligible when the ratio of the decay to the interaction m.f.p., λ_d/λ_i (which is a function of the energy) is either very large or very small.

Only rather few measurements on the zenithal distribution of the nucleonic component at energies > 10 GeV have been published ([5-8]). In spite of the difficulty of correcting these results for the instrumental effects, they seem to suggest, when compared with the now well established vertical absorption law, the existence of an « anomalous » zenithal effect. For this reason we thought it worthwhile to reanalyze from this point of view the results of a already published experiment ([9]). The measurements have been carried out with a detector of local penetrating showers, which looked particularly suited for the angular analysis required by the present problem because of the large size and the geometry of the counters and absorbers.

2. – Experimental apparatus and punched cards technique for the analysis of the experimental data.

The counters arrangement and the experimental conditions have already been described in I ([9]). The geometry of Geiger counters and absorbers is shown in Fig. 1. Each counter of the trays B and C is connected to a neon

([5]) J. R. Green: *Phys. Rev.*, **80**, 832 (1950).
([6]) W. D. Walker: *Phys. Rev.*, **77**, 686 (1950).
([7]) M. B. Gottlieb: *Phys. Rev.*, **82**, 349 (1951).
([8]) T. G. Stinchomb: *Phys. Rev.*, **83**, 422 (1951).
([9]) M. Cervasi Fidecaro, G. Fidecaro and L. Mezzetti: *Nuovo Cimento*, **1**, 300 (1955) (in the following quoted as I); *Suppl. Nuovo Cimento*, **4**, 873 (1956) (in the following quoted as II).

bulb and a picture is taken whenever a coincidence

$$P = A_0' A_{0,1} B_{\geq 1} C_{\geq 3} D_{\geq 3} E_{\geq 2} \quad (\text{« master » event})$$

is recorded.

Only the events $P^0 = A_0' A_0 B_{\geq 1} C_{\geq 3} D_{\geq 3} E_{\geq 2}$ for which no counter of the tray A has been discharged will be considered here. As it has been shown in I (9), they correspond, except for small efficiency corrections, to penetrating

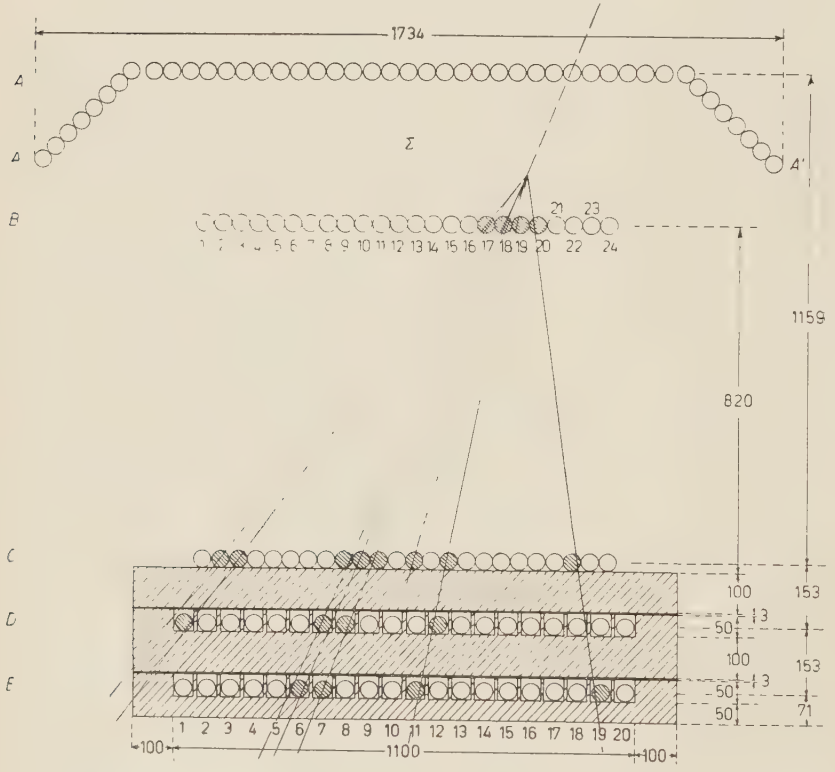

Fig. 1. – Sketch of the counters arrangement (front view).

showers generated in the interaction of incident neutral particles (neutrons) with the nuclei of the thin generator Σ. The measurements of interest in this analysis were taken alternating a paraffin and carbon generator, 18.1 and 16.2 g cm^{-2} respectively. The background was also measured with no material at all in Σ.

The measurements were performed at the Laboratorio della Testa Grigia (Aosta) at 3 500 m above sea level.

For the present analysis 23 000 pictures of the type P^0 obtained in a series of 55 runs have been used. The information was transferred to IBM cards, one card per event. The selections and calculations were performed by means of the machines kindly put at our disposal by the Istituto Nazionale per le Applicazioni del Calcolo.

All the cards went first through a series of internal consistency checks; severe criteria were applied, to be sure that counters and hodoscope had been working properly. Only one run in 55 was discarded on the basis of this check: this corresponds to 1% of the total number of events.

The co-ordinates X_B and X_C of the « center of mass » of the counters discharged in each event respectively in tray B and C were then calculated and punched on the card. The numbers X_B, X_C and $X_B - X_C$ are the basis of the geometrical analysis discussed in the next two sections. All the operations performed by the machines were again carefully checked to eliminate possible punching, calculation and selection mistakes. As a result, the residual errors were estimated to be absolutely negligible.

3·1. – Zenithal distribution of the primaries: geometrical analysis of the experimental data.

The projection α of the zenithal angle of the primary particle on a plane orthogonal to the axis of the Geiger counters will be called here « projected zenithal angle ». In order to evaluate this angle from the information punched on the cards the following schematizations have been used:

1) The direction of the primary particle is assumed to coincide in each event with the axis of the trajectories of the ionizing secondary particles. The error introduced in this way cannot be estimated without a complete knowledge of the kinematics of the event itself. It is easy to see, however, that with this criterium *one assignes to each primary, on the average, a zenithal angle larger than the true one.*

2) The axis of the secondary ionizing particles is assumed to coincide with the straight line through the « centers of mass » of the intersections of the trajectories with trays B and C. Also this criterium, as can be shown from trigonometrical considerations, *favours the inclined directions.*

According to 1) and 2) we shall in the following proceed as if the trajectory of the primary particle actually went through the telescope formed by the two « center of mass counters » in trays B and C. The number of telescopes to be found at a projected direction α, and the corresponding angular width $\Delta\alpha$ are, of course, functions of α. Taking into account the weight of each

angular interval, one can thus calculate from the experimental data the projected zenithal distributions $f(\alpha)$ corresponding to the different experimental conditions (no generators, paraffin generator, etc.).

The random coincidences between counters in tray B or C and the « master » event can introduce a serious error in the determination of the direction of the primary *for an individual event.* The probability of such a coincidence has been determined experimentally to be less than 4% all together. Because of the large average number of secondaries observed in a single event, one can easily recognize that the effect on the zenithal distribution of the primaries is negligible. *Anyway, also this effect would result in a broadening of the observed distribution, favouring again the more inclined directions.*

In order to minimize the instrumental bias on the determination of the direction of the primary, two types of selections have been performed:

a) Only events having the « center of mass » within the 12 central counters of tray C have been accepted. With this limitation, which has been chosen after a preliminary survey of the angular distribution of the secondary particles, the percentage of secondaries escaping the area covered by the counters of tray C is not larger than 20% *in the most unfavourable case*, and one can show that the error introduced in the determination of the angle α becomes negligible.

b) For similar reasons only events having the « center of mass » within the 20 central counters of tray B have been accepted.

About 15000 among the 23000 events examined satisfy conditions *a*) and *b*) at the same time. Of these events 7500 occured with paraffin, 6200 with graphite, 1300 with no generator at all (background) (*).

As already mentioned, the projected zenithal distribution per unit angular interval $\Delta\alpha$ and per unit horizontal area has been calculated separately for each of these three groups of events. All the distributions have been normalized to the same average pressure (679 g cm^{-2}), the barometric coefficient having been determined experimentally from the counting rates of the events P^0. The distributions of events with paraffin and graphite coincide within the experimental errors, and have been therefore added together. The background distribution has been subtracted from the resulting distribution. The validity and the limitations of the « difference » method have already been discussed in I [9], and the conclusions can be easily extended to the analysis of the angular distributions. The « difference » distribution $\bar{f}(\alpha)$ is interpreted as distribution of the primaries of the penetrating showers generated in Σ,

(*) The counting rate with the generators in place was about four times larger than the counting rate for background.

and is shown in Table I together with the distribution of the background events. If one approximates $\bar{f}(\alpha)$ with a law of the type $\exp[-\overline{m}/\cos\alpha]$, one obtains

$$\overline{m} = 8.5 \pm 1.3 .$$

TABLE I.

α degrees	$\bar{f}(\alpha)$ $\mathrm{min^{-1}\,cm^{-2}\,rad^{-1}}$	Background distribution $\mathrm{min^{-1}\,cm^{-2}\,rad^{-1}}$
0° 00′	$(0.594 \pm 0.034)\cdot 10^{-4}$	$(0.206 \pm 0.024)\cdot 10^{-4}$
3° 00′	(0.617 ± 0.026) »	(0.218 ± 0.017) »
6° 00′	(0.612 ± 0.024) »	(0.193 ± 0.017) »
8° 57′	(0.617 ± 0.023) »	(0.165 ± 0.016) »
11° 52′	(0.541 ± 0.024) »	(0.184 ± 0.016) »
14° 42′	(0.471 ± 0.024) »	(0.183 ± 0.017) »
17° 29′	(0.385 ± 0.024) »	(0.196 ± 0.017) »
20° 11′	(0.358 ± 0.024) »	(0.165 ± 0.017) »
22° 47′	(0.344 ± 0.024) »	(0.136 ± 0.016) »
25° 17′	(0.238 ± 0.027) »	(0.178 ± 0.020) »
27° 42′	(0.211 ± 0.027) »	(0.136 ± 0.019) »
30° 00′	(0.205 ± 0.032) »	(0.140 ± 0.020) »
32° 13′	(0.074 ± 0.039) »	(0.183 ± 0.027) »
34° 19′	(0.112 ± 0.049) »	(0.165 ± 0.029) »

3·2. – The zenithal distribution of the neutrons.

In order to find the zenithal distribution of the primary neutrons from the distribution $\bar{f}(\alpha)$ it is necessary to take into account:

1) The geometrical limitations due to the finite length of the counters.

2) The fact that, because of the inefficiency of the anticoincidence counter tray, the experimental distribution contains also a contribution from the charged primaries which is a function of the angle α.

3) The fact that the detection probability of a shower is for each energy a function of the relative position of the shower and the experimental apparatus.

Let $N_0(\theta, E)$ and $N_1(\theta, E)$ be the *differential* energy spectra of incident neutral and charged particles at the zenith angle θ (per unit solid angle); the following general relation can be written

$$(3) \qquad \bar{f}(\alpha)\sigma(\alpha)\Delta\alpha = \int_0^\infty dE \int_{\sigma(\alpha)} \int_{\Omega(\alpha,\Delta\alpha)} d\sigma_\perp \, d\Omega [N_0(E,\theta)P_0(R,\theta,\varphi;E) + N_1(E,\theta)P_1(R,\theta,\varphi;E)] ;$$

$d\sigma$ is the projection of the horizontal surface element $d\sigma$ (Fig. 2) normal to the trajectory of the primary particle. The meaning of the integration domains $\Omega(\alpha, \Delta\alpha)$ and $\sigma(\alpha)$ is evident from Fig. 2. It should be noted that the definition of Ω takes into account the finite length of the counters.

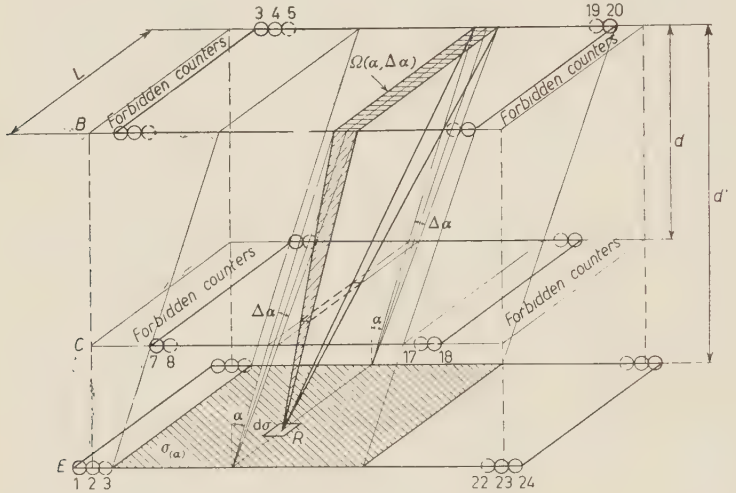

Fig. 2. – Geometrical schematization of the apparatus, for the evaluation of the integral in eq. (3). All the events for which the « center of mass » of the counters discharged in either of the trays B and C happened to fall within the strips indicated as « forbidden counters » were not accepted in the analysis.

The detection probabilities P_0 and P_1 are very complicated functions of the energy E of the incident particle, of its incidence point R on the apparatus and of its zenithal and azimuthal angles, and a complete calculation of (3) appears extremely difficult. A substantial simplification is obtained if one assumes that the detection probability may be written as the product of a function of the energy alone and a purely geometrical factor. For our apparatus, we write for convenience

$$P_0(R, \theta, \varphi; E) = \frac{s}{\lambda \cos\theta}\, p_0(R, \theta, \varphi) q_0(E)\,, \tag{4}$$

(and similarly for P_1), where s is the thickness of the generator and λ the corresponding interaction m.f.p.. The latter can very reasonably be considered as independent from the energy.

Eq. (3) becomes thus

$$\overline{f}(\alpha)\sigma(\alpha)\Delta\alpha = \int_{\sigma(\alpha)} \int_{\Omega(\alpha,\,\Delta\alpha)} d\sigma_\perp\, d\Omega\, \frac{s}{\lambda \cos\theta} \left[J_0(\theta) p_0(R, \theta, \varphi) + J_1(\theta) p_1(R, \theta, \varphi)\right], \tag{5}$$

with

$$J_0(\theta) = \int_0^\infty \mathrm{d}E\, N_0(E, \theta) q_0(E)\,, \tag{6}$$

and similarly for $J_1(\theta)$. The distributions $J_0(\theta)$, $J_1(\theta)$ thus defined do not coincide, in general, with the « true » zenithal distributions discussed in Sect. **1**, but one can easily show that under sufficiently broad conditions the dependence from the angle θ is the same. In particular, if the differential spectra $N(E, \theta)$ satisfy eq. (1) for all values of E for which the « weight functions » $q(E)$ are appreciably different from zero, the same holds for the distributions $J(\theta)$ (*). In the following, we shall therefore refer to $J_0(\theta)$ and $J_1(\theta)$ briefly as zenithal distributions.

In order to simplify further the calculation of (5) the following hypotheses and approximations have been used:

a) The zenithal distribution of the charged primaries (mostly protons) is the same as that of neutral primaries (neutrons):

$$J_1(\theta) = (p/n) J_0(\theta)\,,$$

where p/n is the ratio of the total counting rates of protons and neutrons, as measured experimentally (see I [9]): $p/n = 1.3$.

b) The geometrical detection factor of the showers generated by charged primaries is related to the geometrical detection factor of the showers generated by neutral primaries by the relation:

$$p_1(R, \theta, \varphi) = I(\alpha)\, p_0(R, \theta, \varphi)\,,$$

where $I(\alpha)$ ($\ll 1$) represents the inefficiency of the anticoincidence tray as a function of α, and has been calculated taking into account the geometry of the counters and the results of direct measurements of the integrated inefficiency. With this hypothesis (5) becomes:

$$\bar{f}(\alpha)\sigma(\alpha)\Delta\alpha = (1 + (p/n) I(\alpha)) \int_{\sigma(\alpha)} \int_{\Omega(\gamma, \Delta\alpha)} \mathrm{d}\sigma_\perp \mathrm{d}\Omega \frac{s}{\lambda \cos\theta} J_0(\theta) p_0(R, \theta, \varphi)\,. \tag{7}$$

c) The detection factor $p_0(R, \theta, \varphi)$ is a constant r for all the points R and the values of θ and φ, satisfying the geometrical selections set by the

(*) It should be noted that this result is strongly dependent upon the validity of the basic assumption about the detection probability, eq. (4).

apparatus and by the analysis of the data (and represented by the limits of integration), and zero for all the other values. This hypothesis is certainly not true, and has been introduced for the sake of simplicity. However, it is justified by the reasonable assumption that, *within the limits of integration and for the present experimental arrangement*, p_0 is a monotonically increasing function of the angle θ. This assumption is not contradicted by the results of HODSON ([10]), who finds experimentally a decreasing p_0, because his geometry is quite different form ours. In the present case p_0 increases with θ because the average lateral spread of the particles generated in Σ is quite smaller than the size of the detector (in Hodson's case the situation is reversed): it follows that the number of counters hit by the shower particles in each tray of the detector is on the average an increasing function of the angle θ. The absorption of the secondaries acts on p_0 in the opposite direction but is not likely to compensate for the geometrical effect because of the high energy of the observed events. *The more inclined directions are thus favoured once again by the assumption of a constant* $p_0 = r$.

With these hypotheses (7) becomes:

$$\bar{f}_0(\alpha) = \frac{f(\alpha)}{1 + (p/n)I(\alpha)} = \frac{2sr}{\lambda} J_0(\alpha) G(\alpha) \,, \tag{8}$$

where $G(\alpha)$ is an integral depending on the geometrical parameters of the experimental arrangement and on the behaviour of $J_0(\theta)$.

If one approximates $J_0(\theta)$ with a law of the type $\cos^m \theta$ one gets for $G(\alpha)$ the explicit formula

$$G(\alpha) = \int_0^{\operatorname{tg}^{-1}(L\cos\alpha/\alpha)} \mathrm{d}x \cos^{m+1} x + \frac{1}{m+1} \frac{d}{L\cos\alpha} \left\{ \left(1 + \frac{L^2 \cos^2 \alpha}{d^2} \right)^{-(m+1)/2} - 1 \right\} . \tag{9}$$

This approximation is not the most appropriate one (a better choice would be a law of the type $\exp[-m/\cos\theta]$ (see Sect. 5)), but it simplifies the calculation of the factor $G(\alpha)$. One can show, taking into account the statistical weights of the experimental points, that the error thus introduced in the determination of m is small in comparison with the statistical uncertainty.

The parameter m in (9) has been determined with a successive approximation method. The first step consists in neglecting in (8) the effect of the finite length L of the counters, i.e. assuming $G(\alpha)$ as indipendent from α, and equal to its limit for $L \to \infty$. The method converges quickly and gives for m the value,

$$m = 7.1 \pm 1.3 \tag{10}$$

([10]) A. L. HODSON: *Proc. Phys. Soc.*, A **65**, 702 (1952).

and for the vertical intensity the value

$$rJ_0(0) = (2.97 \pm 0.05) \cdot 10^{-4} \text{ min}^{-1} \text{ cm}^{-2} \text{ sr}^{-1}, \tag{11}$$

where r represents the average geometrical factor already defined. The experimental values of $rJ_0(\theta)$ thus obtained are shown in Fig. 3.

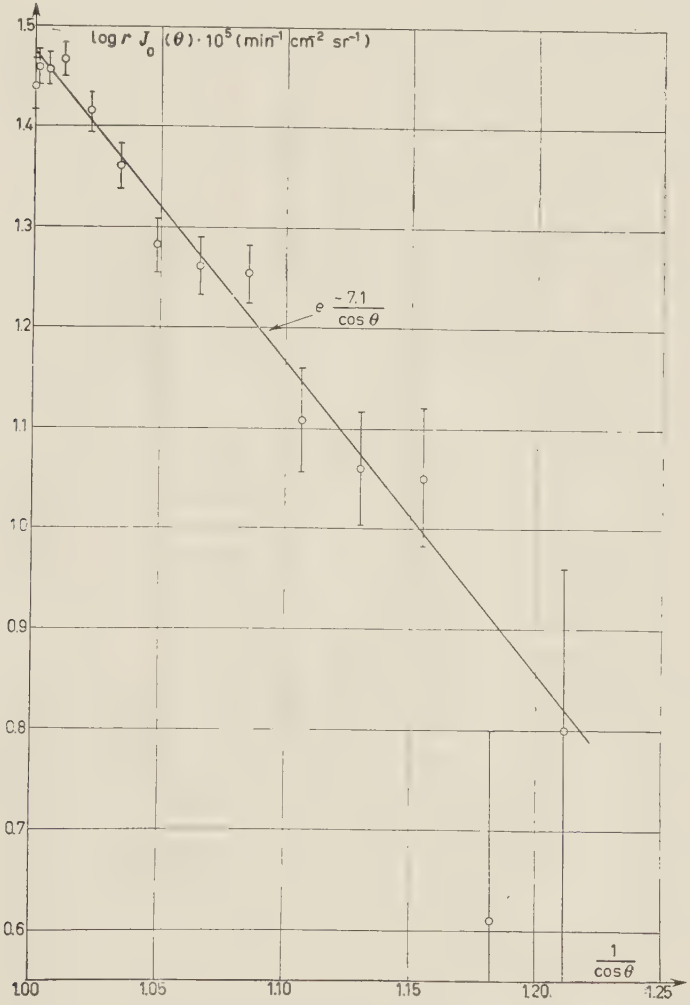

Fig. 3. – Corrected zenithal distribution of the neutral primaries of the observed events.

As already mentioned, it is rather difficult to evaluate quantitatively the effect of the various assumptions made in the preceding analysis. However, the systematic errors connected with the empirical definition of the angle α and the assumptions about the efficiency of the detector, all favour the more

inclined directions. *The value* (10) *obtained for the exponent of the zenithal distribution has therefore to be considered as a lower limit.*

A neutron (or a proton) of high energy is generally associated with an atmospheric shower, whose electrons may discharge one or more counters in tray A. The probability for this to happen is on the average proportional to the projection of the area of tray A on the front of the electronic shower. Thus, the requirement that no anticoincidence counter be discharged favours again the more inclined directions.

3·3. – Zenithal distribution of the neutrons: discussion.

The zenithal distribution of the neutral primaries obtained here is in good agreement with the results of WALKER (6) who finds for the cosine law, at a similar altitude and with selection criteria rather close to the ones used here, $m = 7.0 \pm 1.2$. Larger values of m were obtained by GREEN (5), STINCHCOMB (8) and GOTTLIEB (7), but it is hard to make a comparison without knowing all the details about the instrumental selections and the criteria used to apply corrections.

As regards the absorption mean free path, from the barometric coefficient of our events we get

$$\lambda_a = (121 \pm 12) \text{ g cm}^{-2} \quad \text{(not corrected)} \ (*).$$

This is in agreement with the values previously obtained by several authors (for events in the range $(10 \div 50)$ GeV). A very accurate determination ((129 ± 2) g cm^{-2}) is due to HODSON (10), who discussed thoroughly the corrections to be applied to the result of his measurement ((118 ± 1.1) g cm^{-2}), in order to take into account the angular width of the apparatus and the dependence of the detection efficiency from the zenithal angle of the primary.

The only disagreement comes from the results of STINCHCOMB (8) and GOTTLIEB (7). This point has been discussed by DEUTSCHMANN (11) and it seems that the disagreement has to be attributed to very special experimental selections.

Inserting Hodson's value of λ_a in equation (2) (Sect. **1**) one gets, at the atmospheric depth h at which Walker's and our measurements were carried out

$$m = h/\lambda_a = 5.2 \ .$$

(*) This value is slightly different from the value obtained in I (9) where the neutral and charged primary measurements were considered together.

(11) M. DEUTSCHMANN, in W. HEISENBERG: *Kosmische Strahlung* (Berlin, 1953), p. 104.

The average value of Walker's and our measurements is

$$m = 7.1 \pm 0.8 .$$

As already pointed out the value of m given by equation (10) of the preceding section is almost certainly a lower limit, in the sense that because of the type of analysis applied to the experimental data (Sect. 3·1 and 3·2) systematic errors in the direction of decreasing m are certainly more likely than systematic errors in the opposite direction. We conclude therefore that the zenithal distribution of the nucleon component is not in agreement with the hypothesis of « pure absorption ».

Zenithal distributions in good agreement with the hypothesis of pure absorption have been obtained in experiments on extensive showers. The situation has been summarized and discussed by GREISEN ([12]). KRAYBILL ([13]) and GREISEN ([12]) have pointed out that the agreement (at sea level as well as at mountain altitude) proves that decay processes with mean life such that competition with nuclear absorption is possible are not very important in the development of extensive showers.

One has to be rather cautious in comparing the results of these experiments with those referring to the nucleonic component. What is generally measured in extensive shower experiments is the zenithal distribution of the shower axes, defined as the normals to the « fronts » of the electrons reaching the detection arrangement, as is particularly clearly apparent in the measurements of BASSI *et al.* ([11]). This distribution does not necessarily reproduce the zenithal distribution of the nucleon component of the shower and is determined at least partially by the absorption of the electrophotonic component. The two distributions would coincide in the limiting case of a close equilibrium between the two components, while they are independent in the other limiting case of an autonomous development of the electrophotonic component starting from the π^0's produced in the first nuclear interaction of the primary protons.

4. – Evaluation of the energy of the primaries and angular distribution of the secondaries.

In order to evaluate the average energy of the primaries of the penetrating showers recorded by a particular detector two different methods are usually applied.

([12]) K. GREISEN, in J. G. WILSON: *Progr. in Cosmic Ray Phys.*, vol. III (1956), p. 74.
([13]) H. L. KRAYBILL: *Phys. Rev.*, **93**, 1362 (1954).
([14]) P. BASSI, G. CLARK and B. ROSSI: *Phys. Rev.*, **92**, 441 (1953).

The first method has been mainly employed in counter experiments [15]. It is based on a comparison between the observed rate of penetrating showers and the rate calculated assuming a power law for the energy spectrum of the incident nucleons. The calculation implies, in general, also the knowledge of the zenithal distribution and some more or less arbitrary assumptions about the dependence of the detection probability of the penetrating showers from their energy and position in space relatively to the detector. In our case, following the discussion of Sect. 3·2, we get simply, from eq. (4), (6) and (11)

$$rJ_0(0) = \int_0^\infty \mathrm{d}E N_0(E, 0) r q_0(E) = 2.97 \cdot 10^{-4} \text{ min}^{-1} \text{ cm}^{-2} \text{ sr}^{-1} . \tag{12}$$

It is very difficult to assign *a priori* reasonable values to rq_0 as a function of E. Considering that $N_0(E, 0)$ is a rapidly decreasing function of E, qualitative arguments lead to the rather crude but not too unrealistic approximation

$$\begin{cases} rq_0(E) = 0 & \text{for } E < E_m, \\ rq_0(E) = a & \text{for } E \geqslant E_m, \end{cases} \tag{13}$$

but the actual value of a ($\leqslant 1$) can only be guessed. For a given value of a and a given value of the exponent of the energy spectrum one gets then from (12) and (13) the value of E_m, which in turn can be used to calculate the average energy required. The result is quite sensitive both to the value chosen for a and to the value of the exponent, as shown by the following numerical examples [16]

I) $$a = 0.5 , \quad N_0(E, 0) = 1.5 \cdot 10^{-4} \left(\frac{10}{E}\right)^{2.8} \text{min}^{-1} \text{ cm}^{-2} \text{ sr}^{-1} \text{ GeV}^{-1} ,$$

$$E_m = 12 \text{ GeV} , \quad \bar{E} = 27 \text{ GeV} ;$$

II) $$a = 0.5 , \quad N_0(E, 0) = 1.5 \cdot 10^{-4} \left(\frac{10}{E}\right)^{2.5} \text{min}^{-1} \text{ cm}^{-2} \text{ sr}^{-1} \text{ GeV}^{-1} ,$$

$$E_m = 14 \text{ GeV} , \quad \bar{E} = 42 \text{ GeV} ;$$

III) $$a = 1 , \quad N_0(E, 0) = 1.5 \cdot 10^{-4} \left(\frac{10}{E}\right)^{2.5} \text{min}^{-1} \text{ cm}^{-2} \text{ sr}^{-1} \text{ GeV}^{-1} ,$$

$$E_m = 23 \text{ GeV} , \quad \bar{E} = 68 \text{ GeV}.$$

---

[15] T. G. Walsh and O. Piccioni: *Phys. Rev.*, **80**, 619 (1950).

[16] The vertical neutron intensity $N_0(E, 0)$ has been taken from P. Budini and G. Molière, in W. Heisenberg: *Kosmische Strahlung* (Berlin, 1953), p. 384, with a correcting factor to account for the measured value of the ratio $p/n = 1.3$ (see I [9]).

1962

The second method is based on a comparison between the angular distribution of the secondaries, observed experimentally, and an *a priori* angular distribution in the center of mass system, transformed to the laboratory frame of reference. The energy of the primaries is then determined by the parameter γ of the Lorentz transformation. This method has been often applied to the analysis of high energy interactions in cloud chambers or emulsions. Among the others, DULLER and WALKER ([17]) and CASTAGNOLI *et al.* ([18]) have examined and discussed the assumptions of the method. For a complete discussion, one should refer to these papers.

In order to work out from the experimental data the angular distribution of the ionizing secondaries around the direction of the primary, the events were selected with criteria similar to the ones described in Sect. 3·1, but somewhat restricted according to a preliminary analysis: for instance, only events with « center of mass » in one of the 8 central counters (instead of 12) in tray *C*, have been accepted.

The schematization adopted is also rather similar to the one previously described (Sect. 3·1):

1) The direction of a primary (axis of the shower) is defined in the same way as in Sect. 3·1.

2) The origin of a shower is defined as the intersection of the axis of the shower with the median plane of the generator.

3) The direction of a secondary is determined by the origin of the shower and the counter discharged in tray *C*.

Fig. 4. shows the situation and the formulas used.

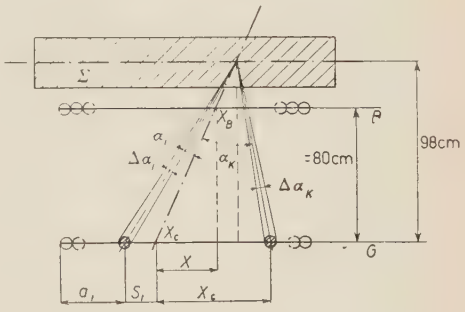

Fig. 4. – Simplified geometry and formulas used for the evaluation of the angular distribution of the secondaries.

It is clear that with these assumptions the information punched on each card gives the projection of the event on a plane π perpendicular to the axis of the Geiger counters. The projected experimental distribution should therefore be compared with the theoretical distribution projected on the same plane. Instead, it has been compared with the theoretical distribution projected on a plane contain-

([17]) N. M. DULLER and W. D. WALKER: *Phys. Rev.*, **93**, 215 (1954).

([18]) C. CASTAGNOLI, G. CORTINI, C. FRANZINETTI, A. MANFREDINI and D. MORENO: *Nuovo Cimento*, **10**, 1539 (1953).

ing the axis of the shower, as if the trajectories of the primary particles were all contained in the vertical plane π. The error is, however, entirely negligible on the average, because of the angular distribution of the primaries being strongly peaked downwards.

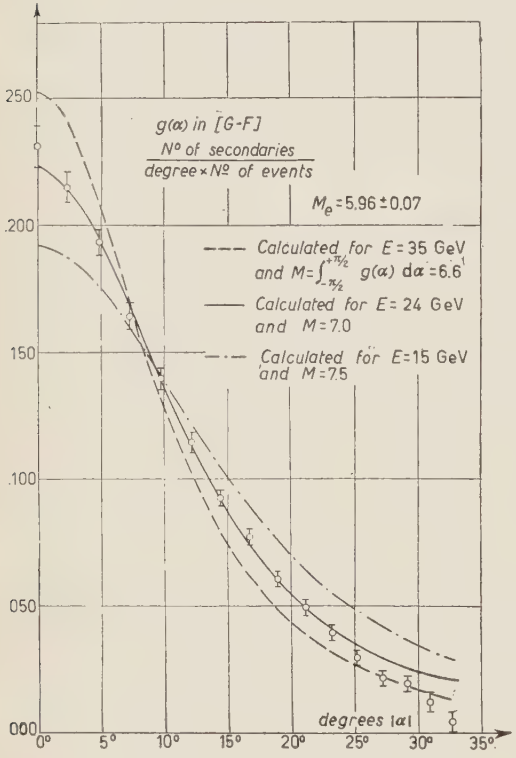

Fig. 5. – Projected angular distribution of charged secondaries from graphite. M_e = experimental multiplicity = average number of charged secondaries per event from $\alpha = 0°$ to $\alpha = \alpha_{max} = 33.5°$. The curves represent Lorentz transformations of an isotropic distribution in the center of mass of a nucleon-nucleon collision.

About 11000 events have been subjected to the punched card analysis. The results, corrected to take into account the finite size of the detector, are shown in Fig. 5 and 6. The curves represent the theoretical distribution

$$(14) \qquad g(\alpha) = K\gamma \frac{1 + \mathrm{tg}^2\,\alpha}{(1 + \gamma^2\,\mathrm{tg}^2\,\alpha)^{\frac{3}{2}}}$$

for a few values of the parameter γ. Equation (14) corresponds to an uniform angular distribution in the center of mass system, the velocity of the particles in the center of mass system being equal to the velocity of the center of mass in the laboratory.

Fig. 5 represents the distribution $(G\text{-}F)$ obtained subtracting from the angular distribution observed with graphite (G), the angular distribution observed without generator (F). Fig. 6 shows the distribution paraffin-graphite $(P\text{-}G)$: according to the « difference method » it represents the angular distribution of the secondaries of the showers generated in hydrogen (n-p collisions).

The normalization factor K in formula (14) has been determined in each case in such a way that the integral $\int_{\alpha_{max}}^{+\alpha_{max}} d\alpha\, g(\alpha)$ equals the average experimental « multiplicity » M_e, as found from the number of counters discharged in tray C:

$$M_e = 5.96 \pm 0.07 \text{ for showers generated in graphite,}$$

$$M_e = 4.9 \pm 0.3 \text{ for showers generated in hydrogen.}$$

These multiplicities are somewhat larger than those obtained in II ([9]) from the events P^0 without geometrical selections.

The curves calculated for $\gamma = 3.64$ (which corresponds to a kinetic energy of the incoming neutron $E = 24$ GeV) fit surprisingly well the experimental points. It seems therefore legitimate to assume as average energy of the primaries of penetrating showers detected by our apparatus the value obtained in this way. This value is in good agreement with the value estimated by DULLER and WALKER ([17]) and ASKOWITH and SITTE ([19]) from an analysis of cloud chamber events selected with criteria very similar to ours. It is also in agreement with the value found by BRENNER and WILLIAMS ([20]). WATASE *et al.* ([21]) have carried out a rough analysis of the lateral spread of the secondaries of the events detected by a counter arrangement rather similar to the present one, finding for showers generated by neutrons in carbon an average energy of 30 GeV. They also find a markedly different lateral spread for the showers generated by neutrons in hydrogen. This difference does not appear to be confirmed by the present experiment.

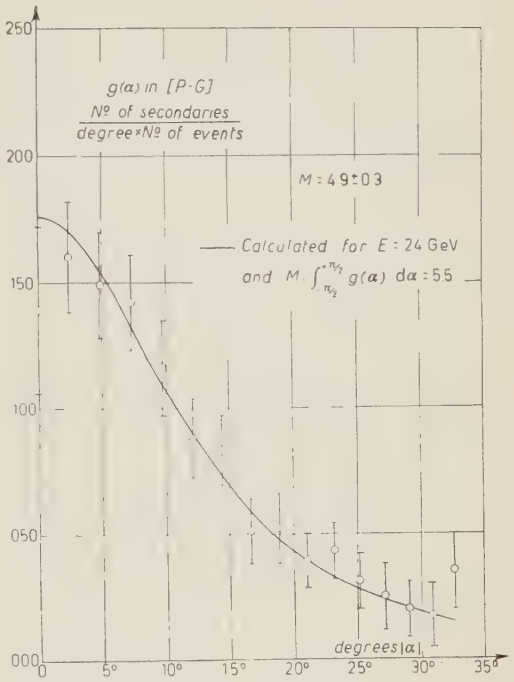

Fig. 6. – Projected angular distribution of charged secondaries from hydrogen.

5. – Theory of the nuclear cascade in the atmosphere and zenithal distribution.

According to the theory of the nucleonic cascade, developed by BUDINI and MOLIÈRE ([22]) the intensity of the « N » component of energy (E, dE) at a vertical depth $h = l\cos\theta$ is given by

$$n(E, l) = AE^{-(s+1)} \exp\left[-l(1 - m_p - \tfrac{2}{3}m_\pi)\right]\left(1 + \frac{lE}{C_\pi}\right)^{-\frac{s}{3}m_\pi c_\pi / E}, \qquad (15)$$

([19]) J. G. ASKOWITH and K. SITTE: *Phys. Rev.*, **97**, 159 (1955).

([20]) A. E. BRENNER and R. W. WILLIAMS: *Phys. Rev.*, **106**, 1020 (1957).

([21]) Y. WATASE, K. SUGA, Y. TANAKA and S. MITANI: *Nuovo Cimento*, **2**, 1183 (1955).

([22]) P. BUDINI and G. MOLIÈRE, in W. HEISEMBERG: *Kosmische Strahlung* (Berlin, 1953), pp. 367-412.

1965

if a power law is assumed for the energy spectrum of the primary protons at the top of the atmosphere.

The discussion of the assumptions and approximations used to derive equation (15) is to be found in the original paper by BUDINI and MOLIÈRE. We remind that s is the exponent of the integral primary spectrum and $m_{\nu} = m_{\nu}(s)$, $m_{\bar{\pi}} = m_{\bar{\pi}}(s)$ are the Mellin transforms of the differential spectra $f_{\nu}(E, E')$, $f_{\bar{\pi}}(E, E')$ of nucleons and pions of energy E generated by pions or nucleons of energy E'. $C_{\pi} = C_{\pi}^{0}/\cos\theta$, where C_{π}^{0} is a quantity (which has the dimension of an energy) proportional to the ratio μ_{π}/τ_{π} of the mass to the mean life of the unstable particles which partecipate to the cascade ($\pi^{\pm}$-mesons). The depths l, h are measured in units of the m.f.p. for nuclear interaction.

By definition the « N » component as given by (15) includes, in addition to all the nucleons, that fraction of the pions present at depth l which will interact in the next layers of atmosphere before decaying spontaneously. The component given by (15) cannot therefore be identified with the component which generates nuclear « local » interactions in a layer of condensed material.

The apparatus of Fig. 1 detects ideally only events generated by neutrons. In order to evaluate their intensity (*integral spectrum*) one has to calculate the numbers of nucleons of energy $> E$ generated by the « N » component at each depth $l' \leqslant l$, using (15) as « source » function

$$\mathcal{N}(E, l) = \int_{0}^{l} \mathrm{d}l' \int_{E}^{\infty} \mathrm{d}E' n(E', l') F_{\nu}(E, E') \exp\left[-(l - l')\right], \tag{16}$$

$F_{\nu}(E, E')$ is the integral spectrum of the generated nucleons. Introducing (15) into (16) and considering the decay factor $(1 + (l'E'/C_{\bar{\pi}}))^{-\frac{2}{3} m_{\pi} C_{\pi}/E'}$ as a slowly varying function of E' (*), one gets

$$\mathcal{N}(E, l) = AE^{-s} M_{\nu}(s - 1) \exp\left[-l\right] \int_{0}^{l} \mathrm{d}l' \exp\left[al'\right] \left(1 + \frac{l'E}{C_{\pi}}\right)^{-b/\cos\theta}, \tag{17}$$

where

$$a = m_{\nu} + \tfrac{2}{3} m_{\pi}\,; \qquad b = \tfrac{2}{3} m_{\pi} C_{\pi}^{0}/E\,.$$

$M_{\nu}(s - 1) = (1/s) m_{\nu}(s)$ is the Mellin transform of $F_{\nu}(E, E')$. Remembering $l = h/\cos\theta$, (17) can be easily written in the following way, which is convenient

(*) This approximation has already been used to deduce (15).

for the numerical calculation

$$(18) \qquad \mathcal{N}(E, h, \cos\theta) =$$

$$= \frac{A}{a} E^{-s} \frac{m_p(s)}{s} \exp\left[-(h+k)/\cos\theta\right] \binom{\cos\theta}{k}^{-b/\cos\theta} \int_{k/\cos\theta}^{(k+ah)/\cos\theta} dv \exp\left[v - \frac{b}{\cos\theta} \ln v\right].$$

where $k = aC_\pi^0/E$.

With the help of the mean value theorem, (18) can also be written

$$(19) \qquad \mathcal{N}(E, h, \cos\theta) =$$

$$= \frac{A}{a} E^{-s} \frac{m_p(s)}{s} \left(1 + \frac{\varepsilon ah}{k}\right)^{-b/\cos\theta} \exp\left[-h/\cos\theta\right](\exp\left[ah/\cos\theta\right] - 1).$$

ε is a number ($0 < \varepsilon \leqslant 1$) which depends on $\cos\theta$ and the other parameters of the problem (E, h, C_π^0, etc.). The factor

$$D = \left(1 + \frac{\varepsilon ah}{k}\right)^{-b/\cos\theta} = \left[(1 + \varepsilon/q)^q\right]^{-\frac{s}{5} m_\pi h/\cos\theta},$$

with $q = C_\pi^0/hE$, represents the effect of the decay of the unstable particles while the other two factors of (19) represent the effect of the multiplication and of the absorption. (19) is useful for the discussion of the limiting cases (f.i. $\tau_\pi \to 0$; $E \gg C_\pi^0/h$; etc.).

It should be noted that (17) depends on the mean life τ_π and on the mass μ_π of the unstable particles only through the ratio C_π^0/E, i.e. through the factor $\mu_\pi/\tau_\pi E$, where E is the minimum energy of the observed neutrons.

Equation (18) has been evaluated numerically using the same values of the parameters as used by BUDINI and MOLIÈRE

$$s = 1.6\,, \qquad m_p = 0.434\,, \qquad m_\pi = 0.071\,,$$

except for the interaction mean free path in air λ_i. For this we have put [23]

$$\lambda_i = 68 \text{ g cm}^{-2}\,.$$

which gives a better fit for the attenuation m.f.p. than the value $\lambda_i = 60$ g cm^{-2} used by BUDINI and MOLIÈRE. The vertical depth is in our case $h\lambda_i = 679$ g cm^{-2}.

([23]) B. ROSSI: *High-Energy Particles* (New York, 1952), p. 491.

As regards the unstable particles the following two assumptions have been used:

a) The unstable particles which partecipate to the nuclear cascade are $\pi^{\pm}$-mesons: $C_{\pi}^{0} = 128$ GeV.

b) The unstable particles have the same nuclear interaction as the pions, but have the mean life and the mass of the $K^{\pm}$-mesons: $C_{\pi}^{0} \to C_{K}^{0} = 1229$ GeV.

In both cases the minimum energy of the detected neutrons was assumed $= 10$ GeV: this value corresponds to an average energy of ~ 24 GeV (see Sec. 4) with $s = 1.6$.

It is easily shown that with these values of the parameters the integral in eq. (18) can be calculated to a very good approximation by expanding the logarithm in a power series near the upper limit of integration and neglecting the quadratic and higher order terms. The functions $J(\theta) = \mathcal{T}(E, h, \cos\theta)$ calculated in this way are all very well represented by the simple expression

$$J(\theta) \sim \exp\left[-\, m/\cos\theta\right], \tag{20}$$

with different values of m, corresponding to the assumptions about the unstable particles.

In the same way one gets the « normal » zenithal distributions

$$J^{(n)}(\theta) \equiv \mathcal{T}\left(E, \frac{h}{\cos\theta}, 1\right) \sim \exp\left[-\, m_n/\cos\theta\right]. \tag{21}$$

The results of the calculations are summarized in Table II. In the first row are values of the vertical absorption mean free path

$$\lambda_a = -\left\{\frac{1}{J\lambda_i}\,\frac{\partial J}{\partial h}\right\}_{\theta=0};$$

the values of m and m_n obtained with approximations (20) and (21) are shown in the second and third row, respectively.

TABLE II.

	$\tau = \infty$ $C^0 = 0$	π-mesons $C_{\pi}^{0} = 128$ GeV	K-mesons $C_{K}^{0} = 1228$ GeV	$\tau = 0$ $C^0 = \infty$
λ_a g cm^{-2}	131.2	125.3	121.9	120.2
m	5.18	5.48	5.58	5.65
m_n	5.18	5.42	5.57	5.65

1968

6. – Conclusions.

As it is well known, the theory of BUDINI and MOLIÈRE predicts fairly well the variation of the vertical intensity with depth, which for rather high energies turns out to be exponential with good approximation. The theoretical value of λ_a/λ_i is sensitive to the value of the exponent s of the primary spectrum: in the present calculations s has been chosen in such a way as to get a reasonable agreement between the experimental value of λ_a and the assumed « geometrical » value of λ_i. Table II shows that the unstable particles have a little, but not negligible effect.

The calculations, however, do not account for the existence of an appreciable anomalous zenithal effect, which should be represented by the difference between the values of m and m_n. In fact the theoretical value of m and the amount of « anomalous » effect depend also on the other parameters of the theory, and particularly on $m_{\pi}(s)$ i.e. on the inelasticity of the elementary collision (see [22], p. 390).

A better agreement with the experimental situation could be certainly obtained with a higher degree of inelasticity and a corresponding change in the numerical values of the other parameters (particularly the interaction path λ_i) to reproduce the correct value of λ_a.

A higher degree of inelasticity and correspondingly an interaction path in air $\sim 100\ \mathrm{g\ cm^{-2}}$ have been recently suggested by BRENNER and WILLIAMS [20] on the basis of some direct measurements of the cross-section for production of penetrating showers in iron, by nucleons of energy ~ 50 GeV.

A more accurate investigation, both theoretical and experimental, of the zenithal distribution of the N-component of cosmic rays appears therefore desirable, as an indipendent method to evaluate the inelasticity coefficient and the interaction cross-section at very high energies.

* * *

We are greatly indebted to Prof. M. PICONE, Director of the Istituto Nazionale per le Applicazioni del Calcolo of the C.N.R., for having put at our disposal the I.B.M. machines of his Institute for the punched card analysis of our data; and to the members of his staff for help and advise in the programming and operation of the machines.

RIASSUNTO

Con un rivelatore di sciami penetranti locali generati in paraffina e in grafite, associato ad un odoscopio di contatori di Geiger di grandi dimensioni, è stata determinata la distribuzione zenitale dei neutroni di energia $\gtrsim 10$ GeV della radiazione cosmica, a 3500 m s.l.m. (679 g cm^{-2}). Vengono discusse in dettaglio le selezioni e gli errori sistematici di origine strumentale, per alcuni dei quali risulta possibile calcolare le corrispondenti correzioni. La distribuzione così corretta risulta bene approssimata da una legge del tipo $\exp[-m/\cos\theta]$ con $m = 7.1 \pm 1.3$, in accordo con i risultati di Walker; la discussione mostra inoltre che questo valore va considerato come un limite inferiore, e risulta pertanto difficilmente conciliabile con l'ipotesi che la distribuzione zenitale sia determinata soltanto dall'assorbimento delle particelle della cascata nell'atmosfera, con c.l.m. $\lambda_a = 130$ g cm^{-2} come determinato da numerosi autori. Dalle informazioni fornite dall'odoscopio viene dedotta anche la distribuzione angolare dei secondari ionizzanti attorno alla direzione di incidenza del neutrone primario. Le distribuzioni ottenute per gli eventi generati in carbonio e in idrogeno sono molto simili. L'analisi in termini di una distribuzione isotropica nel sistema del baricentro dell'urto nucleone-nucleone fornisce per l'energia media degli eventi il valore $E = 24$ GeV. Le distribuzioni zenitali ottenute sperimentalmente sono poste a confronto con quelle che si deducono dalla teoria della cascata nucleonica nell'atmosfera sviluppata da Budini e Molière. Si dimostra che l'instabilità di alcune delle particelle che prendono parte alla cascata non è sufficiente a render conto dell'effetto zenitale « anomalo » indicato dalle misure. Si suggerisce che tale discrepanza possa essere eliminata mediante la scelta di un valore del parametro di analesticità molto maggiore di quello usato da Budini e Molière.

IL NUOVO CIMENTO Vol. IX, N. 1 1° Luglio 1958

Convergence of the S-Matrix (*).

D. R. Yennie (+) and S. Gartenhaus

Stanford University - Stanford, California

(ricevuto il 21 Febbraio 1958)

Summary. — An investigation is made of the convergence of the field-theoretic perturbation expansion of the elements of the S-matrix. For a theory characterized by a coupling linear in the boson field, it is established that if a cut-off is introduced in momentum space, then the transition amplitude for any given process over a finite-time interval, is bounded term by term by an exponential series. The extension of the method to interactions which are not linear, is, for several cases, also included. The implications of the result for theories without a cut-off is discussed from a qualitative point of view.

1. – Introduction.

Caianiello [1] in a series of papers has investigated the convergence of the field theoretic transition matrix as a power series in the unrenormalized coupling constant. For a finite time of interaction, he was able to show that if only a finite number of fermion normal modes F are coupled to the boson field, this power series has, at least, a finite radius of convergence. Caianiello's estimate of the region of convergence depends sensitively, of course, on the value of F and the time of interaction; in particular, as these quantities are increased indefinitely the region of convergence shrinks into the origin. The essential point of Caianiello's technique is that he was able to write the complete n-th order contribution in determinantal form and to place an upper

(*) Supported in part by the United States Air Force through the Office of Scientific Research, Air Research and Development Command.

(+) Now at the University of Minnesota.

(1) E. R. Caianiello: *Nuovo Cimento*, **10**, 223 (1956); see also previous references cited there.

1971

bound on this by Hadamard's inequality. In the present paper, the nth-order contribution will be studied more directly and it will be shown to have a substantially smaller upper bound than estimated originally by CAIANIELLO [2]. With this new upper bound, the series has an infinite radius of convergence: however, its rapidity of convergence decreases as either F or the time of interaction increases. Unfortunately, moreover, the bounds for the various terms given here are in terms of the unrenormalized coupling constant, and further, in a given order, the bound includes contributions from the vacuum-to-vacuum graphs, as well as from the diagrams of interest. The effect of the vacuum diagrams will be further discussed below, while the question of coupling-constant renormalization is not so readily amenable to detailed analysis. It would certainly be very decisive to be able to remove these two restrictions; attempts at such refinements have not met with success.

Other studies of this question of convergence have usually been of a more negative character in that arguments were presented to make plausible the divergence of special types of field theories. Thus, for example, RIDDEL [3] and HURST [4] showed that in n-th order, the number of diagrams [5] contributing to this order increases as $(n!)^3$ and that, thus, assuming negligible cancellations between diagrams, quantum electrodynamics diverges. Below, we shall present arguments that, on the contrary, this theory converges, under certain restrictions, and precisely because of a cancellation among Feynman diagrams. In another investigation, THIRRING [6] considered a theory with a cubic boson interaction and was able to show that in a certain energy region the S-matrix diverges for all values of the coupling constant. As will become evident shortly, a φ^3 interaction is completely dissimilar from a linear coupling between bosons and fermions because of the difference in statistics. Indeed, the latter is shown to converge while for the former, the methods employed here break down completely, resulting in no positive conclusions.

In Sect. 2, a proof of convergence for a particular class of field theories is presented together with a discussion of the extension of the method to slightly different cases. The results thus obtained are then applied in the following section to show that all elements of the S-matrix must have a zero somewhere in the complex g-plane. Finally, Sect. 4 is devoted to a less quantitative discussion of the implications of the results and also a discussion of the limitations inherent in the present method. Also included are several appendices which serve for a mathematical background.

---

[2] See however, A. BUCCAFURRI and E. R. CAIANIELLO: *Nuovo Cimento*, **8**, 170 (1958).

[3] R. J. RIDDEL jr.: *Phys. Rev.*, **91**, 1243 (1953).

[4] C. A. HURST: *Proc. Roy. Soc. London*, A **214**, 44 (1952).

[5] R. P. FEYNMAN: *Phys. Rev.*, **76**, 769 (1949).

[6] W. E. THIRRING: *Helv. Phys. Acta*, **26**, 33 (1953).

1972

2. – Proof of convergence.

As a prototype of field theories of interest, we shall consider an interaction between boson and fermion fields which, for reasons of simplicity, will be taken to be of the form of a linear scalar coupling. It will become evident below that the linearity of the coupling is an essential restriction while its form is immaterial. Specifically, we shall consider a non-local interaction given by the expression

$$H_{\mathrm{I}} = g\int \mathrm{d}\boldsymbol{x}\mathrm{d}\boldsymbol{x}'\mathrm{d}\boldsymbol{x}'' K(\boldsymbol{x}-\boldsymbol{x}', \boldsymbol{x}-\boldsymbol{x}'')\bar{\psi}(x')\psi(x'')\varphi(x) \,. \tag{1}$$

This interaction reduces to the usual local form if $K(\boldsymbol{x}, \boldsymbol{y})$ is given by

$$K(\boldsymbol{x}, \boldsymbol{y}) = \delta(\boldsymbol{x})\,\delta(\boldsymbol{y}) \;;$$

for present purposes, however, $K(\boldsymbol{x}, \boldsymbol{y})$ will be selected so that it provides a cut-off in momentum space. The model here proposed is thus a slight generalization of CAIANIELLO's [1] in which the fermion momenta were sharply cut-off. The resulting theory is unitary but not relativistically invariant. It will be assumed that the system described by (1) is contained in a finite box of volume V and that periodic boundary conditions may be used on its surface. For later applications, it is convenient to define the Fourier transform of $K(\boldsymbol{x}, \boldsymbol{y})$ by the relation

$$K(\boldsymbol{p}, \boldsymbol{p}') = \int \mathrm{d}\boldsymbol{x}\,\mathrm{d}\boldsymbol{y} K(\boldsymbol{x}, \boldsymbol{y}) \exp\,[i\boldsymbol{p}\cdot\boldsymbol{x}] \exp\,[i\boldsymbol{p}'\cdot\boldsymbol{y}] \,.$$

In order to prove the convergence, it suffices to consider explicitly only the meson vacuum-to-vacuum element of the U-matrix, U_0, since the other elements can be treated by an obvious extension of the method. This element U_0 for the time interval, $(-T/2, T/2)$ may be written

$$U_0 = \langle 0\,|\sum_{n=0}^{\infty} \frac{(-i)^{2n}}{(2n)!}\int_{T/2}^{T/2} \ldots \int \mathrm{d}t_1 \ldots \mathrm{d}t_{2n} P[H_{\mathrm{I}}(t_1)H_{\mathrm{I}}(t_2) \ldots H_{\mathrm{I}}(t_{2n})]\,|\,0\rangle \,, \tag{2}$$

where $H_{\mathrm{I}}(t)$ is expressed in the interaction representation and where the odd meson terms vanish and thus have been dropped. Carrying out the operation of taking the meson vacuum expectation value, and using obvious symmetries

in the integrands, U_0 may be written [1]

$$(3)\qquad \sum_{n=0}^{\infty}\frac{(-ig)^{2n}}{2^n n!}\int_{-T/2}^{T/2}\cdots\int \mathrm{d}^4x_1 \ldots \mathrm{d}^4x_{2n}\,\frac{1}{2}\Delta_F(x_1-x_2)\ldots$$

$$\ldots\frac{1}{2}\Delta_F(x_{2n-1}-x_{2n})\langle a|P[j(x_1)\ldots j(x_{2n})]|b\rangle\,,$$

where $|b\rangle$, and $\langle a|$ are the initial and final fermion states and where $j(x)$ is defined by

$$(4)\qquad j(x)=\iint \mathrm{d}\boldsymbol{x}'\,\mathrm{d}\boldsymbol{x}''K(\boldsymbol{x}-\boldsymbol{x}',\boldsymbol{x}-\boldsymbol{x}'')\bar{\psi}(x')\psi(x'')\,.$$

The functions $\Delta_F(x)$ are well known [7] and have the Fourier expansion

$$(5)\qquad \frac{1}{2}\Delta_F(x)=\begin{cases} V^{-1}\sum_{\boldsymbol{k}}\dfrac{\exp[i\boldsymbol{k}\cdot\boldsymbol{x}]}{2\omega_{\boldsymbol{k}}}; & x_0>0,\\ V^{-1}\sum_{\boldsymbol{k}}\dfrac{\exp[-i\boldsymbol{k}\cdot\boldsymbol{x}]}{2\omega_{\boldsymbol{k}}}; & x_0<0.\end{cases}$$

Using a plane-wave expansion for ψ,

$$\psi(\boldsymbol{x},t)=V^{-1}\sum_{\boldsymbol{p},\lambda}a_{\boldsymbol{p},\lambda}(t)u_\lambda(\boldsymbol{p})\sqrt{\frac{m}{|E|}}\exp[i\boldsymbol{p}\cdot\boldsymbol{x}]\,,\qquad(\lambda=1,2,3,4),$$

$j(x,t)$ may be written

$$(6)\qquad j(\boldsymbol{x},t)=V^{-1}\sum\left[\frac{m^2}{|EE'|}\right]^{\frac{1}{2}}\bar{u}(\boldsymbol{p}')u(\boldsymbol{p})\exp[i\boldsymbol{x}\cdot(\boldsymbol{p}-\boldsymbol{p}')]a^+_{\boldsymbol{p}'}(t)a_{\boldsymbol{p}}(t)K(\boldsymbol{p},\boldsymbol{p}')\,,$$

where the sum goes over both momenta and over the four spin and energy states; the spin-energy indices have been suppressed.

Consider now a typical factor in Eq. (3),

$$\iint \mathrm{d}\boldsymbol{x}\,\mathrm{d}\boldsymbol{y}\Delta_F(x-y)j(x)j(y)\,,$$

with the time ordering, although not explicitly indicated, understood. Using

[7] See for example, S. S. Schweber, H. A. Bethe and de Hoffman: *Mesons and Fields*, Sect. **15***b* (1955).

the Fourier expansions Eqs. (5) and (6) and carrying out the trivial spatial integrations, this expression may be displayed in the more useful form

$$(7)\qquad V^{-3}\sum\left[\frac{m^4}{|E_1E_2E_3E_4|}\right]^{\frac{1}{2}}\bar{u}(\boldsymbol{p}_1)u(\boldsymbol{p}_2)\bar{u}(\boldsymbol{p}_3)u(\boldsymbol{p}_4)K(\boldsymbol{p}_1,\boldsymbol{p}_2)K(\boldsymbol{p}_3,\boldsymbol{p}_4)\cdot$$
$$\cdot\,\delta_{\pm\boldsymbol{k}+\boldsymbol{p}_1-\boldsymbol{p}_2}\delta_{\mp\boldsymbol{k}+\boldsymbol{p}_3-\boldsymbol{p}_4}\frac{\exp\left[-i\omega_{\boldsymbol{k}}|x_0-y_0|\right.}{2\omega_{\boldsymbol{k}}}\,a^+_{p_1}(t_i)a_{p_2}(t_i)a^+_{p_3}(t_{i+1})a_{p_4}(t_{i+1})\,.$$

The plus-minus sign in Eq. (7) corresponds to the two possible time orderings and this distinction turns out to be unimportant for the present purpose.

Having disposed of these preliminaries, we shall now obtain a convenient upper bound for any matrix element of the integrand of the $2n$-th term in Eq. (3). The crux of the estimation lies in the fact that *any* matrix element of a^+_p or a_p is always zero or one; thus, independent of any time ordering, the matrix element of a product of these operators is bounded by one. Such a bound will lead to a gross overestimate of the final result because it neglects the fact that for most combinations of the momenta the matrix elements actually vanish. Further, the crudeness of the estimate is emphasized by the fact that it allows more particles in intermediate states than is allowed by the exclusion principle. Indeed, below we shall consider a situation where a refined estimate of the P-bracket of fermion operators is obtained and, consequently an improved upper bound will result. Assuming then that the cut-off function decreases sufficiently rapidly for large momenta, the remaining factors in Eq. (7) can easily be bounded by use of the easily verifiable relations

$$\left[\frac{m^2}{EE'}\right]^{\frac{1}{2}}\bar{u}(\boldsymbol{p}')u(\boldsymbol{p})\;<1\,,$$

and

$$\left|\exp\left[-i\omega_{\boldsymbol{k}}|x_0-y_0|\right]\right|=1\,.$$

Accordingly, the $2n$-th term of U_0 is bounded by

$$\frac{|g|^{2n}}{n!}\;T^{2n}V^{2n}A^n\,,$$

where A is given by the expression

$$A=V^{-3}\sum\delta_{\pm k+p_1-p_2}\delta_{\mp k+p_3-p_4}\frac{K(\boldsymbol{p}_1,\boldsymbol{p}_2)K(\boldsymbol{p}_3,\boldsymbol{p}_4)}{2\omega_{\boldsymbol{k}}}\,.$$

In defining A, factors of V have been explicitly extracted so that A becomes independent of V as the volume tends to infinity. Using Caianiello's sharp cut-off model,

$$K(\boldsymbol{p}, \boldsymbol{p}') = \begin{cases} 0 & |\boldsymbol{p}|, |\boldsymbol{p}'| > P_0, \\ 1 & |\boldsymbol{p}|, |\boldsymbol{p}'| < P_0, \end{cases}$$

we obtain the estimate

$$A \simeq \frac{P_0^q}{\mu}.$$

Our result may thus be summarized by the inequality

$$\text{(8}a\text{)} \qquad \text{Ser}\,|U_0| \leqslant \text{Ser}\left\{\exp\left[|g|^2 T^2 V^2 P_0^q/\mu\right]\right\},$$

where we have introduced a notation which means that the series on the left is bounded term by term by the series on the right.

The convergence proof for other elements of the U-matrix now follows easily. If the initial and final states contain together r mesons, then the only changes would be that the terms in Eq. (3) would have extra plane-wave factors in addition to the Δ_F functions and by the same steps as described above the result would follow. Explicitly, we obtain (except for irrelevant numerical factors) for the case when none of the initial and final boson momenta are equal,

$$\text{(8}b\text{)} \qquad \text{Ser}\,|U_r| \leqslant \text{Ser}\left\{\left[V^{\frac{1}{2}} T P_0^3 |g|/\mu^{\frac{1}{2}}\right] \exp\left[|g|^2 T^2 V^2 P_0^q/\mu\right]\right\}.$$

If some of the initial and final momenta are equal, the net effect is to append a polynomial in g of order r.

The V and T dependence given by the bound of Eq. (8) is of some interest. Ideally, one would have liked the argument of the exponent to be linear in VT (because of the fact, which will be further discussed below, that the energy density is independent of V) instead of quadratic, but in this we have not succeeded in the general case. The V dependence alone, however, can be favorably altered under special circumstances. Consider, for example, an interaction given by Eq. (1) except that now the fermion field is treated non-relativistically to the extent that anti-particles are excluded. The matrix element for going from a single fermion state of fixed momentum to another such state may be bounded in the same way as above except that now we can estimate more closely the expectation value of the P-bracket of the fermion operators. Clearly, for given values of the boson momenta, the nucleon momenta will all be fixed for each time ordering. Thus, the sum over

1976

the five momentum variables in Eq. (7) reduces to a single sum, say over $\boldsymbol{k}$. This eliminates two powers of V and, repeating the same steps as above, we obtain now the bound

$$\text{Ser}\,|\,U^1\,| \leqslant \text{Ser}\left\{\exp\left[|g|^2 T^2 P_0^3/\mu\right]\right\}, \tag{9a}$$

which is completely independent of V. Similarly, a transition of N fermions to N fermions yields the relation

$$\text{Ser}\,|\,U^N\,| \leqslant \text{Ser}\left\{\exp\left[N^2\,|g|^2 T^2 P_0^3/\mu\right]\right\}. \tag{9b}$$

Unfortunately, we have not succeeded in reducing the power of T in the above bounds nor have we been able to find an example where the powers of T were reduced as with the volume above.

For some interactions, other than those given by Eq. (1), the above proof can be applied in a straightforward manner. Examples of such interactions are: a mass renormalization term of the form

$$\overline{\psi}\psi\ ;$$

a β-decay type of interaction,

$$(\overline{\psi}_1\psi_2)(\overline{\psi}_3\psi_4)\ ;$$

and a fixed source theory which has been essentially considered in the last paragraph. On the other hand, interactions of the form,

$$\varphi^2\,, \qquad \overline{\psi}\psi\varphi^2\,, \quad \ldots$$

converge with at least a finite radius by the above method, while for any interactions which contain higher powers of the boson field than Φ^2 the method breaks down. Indeed, THIRRING [6] has further shown that a Φ^3 interaction diverges.

3. – The zeros of the U-matrix.

One of the important consequences of the fact that the elements of the U-matrix are bounded term by term by an exponential series, Eq. (8*a*), is that they are thus entire functions of g^2. (A similar statement holds, of course, for the non-meson vacuum elements, Eq. (8*b*), except for the g^r factor which offers no difficulties.) Consequently, known properties of entire functions may be applied for further study of the U-matrix.

An immediate consequence of this observation is the fact that each element of the U-matrix must have at least one non-trivial zero somewhere in the complex g^2-plane. This statement follows directly from the following theorem which is established in Appendix I:

If $f(z)$ is an entire function and

$$|f(z)| < \exp[A|z|],$$

where A is a positive constant, then either

$$f(z) = \exp[Bz],$$

where B is a constant, or else $f(z)$ has at least one zero.

For the boson vacuum-to-vacuum element, we can select

$$U_0(g^2) = f(g^2)$$

and since generally U_0 cannot be written in the form $\exp[Bg^2]$, it follows from Eq. (8a) that $U_0(g^2)$ must vanish for some, not necessarily real, value of g^2. Similarly, for the case of a total of r bosons in the initial and final states, since generally U_r cannot be written in the form

$$U_r = g^r \exp[Bg^2],$$

it follows from Eq. (8b) that U_r/g^r must have a zero somewhere in the complex g^2-plane. Further, the latter part of Appendix I contains an argument which makes it very plausible that there are a denumerable set of zeros.

Consider now some matrix element of a phyiscal process, say from a state a to a state b. In the Feynman-Dyson approach, one calculates this element by summing only the connected diagrams with the vacuum-to-vacuum factors left out. Let us denote this matrix element by $\langle b|R|a\rangle$. It is well known that the complete matrix element $\langle b|U|a\rangle$ is then given by

$$\langle b|U|a\rangle = \langle b|R|a\rangle \cdot \langle 0|U|0\rangle . \tag{10}$$

Now in the convergence proof above, the bounds were obtained by summing together the contributions from all diagrams, in a given order, including the vacuum-to-vacuum factors. Thus, the physically interesting quantity $\langle b|R|a\rangle$ is the ratio of two entire functions and would itself be entire, if, for every zero in the denominator, there is a zero of, at least, the same order in $\langle b|U|a\rangle$ to cancel it. However, in general, this situation does not arise be-

1978

cause there is always some matrix element of U which does not vanish for the same value of g^2 that the vacuum-to-vacuum factor does. To show this, consider the identity

$$\sum_n \langle a | U^+(g^*) | n \rangle \langle n | U(g) | a \rangle = 1 , \tag{11}$$

which can formally be established by considering the power series expansion of the operator $U^+(g^*) \cdot U(g)$. More rigorously, we observe that each factor in the summand is an entire function of g^2, and in Appendix II it is shown that the sum over states converges to an entire function. Hence the order of summing over states and over powers of g may be interchanged yielding the desired result. Now, if all the matrix elements vanish at the same point in the complex g^2 plane, the left side of Eq. (11) would vanish; but this is impossible. Hence, there exists at least one matrix element of U which fails to vanish at each zero of $\langle 0 | U | 0 \rangle$. Thus, in general, we see that even though the U-matrix has an infinite radius of convergence, the physically more interesting matrix R has only a finite one. This is a basic limitation on the present method.

4. – Discussion.

Up to this point, it has been established that, for an interaction which is restricted to a finite region of space-time and has a momentum cut-off, the elements of the S-matrix, considered as power series in the unrenormalized coupling constant, converge with an infinite radius. This result enabled us subsequently to study the physically more interesting R-matrix and to draw conclusions which were always straightforward and unambiguous. Unfortunately, however, many remaining points cannot be cleared up in a similar manner. Among these one might include questions such as: what happens to the region of convergence in the limit of very large time intervals; or does the above result still hold if a charge renormalization is performed; or what does our result imply about physically more interesting interactions. In this section, we propose to make a detailed discussion of some of these questions albeit from a somewhat less quantitative and more speculative point of view.

Firstly, let us try to understand just precisely what causes the present convergence proof to work and what can be said if some of the restrictions imposed here are relaxed. It is transparent from the work of RIDDEL [3] and HURST [4], that if there is convergence at all in the general case, it must be due to a cancellation among the contributions from various diagrams. The fact that some cancellation between diagrams does take place is well known. For example, in the Feynman method of evaluating the contribution from a given diagram which contains more than one fermion, one may completely

1970

disregard the exclusion principle, for there are other diagrams of the same order which will exactly compensate for this neglect. (This is in contrast to ordinary perturbation theory where the Pauli-principle is explicitly included at every stage.) The remaining question then is, are there enough cancellations from this as well as other sources to insure convergence? We propose to answer this question in the affirmative by means of the following. Brief consideration shows that there are three major reasons why the theory given by Eq. (1) converges. There may be « jamming » in that, because of the momentum cut-off on the fermions, the exclusion-principle decreases substantially the contributions from higher-order diagrams. Secondly, the higher-order terms may be depreciated because the momentum cut-off decreases appreciably the phase space available to many particles. That is, the momentum cut-off on the dependent variables in a sum such as that given by Eq. (7) acts as an additional restriction on the range of values of the independent variables. And lastly, convergence may take place because of cancellations. Let us consider each of these possibilities in turn. If the convergence were due to jamming, then clearly the proof above would be useless since the model would insure convergence in an extremely artificial way. The fact that jamming was not used is most easily seen by referring back to the method employed to estimate the P-bracket of the fermion operators. The replacement of this bracket by unity forces the inclusion of all terms regardless of the exclusion principle. Thus, independent of any momentum cut-off, any number of fermions could exist simultaneously, and consequently the convergence cannot be due to this source. Similarly, the decreasing phase space with increasing numbers of particles was not used in the estimation procedure. This is clear from the discussion immediately preceding Eq. (8a). There, the constant A was evaluated by letting the fermion momenta range up to the cut-off P_0 independent of the momentum conservation restrictions. It follows, therefore, that the convergence must have taken place by cancellations among diagrams, and perhaps it is not unreasonable to assume that this cancellation carries over into the more interesting theory without a cut-off. Indeed, the only plausible way the latter can fail to happen is if there is a non-uniformity in the limit of large P_0. It should also be mentioned that although, cancellation assures convergence, the other two effects may dominate the behavior of the series with regards to questions of rapidity of convergence.

Throughout the analysis thus far, we have restricted our attention to the case of a finite volume and time of interaction as well as a non-invariant cut-off in momentum space. The present method does not seem to be easily adaptable to the situation as V, T and P_0 become arbitrarily large. The basic difficulty is perhaps exemplified by the V^2T^2 dependence of the bounding series given by Eq. (8). A linear VT dependence, on the other hand, might have enabled us to draw conclusions of a more substantial nature. This latter observation

1980

follows because of the expectation that the vacuum-to-vacuum amplitude should be, for asymptotically large V and T, the phase factor

$$\exp[-i\varepsilon VT],$$

where ε is the vacuum self-energy per unit volume and is independent of V. To see this, consider all Feynman diagrams which make up U_0. It is well known that the contributions from these diagrams can all be summed and the result is of the form

$$U_0 = \exp\Big\{-i\sum_n A_n(V, T)g^{2n}\Big\},$$

where A_n is obtained by summing only the contributions from connected diagrams of $2n$ vertices. Each of these contributions to A_n has in the limit of large V and T a four-dimensional δ-function of energy and momentum conservation at each vertex. One of these δ-functions is always superfluous and yields the linear VT dependence. The usual interpretation thus permits one to write the relation

$$\lim_{V,\,T\to\infty} A_n(V, T) = \varepsilon_n VT. \tag{13}$$

In this case, therefore, a linear VT dependence in the bounding series would enable one to determine the properties of the physically more interesting quantity ε. Despite this lack of a linear VT dependence, one might have hoped that one could do all the estimations for finite values of V, T and P_0, carry out a renormalization of mass and charge and then pass to the limit as these parameters increased. It turns out that the present method does not enable one to draw any definite conclusions about the results of such a limiting procedure. Plausibility arguments about such results lead either toward doubt as to the internal consistency of field theory or toward conclusion which seem to require the addition of rules for complete interpretation.

In order to explore this matter further, it is convenient to avoid transients associated with turning the interaction on and off abruptly and to assume it is turned on and off adiabatically. From now on, T will denote the average time for switching on the interaction (if H_1 of Eq. (1) is multiplied by $\exp[-\alpha|t|]$ this means $T\sim 1/\alpha$). With this convention, the previous results are unchanged in form, although they have a somewhat different meaning.

As has been pointed out above, since the present method is not suitable for studying the asymptotic behavior of the series, let us attempt rather to list the various possibilities and study their implications. In the example above, it was observed that as T became infinitely large, the vacuum-to-vacuum amplitude approached unity; that is, because of the assumed adia-

1981

batic variation of the interaction, no transitions are induced from the vacuum to other states. Formally, this assumption may be expressed in the form

$$\lim_{T\to\infty} \langle 0|U^+(T, g^*)|0\rangle\langle 0|U(T, g)|0\rangle = 1 \tag{14}$$

for real values of g. Now consider g to be a complex variable; then for finite T, the left-hand side of Eq. (14) approaches unity on the real axis as T increases. If this limit were of such a nature as not to destroy the analyticity properties of the left-hand side of Eq. (14), then of necessity it would have to be unity in the entire complex g-plane. This result need not be in conflict with Sect. 3 if the zeros of U_0 in Eq. (12) move out with increasing T. Let us assume that this is the case. There thus remain several possibilities for the behavior of the limiting series of the exponent in Eq. (12). If the limiting behavior were sufficiently uniform such that the limit on T could be taken term by term, then the series would be an entire function and the usual methods would be justified. A second alternative is that the limiting series in the exponent has only a finite radius of convergence but it defines an analytic function which may be continued to find its values along the real axis. In this case, the analytic function would approximate the entire function for small g but its analytic continuation, in general, differ from the limiting form of the entire function. Lastly, the limiting series may define a function with a zero radius or one which cannot be continued unambiguously along the real axis. As an example of each of these possibilities consider the series

$$\sum_{n=0}^{\infty} a_n g^n (1 - \exp[-T/n!]) ,$$

which for any finite T will have an infinite radius of convergence provided the a_n's increase less slowly with n than $n!$. On the other hand, the series may have almost any other convergence property if the limit on T is taken term by term. Thus, even though the series in the exponent of Eq. (12) has an increasing radius of convergence as T increases, we are able to say nothing about the behavior of the series in the limit. If the limit function had a zero radius, then the usual methods would be meaningless. However, if the limiting function converges only for small g and can be analytically continued, then one may regard the continuation as representing the true physical content of the theory. Any differences between the limiting form of the entire function and the analytically continued one, might then be regarded as due to the particular limiting procedure used to define the self-energy and not of any real physical significance. This latter view would have to be justified by some other unambiguous method of calculation.

1982

As a particular example of a case where the analytical continuation does work, consider an interaction given by the expression

$$\delta m \bar{\psi} \psi .$$

The details of a calculation of the vacuum-to-vacuum amplitude in the limit of large times will be found in Appendix III; the result is

$$(15) \quad \log U_0 = -\frac{iT}{2} \sum_k \{ \sqrt{K^2 + (m + \delta m)^2} - \sqrt{K^2 + m^2} \}.$$

In this case the power series in δm could be summed exactly and the analytic continuation carried out by inspection. The physical interpretation of Eq. (15) is clear since it represents merely the shift in the zero-point energy of the vacuum. It is to be noted that the computation of only the first few terms in the power series would have led to a completely erroneous answer if the numerical value of $|\delta m|$ exceeded $|m|$. The important point then is that even though the vacuum self-energy has only a finite radius of convergence, the physical content was maintained by its analytic continuation.

In essence, the discussion above the behavior of the series for large times, holds almost equally well for the non-uniformity in the limit of large V and P_0. The usual justification for the V dependence of matrix elements requires the replacement

$$\sum_p \to \frac{V}{(2\pi)^3} \int \mathrm{d}\boldsymbol{p} ,$$

in all momentum sums. For sufficiently high order, with fixed T and P_0, this approximation may depend non-uniformly on V. It is conceivable that for fixed n one may find a sufficiently large V so that the approximation is justified while if V is fixed the approximation may break down for sufficiently large n. This situation may arise because for large n the summations over the independent momentum variables are restricted by the range of the independent ones; this restriction might so cut down the range of the independent variables that the discreteness of the sum becomes important. In any case, the non-uniform behavior for large V can be made plausible just as it was for large T [8]. Similarly, the same argument also follows for the P_0 dependence, which for this particular theory, increases as P_0^4 for large P_0.

---

[8] The point to be emphasized is that in the neighborhood of the place where U_0 of Eq. (12) has a zero, the series in the exponent must reduce to a product of a constant times V times a logarithm. This is not consistent with the analyticity of U_0 which would require that the coefficient of the logarithm be an integer.

1983

The above discussion has been based on the assumption of the validity of Eq. (14); that is, on the assumption that if the interaction is turned on and off very slowly then there will be no transitions from the vacuum to any other state. On the basis of certain conjectures of DYSON [9], even this assumption is open to question. The essence of Dyson's argument is that if the forces between particles are attractive and of long range then the binding energy of a large collection of particles could exceed the energy required to create them. This would result in the eigenvalues of the complete Hamiltonian not being bounded from below; every state would be a decaying one in which more and more particles are created and bound while photons are ejected. The connection with the present discussion is as follows. As the interaction is turned on gradually, a decaying state is produced instead of the physical vacuum. When the interaction is later turned off, some of the components will have separated in space and the system will not return to the bare vacuum [10]. This seems to be in contradiction with the well known fact that if an interaction is turned on and off very slowly, then energy is conserved at every vertex of a Feynman graph. However, this is true only if T approaches infinity for a fixed order n; while for fixed T, the vacuum can make transitions to other states of unperturbed energy of order n/T. Thus no matter how large T is, there are graphs of sufficiently high order to correspond to real transitions. This indicates again a non-uniformity in the limit of large times. Finally, we note that although Dyson's arguments were given for imaginary coupling constants, the difficulties, probably carry over to real values of the charge. For if there is a matrix element from the bare vacuum to some other state, then it cannot vanish identically for real values of e and fail to vanish for imaginary values.

In conclusion, we see that with the present analysis we are unable to conclude anything directly about the analytic properties of the asymptotic quantities which contain the real physical content of the theory. We have indicated, however, that the usual limiting procedures may lead to erroneous or ambiguous results.

* * *

We are grateful to Professor M. M. SCHIFFER of the Mathematics Department for many valuable discussions on the mathematical aspects of this problem especially for the theorem of Appendix I. Also, we are indebted to many colleagues, in particular M. PESHKIN for many illuminating conversations.

[9] F. J. DYSON: *Phys. Rev.*, **85**, 631 (1952).

[10] It is worthy to note in this connection a possible difference between an infinite volume and a finite one. With an infinite volume, the photons can get very far away from the electrons, but with periodic boundary conditions they cannot. In the latter case, the system can possibly return to the vacuum after the interaction is turned off.

Appendix I ([11])

The theorem to be proved is:

If $f(z)$ is entire and $f(z) \leqslant \exp[A|z|]$, where A is a positive constant, then either $f(z) = \exp[Bz]$ where B is a constant or else $f(z)$ has a zero. In order to establish the result, it is convenient to normalize $f(z)$ so that $f(0) = 1$. We shall proceed by assuming that f has no zeros and show that $f(z)$ must be $\exp[Bz]$.

Consider the region inside a very large circle of radius R in the z-plane and define two functions in this region by

$$g(z) = \ln f(z) , \tag{A.1}$$

and

$$h(z) = \frac{g(z)}{2AR - g(z)} . \tag{A.2}$$

Now since $f(z)$ is assumed not to have any zeros, $g(z)$ is analytic; and further, since the real part of $g(z)$ is bounded from above by AR, $h(z)$ is also analytic. Using. eq. (A.2), we see that $h(z)$ is bounded by 1 and further since $h(0) = 0$, we have that $h(z)/z$ is also analytic; and thus by the Maximum Modulus Theorem ([12]) we obtain

$$|h(z)| \leqslant \frac{|z|}{R} .$$

Rewriting this inequality in terms of $g(z)$ by use of eq. (A.2), we obtain

$$|g(z)| \leqslant |2AR - g(z)| \frac{|z|}{R} \leqslant (2AR + |g(z)|) \frac{|z|}{R} ,$$

which implies directly the inequality

$$\left| \frac{g(z)}{z} \right| \left(1 - \frac{|z|}{R}\right) \leqslant 2A .$$

Since this latter inequality is to hold for arbitrarily large R, we may conclude that $|g(z)/z|$ is bounded by a constant, which, by Liouville's Theorem ([13]) and eq. (A.1), proves the assertion.

This method is easily extended to show that $f(z)$ has more than one zero. Since $f(z)$ is entire, and it has a zero at, say, z_0 we can write

$$f(z) = (z - z_0)t(z) ,$$

([11]) The greater part of this appendix was prepared by M. M. Schiffer.

([12]) See for example, E. C. Titchmarsh: *The Theory of Functions* (Oxford. 1939). chapter V.

([13]) See ref. ([12]), chapter II.

1985

where for convenience we have assumed that the zero is simple, and where $t(z)$ is also an entire function. Consider the interior of a very large region of radius $R > \max(2|z_0|, 2)$. By the maximum modulus theorem we have

$$|t(z)| < \frac{2}{R} \exp[AR] \qquad \text{for} \qquad |z| \leqslant R .$$

Thus we have the inequality

$$\mathrm{Re}\,(\ln t(z)) < AR ,$$

which after normalizing $t(0) = 1$ enables us to repeat the above proof and to conclude that either $t(z) = \exp[Bz]$ or else $t(z)$ also has a zero. This argument can be repeated as long as it is known that $f(z)$ is not expressible as a finite product of factors of $(z - z_i)$ multiplied by an exponential of the form $\exp[Bz]$.

Appendix II

The purpose of this appendix is to prove eq. (11), which is a special case of the more general relation

$$U(t, t')U(t', t'') = U(t, t'') , \tag{B.1}$$

where, in our case, $t = t'' = -T/2$ and $t' = T/2$. To establish this equation it clearly suffices to justify the interchange of the order of summing over intermediate states and over powers of g. This will be accomplished by showing that the sum over states yields an entire function of g. In terms of eq. (B.1) this means that the two-power series for the operators on the left may be multiplied together and rearranged to give the power series for the operator on the right. The proof will be explicitly given only for the vacuum expectation value of eq. (B.1). The other matrix elements can be handled with minor unimportant modifications. For reasons of simplicity we take a sharp cut-off in momentum space.

We shall proceed by bounding the vacuum-to-vacuum element of the left side of eq. (B.1). Since the bounding function will turn out to be entire, the matrix element itself will be entire. In order to carry out the proof, it is first necessary to sharpen the inequality in eq. (8*b*). Let us consider the matrix element of U between the meson vacuum and a state in which the i-th mode ($i = 1, 2, \ldots$) has S_i mesons. In the original P-bracket expression, S_i factors will have to be selected from n factors to serve as creation operators for these mesons; this selection can be made in

$$\frac{n!}{(n - \sum_i S_i)!\, S_1!\, S_2! \ldots} , \tag{B.2}$$

ways. We make some particular selection, and leave the remainder of the meson operators to be paired off as Δ_F functions; the resulting matrix element is to be multiplied by eq. (B.2). Suppressing the designation of the fermion state the result is

$$\left.\begin{matrix}\langle S_1, S_2 \ldots | U(t', t'') | 0\rangle \\ \text{or} \\ \langle 0 | U(t, t') | S_1, S_2 \ldots\rangle\end{matrix}\right\} \leqslant \left[\prod_i \frac{1}{\sqrt{S_i!}} \left(\frac{V^{\frac{1}{2}} T_{1,2} P_0^3 |g|}{\sqrt{\mu}}\right)^{S_i}\right] \exp\left[\frac{|g|^2 V^2 T_{1,2}^2 P_0^q}{\mu}\right],$$

where $T_1 = |t' - t''|$ and $T_2 = |t - t'|$. On carrying out the sum over intermediate states the left side of eq. (B.1) is found to be bounded by

$$\exp\left[|g|^2 V^2 P_0^q (T_1^2 + T_2^2 + \alpha T_1 T_2)/\mu\right],$$

where $\alpha \sim 1$ and a constant of proportionality which is independent of g has been omitted. Thus the left side of (B.1) is an entire function and consequently one can interchange the order of summing over intermediate states and over powers of g.

Appendix III

The derivation of eq. (15) is straightforward and follows well-known rules. As has already been noted, we need to sum only the connected diagrams to obtain $\log U_0$. Using for the interaction

$$H_I = -\delta m \bar{\psi}\psi,$$

we obtain in the limit of large times

$$\log U_0 = \frac{VT}{(2\pi)^4} \sum_{n=1}^{\infty} \frac{(i\delta m)^n}{n} \int d^4p \, \mathrm{Tr}\left(\frac{1}{\gamma_\mu p_\mu - im}\right)^n,$$

which may be written in the form

$$\log U_0 = \frac{VT}{(2\pi)^4} \int d^4p \int_0^{\delta m} \frac{dx}{x} \sum_{n=1}^{\infty} (ix)^n \, \mathrm{Tr}\left(\frac{1}{\gamma_\mu p_\mu - im}\right)^n.$$

Assuming we can interchange the sum on n with the taking of the trace, (which is true for a finite number of terms), we perform the sum on n, take the trace, and perform the P_0 integration in that order and obtain thus

$$\log U_0 = -\frac{iVT}{2(2\pi)^3} \int d\boldsymbol{p} \int_0^{\delta m} \frac{dx(m + x)}{\sqrt{p^2 + (m + x)^2}}.$$

1987

The integration on x is now performed, and yields the expression

$$\log U_0 = -\frac{iVT}{2(2\pi)^3}\int \mathrm{d}\boldsymbol{p}\left[\sqrt{p^2+(m+\delta m)^2}-\sqrt{p^2+m^2}\right].$$

which is identical with eq. (15).

RIASSUNTO (*)

Si esamina la convergenza dello sviluppo degli elementi della matrice S secondo la teoria della perturbazione del campo. Per una teoria caratterizzata da un accoppiamento lineare nel campo bosonico si constata che introducendo un taglio nello spazio dei momenti l'ampiezza di transizione per ogni processo in un intervallo di tempo finito è limitata termine a termine da una serie esponenziale. Si espone anche per diversi casi l'estensione del metodo ad interazioni non lineari. Si discutono da un punto di vista qualitativo le conseguenze che dal risultato emergono per le teorie prive di taglio

(*) *Traduzione a cura della Redazione.*

Numerical Calculations on the New Approach to the Cascade Theory - III.

S. K. Srinivasan, J. C. Butcher, B. A. Chartres and H. Messel

The F.B.S. Falkiner Nuclear Research Laboratory (*), *School of Physics, The University of Sydney - Sydney, N.S.W.*

(ricevuto il 25 Marzo 1958)

Summary. — On the basis of the new approach to the cascade theory accurate numerical results on the mean numbers of electrons produced in small thicknesses in a shower initiated by a single electron or photon are presented. Agreement with the experimental results is satisfactory if due allowance is made for tridents.

1. – Introduction.

Since the report of an anomalous electron shower by Schein *et al.* in 1954, a number of anomalous high energy showers have been observed in emulsions (1). More recently Fay (2) at Gottingen has observed similar showers in which the mean number is greater than that predicted by cascade theory. Though most of the showers can be fully accounted for by the theory of bremsstrahlung and pair production, the present experimental evidence cannot wholly exclude multiple processes in which there may be emission of two or more high energy quanta or pair production by charged particles. While on the one hand accurate cross-sections for these higher order processes have to be derived, on the other the cascade theory by itself has to be modified so as to enable easy interpretation of cosmic ray events in nuclear emulsions. A beginning in this direction has been made by Ramakrishnan and Srinivasan (3) who have dealt with the particles with reference to their « primitive »

(*) Also supported by the Nuclear Research Foundation within the University of Sydney.

(1) M. Koshiba and M. F. Kaplon: *Phys. Rev.*, **97**, 193 (1955); **100**, 327 (1955).

(2) H. Fay: *Nuovo Cimento*, **5**, 293 (1957).

(3) A. Ramakrishnam and S. K. Srinivasan: *Proc. Ind. Acad. Sci.*, **44**, 263 (1956).

1989

energies, *i.e.* the energy of the particles at the time of production. Such a modification, apart from relieving the experimenter from the difficulties that are involved in keeping track of the particles, helps him to interpret events which form only part of a shower.

The numerical results relating to the mean number of particles produced between 0 and t rather than the mean number at t (t denotes the thickness in cascade units) have been presented by SRINIVASAN and RANGANATHAN [4] for various values of energy and depth. Since the numbers presented in that paper pertained to large thicknesses, they cannot be checked against experiments. It would be very difficult to make accurate energy measurements for the very large number of particles that are produced in such large thicknesses. Thus from the experimental point of view only calculations relating to small thicknesses of emulsions are of interest. An attempt was made to calculate the mean number for small thicknesses [5] by the saddle point method. However the results were found to be in large deviation from the numbers observed by FAY. The numbers were computed as the difference of two integrals (evaluated by the saddle point method) each of which is so large that the difference itself is within the percentage of error to be expected. The only alternative is to compute the integral accurately without recourse to the saddle point method.

It has long been realized that if the Mellin inverse transform is integrated along a line (through σ, 0) parallel to the imaginary axis, the sequence of contributions to the integral converges slowly. However, BUTCHER, CHARTRES and MESSEL [6] have overcome the difficulty by deforming the path of integration into the parabola $y^2 = 4a(\sigma - x)$. By choosing suitable values of a and σ, they have ensured fairly rapid convergence of the cumulative contributions to the integrand. By the same method, we have now calculated the mean numbers for small thicknesses, using the electronic computer, SILLIAC.

2. – Teoretical mean numbers.

The mean number of electrons with energies greater than E that are produced between 0 and t is given by [3]

$$(1) \qquad \mathcal{E}\{N^i(y;t)\} = \frac{1}{2\pi i}\int_{\sigma-i\infty}^{\sigma+i\infty}\int_0^t \frac{v_1^i(s\,|\,E_0;\tau)\; B_s \exp[(s-1)y]}{s-1}\,\mathrm{d}\tau\,\mathrm{d}s\,, \quad (*)$$

[4] S. K. SRINIVASAN and N. R. RANGANATHAN: *Proc. Ind. Acad. Sci.*, **45**, 69 (1957).

[5] S. K. SRINIVASAN and N. R. RANGANATHAN: *Proc. Ind. Acad. Sci.*, A **45**, 268 (1957).

[6] J. C. BUTCHER, B. A. CHARTRES and H. MESSEL: *Journ. Nucl. Phys.*, **6**, 271 (1958).

(*) Throughout this paper we shall use the symbol $\mathcal{E}$ to denote the mean value.

1990

where $y = \log_e (E_0/E)$ and E_0 is the energy of the primary; $i = 1$ denotes an electron initiated shower and $i = 2$, a photon initiated shower. $v_1^i(s\,|\,E_0;\,t)$ $(i = 1, 2)$, are the Mellin transforms of the product densities of degree one (the differential mean number) of photons and are given by ([7,8])

$$v_1^i(s\,|\,E_0;\,t) = \frac{C_s}{\mu_s - \lambda_s}\{\exp[-\lambda_s t] - \exp[-\mu_s t]\}\,, \tag{2}$$

$$v_1^2(s\,|\,E_0;\,t) = \frac{1}{\mu_s - \lambda_s}\{(-D + \mu_s)\exp[-\lambda_s t] + (D - \lambda_s)\exp[-\mu_s t]\}\,. \tag{3}$$

TABLE I. – $\mathcal{E}\{N^1(y;t)\}$.

$\mathcal{E}\{n^1(y;t)\}$ is given in brackets.

t \ y	4	5	6	7	8	9	10	11
0.5	.524 (1.139)	.750 (1.338)	.994 (1.553)	1.251 (1.781)	1.521 (2.019)	1.801 (2.268)	2.092 (2.527)	2.394 (2.796)
0.6	.729 (1.252)	1.053 (1.530)	1.407 (1.836)	1.786 (2.163)	2.188 (2.512)	2.612 (2.880)	3.057 (3.269)	3.526 (3.678)
0.7	.961 (1.381)	1.400 (1.751)	1.888 (2.162)	2.418 (2.611)	2.988 (3.096)	3.598 (3.616)	4.248 4.173)	4.940 (4.767)
0.8	1.216 (1.524)	1.790 (1.995)	2.437 (2.530)	3.151 (3.123)	3.931 (3.773)	4.777 (4.483)	5.693 (5.254)	6.679 (6.088)
0.9	1.492 (1.677)	2.220 (2.261)	3.054 (2.936)	3.989 (4.548)	5.027 (4.458)	6.170 (5.491)	7.423 (6.530)	8.792 (7.670)
1.0	1.788 (1.837)	2.690 (2.546)	3.740 (3.378)	4.938 (4.336)	6.288 (5.424)	7.797 (6.649)	9.745 (8.020)	11.330 (9.546)
1.1	2.103 (2.003)	3.199 (2.846)	4.497 (3.856)	6.003 (5.039)	7.726 (6.406)	9.682 (7.970)	11.887 (.9747)	14.360 (11.752)
1.2	2.433 (2.172)	4.735 (3.159)	5.326 (4.366)	7.189 (5.806)	9.356 (7.498)	11.851 (9.466)	14.703 (11.733)	17.940 (14.326)
1.3	2.779 (2.343)	4.327 (3.485)	6.226 (4.908)	8.502 (6.638)	11.189 (8.705)	14.329 (11.147)	17.965 (14.002)	22.145 (17.310)

(7) L. JÁNOSSY and H. MESSEL: *Proc. Roy. Irish Acad.*, A **54**, 217 (1950).
(8) B. ROSSI and K. GREISEN: *Rev. Mod. Phys.*, **13**, 240 (1941).

1961

Thus $\mathcal{E}\{N^1(y;t)\}$ and $\mathcal{E}\{N^2(y;t)\}$ are given by

$$(4)\quad \mathcal{E}\{N^1(y;t)\} = \frac{1}{2\pi i}\int_{\sigma-i\infty}^{\sigma+i\infty} \frac{B_s C_s}{\mu_s-\lambda_s}\left\{\frac{1-\exp[-\lambda_s t]}{\lambda_s} - \frac{1-\exp[-\mu_s t]}{\mu_s}\right\}\frac{\exp[(s-1)]y}{s-1}\,\mathrm{d}s\,,$$

$$(5)\quad \mathcal{E}\{N^2(y;t)\} = \frac{1}{2\pi i}\int_{\sigma-i\infty}^{\sigma+i\infty} \frac{B_s}{(\mu_s-\lambda_s)(s-1)}\left\{\frac{\mu_s-D}{\lambda_s}(1-\exp[-\lambda_s t]) + \frac{D-\lambda_s}{\mu_s}(1-\exp[-\mu_s t])\right\}\exp[y(s-1)]\,\mathrm{d}s\,.$$

TABLE II. – $\mathcal{E}\{N^2(y;t)\}$.

$\mathcal{E}\{n^2(y;t)\}$ is given in brackets.

t \ y	4	5	6	7	8	9	10	11
0.5	.710 (.682)	.766 (.746)	.822 (.806)	.879 (.865)	.938 (.925)	1.000 (.987)	1.063 (1.050)	1.128 (1.115)
0.6	.063 (.817)	.951 (.917)	1.044 (1.015)	1.141 (1.114)	1.243 (1.216)	1.349 (1.323)	1.459 (1.432)	1.573 (1.546)
0.7	1.025 (.955)	1.157 (1.102)	1.298 (1.249)	1.450 (1.403)	1.611 (1.564)	1.781 (1.733)	1.959 (1.910)	2.146 (2.095)
0.8	1.198 (1.097)	1.384 (1.300)	1.590 (1.511)	1.813 (1.736)	2.054 (1.975)	2.311 (2.229)	2.584 (2.499)	2.872 (2.784)
0.9	1.382 (1.243)	1.636 (1.513)	1.922 (1.803)	2.237 (2.117)	2.582 (2.457)	2.954 (2.823)	3.354 (3.216)	3.781 (3.637)
1.0	1.579 (1.391)	1.914 (1.741)	2.298 (2.125)	2.729 (2.550)	3.206 (3.016)	3.727 (3.526)	4.293 (4.080)	4.906 (4.680)
1.1	1.788 (1.541)	2.219 (1.982)	2.722 (2.479)	3.295 (3.037)	3.935 (3.659)	4.645 (4.349)	5.426 (5.109)	6.281 (5.492)
1.2	2.011 (1.694)	2.553 (2.237)	3.196 (2.864)	3.939 (3.580)	4.782 (4.392)	5.728 (5.304)	6.781 (6.322)	7.947 (7.452)
1.3	2.246 (1.847)	2.916 (2.505)	3.723 (3.280)	4.668 (4.182)	5.756 (5.220)	6.992 (6.403)	8.385 (7.741)	9.947 (9.243)

1992

$\mathcal{E}\{N^1(y;t)\}$ and $\mathcal{E}\{N^2(y;t)\}$ are given in tables I and II. For comparison, we have also tabulated the corresponding mean numbers $\mathcal{E}\{n^1(y;t)\}$ and $\mathcal{E}\{n^2(y;t)\}$ that exist at t. For a given y, $\mathcal{E}\{N^1(y;t)\}$ is less than $\mathcal{E}\{n^1(y;t)\}$ for very small t, as is to be expected, since the primary is not counted in the former. Of course $\mathcal{E}\{N^2(y;t)\}$ is always greater than $\mathcal{E}\{n^2(y;t)\}$ for any given y and t.

3. – Comparison with experimental data.

The experimental results obtained by FAY (2) can now be compared with the mean numbers given above. We first note that the energy referred to by FAY is the total energy of the pair and the shower is initiated by a pair of electrons obtained from photon materialization. From a physical point of view, it is clear that the mean number of pairs each with a total energy greater than E produced by a pair of total energy E_0 is exactly the same as

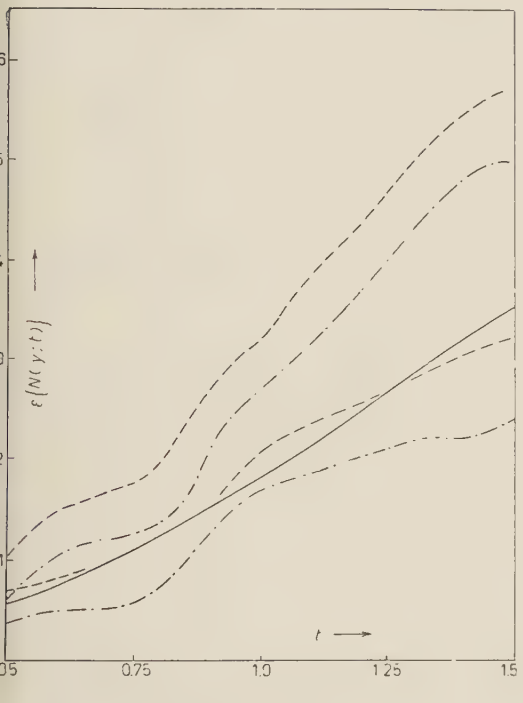

Fig. 1. – Mean number of pairs plotted against thickness measured in radiation units; $y=4$. Broken curves denote the total number of observed pairs while broken curves with dots denote the total number of pairs excluding tridents.

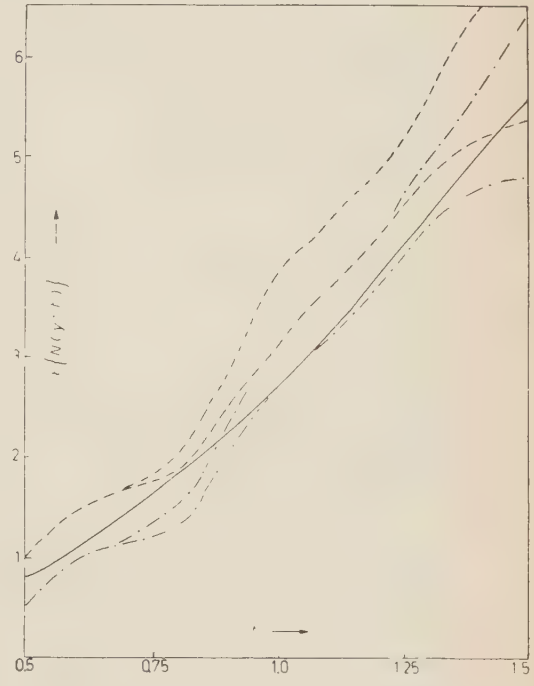

Fig. 2. – Mean number of pairs plotted against thickness measure in radiation units; $y=5$. Broken curves denote the total number of observed pairs, while broken curves with dots denote the total number of pairs excluding tridents.

the mean number of single electrons with energies greater than E produced by a single electron of energy E_0 (*). Hence the numbers presented in Table I can be directly compared with Fay's results. Since Fay's data are based on six showers, the statistics can be expected to be reasonably good. Further as the energies involved are fairly high we have used the data based on scattering measurements, rather than on opening angle (+).

In Fig. 1 and 2, we have plotted the theoretical mean numbers of pairs and the experimental limits against t for $y = 4$ and 5. For comparison we have also indicated the extent to which the experimental curves will be depressed if the reported tridents are subtracted (×). It will be found that there is good agreement between the theoretical curve and the depressed curves (obtained by subtracting the tridents). Calculations relating to higher moments of the distribution can be expected to give a decisive answer to the role played by tridents and other multiple processes.

* * *

In conclusion, we would like to thank Dr. Fay of the Max Planck Institute for supplying us the details of his experimental results.

Appendix

The mean number of electron pairs (the total energy of each pair being greater than E) produced in a shower initiated by an electron of energy E_0 is given by (9)

$$\mathcal{E}\{M(y;t)\} = \frac{1}{2\pi i}\int_{\sigma-i\infty}^{\sigma+i\infty} K(s;t)\exp[y(s-1)]\,\mathrm{d}s\,, \tag{A.1}$$

(*) In view of the fact that such a result does not hold good for higher order moments, a formal proof is presented in Appendix.

(+) We are thankful to Dr. Solntseff for clarifying this point.

(×) We are aware that real tridents cannot be distinguished from pseudo tridents experimentally.

(9) S. K. Srinivasan: *Ph. D. Thesis*, University of Madras (1957).

where

$$K(s;t) = \frac{DC_s}{(\mu_s - \lambda_s)(s-1)} \left\{ \frac{1-\exp[-\lambda_s t]}{\lambda_s} - \frac{1-\exp[-\mu_s t]}{\mu_s} \right\}. \tag{A.2}$$

We then observe that the probability that an electron is produced in the energy range $(E_0, E_0 + \mathrm{d}E_0)$ at $t = 0$ given that a photon of energy E_0 materializes at $t = 0$ is

$$\frac{1}{D}\varrho(E_0, E_0')\,\mathrm{d}E_0\,,$$

where ϱ is the differential cross-section for pair production and D, the total cross-section. Hence $\mathcal{E}\{M'(y';t)\}$ the mean number corresponding to a shower produced by an electron pair of total energy E_0' is given by

$$\mathcal{E}\{M'(E_0'; t)\} = \frac{1}{D}\int_0^{E_0'} \mathcal{E}\{M(y;t)\}[\varrho(E_0; E_0') + \varrho(E_0' - E_0', E_0')]\,\mathrm{d}E_0 = \tag{A.3}$$

$$= \frac{2}{D}\int_0^{E_0'} \frac{1}{2\pi i}\int_{\sigma-i\infty}^{\sigma+i\infty} K(s;t)\exp[y(s-1)]\varrho(E_0, E_0')\,\mathrm{d}E_0\,\mathrm{d}s\,.$$

The dependence of $\mathcal{E}\{M(y;t)\}$ on E_0 is through $\exp[y(s-1)]$ or $(E_0/E)^{s-1}$. Interchanging the order of integration over E_0 and s and observing that

$$2\int_0^{E_0'} \left(\frac{E_0}{E}\right)^{s-1} \varrho(E_0; E_0')\,\mathrm{d}E_0 = \left(\frac{E_0'}{E}\right)^{-s1} B_s\,, \tag{A.4}$$

we obtain

$$\mathcal{E}\{M(E|E_0'\,t)\} = \frac{1}{2\pi i}\int \frac{K(s;t)}{D} B_s \exp[y'(s-1)]\,\mathrm{d}s\,, \tag{A.5}$$

where $y' = \log E_0'|E$. Substituting the expression for $K(s;t)$ in (A.5), we find

$$\mathcal{E}\{M'(y';t)\} = \tag{A.6}$$

$$= \frac{1}{2\pi i}\int_{\sigma-i\infty}^{\sigma+i\infty} \frac{B_s C_s}{(\mu_s - \lambda_s)(s-1)} \exp[y'(s-1)] \left(\frac{1-\exp[-\lambda_s t]}{\lambda_s} - \frac{1-\exp[-\mu_s t]}{\mu_s}\right) \mathrm{d}s\,.$$

1995

Comparing (A.6) with (4), we note

$$\mathcal{E}\{M'(y';t)\} = \mathcal{E}\{N(y;t)\} \tag{A.7}$$

provided $y' = y$.

RIASSUNTO (*)

Sulla base del nuovo trattamento della teoria della cascata si presentano accurati risultati numerici sul numero medio di elettroni generati in piccoli spessori in uno sciame iniziatosi con un singolo elettrone o fotone. L'accordo coi risultati sperimentali è soddisfacente se si tien conto dei tridenti.

(*) *Traduzione a cura della Redazione.*

Energy Spectra of Photoneutrons From Cr and Ta.

G. Cortini, C. Milone and A. Rubbino

Istituto di Fisica dell'Università - Catania
Centro Siciliano di Fisica Nucleare - Catania

F. Ferrero

Istituto di Fisica dell'Università - Torino
Istituto Nazionale di Fisica Nucleare - Sezione di Torino

(ricevuto il 26 Marzo 1958)

Summary. — The energy spectra of photoneutrons emitted at 90° by Cr and Ta under bremsstrahlung of 20 and 30 MeV are investigated by means of the recoil protons in photoemulsion. A scanning method was followed, which gives some advantage for the study of the high energy tail of the spectra. The yield variations are consistent with the second maximum in the cross-section by Ferrero *et al.* [1]. The interpretation of the second maximum on the ground of a quasi-deuteron absorption process seems to be excluded. A temptative explanation of experimental results is discussed.

1. – Introduction.

Recent measurements [1,2] have shown that there exists an anomaly in the yield of the high energy photoneutrons ($E_n > E_0 = 5$ MeV) under bombardment of bremsstrahlung γ-rays.

This anomaly demostrates that the (γ, n) cross-section shows a second maximum at an energy higher than that corresponding to the well known giant resonance.

[1] F. Ferrero, A. Malvano and C. Tribuno: *Nuovo Cimento*, **6**, 385 (1957).
[2] See M. Soga and J. Fujita: *Nuovo Cimento*, **6**, 1494 (1957), reference [14].

1997

The present experiment was made with the aim of investigating the energy spectra of the photoneutrons from two of the elements (Cr and Ta) showing the anomaly stated above. For each element, the exposure was made with two values of the γ-spectra maximum energy, so as to select in some measure the contribution to the observed neutron spectra coming from the second resonance maximum.

Generally speaking, the experimental data available on the photoneutron spectra are rather limited ([3-6])

The total Ta(γ, n) cross-section was investigated carefully by CARVER *et al.* ([7]), but without neutron energy discrimination.

Similar work was made on the Cr photoeffect by GOLDEMBERG *et al.* ([8]).

2. – Experimental method.

2·1. *Exposures of plates.* – The γ-ray beam from the B.B.C. betatron, hit the whole mass of a target, S (Fig. 1), consisting in a cylinder of diameter 2 cm, and height 2 cm, coaxial with the beam.

The target S was at 246 cm from the target of the betatron.

The betatron was operated in different cases at 20 MeV and at 30 MeV β-energy. Exposures were made with Cr and Ta targets in the natural isotopic composition, and also without the target, in order to measure the background track density.

The dose of the irradiation was measured by means of a thick aluminium walled ionization chamber ([9]).

The photoneutrons emitted at angles of $\sim 90°$ with the photon beam were detected by means of the proton recoil tracks in the 8 plates L (Ilford C2 emulsions, 200 μm thick, 1×3 sq. inches) ([10]).

The plates were screened against the neutrons coming directly from the betatron by means of a water wall 60 cm thick (Fig. 1). Also, a foil of lead 6 mm thick screened the plates against the low energy photons coming from the target.

([3]) P. R. BYERLEY and W. E. STEPHENS: *Phys. Rev.*, **81**, 473 (1951); **83**, 54 (1951).

([4]) G. A. PRICE: *Phys. Rev.*, **93**, 1279 (1954).

([5]) W. R. DIXON: *Can. Journ. Phys.*, **33**, 785 (1955).

([6]) M. E. TOMS and W. E. STEPHENS: *Phys. Rev.*, **108**, 77 (1957).

([7]) J. H. CARVER, R. D. EDGE and K. H. LOKAN: *Proc. Phys. Soc.*, A **70**, 415 (1957).

([8]) J. GOLDEMBERG and L. KATZ: *Can. Journ. Phys.*, **32**, 49 (1954).

([9]) F. FERRERO, R. MALVANO and C. TRIBUNO: *Nuovo Cimento*, **5**, 510 (1957).

([10]) We are very grateful to Dr. WALLER and Ilford Ltd. for helpful assistance in the quick supplying of the plates.

2·2. *Scanning and treatment of data.* – The plates, processed by standard methods, were scanned with 55× immersion oil Koristka objectives and 8× eyepieces. Binocular Koristka microscopes were employed.

This « slow » scanning was made in order to determine the investigated neutron spectra starting from rather low neutron energies (1 MeV, corresponding to 14 μm tracks). The conventional way of selecting tracks was followed ([11-21]): the tracks taking origin and coming to rest in the emulsion were considered only if their original direction fell into a « square pyramid » centered in the neutron beam direction and having a semiaperture of 15°.

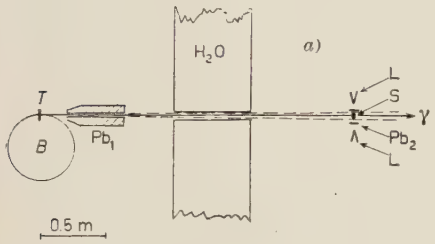

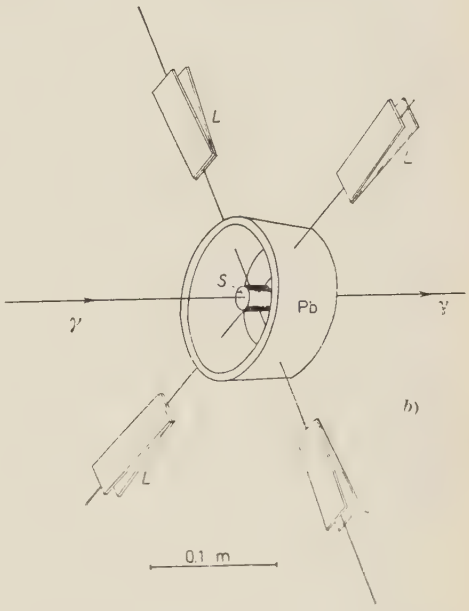

Fig. 1. – *a*) Experimental apparatus: B = betatron, T = target of the betatron; Pb_1 = lead collimator; S = scatterer target, L = photoplates; H_2O = water screen against neutrons from the betatron; Pb_2 = lead screen against low energy photon diffusion from S. *b*) S = scatterer target; L = photoplates; Pb = lead screen against low energy photon diffusion from S.

([11]) L. Rosen: *Nucleonics*, **11**, 7, 32 and **11**, 8, 38 (1953).
([12]) V. F. W. Weisskopf and D. H. Ewing: *Phys. Rev.*, **57**, 472 (1940).
([13]) H. Fesbach and V. F. Weisskopf: *Phys. Rev.*, **76**, 1550 (1949).
([14]) L. Katz and A. G. W. Cameron: *Can. Journ. Phys.*, **39**, 437 (1957).
([15]) S. A. Moszkowsky: *Handbuch der Physik*, **39**, 437 (1957).
([16]) L. I. Schiff: *Phys. Rev.*, **73**, 1311 (1948).
([17]) D. H. Wilkinson: *Physica*, **22**, 1039 (1956).
([18]) J. S. Levinger: *Phys. Rev.*, **84**, 43 (1951).
([19]) D. Walker: *Phys. Rev.*, **81**, 634 (1951); C. Levinthal and A. Silverman: *Phys. Rev.*, **82**, 822 (1951); J. C. Keck: *Phys. Rev.*, **85**, 410 (1952); J. W. Rosengren, and J. M. Dudley: *Phys. Rev.*, **89**, 603 (1953); A. Wattemberg, B. T. Feld and R. D. Goldbole: *Phys. Rev.*, **90**, 380 (1953).
([20]) M. M. Hoffmann and A. G. W. Cameron: *Phys. Rev.*, **92**, 1184 (1953).
([21]) H. T. Richards: *Phys. Rev.*, **59**, 796 (1941).

1999

In order to improve the statistics of the high energy « tail » of the spectrum we also made an additional « fast » scanning with 30× (instead of 55×) immersion oil Koristka objectives, and putting a much higher limitation on the minimum lenght l of the considered tracks ($l > 170$ μm). On the other hand the only required angular condition was on the dip angle θ ($|\theta| \leqslant 15°$).

As long as the high energy tail of a spectrum is concerned, this scanning method is faster by a factor of ~ 8. Besides, if azimuth angles $\varphi > 15°$ are considered, arriving for instance to $|\theta| \leqslant 30°$, another factor of about 2 is gained (see appendix).

A small area already scanned by the « slow » method, was re-examined by fast scanning in order to see if there was an appreciable loss of tracks. The result was negative: all the tracks fitting the required conditions were found again.

The obtained experimental data from the slow scanning were treated in the conventional way ([11]) taking into account (i) the useful solid angle of the recoil tracks in the center of mass system; (ii) the probability of escape of the tracks from the emulsion; (iii) the cross section for n, p collisions in the emulsion; (iv) the number of hydrogen atoms per unit of volume of nuclear emulsion; (v) the γ-ray absorption in the target S, and (vi) the neutron absorption in the target S and in the 6 mm lead screen.

Of course, the fast scanning, and the use of tracks rather inclined with respect to the neutron beam, makes it necessary to use a treatment of the experimental data somewhat more elaborate than the conventional one. This treatment is described in the appendix, where we also discuss the usefulness of this method.

2·3. *Background.* – The water wall proved to be extremely efficient in eliminating spurious neutrons.

The background was measured (i) by the scanning of the plates exposed without target, and (ii) by considering the tracks with origin in the emulsion but having wrong directions. Both methods showed that the background was negligible (less than 3%, that is much less than the statistical errors).

In the high energy region, the only background proved to come from cosmic ray stars. It was, also, negligible (3% for Ta and 6% for Cr plates).

3. – Results.

Table I shows the exposure and the scanning data.

The spectra obtained by the « slow » scanning were integrated with the much more precise high energy tails obtained by the fast scanning. The theo-

2000

TABLE I.

Element	Cr (*)		$^{181}_{73}$Ta	
Weight (g)	21.6		49	
(γ, n) Threshold (MeV)	11.54		7.6	
$E_{\gamma max}$ (MeV)	20	30	20	30
Dose (Roentgen)	1458	2607	1461	2788
— Slow scanning ($\varphi \leqslant 15°$):				
Scanned volume (mm^3)	127	113	62	124
Number of tracks $E_n \leqslant 5$ MeV	342	895	343	1286
Number of tracks $E_n > 5$ MeV	11	37	22	78
— Fast scanning ($E_n > 5$ MeV)				
Scanned volume (mm^3)	—	176	60	271
Number of tracks $\varphi \leqslant 15°$	—	63	15	177
Number of tracks $15° < \varphi \leqslant 30°$	—	48	13	141

(*) Cr element of natural isotopic composition: $^{50}_{24}$Cr: 4.4 %; $^{52}_{24}$Cr: 83.7 %; $^{53}_{24}$Cr: 9.5 %; $^{54}_{24}$Cr: 2.4 %. The indicated threshold for Cr is that of the most abundant isotope ^{52}Cr.

retical relation derived in the appendix (eq. (9)) was used to make the normalization.

The results are shown in Fig. 2 and 3.

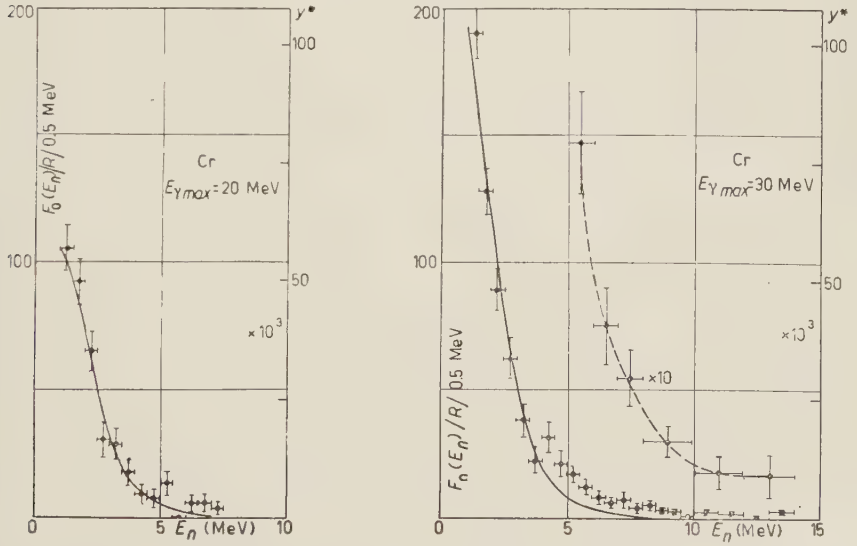

Fig. 2. – Energy spectrum of the photoneutrons from Cr. Experimental figures for the high energy tail are multiplied ×10. The continuous curve is the calculated evaporation spectrum (see text). Y*= neutrons /R/0.5 MeV/mole/$\Delta\Omega$.

3·1. *Low energy neutrons.* – The energy distribution of neutrons in the low-energy range can be compared, in the conventional way, with the evaporation theory ([12]) by means of the expression:

$$(1) \qquad F(E_n) = K \cdot E_n \cdot \sigma(E_n) \int_{B_0 + E_n}^{E_\beta} \omega(E_R) \cdot \sigma_{\gamma n}(E_\gamma) \cdot I(E_\gamma, E_\beta)\, \mathrm{d}E_\gamma ,$$

where: E_n = neutron energy;

$\sigma(E_n)$ = reaction cross-section for neutrons of energy E_n on residual nucleus;

B_0 = binding energy;

$\omega(E_R)$ = energy level density in residual nucleus with excitation energy $E_R = E_\gamma - B_0 - E_n$;

$\sigma_{\gamma n}(E_\gamma)$ = cross-section for the (γ, n) process;

$I(E_\gamma, E_\beta)$ = bremsstrahlung spectrum with maximum energy E_β.

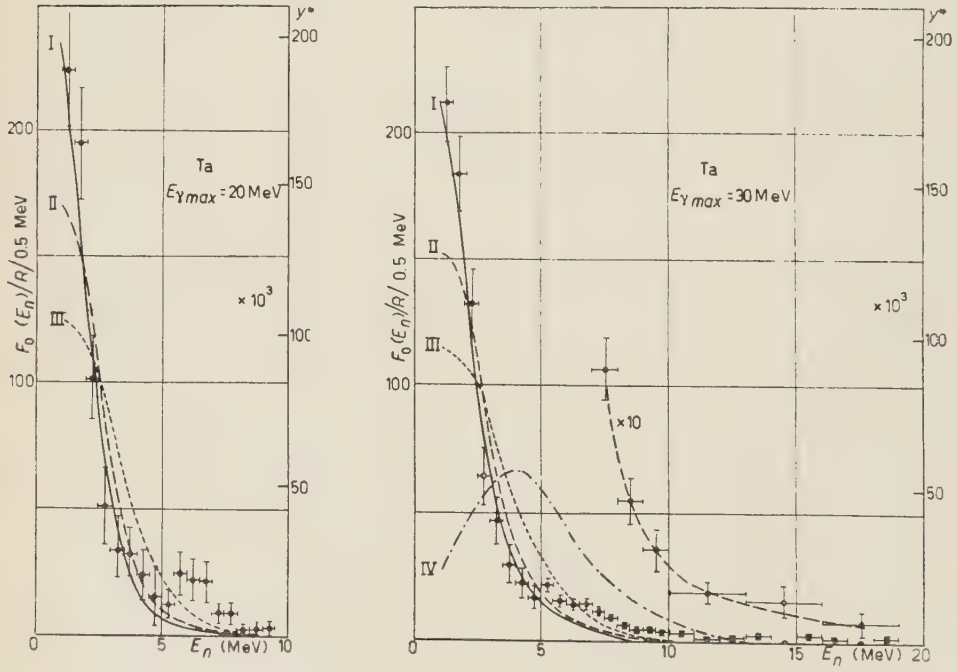

Fig. 3. – Energy spectrum of the photoneutrons from Ta. Experimental figures for the high energy tail are multiplied $\times 10$. The curves I, II, III and IV are the evaporation spectra calculated under different assumptions for the level density (see text).

2002

We made the calculations, inserting in eq. (1) the values available from the following authors: FESBACH *et al.* [13] for $\sigma(E_R)$, KATZ *et al.* [14] for $I(E_\gamma, E_\beta)$, GOLDEMBERG *et al.* [8] for the $\sigma_{\gamma n}$ of Cr, and CARVER *et al.* [7] for the $\sigma_{\gamma n}$ of Ta.

For the level density we used various different expressions.

The full line in Fig. 2, 3 gives the calculated spectrum under the assumption that the level density can be represented as [15]

$$\omega(E_R) = C \exp\left[2\sqrt{\alpha E_R}\right]; \qquad \alpha = \frac{\pi^2 A}{160}.$$

Alternative density level formulas deduced by different authors were used to calculate curve II [12], curve III [4] and curve IV [16]. The 4 theoretical curves I, II, III, IV are normalized to the experimental yield.

It is seen that the best fit with experiment is obtained under the first assumption.

However, it must be kept in mind that some caution is required about this sort of reasoning, because the direct emission of neutrons following resonance absorption could give a considerable contribution to the low energy part of the spectrum [17] and distort it appreciably. Similar effects can be given by the processes $(\gamma, 2n)$ and (γ, pn).

3·2. *High energy neutrons.* – The high energy « tails » in the spectra are, more directly related to our original problem, and we will discuss them in some detail. Unfortunately, in this region our results are still rather poor.

The first point is not a new one. Indeed several authors [3] to [6] found a small peak in the neutron spectrum at about $4 \div 6$ MeV, for lead, copper and bismuth, out of the evaporation theoretical curves. The peaks found by each single worker, are hardly statistically significant. We feel that all the quoted results, together with ours, definitely proof that such peaks really exist. In the 30 MeV spectra the high energy tails following these peaks account for $\sim 10\%$ of the total number of neutrons.

The tantalium yields at 20 and 30 MeV show the correct difference predicted by FERRERO *et al.* [1]. For $E_n > 5$ MeV there is an increase of a factor 1.20 ± 0.10 from the 20 MeV to the 30 MeV results. Taking into account that the Si detector used by FERRERO and co-workers reaches its full sensitivity only for $E_n \sim 6.5$ MeV our results give an increase of $\sim 30\%$, in good agreement with the Turin work, within experimental errors. It is remarkable that the whole difference between the 20 MeV and the 30 MeV spectra is in the neutron energy range from 10 to 19 MeV, that is in a range where no neutron is found at 20 MeV irradiation (under which the range of energy $E_n > 12$ MeV is interdicted by energy conservation). For $E_n < 10$ MeV, the two neutron spectra can be considered coincident within statistical errors.

2003

The Cr neutron yields are also in agreement with the measurements by FERRERO *et al.*, within the large statistical errors, with an increase of a factor ~ 3 from 20 to 30 MeV. In this case, however, the greater part of the observed increase is due to low energy ($5 \div 10$) MeV neutrons. Unfortunately we cannot deduce too many definite conclusions from this fact, for the lack of angular distributions and of a neutron spectrum at 25 MeV, that is at an energy which falls between the first and the second maximum found by FERRERO *et al.*

4. – Discussion.

The existence of a second resonance maximum for direct emission neutrons ($E_n > 5$ MeV), seems to be a rather diffused property of the nuclear photoeffect ([1]). It could be explained with the build up of a new mode of absorption in the 25 MeV energy range. For instance, one could assume that a quasi-deuteron absorption scheme ([18]) would be started in this energy region. Indeed, an order-of-magnitude estimate ([17]) gives for this sort of process a threshold as low as $\sim 55\, A^{-\frac{1}{3}}$ MeV, that is ~ 15 MeV for Cr and ~ 10 MeV for Ta.

Besides, a number of papers ([19,20]), demonstrate that this type of absorption is certainly important at high photon energies, and seems to be the most important one already at ~ 40 MeV bremsstrahlung irradiation ([20]).

However, the neutron spectrum in the case of the quasi-deuteron model has a characteristic form of the type $E_n^{-m_i}$, with $m_i = \text{constant} = m_1$ for $E_n < \frac{1}{2} E_{\beta_1} - B_0$, and $m_i = \text{constant} = m_2 > m_1$ at greater energy, B_0 being the binding energy of the last neutron in the bombarded nucleus.

This spectrum ought to be roughly the same for all elements, if one makes allowance of the different values of B_0.

About the values of m_2 there is no good agreement between the different authors ([19,20]). The measurements at rather low energy (40 MeV) seem to point to a value $m_2 = 4.4$. Our curves have lower value of m_2 than this (*i.e.* they have lower inclination in a log-log plot).

In any case, the high energy tail of the Ta spectrum which accounts for the whole second maximum rise of the yield curve, has definitely too high an energy for being explained with a quasi deuteron process.

Therefore, we consider this explanation to be very improbable, and we can try to fit the experimental results in the frame of the Wilkinson photoeffect model ([17]).

It is expected that the excited neutrons of low angular momentum, having smaller centrifugal barrier, give an appreciable contribution to the « direct » emission of high energy particles, even if their weight in the total absorption cross-section is relatively small. Now, the energy absorption E_γ associated

with $l \rightleftarrows l+1$ transitions having low values of l is often higher (in a square potential well) than that associated with higher l values. This would explain the second resonance maximum.

Now, in order to find a correlation between the neutron spectra and the yield curves, we can test the following temptative assumption. We suppose that all the photoneutrons come from the same shell of the bombarded nucleus. or from shells having about the same energy location in it. Then, the residual nucleus will be left always with about the same excitation energy ε, which must be rather small ((1÷3) MeV). The peaks mentioned under (i) in the last paragraph, roughly correspond to the energy of the giant resonance and this fact agrees with the mentioned assumptions [5]. Besides, the location of the thresholds in the yield curves by FERRERO *et al.* [1] shows that the residual nucleus must be left with a minimum excitation energy of ~ 2 MeV.

Now let be:

$B = B_0 + \varepsilon$

$\sigma_d(E_\gamma)$ the cross-section for (γ, n) direct process;

$F_{\beta_1}(E_n)$ the observed neutron spectrum under irradiation of bremsstrahlung, with electron energy E_{β_1};

$R_{E_0}(E_\beta)$ the activity observed in a neutron threshold detector, having the threshold E_0, under bombardment of the target by bremsstrahlung, with electron energy E_β.

We have, under the stated assumptions

$$E_\gamma = E_n + B\,,$$

$$F_{\beta_1}(E_n) = \sigma_d(E_n + B)\, I_\gamma(E_n + B,\, E_{\beta_0}) = \sigma_d(E_\gamma)\, I_\gamma(E_\gamma,\, E_{\beta_0})\,,$$

that is

$$\sigma_d(E_\gamma) = \frac{F_{\beta_0}(E_\gamma - B)}{I_\gamma(E_\gamma,\, E_{\beta_0})}\,.$$

Therefore, assuming that E_0 is a neutron energy so high that only the direct process can contribute to R_{E_0}, we obtain:

$$R_{E_0}(E_\beta) = \int_{E_0+B}^{E_\beta} F_{\beta_0}(E_\gamma - B)\, \frac{I(E_\gamma,\, E_\beta)}{I(E_\gamma,\, E_{\beta_0})}\, \mathrm{d}E_\gamma\,. \tag{2}$$

In the cases of Ta and Cr, FERRERO *et al.* [1] measured $R_{E_0}(E_\beta)$ with $E_0 \sim 5$ MeV and E_β variable in the range $E_\beta < 30$ MeV, while we measured $F_{\beta_1}(E_n)$ for $E_{\beta_1} = 20$ and 30 MeV.

Therefore we can try to test eq. (2), calculating the expected form of $R_{E_n}(E_\beta)$ from our F results, under the extreme assumptions stated above. The calculations were made numerically using the known bremsstrahlung functions ([14]). Fig. 4 shows the results (full line) in comparison with the R functions measured by FERRERO *et al.* ([1]) (broken line).

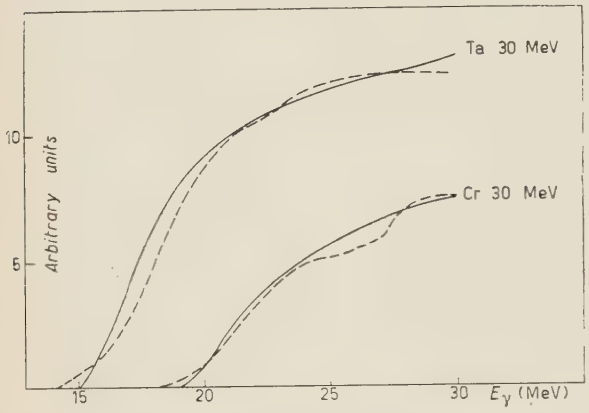

Fig. 4. – Experimental yields of high energy neutrons (broken lines) compared to the calculated yields derived by our spectra (full lines).

It is seen that there is a remarkable similarity between our calculated curves and the yield curves obtained by FERRERO *et al.*

In the Ta case, with $\varepsilon = 2$ MeV, one obtains an agreement as good as can be expected. The second maximum rise is not clearly visible, but this could be attributed to a « round off » of a curve calculated starting from a reduced number of experimental results.

In the Cr case, with $\varepsilon = 1$ we see a somewhat greater difference.

This different situation, could be explained simply with the fact that the second maximum in Cr is much more pronounced than in the Ta case.

On the other hand, it could also be fitted with the Wilkinson model supposing that the above « one level » assumption is correct only in the Ta case, and not in the Cr case.

The neutron spectrum from the direct photoemission process is related to the value of the initial and final energy levels involved in the transition. These energy levels can very well be distributed in different ways for different nuclei, so as to give rise to some variation of the neutron spectra.

Indeed, in the case of Cr, the low angular momentum transition is expected to be a $2s \to 2p$ transition which corresponds to an initial energy level considerably lower than that of the principal $1d \to 1f$ transition. On the other hand, the transitions involved in the case of Ta could be the $3p \to 3d$ and $1h \to 1i$; in this case a definite location cannot be assigned to the involved shell levels because of the well known uncertainties of the shell model in this region. Moreover the Ta nucleus has a large spheroidal deformation. Our results could be explained by supposing that the initial level of the low angular momentum transition has about the same energy as that of the principal transition. Very rough estimates of the strength of indicated transitions, making allowance for the penetrations through the centrifugal barriers, give

2006

the correct order of magnitude for the yields. We feel that at the present stage of development of the theory and of the experimental knowledge it is not worth while making more quantitative and detailed considerations. Further work is in progress.

5. – Conclusions.

Summarizing, the results of the present work are the following:

(i) The well-known high energy tail of the photoneutrons, coming from some direct process, shows, also in Cr and Ta, the small maxima at (5÷6) MeV neutron energy, already found in other elements. The tail accounts for $\sim 10\%$ of all the photoneutrons observed ($E_n > 1$ MeV).

(ii) The increase in the yield of the high energy tails from 20 to 30 MeV in Cr and Ta is consistent with the second maximum in the cross-section found by FERRERO *et al.* [1].

(iii) The interpretation of this second maximum on the ground of a quasi-deuteron absorption process seems to be excluded. A $(\gamma, 2n)$ process is also excluded.

(iv) Our data, together with the Ferrero results, are not in contradiction with Wilkinson's absorption model, with some particularization of the shells from which the high energy neutrons are supposed to come.

* * *

Our thanks are due to Prof. R. RICAMO and Prof. G. WATAGHIN who put at our disposal the means for making the present work.

We thank Prof. M. CINI, Dr. A. AGODI and Dr. R. MALVANO for many illuminating discussions. We thank also all the colleagues of the laboratories of Catania and Turin for friendly help in the exposure and processing of plates.

APPENDIX

Use of tracks with $|\vartheta| < 15°$ and $15° < |\varphi| < 30°$.

Suppose that a neutron incides on a photoplate at grazing incidence, *i.e.* with an angle $\simeq 0$, and collides with a hydrogen nucleus of the emulsion.

The neutron energy E_n, the recoil proton energy E_p and the angle ψ between the directions of flight of the two particles are connected by the well

2007

known relation:

$$E_p = E_n \cos^2 \psi \,. \tag{3}$$

Let ϑ be the dip angle of the proton track and φ its azimuth angle, counted from the direction of flight of the incident neutron beam. Then

$$\cos \psi = \cos \vartheta \cos \varphi \,. \tag{4}$$

The method generally followed ([21,11]) for analysing the recoil proton experimental spectra is to consider only the proton tracks having initial direction included in a « square » pyramid defined by $|\varphi| < \vartheta_0$ $|\vartheta| < \vartheta_0$.

The limiting angle is small (for instance $\vartheta_0 = 15°$), and therefore it is possible to ignore the small percentage difference between the neutron energy E_n and the recoil proton energy E_p, or, at most, to apply to E_p a mean correction deduced by eq. (3), weighting on the angular distribution of protons. The measured range l of the proton tracks ending in emulsion gives directly $E_n \simeq E_p$.

In order to obtain the incident neutron spectrum, the experimental proton spectrum must be multiplied by the factor

$$f(E_n) = \frac{K}{\Theta P(E_n) \sigma(E_n)} \,, \tag{5}$$

where: Θ = solid angle subtended by the considered pyramid in the center of mass system;

$\sigma(E_n)$ = cross-section for the neutron-proton collision;

$P(E_n)$ = probability that the proton track ends its range in the emulsion.

The constant K is 4π divided by the number of hydrogen atoms in the scanned volume.

This procedure has some important advantages. It spares many time-consuming calculations. The proton energy distribution is similar to that of neutrons, and not much softer, as it becomes (see eq. (3)) if one takes into account all proton tracks; for high values of ψ one would be obliged to consider a lot of very short tracks and the measured values of E_n would depend critically on the measurement of ψ. Besides, the background of spurious tracks, which have a quasi isotropic distribution and generally are of low energy, would affect much more the measured spectra.

However, if one is interested in obtaining the maximum accuracy for the high energy « tail » of a neutron spectrum it can be useful to take a « rectangular » pyramid defined by

$$|\vartheta| < \vartheta_0 \,, \qquad |\varphi| < \varphi_0 \,, \qquad \text{with } \varphi_0 > \vartheta_0 \tag{6}$$

putting at the same time a limitation on the minimum lenght of proton tracks to be considered (that is $E_p > E_{p_0}$).

2008

This requires some additional calculations, and the choice of the method must be made from a balance between the scanning time and the time requested for the necessary treatment of data.

Let us examine this treatment.

a) Calculation of the incident flux of neutrons. – The flux of neutrons is calculated taking into account the relation between the solid angle Θ in the center of mass system and the solid angle Ω in the laboratory system.

We have:

$$(7) \qquad \mathrm{d}\Theta = 4\cos\psi\,\mathrm{d}\Omega\,.$$

Making use of the « natural » spherical co-ordinate system of the plate (ϑ = dip angle = « latitude », φ = « longitude ») we obtain

$$(8) \qquad \mathrm{d}\Theta = 4\cos\vartheta\cos\varphi\,\mathrm{d}\Omega = 4\cos\varphi\cos^2\vartheta\,\mathrm{d}\vartheta\,\mathrm{d}\varphi\,.$$

The advantage of this equation is that the two variables φ and ϑ are separated.

By integration, with the limiting conditions (6), one obtains:

$$(9) \qquad \Theta = 8[\sin\vartheta_0\cos\vartheta_0 + \vartheta_0]\sin\varphi_0 = A(\vartheta_0)\sin\varphi_0\,.$$

In the limiting case $\varphi_0 = \vartheta_0 \ll \pi/2$ this reduces to the known value ([21])

$$\Theta = 16\sin^2\vartheta_0\,.$$

Eq. (9) shows that if one takes different values of φ_0, for a fixed value of ϑ_0 the number of neutrons giving recoil protons in the pyramid (6) varies as $\sin\varphi_0$. For instance taking $\varphi_0 = 30°$ instead of $\varphi_0 = 15° = \vartheta_0$ one gains a factor $0.50/0.26 \sim 2$. From the statistical point of view, this advantage is somewhat increased by the fact that $P(l)$ is a decreasing function, that is, that shorter proton tracks have a higher probability of ending in the emulsion.

b) Correction for the tracks which do not come to rest in the emulsion. – In equation (3) is implicit the simplifying assumption

$$E_n \simeq E_p\,,$$

from which follows

$$P(l) = P(E_p) \simeq P(E_n)\,.$$

This assumption must fall, so that the probability P must be calculated starting from the energy E_p of any observed proton. However, the form of the function $P(l)$ remains *unaltered.*

Indeed, the probability that a track of length l comes to rest in the emulsion is dependent on l, on the maximum accepted dip angle ϑ_0 and, besides, on the distribution in ϑ of the tracks. Now, as long as the angular distribution of protons is isotropic in the center of mass system, eq. (8) says that the ϑ distribution of the tracks having any fixed value of φ is independent of φ.

So, the practical procedure of treating the data is as follows.

a) Proton tracks fitting the conditions (6) are sorted following their energy E_p and their azimuth angle φ.

b) For $\varphi < 15°$ the normal procedure is applied.

c) For $\varphi > 15°$ the tracks are sorted in a number of φ intervals, chosen in a convenient way, so that $\cos^2\varphi$ may be considered a constant, $\langle\cos^2\varphi\rangle$ say, within each of them.

d) The number of proton tracks in any chosen E_p, interval is corrected by applying the appropriated $P(l)$ correction.

e) The corrected number of tracks is inserted in the E_n spectrum by application of eq.

$$E_n = \frac{E_p}{\cos^2\varphi\,\cos^2\vartheta} \simeq \frac{E_p}{\langle\cos^2\varphi\rangle}\,.$$

RIASSUNTO

Si studiano gli spettri energetici dei fotoneutroni emessi a 90° dal Cr e dal Ta per effetto dei raggi γ di bremsstrahlung di 20 e 30 MeV. A tale scopo si utilizzano i protoni di rinculo trovati in emulsioni nucleari, mediante un metodo di esplorazione particolarmente adatto allo studio della parte più energica di ogni singolo spettro. I risultati sono in accordo con quelli di FERRERO *et al.* [1]) relativi all'esistenza di un secondo massimo della sezione d'urto. La possibilità di interpretare il secondo massimo mediante un processo d'assorbimento del tipo quasi-deutone sembra da escludere. Un tentativo di spiegazione dei risultati sperimentali viene preso in esame e discusso.

2010

IL NUOVO CIMENTO Vol. IX, N. 1 1° Luglio 1958

On the Derivation of Rate Equations.

R. Ingraham

Department of Physics, New Mexico College of A. & M., State College - New Mexico

(ricevuto il 28 Marzo 1958)

Summary. — Reasons are given four doubting that irreversible behavior can be *derived* from mechanics without the various traditional averaging processes. A critical study of the Van Hove-Brout-Prigogine long time-weak coupling theory which dispenses with these averages is made. The two main objections are 1) mathematical inconsistencies in the quantum-mechanical formulation of the « diagonal singularity » of the mixing perturbation, supposedly responsible for the irreversibility, and 2) a physically inadmissible prescription for treating poles in improper energy integrals. Particular consequences are 1) an ambiguous prescription for evaluating the long time-weak coupling limit of improper integrals and 2) violation of the unitarity of the transition operator, respectively. Diagonal singularity in the « continuum limit » is reformulated. The limit transition operator is explicitly evaluated and exhibits only reversible behavior.

1. – Introduction.

Rate equations describing the time evolution of the relative populations x_n of the levels n of a physical system, of the form

$$\dot{x}_n = \sum_{m \neq n} (W_{nm} x_m - W_{mn} x_n) \equiv \sum_m A_{nm} x_m \,, \tag{1.1}$$

have irreversibility (*e.g.*, dissipativity, entropy increase) built into them. Here W_{nm} is the probability per unit time of the transition $n \to m$, and the conservation of the number of constituent elements of the system is expressed by $\sum A_{nm} = 0$. For instance, one can prove quite generally from Eq. (1.1),

2011

assuming about the W_{mn} only that one has detailed balance at equilibrium,

$$\exp[-\beta E_m]W_{nm} = \exp[-\beta E_n]W_{mn}\,, \tag{1.2}$$

that the system relaxes to a Boltzmann distribution at $t = \infty$ and that therefore its entropy increases up to its maximum value [1]. Again, the time-behavior of the total energy is determinable from the exact solution of Eq. (1.1) as [1]

$$E(t) = \sum_n \left(Z^{-1}E_n \exp[-\beta E_n] + \sum_{j=1}^{\infty} c_j \psi_j(n) E_n \exp[\lambda_j t]\right)\,. \tag{1.3}$$

Hence energy is dissipated since the $\lambda_j < 0$. For a collection of oscillators at a definite temperature immersed in a heat bath at a lower temperature this takes the simple single lifetime form of Landau-Teller [2]

$$\frac{E(t) - E(\infty)}{E(0) - E(\infty)} = \exp[-\tau]\,, \tag{1.4}$$

where $\tau \equiv \varkappa t(1 - \exp[-\theta])$ ($\varkappa$ is an inverse time characteristic of the interaction, and $\theta = \hbar\omega/kT$) is the dimensionless time.

Derivations of rate-type equations themselves, or irreversible behavior of the type proceeding from a rate equation, from the reversible equations of mechanics have been mainly of one kind. Examples are: the derivation of the Boltzmann equation for a single gas particle in classical [3] and in quantum mechanics [4], the formulation of classical and quantum mechanical H-theorems [5], and the classical [1,2] and lately quantum mechanical treatments [6]

---

[1] See E. Montroll and K. Shuler: *Technical Note BN-94* (Institute for Fluid Dynamics and Applied Mathematics, University of Maryland); Part 3. The extra assumption that the largest eigenvalue of a certain symmetric matrix constructible from W is zero and is non-degenerate is also made here. But recently Dr. Shoon Kim has proved the remarkable fact that the latter property follows merely from the detailed balance assumption (1.2).

[2] E. Montroll and K. Shuler: *Technical Note BN-70* (Institute for Fluid Dynamics and Applied Mathematics, University of Maryland); Part 1.

[3] J. Kirkwood: *Journ. Chem. Phys.*, **14**, 180 (1946); **15**, 72 (1947); M. Born. and H. Green: *A General Kinetic Theory of Liquids* (Cambridge, 1949); N. Bogoljubov: *Journ. Phys. USSR*, **10**, 265 (1946).

[4] H. Mori and S. Ono: *Progr. Theor. Phys.*, (*Japan*), **8**, 327 (1952); S. Ono: *Progr. Theor. Phys.* (*Japan*), **12**, 113 (1954); J. Ross and J. Kirkwood: *Journ. Chem. Phys.*, **22**, 1094 (1954).

[5] See say R. Tolman: *The Principles of Statistical Mechanics* (Oxford, 1938); Chapter 12.

[6] F. Bloch: *Phys. Rev.*, **105**, 1206 (1957).

2012

of small systems immersed in heat baths. What we want to emphasize here is that all these treatments have a common guiding principle: that one can obtain irreversible effects only by sacrificing the maximum information about the system to which we are in principle entitled by mechanics. Allow us to belabor for a moment this perhaps well-known point because of its importance for this paper. To get a Boltzmann equation one averages away a precise knowledge of the positions in phase space of all the other particles of the gas to come from the n-particle distribution, whose exact behavior one knows in principle, to the 1-particle distribution of interest. In addition, one often performs certain time averages as well. In the formulation of H-theorems, one defines an entropy in terms of a coarse-grained distribution which is a certain average of the fine-grained distribution, so that one is effectively giving up some information about *all* of the particles of the system impartially. This entropy is then found to increase in time. In heat bath relaxation problems one divides the system into two parts, a large and a small component, where one wants to follows the evolution of the small subsystem in a detailed way. One renounces, however, a detailed knowledge of the large subsystem by treating it as a thermodynamical system of which only a few gross properties, such as its temperature, are known.

Another, quite different, idea as to the derivation of irreversibility has been presented by VAN HOVE in quantum mechanics (7) and by BROUT and PRIGOGINE in classical mechanics (8). They assert that irreversibility is a consequence of a few weak assumptions on the « big » system like the largeness of self-energy effects relative to proper interaction effects and the weakness of the coupling, so that if the initial spread is smooth enough, one will see irreversible behavior emerging after long times. What is important here is that they want to obtain irreversible effects while retaining the maximum information permitted by statistical mechanics. That is, they derive rate equations without any of the averaging processes inherent in all the theories described above. This paper is a critical study of their method, prompted by the strong feeling that both schools of thought cannot be right.

It is shown that these attempts fail. That is, the rate equations which are finally written down are not mathematical consequences of the equations from which they start. Viewed simply as postulated, these rate equations might well have some physical validity—we do not, however, go into this question. Our point is that they cannot be *derived* by the method of I and II from the basic mechanical equations. The rate equations were « derived » on the basis of an ambiguous, « continuum limit » formalism for evaluating improper energy integrals in combination with a physically unsuitable prescription

(7) L. VAN HOVE: *Physica*, **21**, 517 (1955), referred to hereafter as I.

(8) R. BROUT and I. PRIGOGINE: *Physica*, **22**, 621 (1956), referred to hereafter as II.

2013

for handling the singularities. Underlying both these faults is the failure to describe adequately the passage to the limit $N \to \infty$ of a large but finite system of N degrees of freedom. For example, the « continuum limit » as given in I contains mathematical inconsistencies, and allows the formalism to converge to several different answers as desired, depending on how it is manipulated. These meaningless features do not arise if the limit $N \to \infty$ in systems of « large self-energy » etc., is formulated carefully. Again, the prescription for handling energy poles in both I and II is physically inadmissible in that it could never be attained as the limit $N \to \infty$ of a sequence of finite systems, regardless of the great liberty we have in specifying just how the spectrum shall fill up to the continuum. Further clarification of these objections will be postponed to Sect. **3** and **4** where the details will be made abundantly clear. Of course, we know such results must fail mathematically since they violate the well-known theorems in classical and quantum mechanics on the conservation of the energy, the microscopic entropy, and so on of a closed system. These theorems hold regardless of the « size » of the system, the weakness of the coupling, the time interval, the initial configuration, etc. *i.e.*, they hold in the relevant limits, those taken in I and II.

These authors exploit the facility with integrals gained by field theorists in attacking perturbation theory to all orders. Therefore, as an introduction to their more complicated cases, we shall treat perhaps the simplest case in quantum mechanics by this power series method in the next section. It will serve the double purpose of familiarizing the reader with these perturbation techniques applied to the case of a *finite time interval* (not encountered or, at least, needed heretofore in field theory) and of providing us with a check that we get back the expected properties associated with reversibility (unitarity of the transition operator, etc.) by this method. In fact, we think that this exercise may also have an independent interest, since it provides an explicit way to examine transient behavior of systems too complicated to solve in closed form otherwise but still simple enough so that the power series may be summed for some particular finite time or set of times (9).

2. - The linearly perturbed oscillator by the power series method.

Consider a linearly perturbed oscillator with Hamiltonian

$$H = H_0 + \lambda Q \,, \tag{2.1}$$

where H_0 is the usual free Hamiltonian, Q is the oscillator displacement, and λ is a small parameter. The solution of the Schrödinger equation in interaction

(9) By the substitution $it \to \beta$ and the taking of the trace one has then also the partition function of the system at a set of non-zero temperatures.

representation (defined by $\Phi(t) = \exp[iH_0 t]\Psi(t)$, where $\Phi(t)$ and $\Psi(t)$ are the state vectors in interaction and Schrödinger representations respectively) is

$$\Phi(t) = U(t)\,\Phi(0)\,, \tag{2.2}$$

where

$$U(t) = \exp[iH_0 t]\exp[-iHt] \tag{2.3}$$

is the unitary transition operator (units: $\hbar = 1$). We want to study the time evolution of the system as transitions between the stationary states $|n\rangle$ of the unperturbed system, hence we shall expand $U(t)$ as a power series in λ and then take matrix elements with respect to the $|n\rangle$. We get first [10]

$$\begin{cases} U(t) = \sum_{p=0}^{\infty} U_p(t)\,, \\ U_p(t) = (-i\lambda)^p \int_0^t \mathrm{d}t_1 \int_0^{t_1} \mathrm{d}t_2 \ldots \int_0^{t_{p-1}} \mathrm{d}t_p\, Q_{\mathrm{int}}(1)\,Q_{\mathrm{int}}(2)\ldots Q_{\mathrm{int}}(p)\,, \end{cases} \tag{2.4}$$

where $Q_{\mathrm{int}}(k)$ stands for $Q_{\mathrm{int}}(t_k)$ and

$$Q_{\mathrm{int}}(t) \equiv \exp[iH_0 t]Q\exp[-iH_0 t] = a\exp[-i\omega t] + a^*\exp[i\omega t]\,. \tag{2.5}$$

The creation and annihilation operators satisfy

$$[a, a^*] = 1\,, \tag{2.6}$$

ω is the oscillator frequency, and the normalization of Q_{int} has been absorbed into λ. This is the form in which the integrations are actually performed in I and II; it is rendered difficult by the appearance of the integration variables also in the limits of integration. In our simple case (which is also the case of the various field theories) one can use first the time-ordering formalism to make all the integrals independent (all with the common limits 0 to t) and, second, because the perturbing energy is simply a sum of an annihilation and a creation operator, express the time-ordered integrand as a sum of « normal » products. The time-ordering formalism can of course be used on the more general perturbations of I and II, but there is generally no advantage in this because then the time-ordered integrands do not admit a simple decomposition into sums of operator products in « normal » form. Although the following is of course

[10] One way of getting this expansion is to verify that $i\dot{U} = \lambda Q_{\mathrm{int}} U$, of which the solution is known to be Eq. (2.4).

very well known from field theory, we want to go through it in some detail for the benefit of readers in statistical mechanics who may not be so familiar with these techniques as the field theorists.

We can write the right member of Eq. (2.4) with all the integrals of the form $\int_0^t$ if we multiply by $(p!)^{-1}$ and prefix the integrand with P (which, acting on a product of operator functions of time, orders them with the later times standing to the left). Now if we write $Q_{\text{int}}(k) = Q^-(k) + Q^+(k)$ (we drop the subscript «int») where

$$Q^-(k) \equiv a \exp[-i\omega t_k], \qquad Q^+(k) \equiv a^* \exp[i\omega t_k], \tag{2.7}$$

the formula

$$PQ(1)Q(2) = Q^+(1)Q(2) + Q(2)Q^-(1) + \\ + [Q^-(1), Q(2)]\theta(1-2) + [Q(2), Q^+(1)]\theta(2-1), \tag{2.8}$$

where $\theta(1\text{-}2) \equiv \theta(t_1 - t_2)$ etc. and $\theta(x) = +1$ if $x > 0$, $= 0$ if $x < 0$, follows directly from the definition of P. The first two terms (four if we expand $Q(2)$ into its positive and negative frequency parts) has the property that in each term the annihilators stand to the right of the creators, and is defined as the normal form of the (two factor) product $Q(1)Q(2)$ and written $:Q(1)Q(2):$. (The normal form of a product of any number of Q's is defined the same way.) The second two terms are ordinary numbers and define the function of $t_1 - t_2$

$$D_c(1-2) \equiv \exp[-i\omega(t_1 - t_2)]\theta(1-2) + \exp[i\omega(t_1 - t_2]\theta(2-1), \tag{2.9}$$

which will be of great importance for the topic at hand. The commutators were evaluated with Eq. (2.6). A theorem in field theory then says that by iterating Eq. (2.8), the time-ordered product of $Q(1)\cdots Q(p)$ can be reduced to a sum of products of Q's in normal form, each multiplied by a number of D_c functions:

$$PQ(1)\cdots Q(p) = \sum_{\text{partitions}} :Q(l_1)\cdots Q(l_{p-2q}): D_c(i_1 - j_1)\cdots D_c(i_q - j_q). \tag{2.10}$$

The precise definition of the sum over partitions is as follows: one selects q $(0 \leqslant q \leqslant [p/2])$ pairs of integers from $1, \ldots p$: (i_1, j_1), (i_2, j_2), ..., (i_q, j_q); one replaces the pair $Q(i_1)$, $Q(j_1)$ by $D_c(i_1 - j_1)$; ..., $Q(i_q)$, $Q(j_q)$ by $D_c(i_q - j_q)$, then collects the remaining Q's, $Q(l_1)$, $Q(l_2)$, ..., $Q(l_{p-2q})$ into the ordered product

2016

$:Q(l_1)\dots Q(l_{p-2q}):$. This is then done in all possible ways [11] for each q between 0 and $[p/2]$. Therefore we get

$$U_p(t) = \frac{(-i\lambda)^p}{p!}\int_0^t \mathrm{d}t_1 \dots \int_0^t \mathrm{d}t_p \sum_{\text{partitions}} :Q(l_1)\dots Q(l_{p-2q}): D_c(i_1 - j_1)\dots D(i_q - j_q)\,. \tag{2.11}$$

The integrand is thus decomposed into a sum of terms of the type

$$D_c(1-2)D_c(3-4)\dots D_c(2q-1-2q)Q^+(2q+1)\dots \cdot Q^+(2q+k)Q^-(2q+k+1)\dots Q^-(p) \tag{2.12}$$

and the integrals can be performed. We use

$$\begin{cases} \displaystyle\int_0^t Q^+(t')\,\mathrm{d}t' = \frac{1}{i\omega}\,(\exp[-i\omega t]-1)a^* \equiv \frac{1}{i\omega}\,\varrho(t)a^* \\ \displaystyle\int_0^t Q^-(t')\,\mathrm{d}t' = -\frac{1}{i\omega}\,\varrho(t)^* a \end{cases} \tag{2.13}$$

and the most interesting for our purposes,

$$\int_0^t \mathrm{d}t' \int_0^t \mathrm{d}t''\, D_c(t'-t'') = 2\left(\frac{t}{i\omega} - \frac{1}{\omega^2}\,\varrho(t)^*\right). \tag{2.14}$$

The integral of the expression (2.12) becomes

$$\left[\frac{\varrho(t)}{i\omega}\right]^k \left[\frac{\varrho(t)^*}{-i\omega}\right]^{p-k-2q} 2^q \left[\frac{t}{i\omega} - \frac{1}{\omega^2}\,\varrho(t)^*\right]^q (a^*)^k a^{p-k-2q}\,. \tag{2.15}$$

Multiplying by $(-i\lambda)^p/p!$ and summing over partitions, then over p, we have evaluated $U(t)$ explicitly as a power series. Eq. (2.15) is in convenient form for studying the transitions between the levels n of the unperturbed oscillator, for instance the term (2.15) contributes only to the transitions $n \to n+2q+2k-p$ involving the net exchange of $2q+2k-p$ quanta. In Eq. (2.11) with Eq. (2.15) we have reached a form sufficient for our purpose here.

[11] The ordered product :: and D_c are symmetric functions of their arguments, and the « partitions » are therefore defined modulo any permutation of indices within these arguments.

2017

Now note that since

$$\varrho(t) = \varrho(t)^* = 0 \quad \text{for} \quad t = M\frac{2\pi}{\omega} \qquad (M = 0, 1, 2, \ldots), \tag{2.16}$$

the operator $U_p(t)$ vanishes at multiples of the period of the system if it contains any creation or annihilation operators at all. Therefore all $U_p(t)$ vanish for p odd, and for p even $= 2q$ only those $(2q-1)!!$ equal terms $2^q[t/i\omega]^q$ arising from the $(2q-1)!!$ ways of picking q pairs of integers from $1, \ldots, 2q$ survive in the sum over partitions. Therefore at these times we get

$$U(t) = \sum_{q=0}^{\infty} \frac{(-i\lambda)^{2q}}{(2q)!}(2q-1)!!\,2^q\left[\frac{t}{i\omega}\right]^q . \tag{2.17}$$

(For later reference note that Eq. (2.17) is also obtained if we take $\operatorname{Lim} U(t)$ as $\lambda \to 0$, $t \to \infty$ such that $\lambda^2 t$ remains constant.) With the identity $(2q)! = 2^q q!(2q-1)!!$ we can explicitly sum the series and get

$$U(t) = \exp\left[i\frac{\lambda^2}{\omega}t\right] \qquad \left(t = \frac{2\pi}{\omega},\ \frac{4\pi}{\omega},\ \frac{6\pi}{\omega}, \ldots\right). \tag{2.18}$$

So $U(t)$ reduces to a constant matrix, which is necessarily a unit since we are assured by the definition (2.3) of $U(t)$ that it must be unitary at all times. Combining Eq. (2.18) with Eq. (2.3), we see that

$$\exp[-iHt] = \exp\left[-i\left(H_0 - \frac{\lambda^2}{\omega}\right)t\right], \tag{2.19}$$

at these times, so that there is a level shift $\Delta = -\lambda^2/\omega$ independent of the level, but of course no line width leading to a decay. In terms of the original λ of Eq. (2.1) this shift $-\lambda^2/\hbar\omega$ (ordinary units) reads $\Delta = -\lambda^2/2k$, k the spring constant, which is just the answer obtained by solving the problem directly. The answer (2.19) tells us that the system is evolving (at least at this discrete set of times) in a conservative and reversible way.

The value of this little example lies in the formal similarity of the analysis with that of I and II. There the double limiting process on λ and t mentioned above serves the same purpose as the choice of the finite times $M(2\pi/\omega)$ here: it picks out of an intractably large number of terms in $U_p(t)$ those few of the highest algebraic degree in t which can occur, which leads to an explicitly summable series. The main qualitative difference is that here the levels are discrete, so that the integration tricks which lead to a specious irreversibility cannot be performed.

2018

3. – The quantum mechanical derivation.

The system treated in I is specified by the perturbed Hamiltonian $H_0+\lambda V$. The two basic assumptions about the perturbation V are

$$(3.1)\quad \langle E'\alpha'|VAV|E\alpha\rangle = \\ = \int \mathrm{d}E''\,\mathrm{d}\alpha''\,A''\{\delta(E'-E)\,\delta(\alpha'-\alpha)\,W(E''\alpha'';\,E\alpha)+\langle E'\alpha'|\,Y(E''\alpha'')\,|E\alpha\rangle\},$$

where A is any constant of the unperturbed motion with eigenvalues A'', and

$$(3.2)\qquad W(E\alpha';\,E\alpha)\not\equiv 0\,.$$

Here E, α etc., are eigenvalues of a complete set of commuting observables (E is the energy), $W(E''\alpha'';\,E\alpha)\geqslant 0$, and $\langle E'\alpha'|\,Y(E''\alpha'')\,|E\alpha\rangle$ is assumed to have no $\delta(E'-E)$ singularity. The $\langle E'\alpha'|\,V\,|E\alpha\rangle$ themselves are assumed to be well defined for all values of the eigenvalues, in particular they have no $\delta(E'-E)$ singularity. The assumption that E runs over a continuous spectrum is essential, although the other degrees of freedom α may have discrete or continuous spectra indifferently.

The assumption (3.1) is supposed to express the characteristic of « big » systems responsible for self-energy effects large compared to the interaction energy of two different states, while the additional assumption (3.2) is to guarantee the irreversible effects. We shall postpone discussion of the physical content of these assumptions until we come to the critical evaluation of this method later in this section.

Then where $\hat{U}(t)\equiv$ the « $\lambda^2 t$ limit » (as we shall say) of the transition operator $U(t)$ in interaction representation,

$$(3.3)\qquad \hat{U}(t)\equiv \operatorname*{Lim}_{\lambda^2 t} U(t)\,,$$

meaning the limit

$$(3.4)\qquad \lambda\to 0 \quad \text{and} \quad t\to\infty \quad \text{such that} \quad \lambda^2 t=\text{const}\,,$$

the diagonal elements of the density matrix of the pure state E, α of the system at time t, $\langle E\alpha|\,\varrho(t)\,|E\alpha\rangle$, which are the population densities at the level E, α, take the following simple form in the $\lambda^2 t$ limit:

$$(3.5)\qquad \langle E\alpha|\,\varrho(t)\,|E\alpha\rangle \equiv \int \mathrm{d}E'\,\mathrm{d}\alpha'\,\mathrm{d}E''\,\mathrm{d}\alpha''\langle E\alpha|\,\hat{U}(t)\,|E'\alpha'\rangle^*\cdot \\ \cdot\langle E\alpha|\,\hat{U}(t)\,|E''\alpha''\rangle c(E'\alpha')^* c(E\alpha) = \int \mathrm{d}\alpha'\;P_t(E\alpha;\,E\alpha')\,|c(E\alpha)|^2\,.$$

2019

Here the initial state is $q = \int |E\alpha\rangle \, dE \, d\alpha \, c(E\alpha)$. VAN HOVE then proves that the quantity $P_t(E\alpha; E\alpha')$ satisfies a rate equation with transition probabilities $(E, \alpha) \leftarrow (E, \alpha')$ per unit time given by

$$2\pi\lambda^2 W(E\alpha'; E\alpha) . \tag{3.6}$$

By his assumption (3.2) these are non-vanishing. He thus apparently has arrived at rate equation type behavior at times $t = O(\lambda^{-2})$ without any of the averaging processes traditionally employed.

Our program in this section is first to point out the dubious features of this derivation. These are, mainly, 1) a contradiction of the unitarity of $\hat{U}(t)$ by the assumption (3.2) due to a physically inadmissible prescription for handling singular energy integrals; and 2) an essential ambiguity in evaluating the multiply improper integrals leading to $\hat{U}(t)$ whose root is the failure of the ansatz (3.1) correctly to describe the characteristic of « big » systems mentioned above. Secondly, by a better formulation of this characteristic and a more careful passage to the « continuum limit », we intend to show that rate equation type behavior does not occur.

First, then, let us write down the power series expansion of $U(t)$. One gets ([12]) Eq. (2.4) with $Q_{\text{int}} \to V_{\text{int}}$. ($V_{\text{int}}$ will now in general have no simple, single frequency time dependence like the right member of Eq. (2.5).) Taking matrix elements in the $(E, \alpha) - q$ diagonal representation, one finds to evaluate the integrals

$$\begin{aligned} \langle q' | U_p(t) | q \rangle = (-i\lambda)^p \int_0^t dt_p \int_0^{t_p} dt_{p-1} \dots \int_0^{t_2} dt_1 \int dq_{p-1} \dots dq_1 \cdot \\ \cdot \{ \exp [iE't_p] \langle q' | V | q_{p-1} \rangle \exp [-iE_{p-1}(t_p - t_{p-1})] \langle q_{p-1} | V | q_{p-2} \rangle \dots \\ \dots \exp [iE_2(t_3 - t_2)] \langle q_2 | V | q_1 \rangle \exp [-iE_1(t_2 - t_1)] \langle q_1 | V | q \rangle \exp [-iEt_1] \} . \end{aligned} \tag{3.7}$$

Our purpose now is not to recapitulate the whole vast and complex formalism of I but only to pick out of it those results which we need. It turns out that in the $\lambda^2 t$ limit the diagonal parts U_p^p of the U_p, with p even take the simple form ([13])

$$\langle q' | \hat{U}_p^p(t) \, q \rangle = \frac{[-\lambda^2 t F_0(q)]^m}{m!} \delta(q' - q) , \quad p = 2m, \tag{3.8}$$

([12]) I actually evaluates $\exp [-iHt]$ which is obtained from our result by prefixing the factor $\exp [-iH_0 t]$.

([13]) I, Eq. (5.7) with I, Eq. (5.5) and (5.4).

20201

where $F_0(q)$ will be defined later. For $\hat{U}_2$ in particular we have

$$\langle q' \,|\, \hat{U}_2(t) \,|\, q\rangle = \langle q' \,|\, \hat{U}_2^D(t) \,|\, q\rangle = -\lambda^2 t F_0(q)\,\delta(q'-q). \tag{3.9}$$

We note that $\hat{U}_2(t)$ is thus diagonal [14]. We give the proof of Eq. (3.9), which should suffice to illustrate the integration and limiting techniques leading to all these results. From Eq. (3.7) one gets

$$\langle q' \,|\, U_2(t) \,|\, q\rangle = (-i\lambda)^2 \int_0^t \mathrm{d}t_2 \exp\,[i(E'-E)t_2]\cdot \tag{3.10}$$

$$\cdot\left[\int_0^{t_2} \mathrm{d}t_1 \int \mathrm{d}q_1 \exp\,[i(E-E_1)(t_2-t_1)]\langle q' \,|\, V \,|\, q_1\rangle\langle q_1 \,|\, V \,|\, q\rangle\right],$$

after a slight manipulation of the exponentials. The ansatz (3.1) is now used to replace the $V \exp\,[i(E-H_0)(t_2-t_1)]V$ by its W part (the Y part gives zero in the $\lambda^2 t$ limit):

$$\begin{cases} \int \mathrm{d}q_1 A_1 \langle q' \,|\, V \,|\, q_1\rangle\langle q_1 \,|\, V \,|\, q\rangle \to \delta(q'-q)\int \mathrm{d}q_1 A_1 W(q_1; q), \\ A_1 = \exp\,[i(E-E_1)(t_2-t_1)]\,. \end{cases} \tag{3.11}$$

Then the $\exp\,[i(E'-E)t_2]$ can be replaced by 1 since it multiplies a $\delta(E'-E)$ and one obtains

$$\langle q' \,|\, \hat{U}_2(t) \,|\, q\rangle = \operatorname*{Lim}_{\lambda^2 t} \left\{(-i\lambda)^2\,\delta(q'-q)\int_0^t \mathrm{d}t_2 \cdot \right. \tag{3.12}$$

$$\left. \cdot\left[\int_0^{t_2} \mathrm{d}t_1 \int \mathrm{d}q_1 \exp\,[i(E-E_1)(t_2-t_1)]W(q_1; q)\right]\right\}.$$

Now we define μ and $F_\mu(q)$ by

$$\text{L.T.} \int_0^T \mathrm{d}\tau \int \mathrm{d}\varepsilon\, \mathrm{d}\alpha_1 \exp\,[-i\varepsilon\tau]W(E+\varepsilon, \alpha_1; E\alpha) \equiv T^\mu F_\mu(q)\,, \qquad (T>0), \tag{3.13}$$

where L.T. shall signify the leading term, *i.e.* the dominant term as $T \to \infty$ (In a sum of products of powers of T with exponentials in T, this will be the term of highest algebraic degree in T.) We emphasize that the integral (3.13) is improper due to the pole in the ε integral at $\varepsilon = 0$ and must be further de-

[14] I, Eq. (4.3). For $\hat{U}_2 = \hat{U}_2^W + \hat{U}_2^Y$ and $\hat{U}_2^Y$ vanishes by the first equation at the top of page 526.

1121

fined. *It can, in the last analysis, only be defined by our precise mode of passing from a discrete energy spectrum to the continuous spectrum of the « continuum limit. »* We shall discuss this crucial point later at the proper time. Van Hove's choice of definition of $\int \mathrm{d}\varepsilon\, f(\varepsilon)$ is in every case

$$\left(\frac{1}{\varepsilon}\right)_{VH} \equiv \operatorname*{Lim}_{\eta \to 0_+} \left(\frac{1}{\varepsilon - i\eta}\right), \tag{3.14}$$

which leads to $\mu = 0$ and

$$F_0(q) = \pi \int \mathrm{d}\alpha_1\, W(E\alpha_1;\, E\alpha) - i\mathcal{P}\int \mathrm{d}\alpha_1\, \mathrm{d}\varepsilon\, \frac{W(E+\varepsilon,\, \alpha,;\, E\alpha)}{\varepsilon}, \tag{3.15}$$

where $\mathcal{P}$ means the Cauchy principal part. Incidentally the choice (3.14) is made only tacitly in I; it is concealed in the integral formula ([15])

$$\int_0^T \mathrm{d}t \int \mathrm{d}\varepsilon\, \exp\,[i\varepsilon t]\, f(\varepsilon) = \pi\, \mathrm{Sgn}\, T\, f(0) + i\mathcal{P}\int \mathrm{d}\varepsilon \frac{f(\varepsilon)}{\varepsilon}, \tag{3.16}$$

which is simply quoted as « the well known asymptotic formula. » The double integral inside the square brackets in Eq. (3.12) takes the form of the left member of Eq. (3.13) with the substitutions $E_1 - E = \varepsilon$, $t_2 - t_1 = \tau$, and $t_2 = T$. Hence the double integral is independent of t_2 and equals $F_0(q)$. The remaining t_1 integral gives simply t so that one gets finally Eq. (3.9). A strictly analogous procedure gives Eq. (3.8) for the $\hat{U}_p^D$ with p even, if one decomposes the rightmost VAV product according to the ansatz (3.1), drops the Y part, then decomposes the next VAV product, drops the Y part, and so on for all $p/2$ VAV products in the integrand of Eq. (3.7). (In fact it gives $\hat{U}_p = \hat{U}_p^D$ so that the even $\hat{U}_p$ for $p > 2$ are also diagonal, although we need not use this fact here.)

The requirement that $U(t)$ be unitary gives

$$\left|\begin{array}{ll} a) & U_1^* = -\,U_1\,, \\ b) & U_2^* + U_2 = -\,U_1^* U_1\,, \\ c) & U_3^* + U_2^* U_1 + U_1^* U_2 + U_3 = 0\,, \\ d) & U_4^* + U_3^* U_1 + U_2^* U_2 + U_1^* U_3 + U_4 = 0\,, \\ & \text{etc.} \end{array}\right. \tag{3.17}$$

([15]) I, Eq. (3.3).

2052

These must hold of course at all times and for all values of λ, that is, they hold for the $\hat{U}_p$. Eq. (*a*) is satisfied merely in virtue of the hermiticity of V; Eq. (*b*), it can easily be verified, is satisfied identically here. We skip requirement (*c*) and examine (*d*). Now

$$\hat{U}_3^* \hat{U}_1 = \hat{U}_1^* \hat{U}_3 = 0 \,. \tag{3.18}$$

This follows from I, Eq. (6.6),

$$\langle \Phi_n | \Phi'_{n'} \rangle = 0 \,, \qquad n \neq n'. \tag{3.19}$$

where $\Phi_p[\ \tilde{U}_p(t)\varphi] = U_p(t)\varphi$ for p odd, in virtue of the arbitrariness of the initial states φ and φ'. (Proof of $\tilde{U}_p(t) = U_p(t)$ for p odd: definition of $\tilde{U}_p(t)$ in I, Eq. (6.2) with the remark that $U^W(t)$ arises only from the even $U_p(t)$, compare I Eq. (5.5), so that $U_p^W(t) = 0$ for p odd.) Therefore, *looking only at the diagonal part of Eq.* (*d*) in the $\lambda^2 t$ limit, we must have from Eq. (3.18)

$$\hat{U}_4^{*D} + \hat{U}_4^D = -(\hat{U}_2^* \hat{U}_2)^D \,. \tag{3.20}$$

Substituting into this equation from Eq. (3.8) for $p = 4$ and Eq. (3.9) and dividing out the common factor $\lambda^4 t^2 \delta(q' - q)$, we get

$$[F_0(q)^*]^2 + [F_0(q)]^2 = -2\,|F_0(q)|^2 \,. \tag{3.21}$$

Eq. (3.21) says that $\mathrm{Re}\, F_0(q) = 0$, or, with Eq. (3.15)

$$W(E\alpha_1;\, E\alpha) \equiv 0 \tag{3.22}$$

since $W(q_1; q)$ is non-negative and supposed to be continuous. This contradicts the assumption (3.2), gives no level widths for decay ([16]):

$$\Gamma(q) \equiv \lambda^2\, \mathrm{Re}\, F_0(q) = \pi\lambda^2 \int \mathrm{d}\alpha_1\, W(E\alpha_1;\, E\alpha) = 0 \,, \tag{3.23}$$

and gives vanishing transition probabilities (3.6) in the rate equation, so that it reduces to the triviality $\dot{P}_i(E\alpha; E\alpha') = 0$. That is to say, if we accept ansatz (3.1), then the unitarity of the transition operator for these systems puts some strong restrictions on the definition of the improper energy integral in Eq. (3.13), which is supposed to represent some reasonable limit of the sum over energies in the discrete cases. Namely, the restriction that $F(q)$ be

([16]) See I, p. 527 for this interpretation.

2023

pure imaginary. The prescription (3.14) is thus excluded, whereas an example of an admissible prescription would be $\mathcal{P}(1/\varepsilon)$.

The above was an *ad hominem* argument demonstrating that I fails to derive a rate equation even on the basis of its own assumptions. Now we want to present an argument that supersedes the above by showing that those assumptions themselves are untenable. The matrix elements of $\hat{U}_2$ have been evaluated above, Eq. (3.9); this leads immediately to

$$\langle q' \,|\, \hat{U}_2^* \hat{U}_2 \,|\, q \rangle = \lambda^4 t^2 \,|\, F_0(q) \,|^2 \, \delta(q' - q) \,. \tag{3.24}$$

This method of evaluation corresponds to applying the ansatz (3.1) first to the *rightmost* VAV product, then to the remaining VAV product, always dropping Y parts, in the quadruple time integral for $U_2^* U_2$ one gets from the power series expansion (3.7). But now there is another method of evaluating this expression. Namely, one can apply the ansatz (3.1) first to the *middle* VAV product, and then to the remaining (outside) VAV product in this quadruple time integral, dropping Y parts at each step (as is always understood). If one does this, one gets at first [17]

$$\langle q' \,|\, U_2^* U_2 \,|\, q \rangle' = \lambda^4 \, \delta(q' - q) \int_0^t \mathrm{d}t_2' \int_0^{t_2'} \mathrm{d}t_1' \int_0^t \mathrm{d}t_2 \int_0^{t_2} \mathrm{d}t_1 \int \mathrm{d}q_2 \, \mathrm{d}q_1 \cdot \tag{3.25}$$

$$\cdot \left\{ \exp\left[i E_2 \tau_2' \right] W(q_2 ; q_1) \exp\left[- i E_1 (\tau_2' - \tau_1') \right] W(q_1 ; q) \exp\left[- i E \tau_1' \right] \right\}, \qquad \tau_j' \equiv t_j - t_j' \,.$$

The prime on the matrix element indicates that it is evaluated by this second possible method. But is clear already at this stage that the two methods cannot yield the same result in general. For the first method gives a result proportional to $|F_0(q)|^2$ which is of the form $|\int \mathrm{d}q_1 \, W(q_1 ; q) f(q_1)|^2$ in the W kernel, whereas the second method gives a result of the form $\int \mathrm{d}q_2 \, \mathrm{d}q_1 \, h(q_2) \cdot W(q_2 ; q_1) \, k(q_1) \, W(q_1 ; q)$ in the W kernel. For arbitrary $W(q_1 ; q)$ these cannot be the same. According to I, in fact, the integral on the right in Eq. (3.25) would yield [18]

$$\langle q' \,|\, \hat{U}_2^* \hat{U}_2 \,|\, q \rangle' = (2\pi\lambda^2)^2 \frac{t^2}{2} \left| \int \mathrm{d}\alpha_2 \, \mathrm{d}\alpha_1 \, W(E\alpha_2 ; E\alpha_1) W(E\alpha_1 ; E\alpha) \right| \delta(q' - q) \,. \tag{3.26}$$

[17] This can be obtained directly from the formula given for $\langle \Phi_n \,|\, \Phi_n' \rangle$ (second formula on p. 529 of I) by taking $n=2$ and replacing $u^W(t)$ by $\exp[-iH_0 t]$. For this formula was in fact obtained by substituting $u^W(t_n - t_{n-1})$ for the $\exp[-iH_0(t_n - t_{n-1})]$ in $\varphi'^* U_n(t)^* U_n(t) \varphi$ (for reasons which don't concern us here) and then applying the ansatz (3.1) first to the *middle* VAV product, dropping the Y part, etc., and so on.

[18] In accordance with footnote [17], we must replace $u^W(t)$ by $\exp[-iH_0 t]$ everywhere in the integrand of I, Eq. (6.5), which amounts to setting $\lambda = 0$ in the exponentials there; and we specialize to $n=2$.

2024

Note in particular that the right member of Eq. (3.26) involves only the energy diagonal part of W, whereas $|F_0(q)|^2$ (see Eq. (3.15)) depends also on the energy off diagonal part.

We have thus obtained two different answers for $\hat{U}_2^* \hat{U}_2$ by applying the ansatz (3.1) in two different ways. One first might conclude that we have somehow overlooked certain combinations non-vanishing in the $\lambda^2 t$ limit by dropping the V parts in one of the two methods. But this is not tenable since if we had specialized to systems having strictly vanishing V parts, we would continue to get the same disagreement. The analysis which follows shows that the basic reason for this ambiguity is the self-inconsistency of the ansatz (3.1) in conjunction with the unsuitable prescription (3.14) for handling the singularities. The values of the integrals representing most of the $\hat{U}_\nu$, $\hat{U}_\nu^* \hat{U}_\varrho$ etc., in the « continuum limit » theory I, are afflicted with the same ambiguity; that is to say, with the ansatz (3.1) they are not well defined. A further type of ambiguity, which is avoided if one limits himself to multiple time integrals involving an *even* number of V's, arises from an inadequate prescription of just how the « continuum limit » is approached. The following example should suffice. Consider U_p for $p = 2m+1$ odd and apply the decomposition (3.1) successively to the m pairs VAV beginning with the rightmost pair. One gets

$$\langle q' | \hat{U}_\nu | q \rangle = \operatorname*{Lim}_{\lambda^2 t} \left\{ (-i\lambda)^p [F_0(q)]^m \left[\frac{t^m \exp\,[i(E'-E)t] - \delta_0^m}{i(E'-E)} \right] \langle q' | V | q \rangle \right\}. \tag{3.27}$$

Therefore for $m \neq 0$, $\langle E\alpha' | \hat{U}_\nu | E\alpha \rangle = 0$ or is divergent according as the $\lambda^2 t$ limit is taken first and then the limit $E' \to E$ or vice-versa.

We are therefore motivated to look more closely at the ansatz (3.1). This is supposed to express the limiting form of the following characteristic for systems of a large number N of degrees of freedom:

(3.28) *The diagonal terms in the product V^2 are larger than the off diagonal terms by a factor $O(N)$.*

Since the matrix elements of V are all about the same size, this means that in the sum

$$\sum_{q_1} \langle q' | V | q_1 \rangle \langle q_1 | V | q \rangle , \tag{3.28'}$$

there are roughly N times as many non-zero summands for $q' = q$ as there are for $q' \neq q$.

Now setting $A \equiv 1$ in Eq. (3.1), we get what appears to be a sort of continuum analogue of property (3.28); for the diagonal terms of V^2 are larger

than the off diagonal ones by a factor $\delta(E-E)\gg 1$ (N.B. $\langle q_1|Y(q')|q\rangle$ has no $\delta(E'-E)$ singularity by the assumption following Eq. (3.2).) Here let us assume with I

$$W(q_1;q)\simeq\langle q'|Y(q_1)|q\rangle = O(1)\,, \tag{3.29}$$

i.e., that these expressions are everywhere finite valued functions of their arguments with moderate average values of the order of unity, say, in suitable energy units. But since the A'' in Eq. (3.1) are arbitrary, equating their coefficients on both sides gives the equivalent statement of the ansatz

$$\langle q'|V|q_1\rangle\langle q_1|V|q\rangle = \delta(q'-q)\,W(q_1;q)+\langle q'|Y(q_1)|q\rangle\,. \tag{3.30}$$

This is clearly inconsistent with *any* estimate of the size of the ME (matrix elements) $\langle q'|V|q\rangle$. For taking $E'\neq E$ and any E_1 (we suppress the unimportant α dependence) one gets

$$\langle E_1|V|E\rangle = O\left[\{\langle E'|V|E_1\rangle\langle E_1|V|E\rangle\}^{\frac{1}{2}}\right] = O\left[\langle E'|Y(E_1)|E\rangle^{\frac{1}{2}}\right] = O(1)\,,$$

by Eq. (3.29). But then taking $E'=E$ and this E_1, one gets

$$\langle E_1|V|E\rangle = O\left[\{\delta(E-E)\,W(E_1;E)\}^{\frac{1}{2}}\right] = \left\{\delta(E-E)\right\}^{\frac{1}{2}}O(1)\gg O(1)\,,$$

by Eq. (3.29). That is, the equations (3.30) for the various values of the arguments are inconsistent.

The trouble lies in the following: the equivalent form of the anzatz, Eq. (3.30), shows that it concerns the *individual* ME $\langle q'|V|q\rangle$. Since these are all of about the same size, there cannot be any function which gets large of $O(N)$ in this equation. The property expressed by the statement (3.28), or (3.28′), which does involve a number $O(N)$ is a combinatorial property of the *sum* of these ME over all intermediate states and thus represents additional information not containable in any equation about the individual ME. The attempt to include the (continuum analogue of the) statement (3.28′) in Eq. (3.30) by putting in a function $\delta(q'-q)$ which does get large at certain values of the arguments must therefore lead to a mathematical inconsistency.

We shall therefore go back to the discrete case $N<\infty$, formulate the property (3.28) accurately, and then attempt to answer the question of whether a large system shows rate equation behavior in some asymptotic region by letting $N\to\infty$ at a suitable point. Let $\langle q'|V|q\rangle$ represent now the actual ME of the perturbing energy (not its density) of a large system of N degrees of freedom, and define

$$\langle q'|V|q_1\rangle\langle q_1|V|q\rangle \equiv \delta_{q'q}\omega(q_1;q)+\langle q'|y(q_1)|q\rangle\,, \tag{3.31}$$

2020

where $\langle q|y(q_1)|q\rangle = 0$. This defines

$$\omega(q_1; q) = |\langle q_1|V|q\rangle|^2 \geq 0\,,$$

with a similar expression for $\langle q'|y(q_1)|q\rangle$ which we shall not need. The property (3.28) is expressed by

$$\sum_{q_1} \omega(q_1; q) \simeq N \sum_{q_1} \langle q'|\overline{y(q_1)|q}\rangle\,, \tag{3.32}$$

where the bar denotes some average over q'. We actually want to assume a stronger ansatz, namely

$$\sum_{\alpha_1} \omega(E\alpha_1; E\alpha) \equiv N\omega(q) \simeq N \sum_{\alpha_1} \langle E\alpha'|y(E\alpha_1)|q\rangle\,, \qquad \text{(any } \alpha'\text{)}, \tag{3.33}$$

so that we shall be permitted to neglect *all* y parts relative to $N\omega(q)$ (*). The assumptions (3.32) and (3.33) say that not only is the self-energy via all intermediate states «large» but so is the self-energy via only those intermediate states on the same energy shell «large» in the same sense. Since α_1 represents a very large phase space indeed, this is an admissible assumption.

CASE A: $\qquad \omega(E\alpha_1; E\alpha) \equiv 0\,.$

This exceptional case, which actually violates our assumptions, will be treated first, as a useful formal preliminary. The integral for the ME of $U_2(t)$ is given by Eq. (3.7) with $\int dq \to \sum_q$. To evaluate $U_2(t)$, note that everything goes just as before with obvious formal changes and one arrives at the equation corresponding to Eq. (3.12) after decomposing the VAV product by means of the identity (3.31) and dropping the y part (as will always be done hereafter) in accordance with the assumption (3.32):

$$\langle q'|\hat{U}_2(t)|q\rangle = \tag{3.34}$$

$$= \mathrm{Lim}\left\{(-i\lambda)^2 \delta_{q'q} \int_0^t dt_2 \left[\int_0^{t_2} dt_1 \sum_{q_1} \exp\left[i(E - E_1)(t_2 - t_1)\right]\omega(q_1; q)\right]\right\}.$$

The nature of the limit we leave open for the moment. Now define μ and

(*) This way of writing the sum $\sum \omega$, with $\omega(q) \cong \langle q'|y(q_1)|q\rangle \cong |\langle q'|V|q\rangle|^2 = O(1)$ say, emphasizes explicitly that the sum $= O(N)$.

21217

$f_\mu(q)$ by

$$\text{(3.35)} \qquad \text{L.T.}\int_0^T d\tau \sum_{\varepsilon,\alpha_1} \exp[-i\varepsilon\tau]\omega(E+\varepsilon,\alpha_1;E\alpha) \equiv T^\mu f_\mu(q)\,, \qquad (T>0)\,,$$

corresponding to Eq. (3.13). This integral is proper, and one gets $\mu=0$ and

$$\text{(3.36)} \qquad f_0(q) = -i\sum_{\varepsilon\neq 0,\alpha_1} \frac{\omega(E+\varepsilon,\alpha_1;E\alpha)}{\varepsilon}\,,$$

where by the assumption $\omega(E\alpha_1;E\alpha)\equiv 0$ the summation over the energy difference ε effectively excludes $\varepsilon=0$. In any limit $t\to\infty$ we shall need to keep only the leading term of the double integral inside the square brackets in Eq. (3.34), so that we keep only the term $f_0(q)$ which is a constant, just as before. The remaining time integral introduces a t, so that we want to define Lim appearing in Eq. (3.34) as the $\lambda^2 t$ limit. With this convention as to the meaning of $\hat{U}$, we end up with

$$\text{(3.37)} \qquad \langle q'|\hat{U}_2|q\rangle = -\lambda^2 t f_0(q)\,\delta_{q'q}\,,$$

corresponding to Eq. (3.9). It is easy to see that, proceeding this way, we get in general in the $\lambda^2 t$ limit

$$\text{(3.38)} \qquad \langle q'|\hat{U}_p(t)|q\rangle = \frac{[-\lambda^2 t f_0(q)]^m}{m!}\,\delta_{q'q}\,, \qquad p\equiv 2m \text{ even},$$

and

$$\text{(3.39)} \qquad \langle q'|\hat{U}_p(t)|q\rangle = \operatorname*{Lim}_{\lambda^2 t}\left\{(-i\lambda)^p[f_0(q)]^m\cdot\right.$$
$$\left.\cdot\left[\frac{t^m\exp[i(E'-E)t]-\delta_0^m}{i(E'-E)}\right]\langle q'|V|q\rangle\right\}=0\,, \qquad p\equiv 2m+1 \text{ odd}.$$

The last equation follows unambiguously now, for case A implies $\langle E\alpha_1|V|E\alpha\rangle=0$ so that the middle member of Eq. (3.39) $\propto \lambda(\lambda^2 t)^m\to 0$. Hence the series for $\hat{U}(t)$ can be explicitly summed and we get

$$\text{(3.40)} \qquad \langle q'|\hat{U}(t)|q\rangle = \exp[-\lambda^2 t f_0(q)]\,\delta_{q'q}\,.$$

Since $f_0(q)$ (see Eq. (3.36)) is pure imaginary, this leads to a unitary $\hat{U}(t)$, a level shift

$$\text{(3.41)} \qquad \Delta_q = -\lambda^2\sum_{\varepsilon\neq 0,\alpha_1}\frac{\omega(E+\varepsilon,\alpha_1;E\alpha)}{\varepsilon}\,,$$

but of course no level widths for decay.

If we now consider the limit of very large N, sums can be replaced by integrals weighted by a very large density of states $\varrho(q)$, Moreover, if we require, say, that the spectrum fill up « evenly » as $N \to \infty$, then from Eq. (3.36)

$$f_0(q) \to \Phi_0(q) \equiv i\mathcal{P}\int \mathrm{d}q_1 \frac{\Omega(q_1;\, q)}{\varepsilon}\,, \tag{3.42}$$

defined with the principal part $\mathcal{P}$, is a reasonable prescription for the pole. The limit of this sum in which the two ε_i bracketing $\varepsilon = 0$ are always equally spaced from $\varepsilon = 0$ is in fact equivalent to the definition of $\mathcal{P}$. In Eq. (3.42)

$$\Omega(q_1; q) = \varrho(q_1)\,\omega(q_1; q)\,.$$

Strictly speaking, there is no continuum limit, in the sense that the spectrum becomes continuous, for the $\varrho(q_1)$ would be infinite at every point of a finite energy interval, whence so would $\Omega(q_1; q)$, giving meaningless expressions for $\Phi_0(q)$ and the $\hat{U}_p(t)$. Here we are assuming, as seems to us to be the typical case, that as $N \to \infty$ the ME of V stay about the same size, so that $\Omega(q_1; q)$, must become infinite with $\varrho(q_1)$. Hence the physically realistic situation is characterized by a very large valued function $\Omega(q_1; q)$. This however will be expected not to give inordinately large level shifts $-\lambda^2\mathcal{P}\int \mathrm{d}q_1\,\Omega(q_1; q)/\varepsilon$ because of cancellations in the integral (remember that $\Omega(q_1; q) \geqslant 0$). The ME *densities* of $\hat{U}_p(t)$ are given by Eq. (3.38) and (3.39) with $f_0(q) \to \Phi_0(q)$ $\delta_{q'q} \to \delta(q' - q)$. By case A, $\lim_{E' \to E} \langle q' \,|\, V \,|\, q\rangle = 0$, hence if we merely demand $[\mathrm{d}\langle q' \,|\, V \,|\, q\rangle / \mathrm{d}E']_E < \infty$ for large N, then the conclusion $\hat{U}_p(t) = 0$, p odd, continues to hold, the order of performing the $\lambda^2 t$ and $E' \to E$ limits introducing no ambiguity. (The expression $\langle q' \,|\, V \,|\, q\rangle$ is the ME of V, *not* the ME density of course.) Hence in the limit $N \to \infty$

$$\hat{U}(t) = \exp\left[-\lambda^2 t \Phi_0\right], \tag{3.43}$$

where Φ_0 is the q-diagonal operator with eigenvalue $\Phi_0(q)$, and is unitary. From the absence of any decay part, etc., it is obvious that this system will show no rate equation type behavior.

Case B: $$\omega(E\alpha_1; E\alpha) \not\equiv 0\,.$$

This is the more interesting case, and that envisaged in I. From the power series expansion (3.7) with $\int \mathrm{d}q \to \sum_q$ it is seen immediately that the leading term of $U_p(t) \propto t^p$ and that this term is the unique term in which all the energies in the exponentials are equal. Thus the limit of interest is the λt

20129

limit, denoted $\overline{U}(t)$, and we get, performing the time integrals at once

$$\langle q'|\overline{U}(t)|q\rangle = (-i\lambda)^p \frac{t^p}{p!}\delta_{E'E}\sum_{\alpha_{p-1},\ldots\alpha_1}\langle E\alpha'|V|E\alpha_{p-1}\rangle\cdot \cdot\langle E\alpha_{p-1}|V|E\alpha_{p-2}\rangle\ldots\langle E\alpha_1|V|E\alpha\rangle\,. \tag{3.44}$$

Using the identity (3.31) and the ansatz (3.33), we can write

$$\sum_{\alpha_1}\langle E\alpha_2|V|E\alpha_1\rangle\langle E\alpha_1|V|E\alpha\rangle \simeq N\omega(q)\,\delta_{\alpha_2\alpha}\,, \tag{3.45}$$

dropping the y part. Performing this decomposition in Eq. (3.44) from right to left, we arrive at

$$\langle q'|\overline{U}_p(t)|q\rangle = (-i\lambda)^p\frac{t^p}{p!}[N\omega(q)]^m\delta_{q'q}\,, \qquad p=2m \text{ even}; \tag{3.46}$$

$$\langle q'|\overline{U}_p(t)|q\rangle = [N\omega(q)]^{-\frac{1}{2}}(-i\lambda)^p\frac{t^p}{p!}[N\omega(q)]^{m+\frac{1}{2}}\langle E\alpha'|V|E\alpha\rangle\delta_{E'E}\,, \tag{3.47}$$

$$p=2m+1 \text{ odd}.$$

It is worth emphasizing that since we are here dealing with finite sums where no improper expressions can occur, these expressions, are the unique, well-defined ME of $\overline{U}_p$ and would have been attained with any other mode of making the decomposition (3.45). From the last equations one sees that the series can be explicitly summed, and we get

$$\overline{U}(t) = \cos[\lambda t(N\omega)^{\frac{1}{2}}] - \Lambda(N\omega)^{-\frac{1}{2}}\sin[\lambda t(N\omega)^{\frac{1}{2}}]\,, \tag{3.48}$$

where $\omega^{\frac{1}{2}}$, $\omega^{-\frac{1}{2}}$ are q-diagonal operators with eigenvalues $[\omega(q)]^{\frac{1}{2}}$, $[\omega(q)]^{-\frac{1}{2}}$ respectively, and Λ is an energy diagonal operator defined by

$$\begin{cases}\langle E\,\alpha'|\Lambda|E\alpha\rangle = \langle E\alpha'|V|E\alpha\rangle\,,\\ \langle E'\alpha'|\Lambda|E\alpha\rangle = 0\,, \qquad E'\neq E.\end{cases} \tag{3.49}$$

In the limit of large N

$$N\omega(q)\to\Omega(q)\equiv\int d\alpha_1\,\Omega'(E\alpha_1;\,E\alpha)\,, \tag{3.50}$$

where $\Omega'(E\alpha_1;\,E\alpha)$ $\varrho_E(\alpha_1)\omega(E\alpha_1;\,E\alpha)$ and $\varrho_E(\alpha_1)$ is the density of the substates α_1 at $(E,\,\alpha_1)$. $\overline{U}(t)$ goes into the expression (3.48) with $N\omega$ replaced

by Ω given by Eq. (3.50). Λ is an operator defined by Eq. (3.49) where these are still the ME, *not* the ME densities, of V in the limit $N \to \infty$. Note that here unlike case A, we can talk about the continuum limit in the sense of a strictly continuous spectrum. Eq. (3.50) shows that we get an identically divergent integral for $\Omega(q)$ and thus a meaningless expression for $U(t)$ only in the case that there is a continuous distribution of substates α in any finite interval (α_1, α_2). The question of unitarity perishes gracefully by inanation in this case. If we exclude this case $\Omega(q) = \infty$, it can be shown that $\overline{U}(t)$ is unitary. The proof is essentially the same in either the discrete or continuum case; we verify, for example, the necessary condition (3.17) b in the discrete formalism:

$$\overline{U}_2^* = \overline{U}_2 = -\frac{\lambda^2 t^2}{2} N\omega\,, \tag{3.51}$$

and

$$\langle q' | \overline{U}_1^2 | q\rangle = -\lambda^2 t^2 \delta_{E'E} \sum_{\alpha_1} \langle E\alpha' | V | E\alpha_1\rangle\langle E\alpha_1 | V | E\alpha\rangle = \tag{3.52}$$

$$= -\lambda^2 t^2\, \delta_{E'E} N\omega(q)\, \delta_{\alpha'\alpha} = -\lambda^2 t^2 N\omega(q)\, \delta_{q'q}\,.$$

Therefore $\overline{U}_2^* + \overline{U}_2 = \overline{U}_1^2$.

Finally, it is clear from the oscillatory nature of $\overline{U}(t)$ that the relative populations

$$x_q(t) \equiv \sum_{q_1 q_2} \langle q | \overline{U}(t) | q_1\rangle\langle q | \overline{U}(t) | q_2\rangle^* c(q_1) c(q_2)^*\,, \tag{3.53}$$

where $c(q)$ are the q-components of the initial state, could never satisfy a rate type equation. For example, for the simple initial distribution $c(q) = \delta_{qq_0}$, q_0 some fixed state, they become

$$x_q(t) = \cos^2\left[\lambda t\{N\omega(q_0)\}^{\frac{1}{2}}\right]\delta_{qq_0} + |\langle E_0\alpha | V | q_0\rangle|^2 \cdot \tag{3.54}$$

$$\cdot \{N\omega(q_0)\}^{-1} \sin^2\left[\lambda t\{N\omega(q_0)\}^{\frac{1}{2}}\right]\delta_{EE_0}\,,$$

since the completely diagonal part of V can be taken zero. In the limit $N \to \infty$ this reads

$$X_q(t) = \cos^2\left[\lambda t \Omega(q_0)^{\frac{1}{2}}\right]\delta(q - q_0) + \langle E_0\alpha | \Theta | q_0\rangle \cdot \tag{3.55}$$

$$\cdot\, \Omega(q_0)^{-1} \sin^2\left[\lambda t\, \Omega(q_0)^{\frac{1}{2}}\right]\delta(E - E_0)\,,$$

for the relative population densities $X_q(t)$ where the ME of Θ are the α densities of the quantities $|\langle E_0\alpha | V | q_0\rangle|^2$. In fact

$$X_q(t) = P_t(E_0\alpha;\, E_0\alpha_0)\,\delta(E - E_0) \tag{3.56}$$

20231

in terms of the quantity introduced in I (see our Eq. (3.5)). $X_\varrho(t)$ satisfies no rate equation as is obvious from Eq. (3.55).

Thus we have seen that in the case of systems with « large » self-energies and *real* first order processes, which is the case B and the case envisaged in I, the $\lambda^2 t$ limit has no significance because there exist an infinite variety of divergent terms proportional to powers of $\lambda^2 t^\theta$ $(1 < \theta \leqslant 2)$ which are left out of account. The transition operator does, on the other hand, assume a simple and explicitly evaluable form in the long time-weak coupling limit $\lambda \to 0$ and $t \to \infty$ such that $\lambda t = \text{const}$. This λt limit of $U(t)$ is of course unitary and the system shows no rate equation type behavior in this asymptotic region.

4. – The classical derivation.

The classical derivation ([8]) II is, as far as the mathematics goes, almost identical with the quantum mechanical derivation I, so we can be briefer in this section. The system treated is defined by the perturbed Hamiltonian $H_0 + \lambda V$ and its distribution function ϱ satisfies the Liouville equation

$$\frac{\mathrm{d}\varrho}{\mathrm{d}t} \equiv \frac{\partial \varrho}{\partial t} + L\varrho = 0\,, \tag{4.1}$$

where L is the Liouville operator

$$\sum_i \left(\frac{\partial H}{\partial J_i} \frac{\partial}{\partial \alpha_i} - \frac{\partial H}{\partial \alpha_i} \frac{\partial}{\partial J_i} \right),$$

for the perturbed system. The continuity equation (4.1) is the classical analogue of the unitarity of $\exp[-iHt]$ in the quantum mechanical theory. The unperturbed system is multiply periodic and is described by the action and angle variables J_i, α_i $(i = 1, ..., N)$. One expands ϱ into a Fourier series (with respect to the angle variables as is always hereafter understood) whence the time dependence of ϱ_0 is entirely contained in the quantities $\alpha_i - \omega_i t$, where $\omega_i(J) \equiv \partial H_0 / \partial J_i = \text{const}$ $(i = 1, ..., N)$ are the frequencies of the unperturbed system:

$$\varrho(t) = \sum_{(n)} \varrho_{(n)}(J_1, ..., J_N) \exp\left[i \sum n_i(\alpha_i - \omega_i t) \right], \qquad (n) \equiv \{n_1, n_2, ..., n_N\}. \tag{4.2}$$

One assumes that the effect of the perturbation is to make the Fourier components $\varrho_{(n)}$ time dependent through the time dependence of the J_i which are no longer constants of the motion. Substituting the expansion (4.2) and the Fourier expansion of L into Eq. (4.1), one gets the equation describing

2032

the time development of the $\varrho_{(n)}$:

$$\frac{\partial \varrho_{(n)}}{\partial t} = \sum_{(n')} \langle (n) | \exp\left[i \sum n_i \omega_i t \right] \lambda \delta L \exp\left[- i \sum n'_i \omega_i t \right] | (n') \rangle \varrho_{(n')} , \tag{4.3}$$

where the Fourier components of $\delta L \equiv (L - L_0)/\lambda$ are

$$\langle (n) | \delta L | (n') \rangle \quad \frac{1}{(2\pi)^N} \int \mathrm{d}\alpha_1 \ldots \mathrm{d}\alpha_N \exp\left[- i \sum n_i \alpha_i \right] \delta L \exp\left[i \sum n'_i \alpha_i \right] = \tag{4.4}$$

$$= i \sum_k \left[n'_k \left(\frac{\partial}{\partial J_l} \right) V_{(n-n')} - n_k V_{(n-n')} \left(\frac{\partial}{\partial J_l} \right) \right] .$$

Here $(\partial/\partial J_k)$ acts on whatever follows $\langle | \delta L | \rangle$ as well as on $V_{(n-n')}$, and the $V_{(n-n')}$ are the Fourier components of V (defined by the first equation of (4.4) with $\delta L \to V$). $V_{(0)} = 0$ is assumed without limiting generality, since this part could be absorbed into the phase-independent H_0. Hence

$$\langle (n) | \delta L | (n) \rangle = 0 , \tag{4.5}$$

or δL has no completely diagonal elements. Eq. (4.3) is solved as a power series in λ under the initial conditions $\varrho_{(0)}(0) \neq 0$, $\varrho_{(n)}(0) = 0$ for $(n) \neq (0)$ corresponding to a phase-independent initial distribution. Writing

$$\varrho_{(n)}(t) = \langle (n) | U(t) | (0) \rangle \varrho_{(0)}(0) ,$$

we get [19]

$$\langle (n) | U_p(t) | (0) \rangle = \lambda^p \int_0^t \mathrm{d}t_p \int_0^{t_p} \mathrm{d}t_{p-1} \ldots \int_0^{t_2} \mathrm{d}t_1 \sum_{(n_{p-1}),(n_{p-2}),\ldots(n_1)} \cdot \tag{4.6}$$

$$\cdot \left\{ \exp\left[iEt_p \right] \langle (n) | \delta L | (n_{p-1}) \rangle \exp\left[- iE_{p-1}(t_p - t_{p-1}) \right] \langle (n_{p-1}) | \delta L | (n_{p-2}) \right\} \ldots$$

$$\ldots \exp\left[- iE_2(t_3 - t_2) \right] \langle (n_2) | \delta L | (n_1) \rangle \exp\left[- iE_1(t_2 - t_1) \right] \langle (n_1) | \delta L | (0) \rangle \Big\} .$$

Here we have taken the liberty of making some trivial notational changes in Eq. (2.14) of II to facilitate comparison with our Eq. (3.7): E means $\sum_i n_i \omega_i$ and E_q means likewise $\sum_i (n_q)_i \omega_i$. We have numbered our dummy times in the reverse order, as well as replaced (n'), (n''), ..., etc., by (n_{p-1})

[19] II has several errata. For example, II, Eq. (2.14) is correct and coincides with Eq. (4.6) if $i\delta L$ there is replaced by δL [where δL is given by II, Eq. (2.11)]. Moreover, the signs in the exponent of the third term should be switched.

20833

$(n_{p-2}), \ldots, (n_1)$. If one makes in Eq. (4.6) the substitutions

$$(4.7) \qquad \begin{cases} E \to E', \quad 0 \to E, \quad \delta L \to -iV, \quad (n) \to (E', \alpha'), \\ (n_q) \to (E_q, \alpha_q), \quad (0) \to (E, \alpha) \end{cases}$$

and replaces sums by integrals, it becomes formally identical with Eq. (3.7). Hence we can take over the results of performing the time integrations derived in Sect. 3.

The physical assumptions about the system are just those formulated in the last part of Sect. 3. As a result

$$\sum_{(n_1)} \langle (n) | \delta L | (n_1) \rangle \langle (n_1) | \delta L | (0) \rangle$$

is supposed to have $0(N)$ times as many non-vanishing terms for $(n) = (0)$ as for $(n) \neq (0)$, which justifies the neglect of the off diagonal relative to the diagonal ME of $(\delta L)^2$. In fact this is assumed to hold also when the intermediate states are restricted by $E_1 = \sum (n_1)_i \omega_i = 0$. With the transcription (4.7) these become precisely the assumptions (3.32) and (3.33), so that the above approximation corresponds exactly to neglecting y terms in the formalism of I.

The authors now choose to regard their discrete energy sums as replaced « in the limit » by integrals over a continuous spectrum (although, as we have seen in Sect. 3, it is crucially important that this limit is not taken prematurely) and they use the prescription (3.16) of Van Hove for handling these improper integrals. Hence they emerge in a $\lambda^2 t$ limit with the result (3.8) for the even $\hat{U}_p(t)$ and zero for the odd $\hat{U}_p(t)$, or, if we sum, the result

$$\langle q' | \hat{U}(t) | q \rangle \equiv \operatorname{Lim}_{\lambda^2 t} \langle q' | U(t) | q \rangle = \exp [-\lambda^2 t F_0(q)] \, \delta(q' - q) ,$$

with $F_0(q)$ given by Eq. (3.15). Now we recall that $W(E\alpha_1; E\alpha) = \langle E\alpha | V | E\alpha_1 \rangle \cdot \langle E\alpha_1 | V | E\alpha \rangle$ so that transcribing back to the language of II via Eq. (4.7), we get

$$(4.8) \qquad F_0(q) = \pi \int d\alpha_1 \langle E\alpha | V | E\alpha_1 \rangle \langle E\alpha_1 | V | E\alpha \rangle + \text{etc.} \to$$

$$\to -\pi \sum_{(n)}{}' \langle (0) | \delta L | (n) \rangle \langle (n) | \delta L | (0) \rangle \equiv -\pi \langle (0) | (\delta L)^2 | (0) \rangle' ,$$

where the authors of II neglect the level shift (last term in the right member of Eq. (3.15)), and where the prime on $\sum$ restricts one to those (n) giving zero energy:

$$(4.9) \qquad E \equiv \sum n_i \omega_i = 0 + 0(N^{-1}) .$$

2084

Using Eq. (4.4) and $V^*_{(m)} = V_{(-m)}$, one therefore gets

$$(4.10)\qquad \begin{cases} \hat{\varrho}_{(n)}(t) = 0\,, & (n) \neq (0)\,; \\ \hat{\varrho}(t) = \hat{\varrho}_{(0)}(t) \equiv \langle (0)\,|\,\hat{U}(t)\,|\,(0)\rangle\, \varrho_{(0)}(0) = \exp\,[t\Omega]\varrho_{(0)}(0)\,, \end{cases}$$

where

$$(4.11)\qquad \Omega \equiv \pi\lambda^2 \langle (0)\,|\,(\delta L)^2\,|\,(0)\rangle' = \pi\lambda^2 \sum_{(n)}{}' \sum_{k,k'} n_k n_{k'} \left(\frac{\partial}{\partial J_k}\right) |\, V_{(n)}\,|^2 \left(\frac{\partial}{\partial J_k^{\dagger}}\right).$$

This derivation is open to objections which are the exact analogues of those of Sect. 3. The limit distribution function does not verify the Liouville equation (4.1), for from Eq. (4.10) follows ([20])

$$(4.12)\qquad \frac{\mathrm{d}\hat{\varrho}(t)}{\mathrm{d}t} = \Omega\hat{\varrho}(t) \neq 0\,.$$

Hence something mathematically inadmissible has occurred. As is clear now, it is the unphysical prescription (3.16) for handling the improper integrals and, what goes deeper, the faulty replacement of the discrete by the continuous spectrum, which completely changes the character of the limit.

Hence we return to Eq. (4.6), or its transcribed form Eq. (3.7), with energy sums replacing energy integrals. Then the correct evaluation follows as in the last section. Case B is the more interesting case, and the case envisaged in both I and II. We have seen that it leads in fact to a λt limit — the $\lambda^2 t$ limit is meaningless in this case. The answer is then given by the transcription of Eq. (3.48) back into the language of II. We have

$$(4.13)\qquad N\omega(q) \cong \sum_{\lambda_1} \langle E\alpha\,|\,V\,|\,E\alpha_1\rangle\langle E\alpha_1\,|\,V\,|\,E\alpha\rangle \to$$
$$\to i^2 \sum_{(n)}{}' \langle (0)\,|\,\delta L\,|\,(n)\rangle\langle (n)\,|\,\delta L\,|\,(0)\rangle \equiv -\langle (0)\,|\,(\delta L)^2\,|\,(0)\rangle'\,,$$

hence (*)

$$(4.14)\qquad \begin{cases} \langle (n)\,|\,\overline{U}(t)\,|\,(0)\rangle = \delta_{(n)(0)} \cosh\,[\lambda t\{\langle (0)\,|\,(\delta L)^2\,|\,(0)\rangle'\}^{\frac{1}{2}}] + \\ \qquad + \langle (n)\,|\,\delta L\,|\,(0)\rangle\{\langle (0)\,|\,(\delta L)^2\,|\,(0)\rangle'\}^{-\frac{1}{2}} \sinh\,[\lambda t\{\langle (0)\,|\,(\delta L)^2\,|\,(0)\rangle'\}^{\frac{1}{2}}]\,, \\ \qquad\qquad\qquad\qquad\qquad\qquad\qquad\qquad \sum n_i\omega_i = 0\,; \\ \qquad = 0\,, \qquad\qquad\qquad\qquad\qquad\qquad\qquad\qquad \sum n_i\omega_i \neq 0\,; \end{cases}$$

and

$$(4.15)\qquad \bar{\varrho}(t) = \sum_{(n)}{}' \langle (n)\,|\,\overline{U}(t)\,|\,(0)\rangle\, \varrho_{(0)}(0) \exp\,[i \textstyle\sum n_i\alpha_i]\,.$$

([20]) The $\partial/\partial t$ in II, Eq. (2.20) is actually the total derivative $\mathrm{d}/\mathrm{d}t$.

(*) In Eq. (4.14), the second line is defined by its series expansion.

The time dependence in the exponentials has disappeared by the definition of $\sum'_{(n)}$.

Of course, it is just as simple not to make the approximation of dropping the y parts; one gets then the more accurate expression

$$(4.14') \qquad \langle (n) | \bar{U}(t) | (0) \rangle = \sum_{p=0}^{\infty} \frac{\lambda^p t^p}{p!} \sum'_{(n_p), \ldots (n_1)} \langle (n) | \delta L | (n_{p-1}) \rangle \cdot$$

$$\cdot \langle (n_{p-1}) | \delta L | (n_{p-2}) \rangle \ldots \langle (n_1) | \delta L | (0) \rangle , \qquad \sum n_i \omega_i = 0 ;$$

$$= 0 , \qquad \sum n_i \omega_i \neq 0 .$$

To verify that $\bar{\varrho}(t)$ *does* satisfy the Liouville equation (4.1), as it must, let us verify the equivalent set (4.3) for the Fourier components. The $\varrho_{(n)}$ are given by the right members of Eq. (4.14') applied to $\varrho_{(0)}(0)$. Then for (n) such that $\sum n_i \omega_i = 0$, Eq. (4.3) is satisfied since both sides equal

$$(4.16) \qquad \sum_{p=0}^{\infty} \frac{\lambda^p t^{p-1}}{(p-1)!} \sum'_{(n_{p-1}), \ldots (n)_1} \langle (n) | \delta L | (n_{p-1}) \rangle \ldots \langle (n_1) | \delta L | (0) \rangle$$

For (n) such that $E \equiv \sum n_i \omega_i \neq 0$, $\partial \varrho_{(n)} / \partial t = 0$ by Eq. (4.14) and the right member equals the expression (4.16) multiplied by $\exp [iEt]$. But the leading term of $\lambda^p \int dt \exp [iEt] t^{p-1} \propto \lambda^p t^{p-1}$ (*not* $\lambda^p t^p$, due to the presence of the exponential!) so that this right member is the derivative of a function which vanishes in the λt limit and hence must be taken to vanish itself in this limit. Thus $\bar{\varrho}(t)$ satisfies no non-trivial H-theorem; it describes therefore a conservative, entropy-conserving evolution of the large classical system in question.

RIASSUNTO (*)

Si danno ragioni per porre in dubbio che l'irreversibilità possa *derivarsi* dalla meccanica senza ricorrere ai vari processi di media tradizionali facendo uno studio critico della teoria dell'accoppiamento debole a tempo lungo di Van Hove-Brout-Prigogine che non ricorre a tali medie. Le due obiezioni principali sono: 1) incongruenze matematiche nella formulazione meccanico-quantistica della « singolarità diagonale » della perturbazione di miscela che si suppone causa dell'irreversibilità e 2) una prescrizione fisicamente inammissibile per il trattamento dei poli negli integrali impropri dell'energia. Ne consegue in modo particolare, rispettivamente: 1) una prescrizione ambigua per il calcolo del limite dell'accoppiamento debole a tempo lungo degli integrali impropri e 2) la violazione dell'unitarietà dell'operatore di transizione. Si riformula la singolarità diagonale al « limite del continuo ». Si calcola esplicitamente l'operatore di transizione limite che ha comportamento solo reversibile.

(*) *Traduzione a cura della Redazione.*

IL NUOVO CIMENTO Vol. IX, N. 1 1° Luglio 1958

Unitary Transformations of Symmetric PS-PS and PS-PV Interactions.

J. S. R. Chisholm and G. M. Dixon

Department of Mathematics, University College of Wales, Cathays Park, Cardiff, Wales

(ricevuto il 2 Aprile 1958)

Summary. — Exact covariant unitary transformations applied to the Lagrangians of symmetric PS-PS and PS-PV theories exhibit the so-called « equivalence » of the pseudoscalar and pseudovector couplings. The transformation of the PS-PS theory is compared with similar transformations. The value of making unitary transformations is discussed, and some remarks on renormalization problems are made.

1. – Introduction.

In an earlier paper (1), hereafter denoted as I, one of the authors has shown that the interaction in neutral PS-PV meson theory can be transformed by a Dyson-type unitary transformation into an interaction which is exponential in the meson field. In Sect. **2** and **3** of this paper we establish a similar result for symmetric PS-PV theory; in this theory, however, it does not seem possible to introduce multi-meson propagators in the way in which they occur in the neutral theory.

In Sect. **4** a closely similar transformation is applied to symmetric PS-PS theory. The interaction is transformed into one consisting of four terms: one term is the PS-PV coupling term, and the other three contain exponentials in the meson field operator. To second order in the coupling constant this transformation gives results identical with the Foldy (2) transformation; it is

(1) J. S. R. Chisholm: *Phil. Mag.*, **8**, 1, 338 (1956).
(2) L. L. Foldy: *Phys. Rev.*, **84**, 168 (1951).

similar to the result obtained by DRELL and HENLEY ([3]), but is obviously relativistically covariant and takes full account of the non-commutation of the meson field with its time-derivative.

2. – The Evaluation of $\partial_\mu \exp[iG\gamma_5\boldsymbol{\tau}\,\boldsymbol{\varphi}]$.

The transformation in symmetric theory which is analogous to (1) of I is

$$\psi(x) = \exp[iG\gamma_5\boldsymbol{\tau}\cdot\boldsymbol{\varphi})]\zeta(x)\,, \tag{1a}$$

and

$$\psi(x) = \bar{\zeta}(x)\exp[iG\gamma_5\boldsymbol{\tau}\cdot\boldsymbol{\varphi}]\,. \tag{1b}$$

In (1), $\boldsymbol{\tau}$ is the 3-vector of isotopic spin matrices; we have taken $\bar{\psi}(x) = \psi^*(x)\gamma_4$, the matrices $\gamma_1, \ldots, \gamma_5$ all being Hermitian and having squares equal to unity. When we make the substitution (1) in the free nucleon Lagrangian, it is necessary to evaluate the four derivatives $\partial_\mu \exp[iG\gamma_5\boldsymbol{\tau}\cdot\boldsymbol{\varphi}]$, where $\partial_\mu = \partial/\partial x_\mu$. The evaluation of these derivatives forms the major part of the work.

Since $(\boldsymbol{\tau}\cdot\boldsymbol{\varphi})^2 = \sum_r \varphi_r\varphi_r \equiv \boldsymbol{\varphi}^2$, we can write

$$\exp[iG\gamma_5\boldsymbol{\tau}\cdot\boldsymbol{\varphi}] = \sum_{l=0}^{\infty}\left[\frac{(-G^2\boldsymbol{\varphi}^2)^l}{2l\,!} + \frac{(-G^2\boldsymbol{\varphi}^2)^l iG\gamma_5\boldsymbol{\tau}\cdot\boldsymbol{\varphi}}{(2l+1)\,!}\right]. \tag{2}$$

Now

$$\partial_\mu(\boldsymbol{\varphi}^2)^l = \sum_{s=0}^{l-1}(\boldsymbol{\varphi}^2)^{l-s-1}(\partial_\mu\boldsymbol{\varphi}^2)(\boldsymbol{\varphi}^2)^s = l(\boldsymbol{\varphi}^2)^{l-1}(\partial_\mu\boldsymbol{\varphi}^2) + \tfrac{1}{2}l(l-1)(\boldsymbol{\varphi}^2)^{l-2}[\partial_\mu\boldsymbol{\varphi}^2, \boldsymbol{\varphi}^2]$$

and

$$[\partial_\mu\boldsymbol{\varphi}^2, \boldsymbol{\varphi}^2] = 4\boldsymbol{\varphi}^2\lambda_\mu\,,$$

where $\lambda_\mu = [\partial_\mu\varphi, \varphi]$, the commutator for any one of the three meson fields.

Thus for even terms in (2),

$$\partial_\mu(\boldsymbol{\varphi}^2)^l = l(\boldsymbol{\varphi}^2)^{l-1}(\partial_\mu\boldsymbol{\varphi}^2) + 2\lambda_\mu l(l-1)(\boldsymbol{\varphi}^2)^{l-1}\,. \tag{3a}$$

For odd terms in (2), we use (3*a*) and

$$[(\partial_\mu\boldsymbol{\varphi}^2), (\boldsymbol{\tau}\cdot\boldsymbol{\varphi})] = 2\lambda_\mu(\boldsymbol{\tau}\cdot\boldsymbol{\varphi})$$

([3]) S. D. DRELL and E. M. HENLEY: *Phys. Rev.*, **88**, 1053 (1952).

to find

$$(3b)\quad \partial_\mu[\boldsymbol{\varphi}^2(\boldsymbol{\tau}\cdot\boldsymbol{\varphi})] = l(\boldsymbol{\varphi}^2)^{l-1}(\boldsymbol{\tau}\cdot\boldsymbol{\varphi})(\partial_\mu\boldsymbol{\varphi}^2) + 2l^2\lambda_\mu(\boldsymbol{\varphi}^2)^{l-1}(\boldsymbol{\tau}\cdot\boldsymbol{\varphi}) + (\boldsymbol{\varphi}^2)^l(\boldsymbol{\tau}\cdot\partial_\mu\boldsymbol{\varphi})\,.$$

From (3*a*) and (3*b*) we find that $\partial_\mu \exp[iG\gamma_5\boldsymbol{\tau}\cdot\boldsymbol{\varphi}]$ is the sum of

$$(4a)\qquad -2G^2\lambda_\mu\sum_{l=1}^{\infty}\left[\frac{l(l-1)}{2l!}(-G^2\boldsymbol{\varphi}^2)^{l-1} + \frac{l^2}{(2l+1)!}(-G^2\boldsymbol{\varphi}^2)^{l-1}iG\gamma_5\boldsymbol{\tau}\cdot\boldsymbol{\varphi}\right]$$

and

$$(4b)\qquad -G^2\sum_{l=1}^{\infty}\left[\frac{l}{2l!}(-G^2\boldsymbol{\varphi}^2)^{l-1} + \frac{l}{(2l+1)!}(-G^2\boldsymbol{\varphi}^2)^{l-1}iG\gamma_5\boldsymbol{\tau}\cdot\boldsymbol{\varphi}\right](\partial_\mu\boldsymbol{\varphi}^2) + \\ + \sum_{l=0}^{\infty}\frac{iG\gamma_5}{(2l+1)!}(-G^2\boldsymbol{\varphi}^2)^l(\boldsymbol{\tau}\cdot\partial_\mu\boldsymbol{\varphi})\,.$$

In (4*b*) we express all derivatives in terms of $\partial_\mu\boldsymbol{\varphi}$ by using the formula

$$\partial_\mu\boldsymbol{\varphi}^2 = 2(\boldsymbol{\tau}\cdot\boldsymbol{\varphi})(\boldsymbol{\tau}\cdot\partial\boldsymbol{\varphi}) - 2i[\boldsymbol{\varphi},\,\partial_\mu\boldsymbol{\varphi},\,\boldsymbol{\tau}] + 3\lambda_\mu\,.$$

When we substitute this expression in (4*b*), the terms which do not contain λ_μ are

$$(5a)\qquad (iG\gamma_5)\left[\sum_{l=1}^{\infty}\frac{1}{(2l-1)!}(iG\gamma_5\boldsymbol{\tau}\cdot\boldsymbol{\varphi})^{2l-1} + \sum_{l=0}^{\infty}\frac{1}{2l!}(iG\gamma_5\boldsymbol{\tau}\cdot\boldsymbol{\varphi})^{2l}\right](\boldsymbol{\tau}\cdot\partial_\mu\boldsymbol{\varphi}) + \\ + iG^2\sum_{l=1}^{\infty}\left[\frac{2l}{2l!}(iG\gamma_5\boldsymbol{\tau}\cdot\boldsymbol{\varphi})^{2l-2} + \frac{2l}{(2l+1)!}(iG\gamma_5\boldsymbol{\tau}\cdot\boldsymbol{\varphi})^{2l-1}\right][\boldsymbol{\varphi}\,\partial_\mu\boldsymbol{\varphi},\,\boldsymbol{\tau}]$$

Collecting together the terms from (4*a*) and (4*b*) which contain λ_μ, we get

$$(5b)\qquad -\frac{1}{2}G^2\lambda_\mu\sum_{l=1}^{\infty}\left[\frac{1}{(2l-2)!}(iG\gamma_5\boldsymbol{\tau}\cdot\boldsymbol{\varphi})^{2l-2} + \frac{1}{(2l-1)!}(iG\gamma_5\boldsymbol{\tau}\cdot\boldsymbol{\varphi})^{2l-1}\right] - \\ - G^2\lambda_\mu\sum_{l=1}^{\infty}\left[\frac{2l}{2l!}(iG\gamma_5\boldsymbol{\tau}\cdot\boldsymbol{\varphi})^{2l-2} + \frac{2l}{(2l+1)!}(iG\gamma_5\boldsymbol{\tau}\cdot\boldsymbol{\varphi})^{2l-1}\right].$$

The second series in (5*b*) is the same as the series in the second term of (5*a*).

Adding together the terms in (5*a*) and (5*b*) and defining the series $S(A)$ by

$$(6)\qquad S(A) = \sum_{l=1}^{\infty}\left[\frac{2l}{2l!}A^{2l-2} + \frac{2l}{(2l+1)!}A^{2l-1}\right],$$

we have the formula for the derivatives in its final form

$$(7)\qquad \partial_\mu\exp[iG\gamma_5\boldsymbol{\tau}\cdot\boldsymbol{\varphi}] = \exp[iG\gamma_5\boldsymbol{\tau}\cdot\boldsymbol{\varphi}][iG\gamma_5(\boldsymbol{\tau}\cdot\partial_\mu\boldsymbol{\varphi}) - \tfrac{1}{2}G^2\lambda_\mu] + \\ + S(iG\gamma_5\boldsymbol{\tau}\cdot\boldsymbol{\varphi})\,G^2\{i[\boldsymbol{\varphi},\,\partial_\mu\boldsymbol{\varphi},\,\boldsymbol{\tau}] - \lambda_\mu\}\,.$$

The series S has some interesting properties, and behaves in some ways like a « three-dimensional exponential series ».

3. – The Transformation of the PS-PV Lagrangian.

The Lagrangian density for nucleon and meson fields with charge-symmetric PS-PV coupling is

$$\mathcal{L} = \mathcal{L}_1 + \mathcal{L}_2 + \mathcal{L}_3 + \mathcal{L}_4 ,$$

where:

$$\mathcal{L}_1 = \bar{\psi}(x)\gamma_\mu \partial_\mu \psi(x) ,$$

$$\mathcal{L}_2 = M\bar{\psi}(x)\psi(x) ,$$

$$\mathcal{L}_3 = -\tfrac{1}{2}\sum [(\partial_\mu \varphi_r)^2 + m^2\varphi_r^2] ,$$

$$\mathcal{L}_4 = ig\bar{\psi}(x)\gamma_5\gamma_\mu(\boldsymbol{\tau}\cdot\partial_\mu\boldsymbol{\varphi})\psi(x) .$$

Normally $\partial_\mu\boldsymbol{\varphi}$ is placed to the right of $\psi(x)$ in $\mathcal{L}_4$ but we place it to the left to ensure cancellation later. Changing the position simply results in a mass renormalization involving δ-functions with zero argument.

The transformation (1) leaves the free-meson term $\mathcal{L}_3$ unchanged, but affects $\mathcal{L}_1$, $\mathcal{L}_2$ and $\mathcal{L}_4$. The term $\mathcal{L}_2$ becomes

$$M\bar{\zeta}(x)\zeta(x) + M\bar{\zeta}(x)\,(\exp[2iG\gamma_5\boldsymbol{\tau}\cdot\boldsymbol{\varphi}] - 1)\zeta(x) . \tag{8}$$

The first term in (8) is part of the free-fermion Lagrangian. The second term is an exponential interaction term.

The term $\mathcal{L}_4$ becomes

$$ig\bar{\zeta}(x)\exp[iG\gamma_5\boldsymbol{\tau}\cdot\boldsymbol{\varphi}]\gamma_5\gamma_\mu(\boldsymbol{\tau}\cdot\partial_\mu\boldsymbol{\varphi})\exp[iG\gamma_5\boldsymbol{\tau}\cdot\boldsymbol{\varphi}]\zeta(x) .$$

Using the commutation rules for τ-matrices and the meson field operators, we can show that

$$\begin{aligned}(\boldsymbol{\tau}\cdot\partial_\mu\boldsymbol{\varphi})\exp[iG\gamma_5\boldsymbol{\tau}\cdot\boldsymbol{\varphi}] = \exp[iG\gamma_5\boldsymbol{\tau}\cdot\boldsymbol{\varphi}](\boldsymbol{\tau}\cdot\partial_\mu\boldsymbol{\varphi}) + \\ + 2(\boldsymbol{\tau}\cdot\boldsymbol{\varphi})^{-1}\sinh(iG\gamma_5\boldsymbol{\tau}\cdot\boldsymbol{\varphi})[\boldsymbol{\varphi}, \partial_\mu\boldsymbol{\varphi}, \boldsymbol{\tau}] + \\ + iG\gamma_5\lambda_\mu\exp[iG\gamma_5\boldsymbol{\tau}\cdot\boldsymbol{\varphi}] + 2\lambda_\mu(\boldsymbol{\tau}\cdot\boldsymbol{\varphi})^{-1}\sinh(iG\gamma_5\boldsymbol{\tau}\cdot\boldsymbol{\varphi}) .\end{aligned}$$

Thus

$$\begin{aligned}\mathcal{L}_4 = ig\bar{\zeta}(x)\gamma_5\gamma_\mu(\boldsymbol{\tau}\cdot\partial_\mu\boldsymbol{\varphi})\zeta(x) + ig\bar{\zeta}(x)\gamma_5\gamma_\mu(\boldsymbol{\tau}\cdot\boldsymbol{\varphi})^{-1}\cdot \\ \cdot\{1 - \exp[-2iG\gamma_5\boldsymbol{\tau}\cdot\boldsymbol{\varphi}]\}[\boldsymbol{\varphi}, \partial_\mu\boldsymbol{\varphi}, \boldsymbol{\tau}]\zeta(x) - Gg\,\zeta(x)\gamma_\mu\lambda_\mu\zeta(x) + \\ + ig\bar{\zeta}(x)\gamma_5\gamma_\mu(\boldsymbol{\tau}\cdot\boldsymbol{\varphi})^{-1}\{1 - \exp[-2iG\gamma_5\boldsymbol{\tau}\cdot\boldsymbol{\varphi}]\}\lambda_\mu\zeta(x) .\end{aligned} \tag{9a}$$

The forth term in (9*a*) appears as an interaction involving the infinite constant λ_μ. This term and the mass renormalization term preceding it are due to the unsymmetric form of (9*a*), and would appear with a negative sign if the $\boldsymbol{\tau}\cdot\partial_\mu\boldsymbol{\varphi}$ in $\mathcal{L}_4$ were taken to the left instead of to the right; the scalar triple product term would then also occur with a negative sign on the left of the exponential. We can therefore express (9*a*) more symmetrically in the form

$$\begin{aligned}(9b)\qquad \mathcal{L}_4 = {} & ig\bar{\zeta}(x)\gamma_5\gamma_\mu(\boldsymbol{\tau}\cdot\partial_\mu\boldsymbol{\varphi})\zeta(x) + \\ & + \tfrac{1}{2}ig\bar{\zeta}(x)\gamma_5\gamma_\mu\{(\boldsymbol{\tau}\cdot\boldsymbol{\varphi})^{-1}(1-\exp[-2iG\gamma_5\boldsymbol{\tau}\cdot\boldsymbol{\varphi}])[\boldsymbol{\varphi},\partial_\mu\boldsymbol{\varphi},\boldsymbol{\tau}] - \\ & - [\boldsymbol{\varphi},\partial_\mu\boldsymbol{\varphi},\boldsymbol{\tau}](\boldsymbol{\tau}\cdot\boldsymbol{\varphi})^{-1}(1-\exp[-2iG\gamma_5\boldsymbol{\tau}\cdot\boldsymbol{\varphi}])\}\zeta(x)\,.\end{aligned}$$

Now $\mathcal{L}_1$ becomes

$$(10)\qquad \bar{\zeta}(x)\gamma_\mu\partial_\mu\zeta(x) + \bar{\zeta}(x)\gamma_\mu\exp[-iG\gamma_5\boldsymbol{\tau}\cdot\boldsymbol{\varphi}](\partial_\mu\exp[iG\gamma_5\boldsymbol{\tau}\cdot\boldsymbol{\varphi}])\zeta(x)\,.$$

Substituting the expression (7) for $\partial_\mu\exp[iG\gamma_5\boldsymbol{\tau}\cdot\boldsymbol{\varphi}]$ in the second term we obtain (10) in the form

$$\begin{aligned}(11)\qquad & \bar{\zeta}(x)\gamma_\mu\partial_\mu\zeta(x) + \bar{\zeta}(x)\gamma_\mu[iG\gamma_5(\boldsymbol{\tau}\cdot\partial_\mu\boldsymbol{\varphi}) - \tfrac{1}{2}G^2\lambda_\mu]\zeta(x) + \\ & + G^2\bar{\zeta}(x)\gamma_\mu\exp[-iG\gamma_5\boldsymbol{\tau}\cdot\boldsymbol{\varphi}]S(iG\gamma_5\boldsymbol{\tau}\cdot\boldsymbol{\varphi})\{i[\boldsymbol{\varphi},\partial_\mu\boldsymbol{\varphi},\boldsymbol{\tau}] - \lambda_\mu\}\zeta(x)\,.\end{aligned}$$

From the definition (6) we have

$$S(A) = \frac{1}{2A^2}\left(\exp[-A] + (2A-1)\exp[A]\right),$$

so that

$$\exp[-A]S(A) = \frac{1}{2A^2}\left(\exp[-2A] - 1 + 2A\right).$$

Hence (11) can be written

$$\begin{aligned}(12)\qquad & \bar{\zeta}(x)\gamma_\mu\partial_\mu\zeta(x) + \bar{\zeta}(x)\gamma_\mu[iG\gamma_5(\boldsymbol{\tau}\cdot\partial_\mu\boldsymbol{\varphi}) - \tfrac{1}{2}G^2\lambda_\mu]\zeta(x) + \\ & + \tfrac{1}{2}G\bar{\zeta}(x)\gamma_\mu(iG\gamma_5\boldsymbol{\tau}\cdot\boldsymbol{\varphi})^{-2}\{\exp[-2iG\gamma_5\boldsymbol{\tau}\cdot\boldsymbol{\varphi}] - 1 + 2iG\gamma_5\boldsymbol{\tau}\cdot\boldsymbol{\varphi}\}\cdot \\ & \cdot\{i[\boldsymbol{\varphi},\partial_\mu\boldsymbol{\varphi},\boldsymbol{\tau}] - \lambda_\mu\}\zeta(x)\,.\end{aligned}$$

The second term in (12) cancels the first term in (9*b*) if $G = g$; the third term in (12), $-\frac{1}{2}G^2\bar{\zeta}(x)\gamma_\mu\lambda_\mu\zeta(x)$ is a mass renormalization.

Summing the expressions (8), (9) and (12), the transformed Lagrangian is

$$\mathcal{L}' = \mathcal{L}_1' + \mathcal{L}_2' + \mathcal{L}_3 + \mathcal{L}_4'$$

where:

$$\mathcal{L}_1' = \zeta(x)\gamma_\mu\partial_\mu\zeta(x)\,,$$

$$\mathcal{L}_2' = M\bar{\zeta}(x)\zeta(x) - \tfrac{1}{2}g^2\bar{\zeta}(x)\gamma_\mu\lambda_\mu\zeta(x)\,,$$

and

$$\mathcal{L}_4' = M\bar{\zeta}(x)(\exp[2ig\gamma_5\boldsymbol{\tau}\cdot\boldsymbol{\varphi}]-1)\zeta(x) \tag{13}$$
$$+\tfrac{1}{2}ig\bar{\zeta}(x)\gamma_5\gamma_\mu\{(\boldsymbol{\tau}\cdot\boldsymbol{\varphi})^{-1}(1-\exp[-2ig\gamma_5\boldsymbol{\tau}\cdot\boldsymbol{\varphi}])[\boldsymbol{\varphi},\partial_\mu\boldsymbol{\varphi},\boldsymbol{\tau}]-$$
$$-[\boldsymbol{\varphi},\partial_\mu\boldsymbol{\varphi},\boldsymbol{\tau}](\boldsymbol{\tau}\cdot\boldsymbol{\varphi})^{-1}(1-\exp[-2i\gamma_5\boldsymbol{\tau}\cdot\boldsymbol{\varphi}])\}\zeta(x)-$$
$$-\tfrac{1}{2}\bar{\zeta}(x)\gamma_\mu(\boldsymbol{\tau}\cdot\boldsymbol{\varphi})^{-2}\{\exp[-2ig\gamma_5\boldsymbol{\tau}\cdot\boldsymbol{\varphi}]-1+2ig\gamma_5\boldsymbol{\tau}\cdot\boldsymbol{\varphi}\}\cdot$$
$$\cdot\{i[\boldsymbol{\varphi},\partial_\mu\boldsymbol{\varphi},\boldsymbol{\tau}]-\lambda_\mu\}\zeta(x)\,.$$

Again, in the last term of (13), we appear to have an interaction involving λ_μ, but this term vanishes if the remainder of this term is symmetrized. $\mathcal{L}_4'$ is the transformed interaction Lagrangian. It is more complicated than the corresponding Lagrangian for neutral meson theory, given by (4*a*) of I. However, the term

$$M\bar{\zeta}(x)(\exp[2ig\gamma_5\boldsymbol{\tau}\cdot\boldsymbol{\varphi}]-1)\zeta(x) \tag{14}$$

in (13) is analogous to the term (4*a*) of I, and it is of interest to see whether this interaction term can be used to set up multi-meson propagators as in I. In the neutral theory the interaction Lagrangian contains terms of the type

$$M\zeta(x)\frac{(2ig\gamma_5)^n}{n!}[\varphi(x)]^n\zeta(x)\,, \tag{15}$$

for $n=1, 2, 3, \ldots$. When we consider the graphs with an n-meson vertex arising from the term (15), we have $n!$ similar graphs obtained by permuting the n factors $\varphi(x)$. This weight factor $n!$ cancels the $(n!)^{-1}$ term in (15). The result is that we are able to express any matrix element corresponding to particular terms (15) as a simple function of the numbers n_r of lines passing between the vertices, and the summation over the n_r can easily be performed, giving the propagators d_e, d_0, s_e and s_0 of I.

In symmetric theory, the interaction term corresponding to (15) is

$$M\zeta(x)\frac{(2ig\gamma_5)^n}{n!}(\boldsymbol{\tau}\cdot\boldsymbol{\varphi})^n\zeta(x)\,. \tag{16}$$

In order to avoid having to deal with complicated re-arrangements of τ-matrices in (16) when we permute the meson field operators φ_r $(r=1, 2, 3)$ we must write (16) in the form

$$M\zeta(x)\frac{(-4g^2)^l}{2l!}(\boldsymbol{\varphi}^2)^l\zeta(x)\,, \qquad (n=2l)\,. \tag{17a}$$

or

$$M\zeta(x)\frac{(-4g^2)^l}{(2l+1)!}2ig\gamma_5\boldsymbol{\tau}\cdot\boldsymbol{\varphi}\zeta(x)\,, \qquad (n=2l+1). \tag{17b}$$

We can see why the multi-meson propagator concept fails if we consider the number of graphs formed by re-arranging the meson operators in (17*a*). The operators φ_r are linked together in pairs, and the number of arrangements of the $2l$ operators is $2^l l!$, not $2l!$. Thus the $2l!$ factor in (17*a*), and likewise the $(2l+1)!$ factor in (17*b*), is not cancelled; thus the summation over the numbers of lines passing between vertices cannot be easily performed.

4. – The transformation of PS-PS theory.

The Lagrangian density for nucleon and meson fields with charge symmetric PS-PS coupling is

$$\mathcal{L} = \mathcal{L}_1 + \mathcal{L}_2 + \mathcal{L}_3 + \mathcal{L}_4\,,$$

where:

$$\mathcal{L}_1 = \bar{\psi}(x)\gamma_\mu\partial_\mu\psi(x)\,,$$

$$\mathcal{L}_2 = M\bar{\psi}(x)\psi(x)\,,$$

$$\mathcal{L}_3 = -\tfrac{1}{2}\sum_r[(\partial_\mu\varphi_r)^2+m^2\varphi_r^2]\,,$$

$$\mathcal{L}_4 = -ig\bar{\psi}(x)\gamma_5\boldsymbol{\tau}\cdot\boldsymbol{\varphi}\psi(x)\,.$$

We perform a similar unitary transformation (1) on this Lagrangian. The transformation leaves the free-meson term $\mathcal{L}_3$ unchanged, but affects $\mathcal{L}_1$, $\mathcal{L}_2$ and $\mathcal{L}_4$.

The term $\mathcal{L}_2$ becomes, as in (8),

$$M\bar{\zeta}(x)\zeta(x) + M\bar{\zeta}(x)(\exp[2iG\gamma_5\boldsymbol{\tau}\cdot\boldsymbol{\varphi}]-1)\zeta(x)\,. \tag{18}$$

The first term is part of the free-fermion Lagrangian, and the second is an exponential interaction term.

The term $\mathcal{L}_1$ transforms, as in (12), to

$$\begin{aligned}\bar{\zeta}(x)\gamma_\mu\partial_\mu\zeta(x) + \bar{\zeta}(x)[iG\gamma_5(\boldsymbol{\tau}\cdot\partial_\mu\boldsymbol{\varphi}) - \tfrac{1}{2}G^2\lambda_\mu]\zeta(x) - \\ - \tfrac{1}{2}\bar{\zeta}(x)\gamma_\mu(\boldsymbol{\tau}\cdot\boldsymbol{\varphi})^{-2}\{\exp[-2iG\gamma_5\boldsymbol{\tau}\cdot\boldsymbol{\varphi}]-1+2iG\gamma_5\boldsymbol{\tau}\cdot\boldsymbol{\varphi}\}\cdot \\ \cdot\{i[\boldsymbol{\varphi},\,\partial_\mu\boldsymbol{\varphi},\,\boldsymbol{\tau}]-\lambda_\mu\}\zeta(x)\,.\end{aligned} \tag{19}$$

The term $\mathcal{L}_4$ transforms to

$$-ig\bar{\zeta}(x)\gamma_5\exp[2iG\gamma_5\boldsymbol{\tau}\cdot\boldsymbol{\varphi}](\boldsymbol{\tau}\cdot\boldsymbol{\varphi})\zeta(x)\,. \tag{20}$$

If we choose

$$G = g/2M \,, \tag{21}$$

then the first term in the expansion of (20) cancels the second term in the expansion of the exponential in (18), thus eliminating the first order pseudoscalar interaction term.

From (18), (19) and (20) we obtain the transformed Lagrangian in the form

$$\mathcal{L}' = \mathcal{L}'_1 + \mathcal{L}'_2 + \mathcal{L}_3 + \mathcal{L}'_4 + \mathcal{L}'_5 + \mathcal{L}'_6 + \mathcal{L}'_7 \,,$$

where:
$$\mathcal{L}'_1 = \zeta(x)\gamma_\mu \partial_\mu \zeta(x) \,,$$
$$\mathcal{L}'_2 = M\bar{\zeta}(x)\zeta(x) - \tfrac{1}{2}G^2\bar{\zeta}(x)\gamma_\mu\lambda_\mu\zeta(x) \,,$$
$$\mathcal{L}'_4 = M\bar{\zeta}(x)(\exp[2iG\gamma_5\boldsymbol{\tau}\cdot\boldsymbol{\varphi}] - 1 - 2iG\gamma_5\boldsymbol{\tau}\cdot\boldsymbol{\varphi})\zeta(x) \,,$$
$$\mathcal{L}'_5 = -2iMG\bar{\zeta}(x)\gamma_5(\exp[2iG\gamma_5\boldsymbol{\tau}\cdot\boldsymbol{\varphi}] - 1)(\boldsymbol{\tau}\cdot\boldsymbol{\varphi})\zeta(x) \,,$$
$$\mathcal{L}'_6 = iG\bar{\zeta}(x)\gamma_\mu\gamma_5(\boldsymbol{\tau}\cdot\partial_\mu\boldsymbol{\varphi})\zeta(x) \,,$$
$$\mathcal{L}'_7 = \tfrac{1}{2}\bar{\zeta}(x)\gamma_\mu(\boldsymbol{\tau}\cdot\boldsymbol{\varphi})^{-2}\{\exp[-2iG\gamma_5\boldsymbol{\tau}\cdot\boldsymbol{\varphi}] - 1 + 2iG\gamma_5\boldsymbol{\tau}\cdot\boldsymbol{\varphi}\}\cdot$$
$$\cdot\{i[\boldsymbol{\varphi}, \partial_\mu\boldsymbol{\varphi}, \boldsymbol{\tau}] - \lambda_\mu\}\zeta(x) \,.$$

$\mathcal{L}'_1$, $\mathcal{L}'_3$, $\mathcal{L}'_6$ and $\mathcal{L}'_7$ form the transformed interaction Lagrangian. The term in $\mathcal{L}'_2$ which contains λ_μ is a mass renormalization term. The other λ_μ term, occuring in $\mathcal{L}'_7$, disappears when this term is properly symmetrized, as before.

5. – Comparison with similar transformations of PS-PS theory.

To second order in the coupling constant,

$$\mathcal{L}'_4 \sim -2MG^2\zeta(x)\varphi^2\zeta(x) \,,$$
$$\mathcal{L}'_5 \sim 4MG^2\bar{\zeta}(x)\varphi^2\zeta(x) \,,$$
$$\mathcal{L}'_6 \sim iG\,\zeta(x)\gamma_\mu\gamma_5\,(\boldsymbol{\tau}\cdot\partial_\mu\boldsymbol{\varphi})\,\zeta(x)$$
$$\mathcal{L}'_7 \sim G^2\zeta(x)\gamma_\mu\{i[\boldsymbol{\varphi}, \partial_\mu\boldsymbol{\varphi}, \boldsymbol{\tau}] - \lambda_\mu\}\zeta(x) \,.$$

These terms are very similar to those appearing in similar transformations [2-6]

([4]) F. J. Dyson: *Phys. Rev.*, **73**, 929 (1948).
([5]) G. Wentzel: *Phys. Rev.*, **86**, 802 (1952).
([6]) J. M. Berger, L. L. Foldy and R. K. Osborn: *Phys. Rev.*, **87**, 1061 (1952).

of the PS-PS theory. $\mathcal{L}_4'$ and $\mathcal{L}_5'$ contribute the « pair theory » term quadratic in the meson field, and $\mathcal{L}_6'$ the pseudovector coupling term. The second order λ_μ term in $\mathcal{L}_7'$ is a mass renormalization term, and may be omitted; but as we have already noted, all the λ_μ terms in $\mathcal{L}_7'$ disappear when we symmetrize. Terms of fourth power in the nucleon operators do not arise from the transformation; in similar transformations these terms arise partly through the introduction of nucleon operators into the transformation, and partly through the use of the Hamiltonian formalism.

To second order in G we expect our transformation to give the same interaction as, for instance, the Foldy transformation, in which the transforming matrix is $\exp[iS]$, where

$$S = \frac{1}{2}\gamma_5 \operatorname{tg}^{-1}\left(\frac{g\boldsymbol{\tau}\cdot\boldsymbol{\varphi}}{M}\right).$$

To second order in G, $S = G\gamma_5\boldsymbol{\tau}\cdot\boldsymbol{\varphi}$ if $g = 2MG$. Thus the Foldy transformation is the same as ours to second order.

The transformation which we have discussed here has the advantages of being exact to all orders, of exhibiting all the λ_μ infinities arising from non-commutation of the meson field operator with its time-like derivative, and of being obviously relativistically covariant.

6. – Discussion.

In both the PS-PV and PS-PS theories, after we have performed the unitary transformations detailed above, we can use the new interaction Lagrangians to set up rather complex graphical systems involving « multi-meson » vertices at which there are two nucleon lines and an arbitrarily large number of meson lines. As we have explained, it does not seem possible to simplify the graphical systems in symmetric theories by the methods used in I for neutral PS-PV theory.

Nevertheless, it is possible to make perturbation and other types of calculation by working to a given order in the coupling constant. Several calculations of this type have been performed using the transformations of symmetric PS-PS theory discussed in Sect. 5. These calculations usually involve the use of a cut-off (5) which is not needed in the original renormalizable theory. We wish to discuss whether there is in fact any virtue in performing these calculations; in particular, it seems that the use of a cut-off in dealing with a theory which was originally renormalizable requires a lot of justification.

First let us consider the commutation properties of the meson and nucleon

fields. If the interaction Lagrangian does not contain time derivatives of the field quantities, then the canonical formalism leads to nucleon field operators which commute with all meson field operators. If however the interaction Lagrangian contains time derivatives of the fields, the nucleon operators do not commute with all the meson field operators. This difference in the commutation properties does not affect the definition of physical initial and final states, since in all consistent theories, these states are really composed of wave packets whose representative operators commute. However, if we are dealing with operators which involve bound states, the definition of these bound states may well depend greatly on whether or not we use nucleon field operators which commute with the meson operators. Thus for problems other than pure scattering ones, we may well achieve different results in a calculation by performing a unitary transformation of the type (1). It seems quite likely that the use of completely commuting meson and nucleon fields (as in PS-PS theory) is wrong for describing bound states, since in strong close interaction we expect measurements on one field to disturb the other field.

In dealing with pure scattering problems, however, we are inclined to believe that performing a unitary transformation will not change the results of any calculation that depends on working to given order in the coupling constant. The properties of the initial and final physical states involved are unaffected by the transformation, and in the transformations we have discussed the states defined by the ζ operators can be converted into states defined by the ψ operators by an « adiabatic switching off » procedure. So if the calculation being performed were mathematically rigorous and if the « switching off » procedure were justified, we would not expect a unitary transformation to affect the results of an exact calculation. Moreover, since this would be true for all values of the coupling constant, we would expect a result calculated to any given order to be unaffected. The doubtful convergence properties of the perturbation series and other power series approximations casts doubt on this argument, but it is still possible that a unitary transformation does not affect the results of calculations to a given order in the coupling constant in scattering problems. This would mean for instance that the use of a cut-off after making a Foldy transformation was unnecessary, and that if all terms to a given order were included, renormalization procedures would lead to finite results provided that we took account of the mass renormalizations arising from the transformation. However, these finite results would be identical with those obtained from the untransformed theory.

In order to test this conjecture, we are at present attempting to show that the perturbation series matrix elements of a given order in neutral PS-PV theory are identical (apart from the mass renormalization described in I) with those calculated from the « exponential coupling » theory to which it transforms. We have checked this hypothesis for lowest order meson-nucleon scat-

2046

tering. If this turns out to be true generally, it will suggest that in scattering calculations it is not worth while making unitary transformations unless they actually simplify the work; elimination of some of the infinities occurring in a theory, as in the transformation given in I, is of course a very useful simplification.

RIASSUNTO (*)

Le trasformazioni unitarie covarianti esatte applicate alle lagrangiane delle teorie PS-PS e PV-PV simmetriche mostrano la cosiddetta « equivalenza » degli accoppiamenti pseudoscalari e pseudovettoriali. Si confronta la trasformazione della teoria PS-PS con trasformazioni simili. Si discute l'utilità di fare trasformazioni unitarie e si fanno alcune osservazioni sui problemi di rinormalizzazione.

(*) *Traduzione a cura della Redazione.*

Internal Conversion Angular Correlations (*).

E. V. Ivash

University of Texas - Austin, Texas

(ricevuto il 4 Aprile 1958)

Summary. — The angular correlation function is evaluated analytically for the correlation between a γ-ray and an internal conversion electron. A relativistic treatment is presented for the following cases: 1) the 2^{L+1} magnetic pole-2^L electric pole mixture for s, $p_{\frac{1}{2}}$, and $p_{\frac{3}{2}}$ electrons, and 2) the 2^{L+1} electric pole-2^L magnetic pole mixture for $p_{\frac{1}{2}}$ and $p_{\frac{3}{2}}$ electrons.

The problem of angular correlation between a γ-ray and a conversion electron has been considered by a number of authors from varying points of view (1). In particular, the relativistic treatment of the problem for the case of pure conversion of an electron has been given by Rose, Biedenharn and Arfken (2). An extension has been made by Rose and Biedenharn (3) who considered a conversion mixture of 2^L pole magnetic plus a 2^{L+1} pole electric radiation for the s electrons.

It is the purpose of this report to extend still further the treatment of this

---

(*) This paper is based on work done at the Oak Ridge National Laboratory during the summer of 1955 and reported in the Oak Ridge National Laboratory Report ORNL-1972 by E. V. Ivash and M. E. Rose. Originally the intention was to present numerical as well as analytical results, but circumstances have not made this possible, and it was thought appropriate, therefore, to publish the analytical results alone at the present time.

(1) V. B. Berestetzky: *Journ. Exper. Theor. Phys.* (*USSR*), **18**, 1057 (1948); J. W. Gardner: *Proc. Phys. Soc.* (*London*), A **62**, 763 (1949); A **64**, 238 (1951); A **64**, 1136 (1951); D. S. Ling: *Ph. D. dissertation* (University of Michigan, 1948); D. L. Falkoff and G. E. Uhlenbeck: *Phys. Rev.*, **79**, 323 (1950).

(2) M. E. Rose, L. C. Biedenharn and G. B. Arfken: *Phys. Rev.*, **85**, 5 (1952).

(3) M. E. Rose and L. C. Biedenharn: *Oak Ridge National Laboratory Report*, No. 1324.

problem, and to consider analytically the following cases: 1) the 2^{L+1} magnetic pole-2^L electric pole mixture for s, $p_{\frac{1}{2}}$, and $p_{\frac{3}{2}}$ electrons and 2) the 2^{L+1} electric pole-2^L magnetic pole mixture for $p_{\frac{1}{2}}$ and $p_{\frac{3}{2}}$ electrons. The results for pure multipole transitions are, of course, special cases of those for the mixtures. Secondary effects due to the finite size of the nucleus and screening are neglected in the present treatment.

The procedure followed is that of ROSE, BIEDENHARN and ARFKEN [2] in which the Dirac electron current $F^M(\theta)$ is calculated for a 2^L electric pole -2^L magnetic pole conversion mixture. Following these authors the function $F^M(\theta)$ may be written

$$(1) \qquad F^M(\theta) = 2\pi \sum_{\varkappa\varkappa'\tau} \exp\left[i(\Delta_\varkappa - \Delta_{\varkappa'})\right] S(\varkappa)\, S(\varkappa')\, i^{(l\varkappa' - l\varkappa)} \cdot \\ \cdot \langle \varkappa',\, M+\tau \,|\, H_1 \,|\, \psi_i \rangle^* \langle \varkappa,\, M+\tau \,|\, H_1 \,|\, \psi_i \rangle (\chi_{\varkappa'}^{M+\tau} \,|\, \chi_\varkappa^{M+\tau}) \,.$$

The notation used is that of the above-cited reference.

The interaction Hamiltonian H_1 may be written in the form

$$H_1 = \boldsymbol{\alpha} \cdot \boldsymbol{B} + V \,,$$

where

$$\boldsymbol{B} = \alpha \boldsymbol{B}_L^M(m) + \beta \boldsymbol{B}_L^M(e) \,,$$

and

$$V = \beta V_L^M(e) \,.$$

Here $\boldsymbol{B}_L^M(m)$ and $\boldsymbol{B}_L^M(e)$ are vector potentials for outgoing waves corresponding to magnetic and electric radiation respectively, $V_L^M(e)$ is the scalar potential for electric radiation, and α and β are amplitude factors (nuclear matrix elements) for magnetic and electric radiation, respectively, which can be normalized by the condition

$$\alpha^2 + \beta^2 = 1 \,.$$

The quantity α^2/β^2 is the intensity ratio of magnetic to electric multipole conversion. The magnetic multipole field is in the solenoidal gauge.

Using explicit forms [4] for $\boldsymbol{B}_L^M(m)$, $\boldsymbol{B}_L^M(e)$ and $V_L^M(e)$ one finds by straightforward procedures similar to those used by ROSE, BIEDENHARN and ARFKEN [2] the following, more explicit expression for $F^M(\theta)$ for a 2^L electric pole -2^L magnetic pole mixture:

$$(2) \qquad F^M(\theta) = \sum_{\varkappa\varkappa'\nu} T_{\varkappa\varkappa'\nu} \{ \alpha^2 q^*(\varkappa' L' m)\, q(\varkappa L' m)\, S_{mm} + \beta^2 q^*(\varkappa' L e)\, q(\varkappa L e)\, S_{ee} + \\ + 2\alpha\beta \,\mathrm{Re}\, q^*(\varkappa' L' m)\, q(\varkappa L e)\, S_{me} \} ,$$

---

[4] M. E. ROSE: *Theory of Internal Conversion in Beta- and Gamma-Ray Spectroscopy*, edited by K. SIEGBAHN. See also M. E. ROSE: *Multipole Fields* (New York, 1955).

2049

where

$$T_{\varkappa\varkappa'\nu} = S(\varkappa)\,S(\varkappa')(-1)^{j_i+M-\frac{1}{2}} i^{l'-l}(4\pi^2)^{-1}(2j+1)(2j'+1)(2l_1+1)(2j_1+1)\cdot$$
$$\cdot C_{00}^{ll'\nu} W(ljl'j';\tfrac{1}{2}\nu)\exp[i(\Delta_\varkappa - \Delta_{\varkappa'})][(2l+1)(2l'+1)]^{\frac{1}{2}} P_\nu(\cos\theta)\,,$$

$$q(\varkappa L'm) = [(2L'+1)/L'(L'+1)]^{\frac{1}{2}}\, C_{00}^{L'l_i\bar{l}} W(L'l_i j\tfrac{1}{2};\bar{l}j_i)\,S(\varkappa,\varkappa_i,L')\,,$$

$$q\varkappa(Le) = [(2L+1)/L(L+1)]^{\frac{1}{2}}\, C_{00}^{Ll_i l} W(Ll_i j\tfrac{1}{2};lj_i)\,R(\varkappa,\varkappa_i,L)\,,$$

$$S_{mm} = C_{M-M}^{L'L'\nu} W(L'L'jj';\nu j_i)\,,$$

$$S_{ee} = C_{M-M}^{LL\nu} W(LLjj';\nu j_i)\,,$$

$$S_{me} = C_{M-M}^{LL'\nu} W(LL'jj';\nu j_i)\,,$$

and where

$$R(\varkappa,\varkappa_i,L) = L(R_3+R_4-R_5+R_6)_\varkappa + (\varkappa_i-\varkappa)(R_5+R_6)_\varkappa\,,$$

$$S(\varkappa,\varkappa_i,L') = (\varkappa_i+\varkappa)(R_1+R_2)_\varkappa\,.$$

The integrals R_i involving the radial Dirac wave functions are defined in the articles cited in [4]. The quantum numbers j_i, l_i, $\varkappa_i$ specify the initial state of the converted electron, and the notation $\bar{l}_\varkappa = l_{-\varkappa}$ is used.

The function $F^M(\theta)$ may be written as

$$F^M(\theta) = F_e^M(\theta) + F_m^M(\theta) + F_{m.e}^M(\theta)\,, \tag{3}$$

where the three terms on the right hand side are the electric magnetic, and mixed contributions, respectively, and may be calculated from the general expression for a given initial state. The results may be put in the following forms, which are closely related to the angular distributions for emission of electromagnetic radiation:

$$F_m^M(\theta) = \alpha^2(2L'+1)\,C_m(L')\sum_\nu (-1)^{M+1} C_{M-M}^{L'L'\nu} C_{1-1}^{L'L'\nu} P_\nu(\cos\theta)\,b_\nu(L'm)\,, \tag{4a}$$

$$F_e^M(\theta) = \beta^2(2L+1)\,C_e(L)\sum_\nu (-1)^{M+1} C_{M-M}^{LL\nu} C_{1-1}^{LL\nu} P_\nu(\cos\theta)\,b_\nu(Le)\,, \tag{4b}$$

$$F_{me}^M(\theta) = 2\alpha\beta[(2L+1)(2L'+1)]^{\frac{1}{2}}[C_e(L)\,C_m(L')]^{\frac{1}{2}}\cdot$$
$$\cdot\sum_\nu (-1)^{M+1} C_{M-M}^{L'L\nu} C_{1\ -1}^{L'L\nu} P_\nu(\cos\theta)\,b'_\nu(L'L)\,, \tag{4c}$$

where $C_m(L')$ and $C_e(L)$ are conversion coefficients for $2^{L'}$ magnetic pole and 2^L electric pole radiation, respectively. If the b's are set equal to unity, the angular distribution functions become those for electromagnetic radiation de-

0502

fined by BIEDENHARN and ROSE [5]. The quantities $b_\nu(L'm)$, $b_\nu(Le)$, and $b'_\nu(L', L)$, which determine the angular dependence of the conversion process, are given below for the various cases of interest earlier mentioned.

The angular correlation function $W(\theta)$ for a cascade involving a mixed conversion electron ($E_L+M_{L'}$ mixture) and a pure $2^{L_2}\gamma$ multipole may be obtained from $F^M(\theta)$ in a straigthforward fashion, and, following BIEDENHARN and ROSE, be put in the form

$$W(\theta) = I_m C_m(L') W_m + I_e C_e(L) W_e \pm 2(I_e I_m)^{\frac{1}{2}} [C_m(L') C_e(L)]^{\frac{1}{2}} W_{me}\,, \tag{5}$$

where

$$W_m = \sum_\nu b_\nu(L'm)(2L'+1)\, C^{L'L'\nu}_{1-1} C^{L_2L_2\nu}_{1-1} W(JJL'L'; \nu J_1)\cdot \cdot W(JJL_2L_2; \nu J_2) P_\nu(\cos\theta)\,, \tag{6a}$$

$$W_e = \sum_\nu b_\nu(Le)(2L+1)\, C^{LL\nu}_{1-1} C^{L_2L_2\nu}_{1-1} W(JJLL; \nu J_1) W(JJL_2L_2; \nu J_2) P_\nu(\cos\theta)\,, \tag{6b}$$

$$W_{me} = \sum_\nu b'_\nu(L', L)[(2L'+1)(2L+1)]^{\frac{1}{2}} C^{L'L\nu}_{1-1} C^{L_2L_2\nu}_{1-1} W(JJL'L; \nu J_1)\cdot \cdot W(JJL_2L_2; \nu J_2) P_\nu(\cos\theta)\,. \tag{6c}$$

Here $I_m = \alpha^2$, $I_e = \beta^2$; consequently I_m and I_e are proportional to the intensities of the magnetic and electric radiations in the mixed transitions. The particular cascade considered is that in which a nucleus makes a transition from a state of angular momentum J_1 to an intermediate state J with the emission of a conversion electron to a final state J_2 with the emission of a γ-ray of angular momentum L_2.

It remains to give explicit expressions for $b_\nu(Le)$, $b_\nu(L'm)$ and $b'_\nu(L', L)$. Only the results are presented, since the calculations follow in a straightforward manner from Eq. (2). For the E_L+M_{L+1} conversion mixture the correlation function is obtained from Eq. (5) and from the equations below by the substitution $L' \to L+1$. In the case of the M_L+E_{L+1} conversion mixture the substitution $L \to L+1$, $L' \to L$ must be used. If two or more subshells are not resolved the contributions to $W(\theta)$ from each unresolved subshell must be added together, multiplied, of course, by a factor proportional to the probability of conversion from that subshell.

Conversion of K or L_I electrons.

$$b_\nu(L'm) = 1 + \frac{\nu(\nu+1)}{2L'(L'+1) - \nu(\nu+1)} \frac{L'(L'+1)}{(2L'+1)} \frac{|1 - T_m(L')|^2}{L'+1+L'|T_m(L')|^2}\,, \tag{7}$$

[5] L. C. BIEDENHARN and M. E. ROSE: *Rev. Mod. Phys.*, **25**, 729 (1953).

$$(8)\qquad b_\nu(Le) = 1 + \frac{\nu(\nu+1)}{2L(L+1)-\nu(\nu+1)}\,\frac{L}{2L+1}\,\frac{|L+1+T_e(L)|^2}{L(L+1)+|T_e(L)|^2},$$

$$(9)\qquad b'_\nu(L+1,\,L) =$$

$$= \frac{-(L+1)}{[(2L+1)(2L+3)]^{\frac{1}{2}}}\,\frac{\mathrm{Re}\{e^{i\alpha_1}[1-L/T_e(L)][1+(L+2)/(L+1)T^*_m(L+1)]\}}{[1+L(L+1)/|T(L)|^2]^{\frac{1}{2}}[1+(L+2/(L+1)|T_m(L+1)|^2]^{\frac{1}{2}}}$$

$$(10)\qquad b'_\nu(L,\,L+1) =$$

$$= \left[\frac{L(L+2)}{(2L+1)(2L+3)}\right]^{\frac{1}{2}}\,\frac{\mathrm{Re}\{e^{i\alpha_2}[1+(L+1)/LT^*_m(L)][1-(L+1)/T_e(L+1)]\}}{[1+(L+1)/L|T_m(L)|^2]^{\frac{1}{2}}[1+(L+1)(L+2)/|T_e(L+1)|^2]^{\frac{1}{2}}}$$

In these equations

$$T_m(L') = -[(L'+1)S(L'+1,-1,L')\exp[i(\Delta_{L'+1}-\Delta_{-L'})]/L'S(-L',-1,L'),$$

$$T_e(L) = -(LR(L,-1,L)\exp[i(\Delta_L-\Delta_{-L-1}])/R(-L-1,-1,L),$$

$$e^{i\alpha_1} = \frac{R(L,-1,L)S^*(L+2,-1,L+1)\exp[i(\Delta_L-\Delta_{L+2})}{|R(L,-1,L)S(L+2,-1,L+1)|},$$

$$e^{i\alpha_2} = \frac{R(L+1,-1,L+1)S^*(L+1,-1,L)}{R(L+1,-1,L+1)S(L+1,-1,L)|}.$$

For the sake of completeness, results given for this case by Rose *et al.* [2,3] and Biedenharn and Rose [5] (for the M_L+E_{L+1} mixture) have been also included.

Conversion of L_{II} electrons.

$$(11)\qquad b_\nu(L'm) = 1 + \frac{\nu(\nu+1)L'|L'+1+V_m(L')|^2}{[2L'(L'+1)-\nu(\nu+1)](2L'+1)[L'(L'+1)+|V_m(L')|^2]},$$

$$(12)\qquad b_\nu(Le) = 1 + \frac{\nu(\nu+1)L(L+1)|1-V_e(L)|^2}{[2L(L+1)-\nu(\nu+1)](2L+1)[L+1+L|V_e(L)|^2]},$$

$$(13)\qquad b'_\nu(L+1,\,L) - \left[\frac{L(L+2)}{(2L+1)(2L+3)}\right]^{\frac{1}{2}}\cdot$$

$$\cdot\,\frac{\mathrm{Re}\{e^{i\beta_2}[1+(L+1)/LV(L)][1-(L+1)/V^*_m(L+1]\}}{[1+(L+1)/L|V_e(L)|^2]^{\frac{1}{2}}[1+(L+1)(L+2)|V_m(L+1)|^2]^{\frac{1}{2}}},$$

$$(14)\qquad b'_\nu(L,\,L+1) = \frac{-(L+1)}{[(2L+1)(2L+3)]^{\frac{1}{2}}}\cdot$$

$$\cdot\,\frac{\mathrm{Re}\{e^{i\beta_1}[1-L/V^*_m(L)][1+(L+2)/(L+1)V_e(L+1)]\}}{[1+(L+2)(/L-1)|V_e(L+1)|^2]^{\frac{1}{2}}[1+L(L+1)/|V_m(L)|^2]^{\frac{1}{2}}}.$$

2052

Here

$$V_m(L') = -\left(L' S(L', 1, L') \exp\left[i(\Delta_L - \Delta_{-L'-1})\right]\right)/S(-L'-1, 1, L'),$$

$$V_e(L) = -\left((L+1) R(L+1, 1, L) \exp\left[i(\Delta_{L+1} - \Delta_{-L})\right]\right)/L R(-L, 1, L),$$

$$e^{i\beta_1} = \frac{R(L+2, 1, L+1) S^*(L, 1, L) \exp\left[i(\Delta_{L+2} - \Delta_L)\right]}{|R(L+2, 1, L+1) S(L, 1, L)|},$$

$$e^{i\beta_2} = \frac{R(L+1, 1, L) S^*(L+1, 1, L+1)}{|R(L+1, 1, L) S(L+1, 1, L+1)|}.$$

The results for L_{II} conversion follow formally from those for K or L_I conversion by making the substitution $(T_e, T_m) \rightarrow (V_m^*, V_e^*)$ and by modifying the phase factors in an obvious manner. This is a direct consequence of Eq. (2) and of the fact that the values of $\varkappa$ and $\varkappa'$ in the final state for the two cases are negatives of each other.

It will be noted that for $j_i = \frac{1}{2}$ (*i.e.*, for K, L_I and L_{II} electrons) the pure particle parameters obey the recurrence relation

$$b_\nu = 1 + \frac{\nu(\nu+1)[L(L+1) - 3]}{3[2L(L+1) - \nu(\nu+1)]}(b_2 - 1),$$

while all the mixed particle parameters are independent of ν. Thus, only b_2 and b' need be given for numerical computation. The situation is not so simple for $j_i = \frac{3}{2}$. Here, as is seen below, the factor $\nu(\nu+1)$ in the numerator of the preceding expressions is replaced by a quadratic form in $\nu(\nu+1)$, and a three term recurrence formula applies for the pure particle parameters. This means that both b_2 and b_4 need to be given, but it is very seldom that $\nu > 4$ is required. The mixed case for $j_i = \frac{3}{2}$ gives a ν-dependent particle parameter which also fulfills a three term recurrence relation.

Conversion of L_{III} electrons.

a) (15) $$b_\nu(Le) = \frac{2L(L+1)}{2L(L+1) - \nu(\nu+1)}\left[\mathcal{A}_1(\nu^2+\nu)^2 + \mathcal{A}_2(\nu^2+\nu) + 1\right],$$

where

(16) $$\mathcal{A}_1 = \frac{3\pi k\gamma}{2L(L+1)(2L+1)^2 C(L)} \sum_{\varkappa\varkappa'} \mathrm{Re}\, \frac{A_\varkappa A_{\varkappa'}^*}{(2l+1)(2l'+1)},$$

$$(17)\qquad \mathscr{A}_2 = \frac{-3k\pi\gamma}{2L(L+1)(2L+1)^2 C_e(L)} \operatorname{Re}\left\{\frac{2(2L+1)(2L+2)}{(2L+3)^2} A_{-L-2}A^*_{L+1} + \right.$$

$$+ \frac{2(2L+1)(2L+2)}{(2L-1)(2L+3)} A_{-L-2}A^*_{-L} \cdot \frac{(2L+3)(2L+4)+(2L+1)(2L+2)}{(2L+3)^2} |A_{-L-2}|^2 +$$

$$+ \frac{2L(2L+3)+3(2L+1)(2L+2)}{3(2L+3)^2} |A_{L+1}|^2 \cdot \frac{12A_{-L-2}A^*_{L-1}}{(2L-1)(2L+3)} +$$

$$+ \frac{8L(2L+2)A_{L+1}A^*_{-L}}{3(2L-1)(2L+3)} + \frac{(2L-1)(2L+2)+6L(2L+1)}{3(2L-1)^2} |A_{-L}|^2 \cdot$$

$$\cdot \frac{4L(2L+1)A_{L+1}A^*_{L-1}}{(2L-1)(2L+3)} + \frac{4L(2L+1)A_{-L}A^*_{L-1}}{(2L-1)^2} +$$

$$\left. + \frac{(2L-1)(2L-2)+2L(2L+1)}{(2L-1)^2} |A_{L-1}|^2 \right\},$$

in which $A_\varkappa = R(\varkappa, 2, L)e^{i\Delta_\varkappa}$, and

$$(18)\qquad C_e(L) = \frac{6\pi k\gamma}{L(L+1)(2L+1)} \left[\frac{(L+1)(L+2)}{2L+3} |A_{-L-2}|^2 + \right.$$

$$\left. + \frac{L(L+1)}{3(2L+3)} |A_{L+1}|^2 + \frac{L(L+1)}{3(2L-1)} |A_{-L}|^2 + \frac{L(L-1)}{2L-1} |A_{L-1}|^2 \right].$$

b) $$(19)\qquad b_r(L'M) = \frac{2L'(L'+1)}{2L'(L'+1) - \nu(\nu+1)} [\mathscr{B}_1(\nu^2+\nu)^2 + \mathscr{B}_2(\nu^2+\nu) + 1],$$

where

$$(20)\qquad \mathscr{B}_1 = \frac{3\pi k\gamma}{2L'(L'+1)(2L'+1)^2 C_m(L')} \sum_{\varkappa\varkappa'} \operatorname{Re} \frac{B_\varkappa B^*_{\varkappa'}}{(2l+1)(2l'+1)},$$

and

$$(21)\qquad C_m(L') = \frac{6\pi k\gamma}{L'(L'+1(2L'+1)} \left[\frac{(L'+1)(L'+2)}{2L'+3} |B_{L'+2}|^2 + \right.$$

$$\left. + \frac{L'(L'+1)}{3(2L'+3)} |B_{-L'-1}|^2 + \frac{L'(L'+1)}{3(2L'-1)} |B_{L'}|^2 + \frac{L'(L'-1)}{2L'-1} |B_{-L'+1}|^2 \right].$$

$\mathscr{B}_2$ has the same form as $\mathscr{A}_2$, except that $A_\varkappa$, $C_e(L)$ and L are replaced by $B_\varkappa$, $C_m(L')$ and L', respectively, where $B_\varkappa = S(\varkappa, 2, L') \exp[i\Delta\varkappa]S_\varkappa$. Here γ is the fine structure constant ($\simeq 1/137$), and $\varkappa$ and $\varkappa'$ take on the values $-L-2$, $L+1$, $-L$ and $L-1$, and $L'+2$, $-L'-1$), L' and $-L'+1$, respectively.

20054

c) (22) $$b'_\nu(L+1,\,L)=\frac{3\pi k\gamma}{(2L+1)(2L+3)}\,[C_e(L)C_m(L+1)]^{-\frac{1}{2}}[\mathcal{C}_1(\nu^2+\nu)+\mathcal{C}_2],$$

where

(23) $$\mathcal{C}_1=\sum_{\varkappa\varkappa'}\frac{A_\varkappa B^*_{\varkappa'}}{(2l+1)(2l'+1)},$$

(24) $$\mathcal{C}_2=\frac{(2L+4)}{2L+5}\,(A_{-L-2}B^*_{L+3}+A_{-L-2}B^*_{-L-2}+A_{L+1}B^*_{L+3})+$$

$$+\frac{6}{(2L-1)(2L+5)}\,(A_{-L}B^*_{L+3}+A_{L-1}B^*_{L+3}+A_{L-1}B^*_{-L-2})+$$

$$+\frac{2L}{2L-1}\,(A_{-L}B^*_{-L}+A_{L-1}B^*_{L+1}+A_{L-1}B^*_{-L})+\frac{2}{3}A_{L+1}B^*_{L+1}+$$

$$+\frac{(2L+1)(2L+4)+2}{3(2L+3)(2L+5)}A_{L+1}B^*_{-L-2}+\frac{2(2L+1)(2L+3)+2}{3(2L-1)(2L+5)}A_{-L}B^*_{-L-2}+$$

$$+\frac{2L(2L+3)+2}{3(2L-1)(2L+1)}A_{-L}B^*_{L+1}.$$

d) (25) $$b'_\nu(L,\,L+1)=\frac{3\pi k\gamma}{(2L+1)(2L+3)}\,[C_m(L)C_e(L+1)]^{-\frac{1}{2}}[\mathcal{D}_1(\nu^2+\nu)+\mathcal{D}_2],$$

where

(26) $$\mathcal{D}_1=-\sum_{\varkappa\varkappa'}\frac{A_\varkappa B^*_{\varkappa'}}{(2l+1)(2l'+1)},$$

(27) $$\mathcal{D}_2=\frac{2L+4}{2L+5}\,(A_{-L-3}B^*_{L+2}+A_{-L-3}B^*_{-L-1}+A_{L+2}B^*_{L+2})+$$

$$+\frac{2L(2L+3)+2}{3(2L-1)(2L+1)}A_{-L-1}B^*_L+$$

$$+\frac{6}{(2L-1)(2L+5)}\,(A_{-L-3}B^*_L+A_{-L-3}B^*_{-L+1}+A_{L+2}B^*_{-L+1})+\frac{2}{3}A_{-L-1}B^*_{-L-1}+$$

$$+\frac{2L}{2L-1}\,(A_{-L-1}B^*_{-L+1}+A_LB^*_L+A_LB^*_{-L+1})+$$

$$+\frac{(2L+1)(2L+4)+2}{3(2L+3)(2L+5)}A_{L+2}B^*_{-L-1}+\frac{2(2L+3)(2L+1)+2}{3(2L-1)(2L+5)}A_{L+2}B^*_L.$$

* * *

The author would like to thank Dr. M. E. Rose for suggesting this problem and for many valuable discussions.

RIASSUNTO (*)

La funzione di correlazione angolare si calcola analiticamente per la correlazione fra un raggio γ e un elettrone di conversione interna. Si presenta un trattamento relativistico per i seguenti casi: 1) la miscela polo magnetico 2^{L+1} - polo elettrico 2^L per elettroni s, $p_{\frac{1}{2}}$ e $p_{\frac{3}{2}}$ e 2) la miscela polo elettrico 2^{L+1} - polo magnetico 2^L per elettroni $p_{\frac{1}{2}}$ e $p_{\frac{3}{2}}$.

(*) *Traduzione a cura della Redazione.*

IL NUOVO CIMENTO Vol. IX, N. 1 1° Luglio 1958

Causality and Vacuum Polarization due to a Constant and a Radiation Field.

A. Minguzzi

University of Maryland - Washington
Istituto di Fisica dell'Università - Bologna
Istituto Nazionale di Fisica Nucleare - Sezione di Bologna

(ricevuto il 5 Aprile 1958)

Summary. — It is shown that the modification of the vacuum due to the superposition of a constant electromagnetic field and a radiation field can be accounted by a for refraction index which is the limit to the real axis from the upper part of the complex plane of a function of the frequency analytic in the full complex plane with exception of branch points on the real axis. This function is explicitly constructed. It is shown that when the absorption is negligible, the phase velocity of the radiation field in the constant electromagnetic field region is smaller than the light velocity in vacuo.

1. – Introduction.

It is known that an external electromagnetic current $J_\mu(k)$ induces a vacuum polarization current; from the ratio between the polarization current and the driving current one defines the refraction index of the vacuum, which is an invariant function of $k_\mu k_\mu$ and which is the limit to the real axis of an analytic function in the upper part of the complex $k_\mu k_\mu$ plane ([1,2]). This fact bears a strict similarity with the results that have been established for the refraction index of ponderable media. A feature which is common with either treatment is the causality requirement; some authors have exploited these properties of analitycity in order to predict the dispersive part of the

([1]) G. Källén: *Helv. Phys. Acta*, **25**, 417 (1952).
([2]) R. Euwema and J. Wheeler: *Phys. Rev.*, **103**, 803 (1956).

refraction index from the knowledge of the absorptive part ([2,5]). In this work we extend the above consideration to the case in which the vacuum polarization is due to the superposition of a constant electromagnetic field satisfying $H^2 - E^2 > 0$, $\boldsymbol{E}\cdot\boldsymbol{H} = 0$ and a radiation field. It is shown that the refraction index (which actually is a tensor due to the anisotropy introduced by the constant field) as a function of the frequency ω of the radiation field is the limit to the real axis from the upper part of the complex plane of a function analytic in the full complex plane, with the exception of two branch lines ranging respectively from $-\infty$ to $-2m$ and from $2m$ to $+\infty$, m being the electron mass, and the point at infinity is at most a pole; this conclusion allows one in particular to define the refraction index for negative frequencies which turns out to be the same as postulated by KRAMERS ([3]). In a preceding ([6]) work the refraction index for real positive frequencies has been explicitly calculated; here the function is explicitly constructed in the entire complex plane, whose limit to the real ω-axis from the upper part is the actual refraction index.

In the appendix it is even shown that in the frequency range in which there is no absorption, the phase velocity of an electromagnetic wave in the constant field region is smaller than the light velocity in vacuo as it is the case in material media when one is sufficiently far from absorption lines. The corresponding investigation when there is absorption is not simple, but if the similarity with dielectric material is valid, we expect that, whatever the frequency, the phase velocity in the electromagnetic field region is smaller than the light velocity in vacuo.

2. – Properties of the refraction index.

In the bound interaction representation, the vacuum polarization current of the radiation field to first order si

$$\langle J_\mu(x)\rangle_0 = \frac{i}{2}\int [1 + \varepsilon(x-y)]\langle 0\,|\,[J_\mu(x),\, J_\nu(y)]\,|\,0\rangle A_\nu(y)\,\mathrm{d}^4y\,, \tag{1}$$

where $A_\nu(y)$ is the monochromatic radiation field and the commutator takes exactly into account the constant electromagnetic field. No renormalization term is introduced into (1) because the sources of the constant and the

([3]) H. KRAMERS: *Atti del Congresso Internazionale di Fisica*, Ed. Zanichelli (1928).
([4]) J. S. TOLL: *Phys. Rev.*, **104**, 1760 (1956).
([5]) J. S. TOLL: *Thesis*, Princeton (1952) (unpublished).
([6]) A. MINGUZZI: *Nuovo Cimento*, **6**, 501 (1957).

2058

radiation field are situated at infinite distance. The tensor

$$[1 + \varepsilon(x - y)]\langle 0 \,|\, [J_\mu(x), J_\nu(y)] \,|\, 0\rangle \,,$$

whose divergence must vanish on account of charge conservation, is a continuous function in the interior of the future light cone $x_\mu - y_\mu$ and its limit on the light cone is independent of the electromagnetic field strength; and its well known indeterminate behaviour on the light cone is supposed to be circumvented with the regularization procedure. From relativity and gauge invariance and taking into account only the linear term in the radiation field, we expect that:

$$\langle J_\mu(x)\rangle_0 = M_1 F_{\mu l}\left[\frac{\partial^2 A}{\partial x_n \partial x_l} - \frac{\partial^2 A_l}{\partial x_n \partial x}\right] F_{ln} + M_2 \tilde{F}_{\mu l}\left[\frac{\partial^2 A_l}{\partial x_n \partial x_l} - \frac{\partial^2 A_l}{\partial x_n \partial x_l}\right] \tilde{F}_{ln} \,, \tag{2}$$

where $F_{\mu\nu}$ and $\tilde{F}_{\mu\nu}$ are the constant field tensor and its dual tensor respectively and M_1, M_2 are invariant functions of $F_{\mu\nu}F_{\nu\mu}$, $F_{\mu l}F_{lt}(\partial^2/\partial x_\mu x_t)$.

We choose the frame in which the constant field is a constant field pointing in the x_3 direction and the radiation field is propagating normally to the x_3 direction and is polarized either parallel or perpendicularly to the constant magnetic field; these two cases are the only significant ones, because from (2) we get a vanishing vacuum polarization when the radiation field propagates along the magnetic field direction; in addition to this, due to the particular nature of the fields involved, we lose nothing in generality by taking the vacuum current at the point $x_1 = x_2 = x_3 = x_0 = 0$. By comparing (1) and (2), it follows that only the diagonal elements of the tensor $[1 + \varepsilon(-y)]\cdot$ $\cdot\langle 0 \,|\, [J_\mu(0), J_\nu(y)] \,|\, 0\rangle$ must be different from zero; this implies that this tensor must be only combinations of $\delta_{\mu\nu}$, $F_{\mu\nu}F_{\nu l}$, $\tilde{F}_{\mu l}\tilde{F}_{\nu l}$, each term multiplied by invariant functions of $F_{\mu\nu}F_{\mu\nu}$, $F_{\mu l}F_{lt}y_\mu y_t$, $y_\mu y_\mu$, *i.e.* in our frame the commutator is a function of $F_{\mu\nu}F_{\mu\nu}$, $y_1^2 + y_2^2$, $y_\mu y_\mu$.

By introducing polar co-ordinates in the $x_1 - x_2$ plane and integrating (1) over the angle, one gets in the parallel case

$$\langle J_2(\omega)\rangle = \int \mathrm{d}\varrho \, \mathrm{d}z F(\omega, \varrho, z) \,,$$

where

$$F(\omega, \varrho, z) = 2\pi i \varrho J_0(\varrho\omega) \int_0^\infty \langle 0 \,|\, [J_2(0), J_2(y)] \,|\, 0\rangle \exp[i\omega y_0] \mathrm{d}y_0 \,, \tag{3}$$

where $J_0(\varrho\omega)$ is the Bessel function of zero order.

2059

We notice that

$$\langle 0 | [J_2(0), J_2(y)] | 0 \rangle = 0 ,$$

when $y_\mu y_\mu$ is space-like.

Following the procedure of (8), let us consider $F(\omega, \varrho, z)$ as a function of ω, holding constant the parameters ϱ and z; it is an analytic function in the upper part of the complex ω plane. When $F(\omega, \varrho, z)$ is divided by a convenient polynomial in ω, we note that because the electromagnetic interaction is localized, the resulting function is square integrable. By observing that Re $F(\omega, \varrho, z)$ and Im $F(\omega, \varrho, z)$ are respectively even and odd functions of ω, we have

$$(4) \qquad \operatorname{Re} F(\omega_0, \varrho, z) = \sum_\nu \operatorname{Re} F(\omega_\nu, \varrho, z) \prod_{\lambda \neq \nu} \frac{\omega_0^2 - \omega_\lambda^2}{\omega_\nu^2 - \omega_\lambda^2} + \\ + \frac{2}{\pi} \prod_\nu (\omega_0^2 - \omega_\nu^2) P \int_0^\infty \frac{\omega \, d\omega}{\omega^2 - \omega_0^2} \frac{\operatorname{Im} (\omega, \varrho, z)}{\prod_\nu (\omega^2 - \omega_\nu^2)} .$$

If, in the usual way, we introduce into (3) a complet set of states of the hamiltonian of our system, we observe that we can neglect the states containing photons because, from charge conjugation invariance, they cannot be less than three, in order to give a non-vanishing contribution. Consequently the largest contribution arises from the states containing a pair of electrons placed in the magnetic field, whose mutual interaction can be disregarded as long as the magnetic field strength is sufficiently large. Now independently of the magnetic field strength, the energy of the lowest state containing two electrons is $2m$. As a consequence the integration over ω into (4) ranges between $2m$ and infinity.

The successive integrations of (4) over ϱ and z can be freely interchanged with the ω integration, with the final result

$$(5) \qquad \operatorname{Re} \langle J_2(\omega_0) \rangle_0 = \sum_\nu \operatorname{Re} \langle J_2(\omega_\nu) \rangle_0 \prod_{\lambda \neq \nu} \frac{\omega_0^2 - \omega_\lambda^2}{\omega_\nu^2 - \omega_\lambda^2} + \\ + \frac{2}{\pi} \prod_\nu (\omega_0^2 - \omega_\nu^2) P \int_{2m}^\infty \frac{\omega \, d\omega}{\omega^2 - \omega_0^2} \frac{\operatorname{Im} \langle J_2(\omega) \rangle_0}{\prod_\nu (\omega^2 - \omega_\nu^2)} .$$

If we write

$$\langle J_2(\omega) \rangle_0 = e^4 \hbar^2 M_1(\omega) \omega^2$$

and suppose that $M_1(\omega)$ has not a pole at $\omega = 0$, and we let one of the ω_ν

go to zero, one gets:

$$\text{(6)} \qquad \operatorname{Re} M_1(\omega_0) = \sum_\nu \operatorname{Re} M_1(\omega_\nu) \prod_{\lambda \neq \nu} \frac{\omega_0^2 - \omega_\lambda^2}{\omega_\nu^2 - \omega_\lambda^2} + \\ + \frac{2}{\pi} \prod_\nu (\omega_0^2 - \omega_\nu^2) P \int_{2m}^{\infty} \frac{\omega \, \mathrm{d}\omega}{\omega^2 - \omega_0^2} \frac{\operatorname{Im} M_1(\omega)}{\prod_\nu (\omega^2 - \omega_\nu^2)} ,$$

where the degree of the denominator is two less than the degree of the denominator in (5). As we will see $M_1(\omega)$ is square integrable in such a way that we can neglect the denominator in (6). Remembering the connection between the polarization current and the refraction index (6)

$$n_1(\omega) = 1 - \tfrac{1}{2} e^4 h^2 M_1(\omega) ,$$

then (6) can be written

$$\text{(6)} \qquad \operatorname{Re} n_1(\omega) = 1 + \frac{2}{\pi} \int_{2m}^{\infty} \frac{\omega \operatorname{Im} n_1(\omega)}{\omega^2 - \omega_0^2} \mathrm{d}\omega .$$

By introducing the absorption coeffcient $\xi_1(\omega) = 2\omega \operatorname{Im} n_1(\omega)$ (6), *i.e.* the energy of the radiation field absorbed per unit time and volume we can write

$$\operatorname{Re} n_1(\omega) = 1 + \frac{1}{\pi} \int_{2m}^{\infty} \frac{\xi_1(\omega)}{\omega^2 - \omega_0^2} \mathrm{d}\omega ,$$

which is the same formula established by Kramers for dielectric material (3).

Turning now to the perpendicular case by similar reasoning we have a relation which is formally the same as above.

3. - Explicit construction of the $n_1(\omega)$ function in the complex plane.

In the region I of Fig. 1 we define the function

$$M_1(\omega_1) = \frac{2}{(4\pi eh)^2} \lim_{\alpha \to 0} \int_0^1 \mathrm{d}v \int_0^\infty \mathrm{d}s \left[-\frac{1}{s'} + \frac{ehv \sin ehs' v \cos ehs}{\sin ehs'} + 2eh \frac{\cos ehs' v - \cos ehs'}{\sin^3 ehs'} \right] \cdot \\ \cdot \exp \left\{ -ism^2 + \frac{i\omega_I^2}{2} \left[\frac{1}{2} s(1 - v^2) - \frac{\cos ehsv - \cos ehs}{eh \sin ehs'} \right] \right\} ,$$

2061

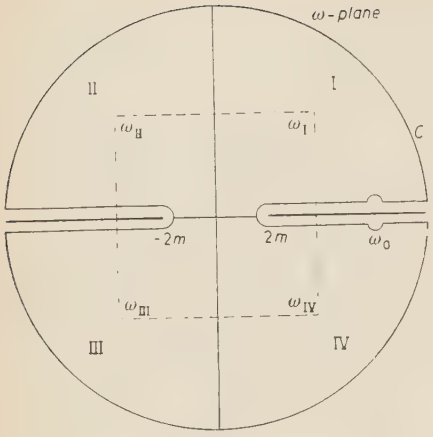

Fig. 1.

where $s' = s(1 - i\alpha)$, whose limit to the real axis coincides with the $M_1(\omega)$ function introduced in (6), and which in I is analytic. If ω_I and ω_{II} are symmetrical points with respect to the positive imaginary ω-axis as in Fig. 1 we define

$$M_1(\omega_{II}) = M_1^*(\omega_i) ,$$

which is analytic in region II. We can state the existence of an analytic function in the region I+II if no singularity occurs on the positive imaginary ω axis, on which from (8) and (9) there are no singularities except possibly branch points. But by a rotation of $\pi/2$ of the s-integration path in (8) one can show that

$$\lim_{\omega_r \to 0_+} M_1(\omega_r + i\omega_i) = \lim_{\omega_r \to 0_+} M_1^*(-\omega_r + i\omega_i)$$

and we have thus defined an analytic function in the region I+II; which at infinity decreases faster than $1/|\omega|^2$.

The defined function being analytic in the region I+II will be analytic in the strip $\mathrm{Im}\,\omega > 0$, $-2m \leqslant \mathrm{Re}\,\omega \leqslant 2m$ and being real on the real axis with the Schwarz reflection principle [9] can be analytically continued into the strip $\mathrm{Im}\,\omega < 0$, $-2m \leqslant \mathrm{Re}\,\omega \leqslant 2m$ and from this to the remaining part of the complex plane. We have consequently

$$M_1(\omega_{III}) = M_1^*(\omega_{II}) , \qquad M_1(\omega_{IV}) = M_1^*(\omega_I) ,$$

which shows that the only singularities of the defined function in the full complex plane are two branch lines ranging from $-2m$ to $-\infty$ and from $2m$ to $+\infty$. A check of the correctness of this procedure is the observation that having defined the function in the region I+IV (II+III) we can continue this function into II+III (I+IV) using again the Schwarz reflection principle because along the imaginary axis the function is real and this procedure gives the same result obtained with the previous procedure.

---

(7) W. Pauli and F. Villars: *Rev. Mod. Phys.*, **21**, 434 (1949).
(8) R. Oehme: *Nuovo Cimento*, **6**, 1316 (1956).
(9) P. H. Morse and H. Feshbach: *Methods of Theoretical Physics* (New York, 1953).

2062

By the application of the Cauchy theorem to the C-path of Fig. 1

$$\oint \frac{M_1(\omega)}{\omega - \omega_0} \, \mathrm{d}\omega = 0 \,,$$

this equation is completely equivalent to the result (7), if we observe that the definition of the $M_1(\omega)$ function for negative frequencies following from (9) is $M_1(-\omega) = M_1^*(\omega)$, which coincides with the definition of $n_1(-\omega)$ one for negative frequencies.

The same procedure applied to $n_2(\omega)$, allows to rearch the same conclusions.

* * *

The author whises to thank Prof. J. Toll for useful discussions about the subject.

I would like to express my gratitude to Prof. J. Toll for the kind hospitality given me in the Physics Department of the University of Maryland.

Appendix

In order to demonstrate that the phase velocity is smaller than the light velocity in vacuo we must show that

$$M_2(\omega) \leqslant 0 \,, \qquad M_1(\omega) \leqslant 0 \,.$$

This is easy to prove when $\omega < 2m$ and we will restrict to this case. When $\omega < 2m$ we can rotate the s-integration path into formula (1′) and (1″) of reference (6), and we obtain,

$$M_2(\omega) = \frac{2}{(4\pi e h)^2} \int_0^\infty \mathrm{d}s \int_0^1 \mathrm{d}v \left[\frac{1}{s} - \operatorname{cotgh} s \left(1 - v^2 + v \frac{\sinh sv}{\sinh s} \right) \right] \exp [R] \,,$$

$$M_1(\omega) = \frac{2}{(4\pi e h)^2} \int_0^\infty \mathrm{d}s \int_0^1 \mathrm{d}v \left[-\frac{1}{s} + \frac{v \sinh sv \operatorname{cotgh} sv}{\sinh s} - 2 \frac{\cosh sv - \cosh s}{\sinh^3 s} \right] \exp [R] \,,$$

$$R = -s \frac{m^2}{|eh|} + \frac{1}{2} \frac{\omega^2}{|eh|} \left[\frac{1}{2} s(1 - v^2) + \frac{\cosh sv - \cosh s}{\sinh s} \right] .$$

21063

Now the sign of $M_2(\omega)$ is the sign of

$$\sinh^2 s - s\,(1 - v^2)\sinh s \cosh s - sv \cosh s \sinh sv\,,$$

which, developed in power series of v is equal to

$$\sum_1^\infty{}_n A_{2n}(v) s^{2n}\,.$$

It is easy to show that

$$A_{2n+2}(v) \leqslant A_{2n}(v)$$

and that $A_2(v) \leqslant 0$ from which follows that $M_2(\omega) \leqslant 0$.

In order to investigate the sign of $M_1(\omega)$ it is necessary to investigate the behaviour of $\exp[R]$, and one can shown that $\exp[R]$ is a not increasing function of v when v ranges between 0 and 1 whatever is s.

Beyond this

$$\varphi(s, v) = \left[\frac{1}{s} - \frac{v \sinh sv \operatorname{cotgh} sv}{\sinh s} + 2\frac{\cosh sv - \cosh s}{\sinh^3 s}\right]\frac{2}{(4\pi eh)^2}\,,$$

is a non-increasing function of v and in correspondence to every s there is a $v_0 = v_0(s)$, such that $\varphi(s, v_0(s)) = 0$ and $\int_0^1 \varphi(s, v)\,\mathrm{d}v < 0$.

We can write

$$-M_1(\omega) = \int_0^\infty \mathrm{d}s\left[\int_0^{v_1(s)} \varphi(s, v)\exp[R]\,\mathrm{d}v + \int_{v_0(s)}^1 \varphi(s, v)\exp[R]\,\mathrm{d}v\right]$$

and from the average theorem

$$-M_1(\omega) = \int_0^\infty \mathrm{d}s \exp[R(\bar{v})]\int_0^{v_1(s)} \varphi(s, v)\,\mathrm{d}v + \int_0^\infty \mathrm{d}s \exp[R(v)]\int_{v_0(s)}^1 \varphi(s, v)\,\mathrm{d}v\,,$$

with $\bar{v} \geqslant \bar{v}$ and consequently $\exp[R(\bar{v})] \geqslant \exp[R(\bar{v})]$.

But

$$\int_0^\infty \mathrm{d}s \exp[R(\underline{v})]\int_0^1 \varphi(s, v)\,\mathrm{d}v \geqslant 0\,,$$

in such a way that we have *a fortiori*

$$-M_1(\omega) \geqslant 0\,.$$

2064

We have thus shown that when there is no absorption the refraction index is greater than unity; this result shows a remarkable similarity to the behaviour of dielectric material when absorption is negligible. The analysis concerning the real part of the refraction index when $\omega > 2m$ is not directly possible, but we can have information if we assume that the already noted similarity with dielectric material occurs even when $\omega > 2m$; and from this follows that $\mathrm{Re}\, n_{1,2}(\omega) < 1$ if one expects « resonance frequencies », *i.e.* frequencies around which absorption becomes very important. Now the actual absorption coefficient is proportional to the transition rate of electrons from negative to positive energy states and the initial and final are continuum levels. Consequently we expect a very smooth behaviour of the absorption coefficient with frequency; and finally we expect $\mathrm{Re}\, n_{1\,2}(\omega) \geqslant 1$ whatever is ω.

RIASSUNTO

Si dimostra che la modificazione del vuoto dovuta alla sovrapposizione di un campo elettromagnetico costante e un campo di radiazione si può descrivere mediante un indice di rifrazione che è il limite sull'asse reale dalla parte superiore del piano complesso di una funzione della frequenza analitica in tutto il piano complesso ad eccezione dei punti di diramazione sull'asse reale. La funzione è esplicitamente costruita. Si mostra che quando l'assorbimento è trascurabile, la velocità di fase del campo di radiazione nella regione del campo elettromagnetico costante è minore della velocità della luce nel vuoto.

2065

Diffraction Scattering and Interactions of 0.57 GeV π^- in Emulsions.

A. Barbaro, G. Baroni and C. Castagnoli

Istituto di Fisica dell'Università - Roma
Istituto Nazionale di Fisica Nucleare - Sezione di Roma

(ricevuto il 7 Aprile 1958)

Summary. — A study of 570 MeV negative pion interactions with nuclei (and nucleons) is carried out with nuclear emulsion technique. Particular attention is given to diffraction scattering. The results on 152.2 m of followed track agree, as far as absorption is concerned, with the predictions of an optical model using dispersion rules, and a Fermi-type nuclear density distribution. The diffraction cross-section, instead, comes out larger than that predicted by the model, and this seems to confirm the results obtained with other techniques.

1. – Introduction.

It is well known that the experimental results for the pion and nucleon absorption cross-sections by nuclei do no agree (1) with the predictions of a simple optical model which considers the nucleus as an opaque sphere of radius $R = r_0 A^{\frac{1}{3}}$. More elaborate models have been therefore proposed, as regards the size and density distribution of nuclei, and better agreement has been thus obtained between theory and experiment (2).

It has been recently observed (3), however that the diffraction cross-section σ_d for high-energy π^- is $(20 \div 30)\%$ higher than that predicted by a tapered optical model, while the agreement for the absorption cross-section, σ_a, is good. This result, obtained with counters technique, would indicate that the

(1) A. Wattenberg: *Handb. d. Phys.*, **40**, 493 (1957).
(2) R. W. Williams: *Phys. Rev.*, **98**, 1387 (1955).
(3) J. W. Cronin, R. Cool and A. Abashian: *Phys. Rev.*, **107**, 1121 (1957).

real potential of the nucleus for pions has to be higher than the value deduced from the optical model using dispersion rules. To verify the existence of such potential, we thought it convenient to examine, with a different technique, the diffraction and absorption of 570 MeV π^- in nuclear emulsion, and to compare the results with the predictions of a high-energy optical model using dispersion relations, and an accurate nuclear density distribution according to a Fermi, tapered model. In this research we have also observed the interaction with nucleons in the emulsion, since up to now there are not many results of this type at energies over the first resonance ([1-8]).

2. – Exposure and track scanning.

During the antiproton research ([9,10]) a stack of stripped G5 emulsions (each 10 cm × 16 cm × 0.06 cm) was exposed to a magnetically selected and focalized beam of negative particles of $p = 700$ MeV/c emitted by a copper target bombarded by 6.2 GeV protons from the Berkeley Bevatron.

Accurate range-measurements of antiprotons belonging to the beam gave a momentum $p = (690 \pm 5)$ MeV/c. There was a variation $\Delta p/p = 0.7\,\%$ per inch, starting from a reference line: only those zones in the emulsion for which $\Delta p/p \sim 1\,\%$ were used. We then assumed for the kinetic energy of the π^- the value $E = (565 \pm 6)$ MeV.

The mean semi-aperture of the beam entering the emulsion stack was $\sim 1°$, the flux was $1 \cdot 10^5$ per cm^2; the fast μ and electron contamination was estimated at $\sim (10 \pm 5)\,\%$ but the exact knowledge of this contamination was not necessary to our purpose namely to study the ratio σ_d/σ_a. Minimum grain count was $g_0 = 25/100\ \mu$m; bubbles and distortion were negligible. Scanning velocity was ~ 0.5 m per man-day.

3. – Diffraction scattering.

3.1. *Scanning efficiency.* – As usual, we have assumed as diffraction scatterings against nuclei those scatterings whose angle in space $\vartheta \leqslant 10°$.

([1]) A. E. Ignatenko: *CERN Symposium* (1956).
([5]) M. Blau and A. R. Oliver: *Phys. Rev.*, **102**, 489 (1956).
([6]) J. Crussard and W. D. Walker: *Phys. Rev.*, **98**, 1416 (1955).
([7]) W. D. Walker, F. Hushfard and W. D. Shepard: *Phys. Rev.*, **104**, 526 (1956).
([8]) J. D. Clark and J. V. Major: *Phil. Mag.*, **2**, 37 (1957).
([9]) O. Chamberlain *et al.*: *Phys. Rev.*, **102**, 921 (1956).
([10]) E. Amaldi, C. Castagnoli, C. Franzinetti, M. Ferro-Luzzi and A. Manfredini: *Nuovo Cimento*, **5**, 1797 (1957).

The majority of the scatterings has been identified by a sudden variation of the direction of the track on the horizontal plane (and only a few on the vertical plane). Hence the scanning efficiency must have increased with increasing α (projection of the angle in space onto the plane of the emulsion), at least for small α. It is obviously very difficult to estimate how the scanning efficiency depends on α. On the other hand it is possible to calculate, with simple geometrical considerations, the loss due to a given cut-off in α. If $F(\vartheta)$ is the angular distribution and if one accepts only those scatterings whose projected angle is $\alpha \geqslant \alpha_0$, then the angular distribution will be:

$$(1) \qquad F_{\alpha>\alpha_0}(\theta) = \frac{1}{\pi} F(\theta) \left\{ \arccos(2s^2 - 1) + \frac{1}{\sum_{\varphi} N(\varphi)} \sum_{\varphi} \left[N(\varphi) \cdot \varphi^2 \cdot s \frac{1 + \mathrm{tg}^2 \alpha_0}{(1 - s^2)^{\frac{1}{2}}} \right] \right.,$$

where φ is the dip-angle of the incident π, $N(\varphi)$ has been determined experimentally, and $s = \mathrm{tg}\,\alpha_0 / \mathrm{tg}\,\vartheta$.

Applying formula (1) for various values of α_0 we ascertained that the efficiency depends on α_0 only for $\alpha_0 \leqslant 2°$; all scattering with $\alpha \leqslant 2°$ have been discarded. It remains to evaluate the general scattering-scanning efficiency. A test performed on the accepted scanners—each one had to follow the same track—allowed us to set the general scanning efficiency $e = 0.86 \pm 0.08$.

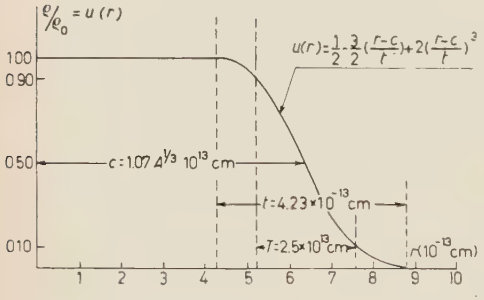

Fig. 1.

Since we have supposed equal to zero the scanning efficiency for $\alpha \leqslant 2°$, the calculation of $\lambda\alpha$ requires an extrapolation to $\alpha = 0$ on the basis of some theoretical model.

3·2. *The theoretical model.* – The values of the parameters in the Fermi tapered model used by us and shown in Fig. 1, are obtained from the scattering of high-energy electrons ([11]). Indeed, an accurate analysis ([2,12,13]) of high-energy experiments indicates that the charge density distribution coincides to within a few percent with the matter density distribution. Supposing furthermore that the proton and neutron radial distributions are identical, the absorption and diffraction cross-sections in

([11]) B. Hahn, D. G. Ravenhall and B. Hofstadter: *Phys. Rev.*, **101**, 1131 (1956).

([12]) T. Coor *et al.*: *Phys. Rev.*, **98**, 1369 (1955).

([13]) F. P. Chen, C. P. Leavitt and A. M. Shapiro: *Phys. Rev.*, **99**, 857 (1955).

2068

emulsion, as calculated with the optical model, are:

$$\sigma_a = 2\pi \sum_j N_j \int_0^\infty \{1 - \exp[-2\bar{\sigma} \varrho_{0j} S_j(b)]\} b \, db \,, \tag{2}$$

$$\sigma_d = 2\pi \sum_j N_j \int_0^\infty |1 - \exp[2i\alpha_j - \bar{\sigma}_j] \varrho_{0j} S_j(b)|^2 b \, db \,, \tag{3}$$

where N_j is the number of nuclei per cubic centimeter of the j^{th} species and $\bar{\sigma}$ indicates $\bar{\sigma} = [Z\sigma^- + (A - Z)\sigma^+](1/A)$. The value of $\bar{\sigma}$ should be diminished according to an observation by SERBER ([14]), on account of the Pauli principle which prohibites elastic collisions with energy transfer too small to carry the bound nucleon into a non-occupied state. On the other hand $\bar{\sigma}$ should be augmented on account of direct pion absorption by 2 or more nucleons. The two corrections practically cancel each other out ([3]), and it is thus justified to use $\bar{\sigma}$ as gotten from the free cross-sections of the pion-nucleon elementary processes. The effective path length within the nucleus $S(b)$ is a function of the impact parameter b graphed by CRONIN *et al.* ([3]).

Parameter α is related to the usual parameter k' which measures the variation of the wave-number when the pion enters the nucleus, as follows:

$$k' = 2\pi \varrho_0 u(r)[ZD_-(k) + (A - Z)D_+(k)] \frac{1}{kA} = \alpha \varrho_0 u(r) \,, \tag{4}$$

where ϱ is the nucleus density, k the wave-number, $D_+(k)$ and $D_-(k)$ the real parts of the scattering amplitudes in the forward direction for the (π^+-p) and (π^--p) cases respectively as obtained from dispersion rules.

Using (2) and (3) and the G5 emulsion composition given by WALLER ([15]) we have obtained the following cross-sections for π^-'s of our energy in 1 cm^3 of emulsion:

$$\sigma_a = 2.57 \cdot 10^{-2} \text{ cm}^{-1}, \quad \sigma_d = 1.19 \cdot 10^{-2} \text{ cm}^{-1}, \quad \frac{\sigma_d}{\sigma_a} = 0.46. \tag{5}$$

In computing σ_a we took into account the electrostatic correction. The corresponding values from a square-well model with $r_0 = 1.4$ fermis would be:

$$\sigma_a = 2.91 \cdot 10^{-2} \text{ cm}^{-1}, \quad \sigma_d = 1.34 \cdot 10^{-2} \text{ cm}^{-1}, \quad \frac{\sigma_d}{\sigma_a} = 0.46.$$

([14]) R. SERBER: *Phys. Rev.*, **72**, 1144 (1947).

([15]) C. WALLER: private communication; A. J. SWINNERTON: *The density and composition of Ilford G5 emulsion.*

2069

The diffraction scattering angular distribution is given by

$$F(\theta)\,\mathrm{d}\theta = \frac{2\pi \mathrm{d}\cos(\theta)}{\sum N_j \sigma_{\mathrm{tot}\,j}} \sum N_j |f_j(\theta)|^2 , \tag{6}$$

where $f_j(\theta)$, the amplitude of the scattered wave as a function of the angle of scatter in space is of the type

$$f_j(\theta) = k_0 \int_0^\infty \{1 - \exp\,[2i\alpha_j - \bar{\sigma}_j]\varrho_{0j} S_j(b)\} J_0(k_0 b \sin\theta) b\,\mathrm{d}b ,$$

where J_0 is the Bessel function of zero-order. θ is the angle in the center of mass system between incident and scattered π^-: in our case, since hydrogen does not contribute to the scattering, θ practically coincides with the laboratorium system angle, also for light elements.

The scattering cross-section at forward angles is the square of the sum of the amplitude for nuclear elastic scattering f_N and Coulomb scattering f_C, and thus contains an interference term $2f_N f_C$. At our energy, Coulomb scattering is not simply given by the Rutherford cross-section for a point charge, but the finite extension of the charge density must be taken into account by means of a form-factor F. We have used the form-factor calculated by CHEN *et al.* [13].

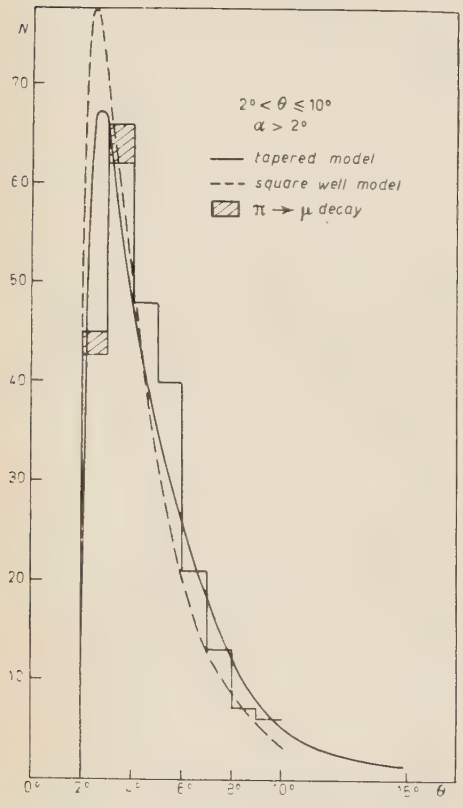

Fig. 2.

3·3. *Results.* – Out of the 498 observed scatterings in the 152.2 m of track followed by the accepted scanners, 255 have $\alpha \geqslant 2°$ and their angular distribution is shown as a histogram in Fig. 2. The solid curve represents the theoretical distribution as given by (6) considering (1) and Coulomb scattering. Notice that the agreement between theoretical curve and experimental histogram is not so good if one uses instead a square-well model

with $r_0 = 1.40$ fermis, as shown by the dashed curve in the figure. Taking into account Coulomb-correction, π-μ decay, and geometrical corrections (1) one finds the effective number of diffraction nuclear scatterings with $\alpha > 0$ and $0 < \theta < 15°$ to be 176.

4. – Collisions against nuclei and nucleons.

Stars, scatterings with $\theta > 10°$, and tracks which disappear in the emulsion have been classified as *collisions against nuclei and nucleons*. After discarding one scanner on the basis of Chauvenet's criterium on the individual λ_a, the star-scanning efficiency has been estimated considering separately for each observer the mean number of prongs of the stars, $\overline{n_s + n_H}$ and the corresponding individual λ_a, and constructing then the graph in Fig. 3. It does give a small indication of small-star losses for some scanners, but we have not performed the correction since it is not a statistically significant loss. We have used 150.5 m of followed track and found 319 interactions, of which 10 scatterings with $\theta > 10°$ have been discarded as probably belonging to the tail of the corrected scattering distribution.

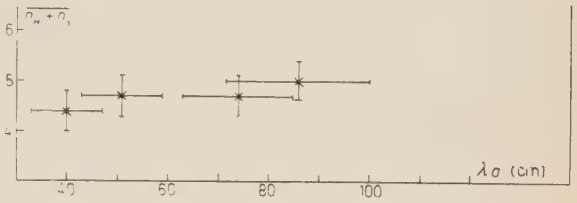

Fig. 3.

TABLE I.

Energy GeV	$\pi^- + p = \pi^- + p$		$\pi^- + p = \begin{cases} \pi^- + \pi^+ + n \\ \pi^- + p + \pi^0 \end{cases}$		$\pi^- + p = \pi^0 + n + (\pi^0)$		$\sigma_{tot.}$(*) mb.
	σ_{el} mb	σ_{el}/σ_t	$\sigma_{1\pi}$	$\sigma_{1\pi}/\sigma_t$	$\sigma_{c.e.}$	$\sigma_{c.e.}/\sigma_t$	
0.57 ([a])	5.5±3.0	0.15	6.8±3.5	0.19	23.6±7.3	0.65	36
0.75 ([5])	11.8±4.0	0.27	14.0±4.4	0.32	18.3±5.3	0.42	44
0.90 ([7])	18.6±3.0	0.40	16.5±2.8	0.35	10 ±3	0.12	46.2
1.5 ([6])	6.7±3.0	0.22	13.8±2.8	0.46	8.4±1.3	0.28	30
4.5 ([16])	4.5	0.16	16.5	0.58	2	0.07	28.7 (+)

(*) The total cross-section values are by COOL *et al.* ([17]).
(+) This value for the cross-section is by N. F. WILKNER (January 1957, unpublished).
(*a*) Present work.

([16]) W. D. WALKER: *Phys. Rev.*, **108**, 872 (1957).
([17]) R. COOL, O. PICCIONI, D. CLARK: *Phys. Rev.* **103**, 1082 (1956).

2071

The selection-criteria in the case of elastic and inelastic collisions against nucleons were those by now commonly practiced (6). It is to be noticed that charge-exchange scatterings appear as a track ending abruptly: the aspect is obviously the same as for the π^--nuclei interaction with emission of neutrons only. Pairs due to the produced π^0 have not been looked for.

The results obtained for the various events are compiled in Table I; for comparison we include the results which we know of at different energies of other authors.

5. – Discussion.

From what has been said so far one finds for the corrected total nuclear interaction length in emulsion the value $\lambda_i = (28.1 \pm 1.7)$ cm, to be compared with the geometrical path $\lambda_g = 26.0$ cm, calculated from the G5 composition and assuming a black nucleus with $r_0 = 1.4$ fermis. Accepting the previous estimation for the contamination of the beam, this result gives for the scanning efficiency 0.93 ± 0.06, which is quite reasonable.

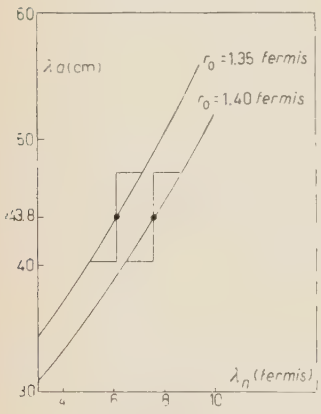

Fig. 4.

From the experimental value of $\lambda_a = (43.8 \pm 3.5)$ cm obtained it is also possible to determine an important parameter: the mean free path in nuclear matter λ_n. Considering for sake of simplicity the square model, we have constructed in Fig. 4 the general dependence of λ_a from λ_n, for the two usual values $r_0 = 1.4$, and $r_0 = 1.35$ fermis One thus obtains respectively $\lambda_n = 7.6 \pm 1.1$ and $\lambda_n = (6.1 \pm 1.1)$ fermis. Hence a π^- of this energy will undergo, on the average, 0.7 collisions when going through a nucleus of medium size within the emulsion.

Furthermore one sees that the optical model suggests a ratio $\sigma_{el}/\sigma_a = \lambda_a/\lambda_{el} = 0.46$ for the tapered as well as the square models of the nucleus, with $r_0 = 1.4$ fermis. We obtain, experimentally, for the value of this ratio, $Q = 0.56 \pm 0.05$. The scanning efficiency—and uncertainties on beam contamination—influence, of course, very little this value.

Our result contradicts that obtained by WILLIAMS (18), who also uses the tapered model based on the emulsion measurements of CRUSSARD and WALKER at 1.5 GeV. He gets $Q = 0.31 \pm 0.05$ instead of 0.56 as expected at that

(18) R. W. WILLIAMS: *CERN Symposium* (1956), p. 324.

energy. But the very small average deflection of the pions in elastic collisions at this energy, renders difficult a good estimation of total scanning efficiency and of bias-free data at very small angles. CRONIN, instead, finds a Q-value 20 to 30% larger than the theoretical value, and attributes this effect to the fact that for pions the real potential of the nucleus may be several times larger than the value deduced from the optical model and the dispersion theory.

Our value of Q, obtained with a different technique, seems to give an indication in the same sense.

It is to be noticed, however, that in order to verify with emulsion technique the extent of the effect one should work at an energy much higher than ours. That is, at about 700 to 900 MeV, so that the Coulomb correction would fall off and one would still have a reasonable scanning efficiency.

RIASSUNTO

Si studia con la tecnica delle emulsioni nucleari la interazione di π^- da 570 MeV contro nuclei (e nucleoni), con particolare riguardo allo scattering di diffrazione. Su 152.2 m di traccia seguita i risultati sull'assorbimento concordano con quelli previsti da un modello ottico che usa le relazioni di dispersione ed una distribuzione di densità nucleare alla Fermi. La sezione d'urto di diffrazione risulta invece più grande di quella prevista dal modello; e ciò sembra confermare i risultati ottenuti con altre tecniche.

Might perhaps Energy be a merely Statistical Concept? (*)

E. Schrödinger

Vienna

(ricevuto il 21 Giugno 1958)

Summary. — Arguments are given in favour of the opinion that the quantum-mechanical frequency, multiplied by Planck's constant, has for microscopic systems *not* the meaning of energy. It is suggested, that the concept of energy and its conservation, just like that of entropy and its increase, has merely a statistical meaning, the energy of a macroscopic system being the product of Planck's constant and a weighted average of the frequencies in question. The wide-spread attitude that the claim for an objective description of physical reality must be given up, is rejected on the ground that the so-called external world is built up exclusively of elements of the single minds, and is characterized as what is common to all, recognized by every healthy and sane person. Hence the demand for a non-subjective description is inevitable, of course without prejudice whether it be deterministic or otherwise.

---

1. – The prevailing opinion is to the contrary. It is claimed, that the conservation of energy and momentum holds for single collisions or similar events in all cases that have been observed. The earliest and indeed very difficult investigations were about the Compton effect. A vast number of single processes have since been fixed and analysed in the Wilson cloud chamber, in photographic emulsions etc. However, I believe that in all cases the kind of interpretation suffices that I put forward thirty years ago (1927) for the Compton effect, *viz.* reflexion of one progressive wave by another one; or to be quite accurate: the interference pattern formed by *one* wave and its reflected wave serves as a sort of (moving) Bragg crystal mirror for the *other*

(*) Based on a lecture, delivered in Vienna on 26th March 1958 at a joint meeting of the Austrian Physical Society and the Chemical-Physical Society.

wave, and *vice-versa*. To this there is, by the way, a close analogy in the reflexion of monochromatic light by the waves of heat motion or by ultrasonic waves in a fluid (Léon Brillouin and others). It is not my objective to go into details about these things here. But allow me to mention: it is usually believed, that the current orthodox theory actually accounts for the « nice linear traces » observed in the Wilson chamber etc. I think this is a mistake, it does not.

The first to raise serious and well argued doubts as to the validity of the conservation laws on the small scale was Franz Exner in his *Vorlesungen über die physikalischen Grundlagen der Naturwissenschaften* (Wien, Deuticke, 1919). This was six or seven years before the advent of quantum- or wave-mechanics. After the latter had been developed and adopted, it became extremely improbable that the conservation of energy retain its meaning as an exact and sharp law. For the concept of energy and its conservation stems from classical mechanics (Galileo, Newton), namely from an integration constant (« constant of the motion ») which in that theory plays a fundamental part. However, the mathematical scheme and the mental image of classical mechanics have turned out to be only an approximation, that holds on a large scale but breaks down entirely in spatial dimensions of about the order of an Å. It cannot even approximately comprehend the details of the motion of elementary particles (supposing that this concept is at all going to survive in the new setting of ideas). That is why I consider it *prima facie* rather improbable, that the notion of energy conservation should hold good even in the domain where the theory from which it hails is no longer competent.

We are reminded of the Second Law, which according to *phenomenological* thermodynamics says that in an isolated system the entropy never decreases and as a rule increases. *Statistical* thermodynamics, by revealing an insight into the true nature of this theorem, at the same time annulls it as a strict law; and that in two ways. *First* it is truly invalidated for systems with a small number of degrees of freedom, and for any system in the neighbourhood of thermodynamic equilibrium; nay, in these cases it is hardly possible to offer a sound definition of entropy or to give it with sufficient precision. *Secondly*, and even more relevantly, the statistical theorem seems *prima facie* to imply a logical contradiction, because it makes bold to deduce from reversible models the unidirectional running down which is the gist of the Second Law. As everybody knows, this dangerous hitch can only be overcome by allowing the « arrow of time »—the direction from past to future—to be defined by the very law of increasing entropy itself. Thus we eventually hit on the problematics of the concept of time.

According to the new physics energy too has something to do with time, though not with time's arrow. There is an uncertainty relation stating, for simultaneous determinations of energy and of time, a lower boundary for the

20755

product of their respective lacks of precision. Moreover some difficulties arise for the concept of an *isolated* system (whose energy might prove to be constant), not only because a system under observation is by principle not isolated, but also because the interaction with the general heat radiation can in actual fact never be excluded.

The said uncertainty relation is usually taken to mean that in principle an infinite time is required for finding out the exact value of the energy. It is difficult to see how « after » doing so we should still manage to ascertain that the value we have found does not change with time. In addition, within a comparatively short span of time, an appreciable interaction with the radiation is to be expected, and thus—if we keep to the idea of energy conservation—some change of the energy of the system under consideration. It may seem that in these remarks we are maliciously pushing things to extremes (which one ought never to do), while in actual fact the situation is not as bad as all that. Please wait, I hope to show that it is even worse.

In the old mechanics the energy was a function in phase-space (p_k, q_k). In the new mechanics this cannot be, since from the general uncertainty relations no point in phase space can be exactly determined. How does the quantum statistician meet this predicament? He writes out what is often called the energy-eigenvalue-equation (or time-independent Schrödinger equation, or most aptly the amplitude equation). It determines the eigenvalues of the frequency. These, multiplied by h, are declared to be the *only admissible* values of the energy; which means falling back into the foot steps of Niels Bohr's pioneer work of 1913, duly hailed then and for ever, for the immense advancement of physics that it brought about, but now (1958) after all superseded for more than thirty years. Anyhow, this « energy spectrum » replaces the phase space of Boltzmann and Gibbs. The weight to allot to every « level » is easily made out from analogy with Liouville's theorem, *viz.* the same for every single eigenvalue, and for degenerate ones according to their multiplicity. Very satisfactory agreement with observations is obtained by this procedure, which might pass for impeccable, were it not in glaring contradiction to the foundations of quantum mechanics. This heretic statement and the following argument refers in the first place to systems of few degrees of freedom, when the multiplicities too are not very great; these are the cases of primary interest.

Then, since every privileged quantum level is associated with a volume h^f of phase space when single, or a small multiple thereof when degenerate (f being the number of pairs of canonically conjugate variables) it is easily seen that the levels are just so densely packed as to disallow one to distinguish unequivocally between neighbouring levels, on account of the uncertainty relations that hold between the pairs of conjugate variables. Hence it does not seem to me consistent to declare those levels as the only admissible ones, since in

2076

doing so one tacitly admits anything between them. I am sure that if an advocate of the orthodox view cares to argue the case with me, the first thing he is going to tell me is, would I please have a look at a line spectrum and *see* that the levels are not blurred but very sharply distinguished and privileged. But this argument is based on the idea that an observed spectral frequency is emitted by single atoms jumping from a certain higher level to a certain lower level, each atom producing in this process a photon with energy equal to the difference of the two levels. This, of course, presupposes the detailed validity of the conservation law, which is just the point under discussion that I do not take for granted.

For macroscopic systems with a very large number of degrees of freedom the multiplicities may, and will as a rule, be very large numbers, so that our above argument breaks down. Still it is known that in this case the eigenvalues are so closely packed, that their discreteness is practically unobservable, whether you regard them as frequencies or as energy levels. They do have an important say in determining the statistical thermodynamics of the system in question. In this the customary relation between the frequency (of the whole macroscopic system!) and its energy must of course be admitted, but the relation may quite conceivably be itself only of a statistical nature. Anyhow the situation is not quite as simple as it might seem. The following discussion is mainly aimed at macroscopic systems.

Must we, in view of the thermodynamical application, regard an eigenfunction of a sharply determined « energy »-eigenvalue as representing a state in which our system has this sharply determined energy?—Certainly not. Why not?

The energy alone or together with a few other macroscopic parameters as volume etc., does not determine the state of the system uniquely, but at best the state of thermodynamic equilibrium that it is going to reach eventually when left to itself. In other words the system can harbour the same amount of energy in very many different ways, among which there are states of equilibrium, but also many far away from equilibrium, *e.g.* with considerable temperature gradients, arbitrary distributions of pressure, concentration, density etc. At first sight it may seem that this variety is fully accounted for by the high degree of multiplicity (degeneracy) of the eigenvalue in question; it ought to be possible to associate the eigenfunctions with the empirical states in such a way that each of the latter is represented by at least one of the former. But this is not so. A non-equilibrium state cannot be represented by an energy eigenfunction. For it is well known and easily seen that when the wave function depends on the time just by one imaginary exponential (one frequency) the system is « completely dead ». No change takes place, nothing depends on time. The proposed association would therefore in every case reduce the system in question to the « sleeping beauty » of the fairy tale:

gradients of temperature or concentration frozen in, chemical reactions stopped midway, a falling brick hung midway in the open air by witchcraft, a radio wave emitted from London not reaching Cambridge etc.—including the irate chef de cuisine, whose hand remains brandished «for a hundred years», threatening to box the ears of the negligent lad, who is petrified in motionless fright, trying to ward off the blow.—But jokes apart, there is another more serious aspect of the same thing, namely that, according to the accepted view an absolutely precise measurement of total energy of a physical system would bring the system into the state of thermodynamic equilibrium or maximum entropy, however far away from this state it may have been when the measuring device was applied. Just imagine your walking into a pharmacist's shop and asking him to make out your *weight* quite exactly. Could he comply with your request, which of course he cannot, he would become guilty of murder.

Thermodynamic equilibrium is only an abstraction, a limiting case that in actual fact is never met with. No system that we observe has a sharply determined energy value, nay we must not even admit this in the mental images we invent in order to describe what is *going on*. For nothing that takes part in what is *going on* has a well defined energy. Is that not rather in favour of the view I am advocating, that energy, just like entropy, is a statistical concept? Any display of physical events, while to the classical view it was taking place within or between systems of well defined energies, is quantummechanically represented by state functions that do *not* depend on time just by one imaginary exponential factor with one single frequency, but by a superposition of several, as a rule a great many such terms, covering a discrete or continuous range of frequencies, though it may be restricted to a narrow domain of the spectrum. Only in this way can one obtain a representation of something *happening*, an evolution in time. (The situation is mathematically analogous to the well known, not to say ill-famed (because wrongly used), wave parcel.) These considerations fortify my conviction that for small systems—with few degrees of freedom—one ought not to consider the product of Planck's constant and the frequency as meaning a definite amount of energy, while for macroscopic systems this relation is, of course, indispensable for the theory of thermodynamics and ought itself to be given a statistical foundation.

The theoretical facts adduced in the preceding paragraphs have been familiar for thirty years. Let me still recall a theoretical discovery that at the time aroused keen interest and is closely related to the same order of ideas. In the case of some small and comparatively simple systems the states which the classical physicist without hesitation deems states of equilibrium, are from the quantummechanical point of view not equilibria. Take for instance the molecule of ammonia (NH_3). It is pictured as an equilateral pyramide with the nitrogen atom at the apex (N), the basis being an equilateral triangle

20178

formed by the three hydrogens. But since the nitrogen might as well be situated on the other side of the said triangle at the mirror point (say at N') one might expect that in the quantummechanical description this gives rise to a twofold degeneracy, two eigenfunctions belonging to the same eigenvalue. However from very general and very fundamental considerations this is not so. Neither the position at N, nor that at N' is associated with an eigenfunction. There are indeed two of them, but their eigenvalues differ slightly, moreover, both are quite « impartial » as regards the positions N and N', they leave this alternative in abeyance. The essential difference between them is that one is symmetric with respect to the plane of the three hydrogens, the other antisymmetric. Suitable linear aggregates of the two functions represent the N-configuration or the N'-configuration respectively, according as the phase difference is adjusted. Naturally none of them is permanent, since the difference in phase is subject to slow secular change on account of the slightly different frequencies of the two proper modes.

Of even greater interest, is the case when the two configurations have not, as with NH_3, exactly the same physical properties (since they differ only by orientation), but can be distinguished by observation, though from the point of view of classical physics we should have to allot them exactly the same energy. I am alluding to stereoisomeres, *i.e.* molecules that are mirror images of one another, but cannot be made to coincide by a mere movement in space. In every other respect the state of affairs is exactly the same. Neither the R-situation nor the L-situation is represented by a genuine eigenfunction. Both the latter are « razemic », that is impartial with regard to R and L, but again in two different manners (and therefore slightly out of tune with one another), one being symmetric, the other antisymmetric with respect to the operation of space reflexion. Since many stereoisomeres can be kept for almost indefinitely long periods without razemisation, the frequency differences must in these cases be exceedingly small. The remarkable thing is that here we meet with states that are ostensible equilibria, but « sub specie aeternitatis » they are not, because they cannot be represented by one eigenfunction with one definite frequency.

2. – Let me join here some remarks which, though not covered by the title of this paper, have to do with our enquiry. The opponents of the Kopenhagen view about *complementarity*, the relation between *object* and *subject* etc., are regularly reproached with wrongly clamouring for a picture of reality, of the real world around us, without reference to the observer, the subject of cognizance. We are blamed for shutting our eyes to the fact (allegedly only discovered in this century by quantum physicists) that the description of objective reality is impossible, because our knowledge about things is based upon our interaction with them, which is essentially mutual, that is to say not only

do the objects make impressions on us but also we on them, and that in an uncontrollable fashion etc. etc.

I cannot share this attitude (which I hope to have summarized impartially), indeed this kind of discrimination between the ego and the world outside appears to me to be based on an epistemology out of date for some time. Naturally our urge to form a picture, valid for all of us, of the world in space and time—which includes of course our own bodies—must not be framed ontologically; this would be rather naive science and ignore philosophical achievements very much older than quantum mechanics. From Democritus to Bertrand Russell there have been thinkers who became aware of the obvious fact that our sensible, perceiving, feeling, thinking ego, and the so called external world consist of the same elements, only comprehended in different arrangements. The elements in themselves (I am following Bertrand Russell) may not be called psychic or physical, mental or material; only after arranging themselves in various patterns do they in conventional language acquire this or that characteristic. In any case the so called external world is built up exclusively of constituents of the ego. It is characterized as what is common to all, recognized by every healthy and sane person. That is what distinguishes it from dreams and hallucinations, also from joy or pain, tooth-ache, sorrow, depression etc.

This « being-shared-by-everybody », this community (1) is the one and only hall-mark of physical reality. Not unfrequently do we resort to this criterion in daily life: I hear a humming; do you hear it too? Is it perhaps the stove or something out in the street or is it only in my ear? Well it seems to me that the Kopenhagen epistemology does not acknowledge this criterion, pays no attention to it. In being satisfied with describing the material world for one observer (while for another one a different description may hold) it leads to the physics of solipsism. This bears even on the linguistic expression used in the analysis of experiment; instead of « we find » or « we measure » (plural) the singular is usually preferred: « I find » or « the observer states ». This is not astonishing. Indeed the one lightquant which *e.g.* in the gamma-ray microscope is supposed to reveal to *me* the place of an electron hardly suffices for poor me, letalone for others.

But jokes apart, I shall not waste the time by tritely ridiculing the attitude that the state-vector (or wave function) undergoes an abrupt change, when « I » choose to inspect a registering tape. (Another person does not inspect it, hence for him no change occurs.) The orthodox school wards off such insulting smiles by calling us to order: would we *at last* take notice of

(1) This is in itself the most remarkable trait of our general experience, considering the complete privacy of an individual's sensations, the absolute seclusion of every mind from every other mind.

0806

the fact that according to them the wave function does not indicate the state of the physical object but its relation to the subject; this relation depends on the knowledge the subject has acquired, which may differ for different subjects, and so must the wave function.—Very well, but this situation is by no means novel. Think of entropy. The entropy of, let me say, a given body of gas has a certain value for him who only knows the energy and the volume—he may take for it the logarithm of the phase volume up to that energy; the entropy of the same body has a different, indeed a smaller value for one who is informed of the inhomogeneous distribution of density and temperature in the gas. Yet I do not think that it has ever occurred to anyone to declare that entropy is *not* a property of a physical system *per se*, but only expresses « my » knowledge about that system. In a certain way of course one may, if one likes, say this about *all* the numerical results of physical measurements, either about all of them or none; however this is an old yarn, an entirely irrelevant matter of taste.

We do feel the yearning for a complete description of the material world in space and time, and we consider far from proven, that this aim cannot be reached. This does not mean that we wish to outwit the uncertainty relation. Yet it ought to be possible, so we believe, to form in our mind of the physical object an idea (Vorstellung) that contains in some way everything that *could be* observed in some way or other by any observer, and not only the record of what *has been* observed simultaneously in a particular case. I mean precisely what someone (was it not Ernst Mach?) has called the completion of facts in thought (Ergänzung der Tatsachen in Gedanken). We prefer to grasp the shape of a solid by visualizing it in threedimensional space instead of by a set of perspective drawings, even though the eye can at any moment only perceive one perspective view. Everyday life is based every minute on « completion in thought » since we rely on the continued existence of objects while they are not observed by anyone; *e.g.* we surmise the nocturnal preservation of our portfolio and its contents, locked up in a drawer at night and taken out in the morning.

It is not now the question whether the wave function (or state vector) yields the desired complete description. I remember reading the other day the very apt statement that with a physical theory one ought never to ask whether it would still have to undergo some change, but in what direction. My point is that at the present stage and as long as the state vector plays the role it does it must be taken to represent « the real world in space and time », it ought not to be sublimed into a probability function for the purpose of making forecasts, depending therefore on the momentary state of our knowledge and changing abruptly when somebody (who?) cares to inspect a photograph or a registering tape; it must not be regarded as « hovering in empty space » between subject and object; the question what *is* now the wave

20881

function (meaning, what is now the actual state of the physical system?) must be regarded as meaningful, even though it can hardly ever be answered exhaustively.

In the first part of this paper I have given reasons for doubting, in the case of energy, the current association between wave function and observation. Here I feel induced to contradict emphatically an opinion that Professor L. Rosenfeld [2] has recently uttered in a meeting at Bristol, to the effect that a mathematically fully developed, good and self-consistent physical theory carries its interpretation in itself, there can be no question of changing the latter, of shuffling about the concepts and formulae.—This does not make much sense to me. I recall a brief paradoxical remark that Einstein made, half in joke, while we were strolling Unter den Linden: Of course every theory is true provided that you suitably associate its symbols with observed quantities.

Rosenfeld's statement is a danger signal. What is at stake today—far more important than the eventual decision for this or that view—is the peril of a progressive narrowing of our field of vision, a mental glaucoma as it were.

[2] *Proc. of the Ninth Symposium* of the Colston Research Society, April 1957.

RIASSUNTO (*)

Si danno argomenti in favore dell'opinione che in meccanica quantistica la frequenza moltiplicata per la costante di Planck *non* ha per i sistemi microscopici il significato di energia. Si esprime l'opinione che i concetti di energia e della sua conservazione, al pari di quelli di entropia e del suo aumento, hanno solo un significato statistico, l'energia di un sistema macroscopico essendo il prodotto della costante di Planck per una media ponderata delle frequenze in questione. L'opinione diffusa che il proposito di dare una descrizione obiettiva della realtà fisica debba essere abbandonato è respinta basandosi sul fatto che il cosiddetto mondo esterno è costituito soltanto di elementi delle singole menti ed è caratterizzato come ciò che è comune a tutti, e riconosciuto da ogni persona sana e ragionevole. Donde è inevitabile la richiesta di una descrizione non soggettiva, naturalmente senza pregiudizio del fatto che essa sia deterministica o di altra natura.

(*) *Traduzione a cura della Redazione.*

2082

NOTE TECNICHE

Un circuito di coincidenza con tempo risolutivo di 2.2 ns e tempo morto dell'ordine di 5 ns di possibile impiego nella fisica nucleare.

U. Pellegrini, B. Rispoli e A. Serra

Istituto Nazionale di Fisica Nucleare, Centro Coordinamento Elettronica (*) - *Roma*
Istituto di Fisica dell'Università - Roma

(ricevuto il 1° Marzo 1958)

Riassunto. — Si descrive un circuito di coincidenza con tempo risolutivo di 2.2 ns che può essere usato bene anche per coincidenze di ordine elevato (quintuple e sestuple). Insieme al circuito proposto vengono presi in esame i classici circuiti di coincidenza rapida e si presentano le misure su di essi effettuate. La caratteristica precipua del nuovo circuito, basato sulla tecnica degli amplificatori distribuiti, è il basso valore del tempo morto (dell'ordine di 5 ns) il che lo rende particolarmente utile negli esperimenti di fisica nucleare allorquando si abbia a che fare con un numero estremamente grande di particelle per unità di tempo.

1. – Introduzione.

Il recente sviluppo della fisica nucleare in relazione alla entrata in funzione delle grosse macchine acceleratrici e dei reattori ad alto flusso neutronico, rende di nuova attualità il problema della strumentazione elettronica ad alto potere risolutivo. In particolare, l'affollamento dei contatori a scintillazione e di Čerenkov richiede l'impiego di coincidenze ad altissimo potere risolutivo, al fine di contenere il numero di coincidenze spurie entro limiti ragionevoli.

(*) Attualmente il Centro è alle dirette dipendenze del Comitato Nazionale per le Ricerche Nucleari.

9183

Tuttavia si richiede che i circuiti di coincidenza abbiano non solo un potere risolutivo elevato, ma anche alta stabilità, elevata sensibilità e piccolo tempo morto. I circuiti sviluppati in questi ultimi anni non sempre realizzano le condizioni optimum per i tre requisiti anzidetti perchè, in genere, presentano poteri risolutivi o sensibilità molto elevati ma lunghi tempi morti.

Per questo motivo abbiamo realizzato un nuovo tipo di coincidenza rapida in cui viene esperimentata con successo la tecnica degli amplificatori distribuiti.

Per poter valutare bene le prestazioni di tale coincidenza ci è sembrato opportuno eseguire uno studio comparativo dei più noti e recenti circuiti impiegati nelle esperienze di fisica nucleare: essi sono stati messi direttamente a confronto misurando, sempre con il medesimo metodo sperimentale, i loro parametri caratteristici.

Come è noto un circuito di coincidenza è un dispositivo capace di dare in uscita un segnale di ampiezza maggiore di un prefissato valore quando a tutti i suoi ingressi arrivano impulsi di determinate caratteristiche entro un intervallo di tempo $\tau \leqslant \tau_m$; il valore di τ_m, che fissa il limite superiore ai possibili valori di τ, viene chiamato tempo *di risoluzione*, mentre con $1/\tau_m$ si indica il *potere risolutivo*. Di solito, la determinazione di τ_m viene fatta sperimentalmente usando un generatore di impulsi rapidi di ampiezza, forma e durata ben determinata (1). L'impulso fornito dal generatore viene mandato con differente ritardo ai vari canali della coincidenza; riportando su di un grafico l'ampiezza dell'impulso d'uscita in funzione del ritardo relativo fra i canali, si ottiene una curva, con un massimo per un ritardo nullo, generalmente simmetrica rispetto al massimo, e che tende per $\tau > \tau_m$ al valore corrispondente all'ampiezza relativa agli impulsi fuori coincidenza. Nel seguito indicheremo tale curva con il nome di « caratteristica della coincidenza », e definiremo *tempo di risoluzione* la semidifferenza delle ascisse relative ai punti della caratteristica la cui ordinata ha un valore metà del massimo.

Il fatto che l'ampiezza dell'impulso di uscita non sia nulla per impulsi fuori coincidenza porta a dovere definire un secondo parametro individuato dal rapporto tra il massimo ed il valore asintotico della caratteristica.

Inoltre ogni circuito, dopo aver registrato una coincidenza, può registrarne una seconda solo se i segnali di comando arrivano, dopo un tempo T detto *tempo morto*. Quando si lavora con sorgenti di radiazioni molto intense è necessario che, oltre al tempo di risoluzione, anche il tempo morto sia il più piccolo possibile perchè, come è noto, da esso dipendono le perdite statistiche di conteggio.

Il problema di ridurre il tempo morto dei circuiti di coincidenza si pone oggi in quanto, per i notevoli progressi realizzati dall'elettronica, è possibile disporre di amplificatori e circuiti di conteggio ad alto potere risolutivo.

I parametri finora elencati vanno completati dando la *sensibilità della coincidenza*, definita dalla minima ampiezza in entrata necessaria per dare un impulso di coincidenza maggiore di qualsiasi degli impulsi fuori coincidenza. Tale definizione non è però completa se non viene specificata anche la forma e la durata degli impulsi di comando.

(1) Nel nostro caso un generatore con relais a mercurio forniva impulsi rettangolari o esponenziali di durata variabile e con tempo di salita notevolmente inferiore a 10^{-9} s.

4103

2. – Circuito di coincidenza proposto.

Il circuito di coincidenza da noi studiato è sostanzialmente un circuito di somma lineare eseguita su una linea a costanti concentrate applicando la tecnica degli amplificatori distribuiti. Lo schema di principio di un circuito di triple è dato in Fig. 1; i pentodi T_1, T_2, T_3 (che per semplicità sono indicati in figura come triodi) sono in regime di conduzione e i cavi coassiali, messi in derivazione all'entrata come formatori di impulsi, sono di ugual lunghezza e di impedenza caratteristica pari a quella dei cavi che connettono le entrate della coincidenza alle sorgenti di impulsi.

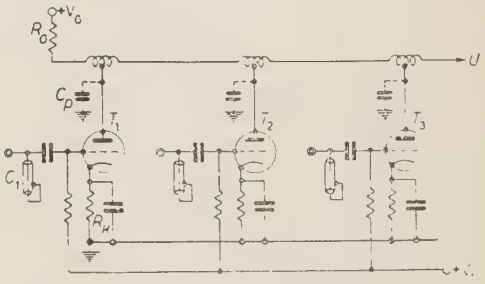

Fig. 1. - Schema di principio di una coincidenza tripla.

Lo schema di Fig. 1 differisce dallo schema classico della coincidenza alla Rossi unicamente perchè le placche delle valvole, invece che essere collegate in parallelo con un carico costituito da una resistenza R_0, sono connesse da una linea a costanti concentrate con impedenza caratteristica $Z_0 = R_0$. Tale tipo di connessione, sebbene più complicato, comporta però notevoli vantaggi quando si voglia raggiungere elevati poteri risolutivi. Infatti nella connessione alla Rossi il tempo di salita sulla placca di n valvole connesse in parallelo è $2.2\, R_0 \times n C_p$; viceversa nella connessione con linea il tempo di salita è il minimo possibile per una data impedenza di carico, dipende solo dalla induttanza e dalla capacità di ogni elemento della linea e quindi non aumenta, come nel circuito di Rossi, con l'aumentare dell'ordine della coincidenza.

In generale in una coincidenza rapida si possono distinguere le seguenti operazioni:

a) ugualizzazione in ampiezza degli impulsi provenienti dai vari canali;

b) formazione di impulsi di breve durata per fissare il potere risolutivo della coincidenza;

c) mescolamento degli impulsi provenienti dai vari canali che si sovrappongono entro il tempo risolutivo;

d) discriminazione in ampiezza per selezionare solo gli impulsi in coincidenza.

La operazione *a*) è compiuta nel nostro caso direttamente dalle valvole a condizione che i segnali di ingresso siano di ampiezza sufficiente (qualche volt) per portarle alla interdizione: l'ampiezza dell'impulso che si ha in placca è allora determinata unicamente da $R_0 i_p/2$, essendo i_p la corrente di placca che risulta stabilizzata dalla reazione negativa in continua dovuta alla resistenza R_k.

L'operazione *b*) è compiuta dai cavi C_1, C_2, C_3, i quali formano impulsi di durata τ_i pari al doppio del tempo di propagazione di un segnale lungo il cavo. Se gli impulsi provenienti dalla sorgente (fotomoltiplicatore) hanno polarità

negativa con un fronte di salita dell'ordine di 10^{-9} s, con una discesa $\geqslant 10^{-8}$ s, e τ_f è molto minore della costante di tempo di discesa degli impulsi di ingresso, si ottengono impulsi negativi di forma pressochè rettangolare di durata τ_f.

L'operazione *c*) per il nostro circuito consiste in una somma lineare nel senso che l'ampiezza del segnale in U è proporzionale al numero di impulsi di ingresso che si sovrappongono.

L'operazione *d*) è invece compiuta da un apposito circuito di discriminazione. Come si vede dalla Fig. 1 le placche sono connesse al centro di bobine di induttanza L; la capacità parassita C_p della placca è pertanto inserita tra due bobine di induttanza $L/2$ mutuamente accoppiate tra loro come è indicato dal circuito equivalente di Fig. 2, che costituisce una linea artificiale formata da celle *m*-derivate.

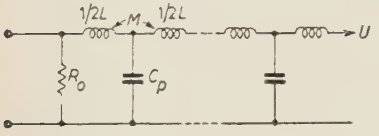

Fig. 2. – Circuito equivalente della linea di placca dello schema di Fig. 1.

Per un tale sistema l'impedenza caratteristica vale

$$Z_0 = \sqrt{(1-K)\frac{L}{C}},$$

dove K è il coefficiente di accoppiamento definito dal rapporto $2M/L$, M essendo il coefficiente di mutua induzione.

Come è mostrato in Fig. 1 la linea è chiusa ad un estremo sulla impedenza caratteristica Z_0. Se una valvola viene portata alla interdizione per un tempo τ_f, sulla placca corrispondente si genera un impulso rettangolare di durata τ_f che si propaga lungo la linea in entrambi i versi; ad un estremo è assorbito da Z_0, mentre in U subirà riflessioni o meno a seconda delle condizioni terminali. Supporremo per semplicità che il circuito seguente abbia impedenza d'entrata Z_0 in modo tale che il segnale si possa propagare senza riflessioni.

Immaginiamo ora che contemporaneamente tre impulsi vengano applicati alle griglie delle tre valvole. Poichè ogni sezione della linea introduce un ritardo $\tau_0 = \sqrt{(1-K)LC}$, i fronti degli impulsi in placca giungono al terminale U ritardati del tempo necessario a percorrere la porzione di linea interposta tra U e il punto nel quale viene iniettato l'impulso. Occorre quindi introdurre un ritardo di compensazione τ_0 per il secondo impulso, $2\tau_0$ per il terzo, il che può farsi semplicemente inserendo in entrata cavi di ritardo di lunghezza opportuna.

Il circuito di coincidenza si presenta così estremamente semplice ed è possibile ottenere grande stabilità. Il tempo risolutivo dipende dalla durata τ_f degli impulsi; tuttavia questo non può essere ridotto al disotto del tempo di salita della linea di placca. Come è ben noto, introducendo le capacità parassite come elementi di una linea a costanti concentrate si minimizza il tempo di salita in quanto questo viene esclusivamente a dipendere dalla frequenza di taglio della linea che è data da

$$\nu_c = \frac{1}{\pi\sqrt{(1+K)LC}}.$$

In pratica sono facilmente realizzabili tempi di salita di $(2 \div 3)$ ns.

20186

Un circuito così concepito presenta i seguenti vantaggi: 1) è molto facile realizzare una coincidenza d'ordine maggiore di tre aggiungendo altrettanti stadi e ritardando progressivamente le rispettive entrate; 2) indipendentemente dall'ordine di coincidenza, l'impulso ha sempre lo stesso tempo di salita potendosi così ottenere un tempo di risoluzione che non peggiora all'aumentare dell'ordine della coincidenza; 3) il tempo di salita è dell'ordine di $\sqrt{(1+K)LC}$ e risulta il minimo possibile per una data impedenza di carico; 4) il tempo morto è molto piccolo ed ha lo stesso ordine di grandezza dell'impulso di coincidenza.

Poichè il circuito si comporta come una somma lineare, il rapporto tra la coincidenza n-pla e le coincidenze $(n-1)$-ple è semplicemente $n/(n-1)$; ne consegue la necessità di un discriminatore particolarmente preciso e di notevole stabilità.

Generalmente per effettuare la discriminazione si ricorre a diodi a germanio che presentano ottime caratteristiche di sensibilità. Noi abbiamo voluto evitarlo per due motivi:

1) l'introduzione di diodi a germanio, anche se convenientemente scelti, comporta inevitabilmente la rinuncia al basso tempo morto a causa dei complessi fenomeni che hanno luogo nei diodi a cristallo quando questi variano il loro stato di conduzione;

2) è preferibile che la linea artificiale sulla quale si effettua la somma sia chiusa sull'impedenza caratteristica e ciò esclude la presenza di circuiti a scatto quali appunto i diodi che passano dal regime di interdizione al regime di conduzione.

Per questi motivi, e per avere un impulso di ampiezza sufficiente, abbiamo adottato la soluzione di usare come discriminatore un amplificatore distribuito a due stadi polarizzati in maniera opportuna.

In Fig. 3 è dato lo schema completo di una coincidenza quintupla seguita dal relativo discriminatore-amplificatore.

Si sono usati pentodi Philips E180F perchè, presentando una elevata transconduttanza insieme ad un ottimo fattore di merito, sono i più adatti a funzionare come valvole limitatrici in quanto hanno interdizione netta con i soli 3 V negativi di griglia.

Per i cavi di ritardo e formatori posti su ogni entrata, è stato scelto, grazie al suo piccolo ingombro, il tipo « Carlo Erba C522 » che presenta una impedenza caratteristica di 52 ohm.

Abbiamo fissato come impedenza della linea di placca e delle linee dell'amplificatore distribuito che segue la coincidenza, il valore di 200 ohm.

Le misure di capacità eseguite sul circuito da noi realizzato risultano le seguenti:

— capacità parassita placca-massa per ciascuna valvola (accesa) con la bobina relativa sconnessa dalla linea ai due estremi: $C_p = 6$ pF;

— capacità parassita griglia-massa per ciascuna valvola (accesa) dell'amplificatore distribuito con la bobina relativa sconnessa dalla linea ai due estremi: $C_g = 11$ pF.

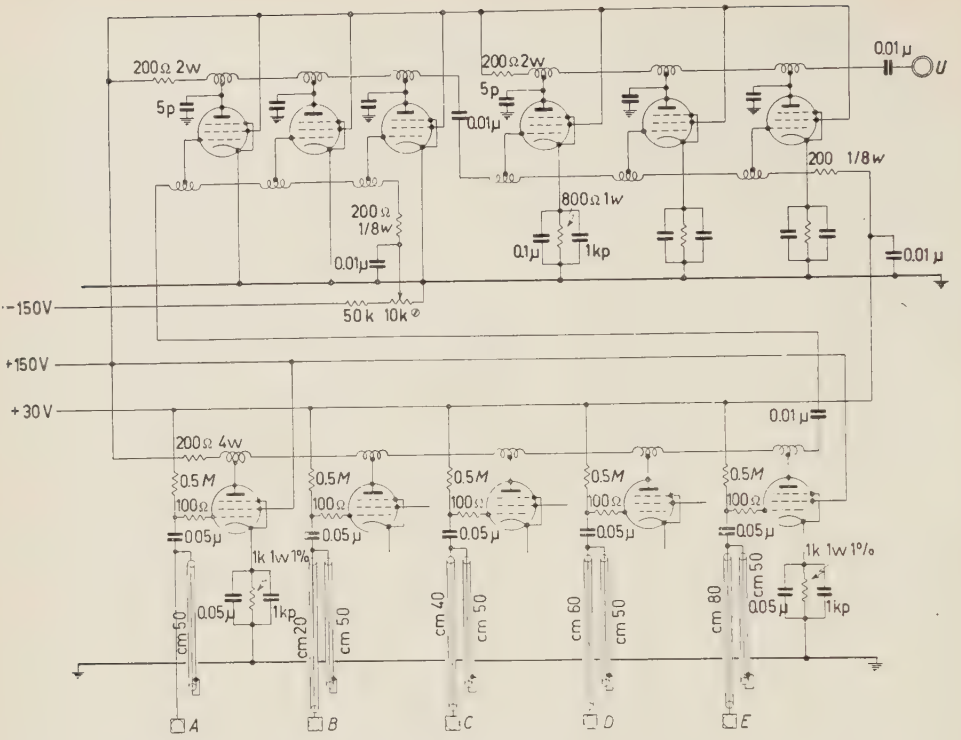

Fig. 3. – Schema completo di una coincidenza quintupla. Tutti i pentodi sono del tipo Philips E180F.

Affinchè tutte le linee abbiano la stessa impedenza caratteristica, tenendo conto che il ritardo per sezione delle linee di griglia e di placca dei due stadi dell'amplificatore debbono essere uguali, occorre aggiungere una capacità di 5 pF sulle linee di placca dell'amplificatore, e fare le bobine di questo diverse da quelle della coincidenza. I dati costruttivi e lo schema di montaggio delle bobine sono dati in Fig. 4.

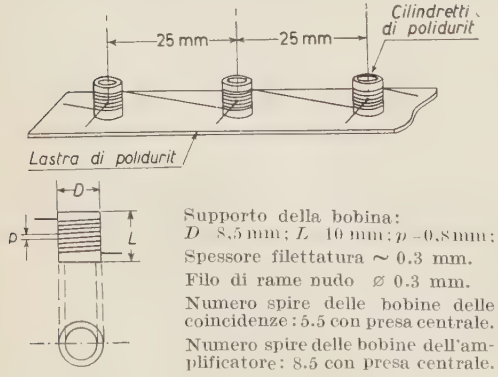

Fig. 4. – Dati costruttivi e schema di montaggio delle bobine.

Il primo stadio dell'amplificatore è normalmente interdetto: la polarizzazione di griglia è regolata in modo che solo gli impulsi di quintupla superino il livello d'interdizione. La discriminazione fra questi e quelli di quadrupla è molto sicura perchè fra essi vi è una differenza di 3 V, mentre bastano 0.5 V per portare una E180F dalla condizione di interdizione netta a una condizione in cui la transconduttanza è superiore a 5 000 μmho.

Il secondo stadio lavora invece vicino alla saturazione e poichè riceve in griglia impulsi negativi si trova nella condizione di massima amplificazione sfruttando il tratto della caratteristica a transconduttanza massima.

Con 50 cm di cavo formatore, equivalente ad un tempo di doppio transito di 5 ns, si ottiene alla uscita dell'amplificatore, la caratteristica *a* della Fig. 5, cui corrisponde un tempo risolutivo di 4 ns. Usando invece cavi di lunghezza 25 cm, questo tempo si riduce a 2.2 ns, come è mostrato dalla curva *b* della Fig. 5; con cavi più corti, il tempo risolutivo non si riduce ulteriormente poichè in questo caso esso è determinato unicamente dal tempo di salita della linea di placca che è di 2 ns.

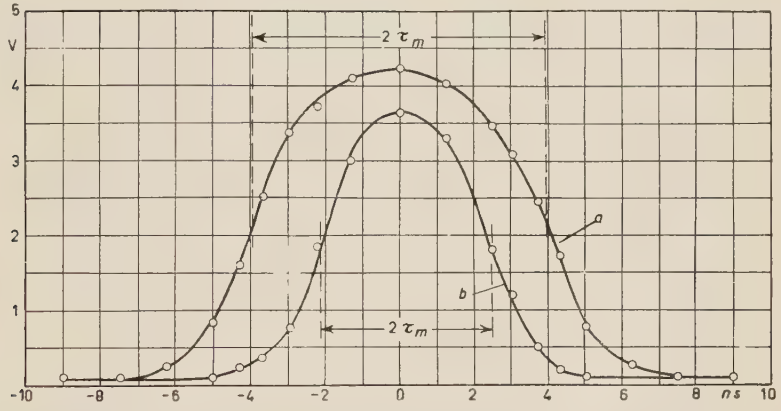

Fig. 5. – Caratteristiche della coincidenza di Fig. 3 relative ad impulsi di durata 5 ns (*a*) e 2.5 ns (*b*).

Le curve di Fig. 5 si riferiscono al canale *A* e sono state ottenute ritardando o anticipando l'impulso in *A* rispetto agli impulsi simultanei negli altri quattro ingressi; le curve relative agli altri canali coincidono con le precedenti entro il 10%.

3. – Analisi dei circuiti di coincidenza più noti.

Nel seguito riportiamo alcuni risultati delle misure da noi effettuate relative ai più noti circuiti di coincidenza.

In Fig. 6 è uno schema di coincidenza del tipo suggerito da GARWIN [2].

Il potere risolutivo di questo circuito è fortemente influenzato dal

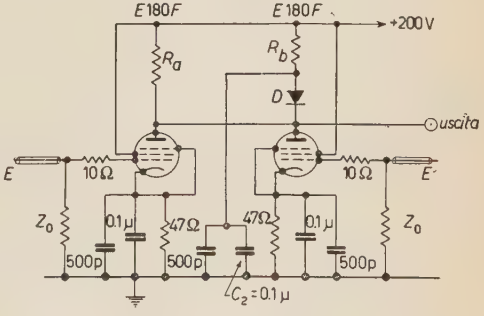

Fig. 6. – Circuito di Garwin.

[2] R. L. GARWIN: *Rev. Sci. Instr.*, **21**, 569 (1950); **24**, 618 (1953).

tempo che il diodo D impiega a passare dallo stato di conduzione a quello di interdizione. Esso è stato provato con un diodo 1N34 e con un diodo a bassissima

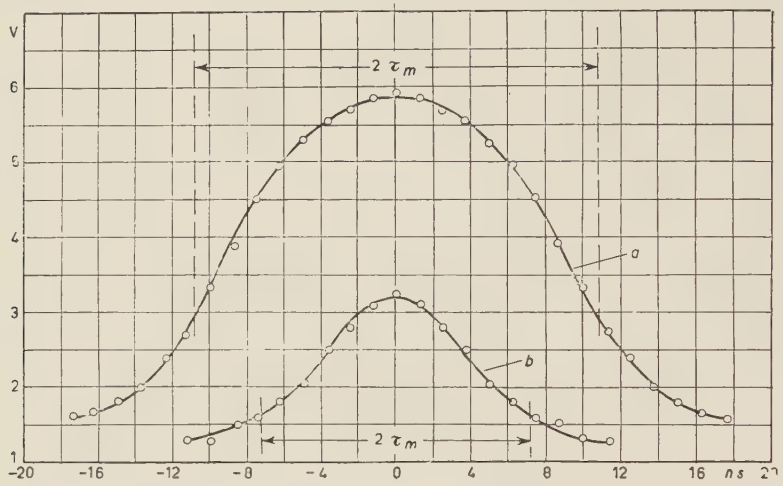

Fig. 7*a*. – Caratteristica del circuito di Fig. 6 con i seguenti componenti: $R_a = 3.9$ K; $R_b = 3.3$ K; $D =$ 1N34. Le curve *a*) e *b*) si riferiscono ad impulsi di comando di ampiezza 3 V e di durata rispettivamente 10 ns, 20 ns.

resistenza tipo 1N270. Le caratteristiche sono date in Fig. 7: dai grafici si osserva che, pur lasciando inalterata la forma e l'ampiezza degli impulsi di entrata, il tempo risolutivo diminuisce e contemporaneamente migliora il rap-

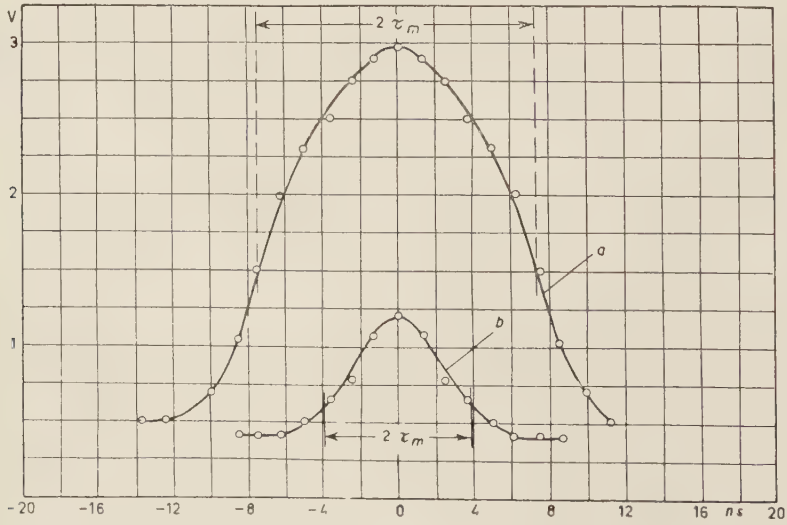

Fig. 7*b*. – Caratteristica del circuito di Fig. 6 con i seguenti componenti: $R_a = 3.3$ K; $R_b = 3.3$ K; $D =$ 1N270. Le curve *a*) e *b*) si riferiscono ad impulsi di comando di ampiezza 3 V e di durata rispettivamente 10 ns, 20 ns.

porto doppia-singola se si usa un diodo 1N270 invece che un normale 1N34, e si danno ad R_a ed R_b i valori indicati in figura.

Se la durata degli impulsi di entrata viene diminuita, si riduce proporzionalmente il tempo risolutivo; tuttavia già per impulsi di 5 ns il rapporto doppia/singola diventa circa 2 e l'ampiezza degli impulsi di uscita scende al di sotto di 1 V.

Un circuito di coincidenza rapida realizzato con un'unica valvola multigriglia è descritto da FISHER e MARSHALL [3]. L'elevato potere risolutivo ed una sufficiente simmetria nelle curve di coincidenza sono raggiunti grazie alla particolare ottica elettronica della valvola 6BN6.

In Fig. 8 è dato il circuito da noi provato e le curve ottenute con impulsi rettangolari applicati direttamente sulle griglie G_1 e G_3. Il massimo di queste curve è spostato di 2 ns rispetto al ritardo zero a causa del tempo di transito degli elettroni fra G_1 e G_3: per questo motivo gli impulsi d'entrata su G_3 devono essere ritardati di questo stesso intervallo di tempo.

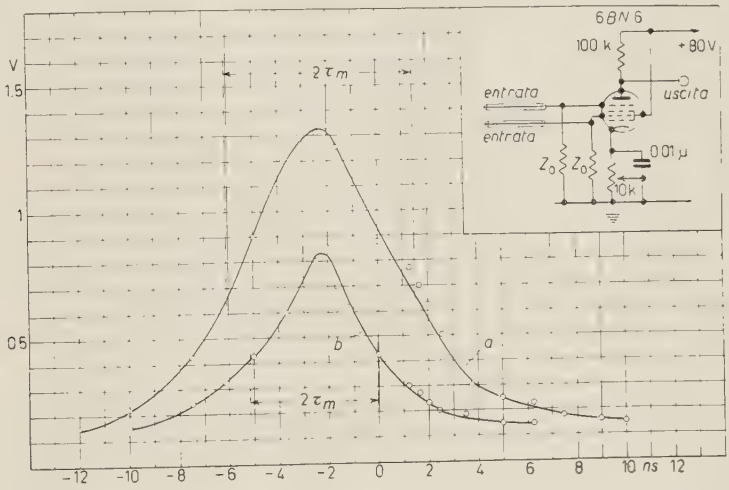

Fig. 8. – Schema della coincidenza con valvola 6BN6 e relativa caratteristica misurata con impulsi d'entrata di 4 V, e durata 5 ns (*a*), 2.5 ns (*b*); gli impulsi d'uscita durano ~ 5 μs.

Un'interessante innovazione nei circuiti di coincidenza rapida è stata introdotta da BELL, GRAHAM e PETCH [4] adottando la tecnica dei cavi formatori di impulsi. Il circuito da noi realizzato è riportato in Fig. 9 insieme con la sua caratteristica.

Il potere risolutivo di questo circuito dipende sia dalla lunghezza del cavo formatore che determina la durata degli impulsi da far coincidere, sia dal comportamento alle alte frequenze del diodo discriminatore.

---

[3] J. FISHER and J. MARSHALL: *Rev. Sci. Instr.*, **23**, 417 (1952).

[4] R. E. BELL, GRAHAM e E. H. PETCH: *Canad. Journ. Phys.*, **30**, 35 (1952).

Copyright

Nei circuiti di coincidenza rapida si possono utilizzare i diodi a cristallo poichè in genere presentano una capacità interelettrodica molto piccola (~ 1 pF) ed una bassa resistenza (~ 10 ohm); quindi le costanti di tempo da loro introdotte influenzano in maniera trascurabile i fronti d'onda degli impulsi di co-

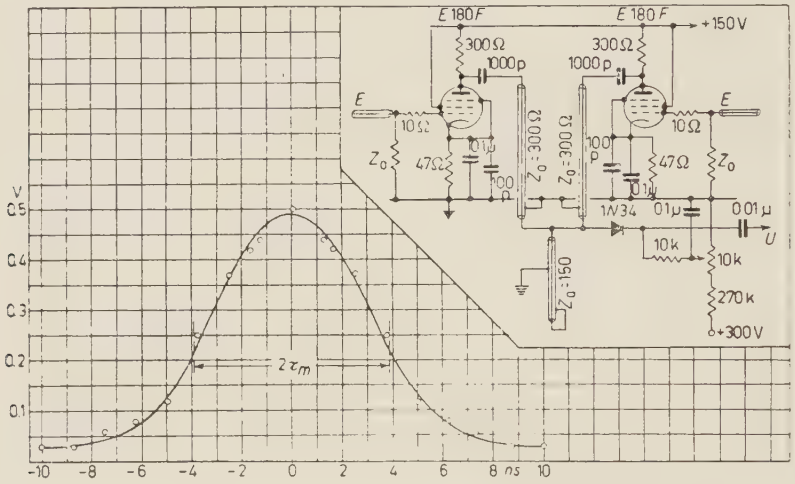

Fig. 9. – Schema della coincidenza di Bell, Graham e Petch e relativa caratteristica ottenuta con impulsi di entrata di ampiezza 2.5 V e caduta esponenziale con costante di tempo 0.25 μs; i cavi da 300 Ω tipo TEKO 10/300 sono lunghi 100 cm; il cavo da 150 Ω tipo TEKO 10/150 è lungo 75 cm equivalente ad un tempo di doppio transito di 5.4 ns.

mando. Inoltre con i diodi si può raggiungere una elevata sensibilità poichè bastano impulsi di una frazione di volt per commutare il loro stato di conduzione.

Un tipo di circuito di coincidenza rapida a diodi è stato descritto da Elmore, De Benedetti e Richings, Minton [5] ed altri.

Il vantaggio di questo circuito sta nella elevata sensibilità, (perchè sente sempre il più piccolo dei due impulsi) e nella facilità con cui può essere adattato ad una coincidenza d'ordine maggiore di 2.

Nel nostro laboratorio abbiamo sperimentato questo circuito adottando lo schema che riportiamo in Fig. 10. Le valvole V_1 in entrata sono poste come limitatrici e gli impulsi vengono formati sulle placche da cavi da 197 ohm tipo Transradio C3T, lunghi 20 cm, che hanno un ritardo di 3.6 ns/m; le valvole V_2, V_3 funzionano da amplificatrici e la V_4 è lo stadio di uscita che fornisce impulsi dell'ordine di qualche decina di volt e di durata circa 3 μs. La caratteristica relativa ad una coincidenza doppia è riportata in Fig. 11; caratteristiche sostanzialmente coincidenti si hanno per circuiti di triple e quadruple da noi studiati.

---

[5] W. C. Elmore: *Rev. Sci. Instr.*, **21**, 649 (1950); G. H. Minton: *Phys. Rev.*, **94**, 758 (1954); S. Debenedetti e H. J. Richings: *Rev. Sci. Instr.*, **23**, 37 (1952).

Molte coincidenze con diodi sono realizzate con circuiti a ponte che si sbilanciano solo quando arrivano contemporaneamente due impulsi di comando. Circuiti di questo tipo sono stati studiati da BALDINGER, HUBER e MAYER, da STRAUCH (6) e da altri.

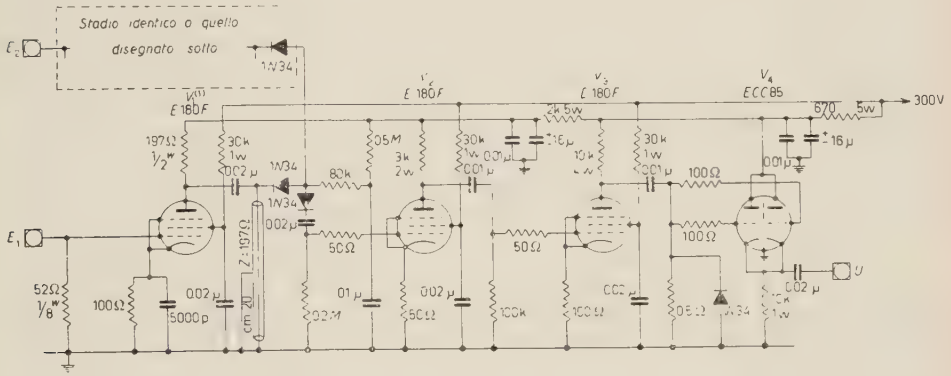

Fig. 10. – Circuito di coincidenza a diodi con relativo amplificatore.

Il circuito da noi realizzato è dato in Fig. 12; la valvola V_1 funziona da amplificatore differenziale, le valvole V_2, V_3 da amplificatrici e la V_4 da stadio di uscita; i diodi D_3, D_4 hanno la funzione di eliminare le singole di polarità opposta agli impulsi di coincidenza.

In Fig. 13 sono date le caratteristiche della coincidenza relativa a diversi tipi di diodi (D_1, D_2) usati. Come si vede il massimo della curva di coincidenza è spostato rispetto allo zero verso i ritardi negativi di un tempo che dipende dal tipo di diodo usato. Tale fenomeno può essere interpretato come conseguenza del comportamento alle alte frequenze dei diodi a cristallo. Infatti D_1 e D_2 mutano il loro stato di conduzione con un certo ritardo rispetto all'istante in cui arriva in E_1 il fronte d'onda di un impulso rapido. Nel caso di coincidenza, affinchè il ponte risulti sbilanciato per tutta la durata del comando, occorre ritardare dello stesso intervallo di tempo l'impulso applicato sulla placca di D_1. Per questo motivo è stato inserito sull'entrata E_2 un cavetto di ritardo; con i

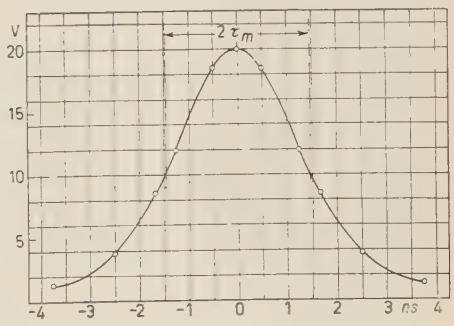

Fig. 11. – Caratteristica del circuito di Fig. 10 ottenuta con comando di ampiezza 2.5 V e caduta esponenziale con costante di tempo 0.25 μs.

(6) E. BALDINGER, P. HUBER e K. P. MEYER: *Helv. Phys. Acta*, **23**, 121 (1950); Z. BAY: *Phys. Rev.*, **79**, 233 (1950); K. STRAUCH: *Rev. Sci. Instr.*, **24**, 283 (1953).

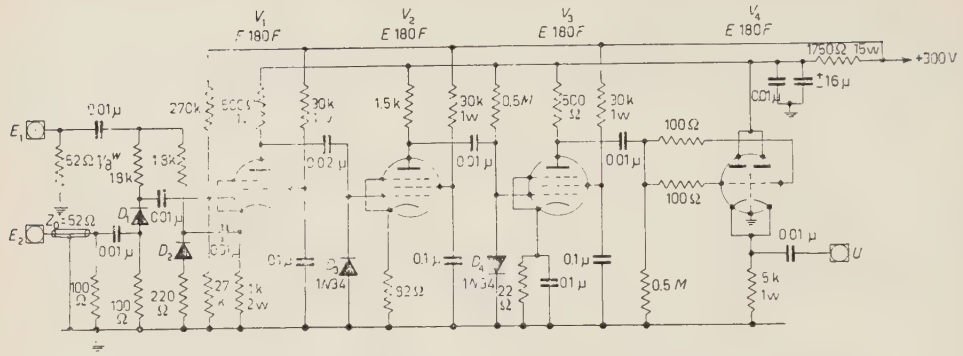

Fig. 12. – Circuito di coincidenza a ponte con relativo amplificatore.

diodi 1N34 abbiamo usato un cavo da 52 tipo « Carlo Erba C522 » di lunghezza, equivalente ad un ritardo di 1.5 ns.

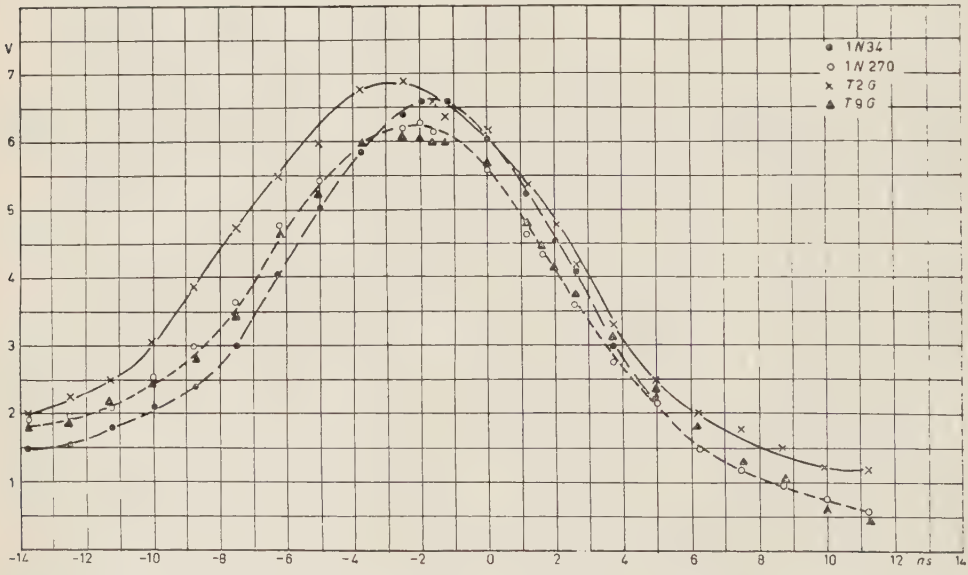

Fig. 13. – Caratteristiche del circuito di Fig. 12 relativo a diversi tipi di diodi, ottenute con impulsi rettangolari di ampiezza 2 V e di durata 2.5 ns.

4. – Conclusioni.

La scelta del circuito di coincidenza da adottare va fatta in base ai particolari requisiti voluti in relazione all'esperimento da effettuare. I parametri che giovano nella scelta sono *a*) ordine della coincidenza, *b*) tempo risolutivo, *c*) tempo morto, *d*) sensibilità.

L'esame dei circuiti da noi effettuato ci permette di formulare alcuni criteri generali per detta scelta.

Cominciamo con l'esaminare il caso delle coincidenze doppie: poichè tutti i circuiti da noi descritti hanno elevato potere risolutivo, gli elementi che determinano la scelta sono il massimo tempo morto e la minima sensibilità ammissibile. Se è richiesto un piccolo tempo morto, è opportuno usare un circuito nel quale si effettui una somma lineare su cavi o su linee come quello di Fig. 9 o quello da noi proposto seguito da un discriminatore rapido, escludendo l'uso di diodi a cristallo ed adottando un amplificatore a larga banda opportunamente polarizzato. Tali circuiti però hanno basse sensibilità perchè occorrono impulsi di comando dell'ordine di alcuni volt ed è pertanto generalmente necessario amplificare mediante amplificatori distribuiti gli impulsi provenienti dai fotomoltiplicatori. Se il requisito essenziale è invece un'alta sensibilità di ingresso sono preferibili i circuiti di coincidenza a diodi e tra questi è particolarmente consigliabile per la sua stabilità il circuito di Fig. 10.

Rimane ora da considerare il caso di coincidenze di ordine maggiore di 2. I circuiti che più facilmente possono usarsi sono il circuito di Fig. 10 e quello da noi proposto. Il primo presenta elevata sensibilità ma lungo tempo morto ed inoltre mal si presta per coincidenze di ordine superiore a 4. Il secondo invece oltre alle ottime caratteristiche già descritte può senz'altro usarsi anche per coincidenze sestuple.

SUMMARY

A new high resolution coincidence circuit has been studied for scintillation or Čerenkov counter experiments. The resolving time has been found to be 2.2 ns and the circuit is suitable for 5-fold or 6-fold coincidence arrangement. The circuit is given in Fig. 3 and the coincidence curve is shown by Fig. 5. The circuit has a sensitivity of about 3 V and dead time of about 5 ns. The characteristics of the circuit as well the characteristics of the conventional coincidence circuits have been measured.

LETTERE ALLA REDAZIONE

(La responsabilità scientifica degli scritti inseriti in questa rubrica è completamente lasciata dalla Direzione del periodico ai singoli autori)

Infrared Absorption Spectra of Some Pyridine Molecular Complexes.

L. Peraldo Bicelli

Istituto di Elettrochimica, Chimica Fisica e Metallurgia del Politecnico - Milano

(ricevuto il 2 Aprile 1958)

Infrared spectra of some pyridine molecular complexes have been investigated.

The complexes: $InCl_3 \cdot 3Py$; $AgNO_3 \cdot 2Py$; $AgClO_4 \cdot 2Py$; $NiCr_2O_7 \cdot 4Py$; $ZnCr_2O_7 \cdot 4Py$ prepared following the usual methods, have been examinated in nujol (or hexachlorobutadiene) mull, using a Perkin-Elmer, Model 21 double beam spectrometer with rock salt optics.

lowing notable exceptions:

1) some absorption bands are split;

2) they are shifted from their usual position.

Splitting of some absorption bands is generally observed for the crystalline forms and may depend upon the magnitude of the interaction forces between molecules in the unit cell.

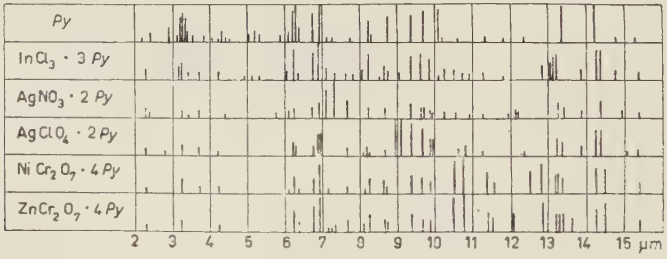

Fig. 1.

The spectra including that of liquid pyridine are given in Fig. 1.

The spectrum of each complex, appears to be almost a superposition of the spectra of pure pyridine and of the corresponding pure salt, with the following notable exceptions:

The second case, the most important one, has been observed in the spectra of donor-acceptor complexes.

For example: the frequencies due to the carbon-carbon stretching vibrations are shifted in the Raman spectrum of the

silver perchlorate-benzene complex (1). X-ray structure of this complex (2) shows definite, though weak, silver-benzene interaction (Ag-C distances 2.6 Å), the silver ions being located over two carbon atoms.

Pyridine is a good electron-donor, while cations, particularly when containing *d* electrons, are vacant-orbital acceptors (3).

The analysis of the spectra gives new evidence these substances to be complexes, formed utilizing the lone pair of electrons of the nitrogen atom of pyridine.

(1) H. J. Taufen, M. J. Murray and F. F. Cleveland: *Journ. Amer. Chem. Soc.*, **63** 3500 (1941).

(2) R. E. Rundle and J. H. Goring: *Journ. Amer. Chem. Soc.*, **72**, 5337 (1950).

(3) R. S. Mulliken: *Journ. Amer. Chem, Soc.*, **72**, 600 (1950); **74**, 811 (1952); *Journ. Phys. Chem.*, **56**, 801 (1952); *Journ. Chim. Phys.*, **51**, 341 (1954).

21017

Energy Dependence of Positron Asymmetry from Polarized Muon Decay in Emulsion.

C. Castagnoli, A. Manfredini

Istituto di Fisica dell'Università - Roma
Istituto Nazionale di Fisica Nucleare - Sezione di Roma

and

A. W. Merrison

Physics Department, University of Liverpool (*)

(ricevuto il 29 Aprile 1958)

Under the hypotheses of a two component neutrino and conservation of leptonic charge it is possible to show (1) that in the polarized muon decay the asymmetry $\alpha(>\varepsilon)$ averaged over decay positrons having energy between ε and 1 (in units of $\varepsilon_{max} = 52.8$ MeV) may be written as

$$(1) \qquad \alpha(>\varepsilon) = \frac{\int_{\varepsilon}^{1} b(\varepsilon)\,\mathrm{d}\varepsilon}{\int_{\varepsilon}^{1} a(\varepsilon)\,\mathrm{d}\varepsilon} = \bar{\alpha} f(\varepsilon)\,,$$

where α is the asymmetry averaged over the whole spectrum and $f(\varepsilon)$ is given by

$$(2) \qquad f(\varepsilon) = \frac{1 + 2\varepsilon - 3\varepsilon^4}{1 - 2\varepsilon^3 + \varepsilon^4}\,,$$

and $a(\varepsilon) = 2\varepsilon^2(3 - 2\varepsilon)$; $b(\varepsilon) = 2\varepsilon^2(2\varepsilon - 1)$ (Fig. 1, curve 1). To verify this theoretical prediction we have studied the energy dependence of the angular asymmetry of 1001 positrons from the decay

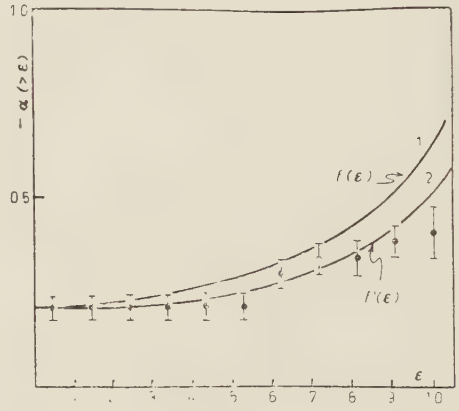

Fig. 1.

of muons coming to rest in nuclear emulsions exposed to the π^+ beam produced by the Liverpool synchrocyclotron and coming itself to rest in the emulsion stack.

(*) Now at CERN, Geneva.

(1) T. D. Lee and C. N. Yang: *Phys. Rev.*, **105**, 1671 (1957).

Experimental details have been given in a previous communication [2]. We just recall that the percentage error on the single positron energy as determined by scattering measurements is almost constant over the whole spectrum ($\sim 8\%$) We have identified 60 catastrophic energy losses ($> 60\%$) by bremsstrahlung and in those cases the energy considered in the spectrum is the energy before the loss. For the various values of ε, the asymmetry parameter $\alpha(>\varepsilon)$ has been computed through the ratio

$$2(B-F)/(B+F)\,,$$

where B and F are the backward and forward intensity. Since the events in the backward and forward hemisphere are statistically uncorrelated the error is thus given by

$$\sigma = 2\sqrt{1-\alpha^2}/\sqrt{N}\,,$$

where N is the number of events used for calculating α.

To compare the experimental values $\alpha(>\varepsilon)$ with the corresponding theoretical values it is necessary to introduce corrections.

1) The theoretical electron spectrum

$$N(\varepsilon,\theta) = a(\varepsilon) + b(\varepsilon)\cos\theta\,,$$

should be modified on account of bremsstrahlung losses, using the radiation loss straggling formula given by Eiges [3].

2) This spectrum should be further modified to take into account ionization energy losses. We have supposed a loss of 6 MeV/cm.

3) Furthermore the spectrum should be modified to include statistical dispersions in the scattering measurements; we have assumed a gaussian distribution characterized by a mean square deviation $\mu=\langle\theta\rangle/\sqrt{n}$, where $\langle\theta\rangle$ is the mean square angle of scattering and n the number of measured cells.

4) It is necessary to include radiative corrections due to the emission of virtual photons and to inner bremsstrahlung; this tends to shift the spectrum towards lower energies. We have used the results of Kinoshita and Sirlin [4].

The corrections have been carried out numerically and graphically and the result was to modify $a(\varepsilon)$ and $b(\varepsilon)$ into two new functions, $a'(\varepsilon)$ and $b'(\varepsilon)$ and so to a new dependence:

$$\alpha'(>\varepsilon) = \frac{\int_{\varepsilon}^{1} b'(\varepsilon)\,\mathrm{d}\varepsilon}{\int_{\varepsilon}^{1} a'(\varepsilon)\,\mathrm{d}\varepsilon} - \alpha f'(\varepsilon)\,,$$

shown in Fig. 1 (curve 2). According to our results, $\overline{\alpha}=0.20\pm0.04$ to be compared with the value $\overline{\alpha}=0.127\pm0.017$ obtained by averaging the results of various authors over ~ 11000 decays.

Within the statistical limits the agreement between the experimental results and the predictions of a simple non-derivative coupling theory of the decay processes $\mu^+ \to e^+ + \nu + \tilde{\nu}$ may be considered satisfactory. These results agree with those obtained with the same technique and 530 events by Smirnitsky and Weissenberg [5], with those obtained with counters [6], and for low energy electrons with those in bubble-chambers [7].

---

[2] C. Castagnoli, *Atti Congresso Internazionale Padova* (Settembre 1957).

[3] L. Eyges: *Phys. Rev.*, **76**, 264 (1949).

[4] T. Kinshita and A. Sirlin: *Phys. Rev.*, **107**, 638 (1957).

[5] V. A Smirnitsky and A. O. Weissemberg: *Nucl. Phys.*, **5**, 33 (1958).

[6] D. Berley, T. Coffin, R. L. Garwin, L. M. Lederman and M. Weinrich: *Phys. Rev.*, **106**, 835 (1957).

[7] I. A. Pless, A. E. Brenner, R. W. Williams, R. Bizzarri, R. H. Hildebrand, R. H. Milburn, A. M. Shapiro, K. Strauch, J. C. Street and L. A. Young; *Phys. Rev.*, **108**, 159 (1958).

2099

Photoprotons from Nitrogen.

G. Cortini, C. Milone and R. Rinzivillo

Istituto di Fisica dell'Università - Catania
Centro Siciliano di Fisica Nucleare - Catania

C. Tribuno

Istituto di Fisica dell'Università - Torino
Istituto Nazionale di Fisica Nucleare - Sezione di Torino

(ricevuto il 9 Maggio 1958)

The spectrum of photoprotons emitted by nitrogen under bremsstrahlung irradiation was investigated by Wright *et al.* [1] for γ-rays to a maximum energy of 23 MeV. These authors used as detector a cloud chamber, which allowed a very good resolution for a proton energy $E_p < \sim 3$ MeV. For higher proton energies the information was derived from the short tracks of recoil nuclei so that the resolution was rather poor.

A nuclear emulsion investigation was also made by Spicer [2] with 11.5 MeV bremsstrahlung γ-rays.

In order to extend the knowledge of the spectrum to proton energies higher than those easily obtainable with the cloud chamber technique, we have made a similar experiment by means of photographic emulsions, with 18, 23 and 30 MeV bremsstrahlung.

The method of irradiation to the Turin betatron has already been described elsewhere [3]. A couple of photoplates, Ilford C2, 200 μm thick, were used, for each exposure. Each plate was square (2 in. $\times$ 2 in.) with a round hole of 25 mm diameter in the centre through which the γ-ray beam passed. The whole system of plates was included in an exposure chamber filled with nitrogen gas at 2.1 atmospheres.

The proton spectrum at $\sim 90°$ from the incident γ-rays was detected in the plates, using standard techniques. The gas target was very well defined, as the distance between the two plates was only 8 mm. The background, evaluated by the tracks entering the emulsions from wrong directions, was very low ($\lesssim 3\%$).

The experimental data are summarized in Table I.

Fig. 1 shows the results for each of the 3 irradiation energies employed.

(1) I. F. Wright, R. D. C. Morrison, J. M. Reid and J. R. Atkinson: *Proc. Phys. Soc.*, A **69**, 77 (1956).

(2) B. M. Spicer: *Austr. Journ. Phys.*, **6**, 391 (1953).

(3) C. Milone, S. Milone Tamburino, R. Rinzivillo, A. Rubbino and C. Tribuno: *Nuovo Cimento*, **7**, 729 (1958).

TABLE I.

$E_{\gamma max}$ (MeV)	18	23	30
Dose (röntgen)	5 000	7 900	8 000
Nitrogen pressure (atm)	2.0	2.1	2.1
Number of tracks	71	1 194	1 590

Thresholds: $N(\gamma, p) = 7.54$ MeV
$N(\gamma, np) = 12.49$ MeV

They are normalized at the same dose, as measured by means of a standard Victoreen chamber.

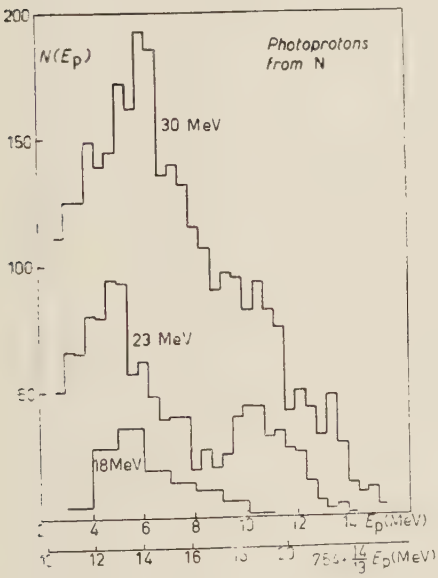

Fig. 1. – Energy spectrum of the photoprotons from N, at 18 MeV, 23 MeV and 30 MeV maximum energy irradiations. $N(E_p)$ (arbitrary units) = number of protons per unit energy interval normalized to the same dose and other experimental conditions. The scale (14/13) $E_p + 7.54$ is also reported.

The absolute yield at 30 MeV was about the same as in the oxygen irradiation ([3]). Therefore, under the assumption that the angular distribution be approximately isotropic, the yield would be $\sim 10^5$ protons/mole/röntgen.

This value can be compared with the cross-section curves deduced from the data by FERGUSON *et al.* ([4]) and by JOHNS *et al.* ([5]) on the (γ, n) process (see Fig. 2).

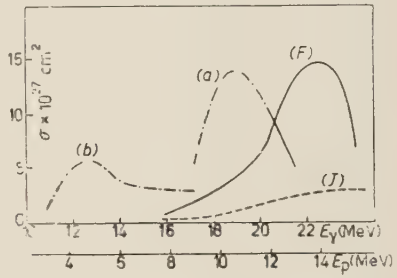

Fig. 2. – Cross sections. Curve (*F*): Ferguson data on neutron production [$(\gamma, n) + (\gamma, np)$ processes]. Curve (*J*): Johns data on radioactivation [only (γ, n) process]. Curves (*a*) and (*b*) could be deduced from the present 23 MeV and 18 MeV data for the (γ, p) process, under particular assumptions (see text).

The measurements by FERGUSON *et al.* were made by means of a neutron detector, while JOHNS *et al.* used the method of radioactivation. Therefore these two cross-section curves give, by subtraction the cross-section curve for the (γ, np) process. From this curve one can calculate the proton yield of the last process at 30 MeV, obtaining about the same figure of 10^5 protons/mole/röntgen, deduced by our data.

This means that a considerable fraction of the protons observed in our 30 MeV plates come from (γ, np) processes. An accurate estimate of their contribution is not possible for the uncertainty on the angular distribution.

The relative photoproton yields for

([4]) E. A. FERGUSON, J. HALPERN, R. NATHANS and P. Y. YERGIN: *Phys. Rev.*, **95**, 776 (1951).

([5]) H. E. JOHNS, R. J. HORSLEY, R. N. H. HASLAM and A. QUINTON: *Phys. Rev.*, **84**, 856 (1951).

18 MeV, 23 MeV and 30 MeV bremsstrahlung maximum energies are as follows:

$$(1) \qquad Y_{18}/Y_{23}/Y_{30} = \\ = (0.25 \pm 0.04)/1/(2.5 \pm 0.14) .$$

The same ratios, as deduced by the (γ, np) cross-section curve (supposed to be negligible for $E_\gamma > 23$ MeV — see Fig. 2) are:

$$(2) \qquad Y_{18}/Y_{23}/Y_{30} = 0.16/1/2.5 .$$

We deduce that the general shape of the (γ, p) cross-section is not very different from that of the (γ, np) cross-section (see later) at high energy ($E_\gamma > > 18$ MeV). However, for $E_\gamma < 18$ MeV the first cross-section is higher as shown by eqs. (1) and (2) as well as by the results obtained by WRIGHT *et al* [1]. If one assumes that the processes generating the photoprotons emitted at 18 MeV leave the residual nucleus in the fundamental state, the cross-section curve *b*) Fig. 2 is obtained.

We do not see any evidence of « fine structure » in the proton spectra, as observed by WRIGHT *et al.* [1] for low proton energies ($E_p < \sim 1.5$ MeV). Indeed, our emulsion detector is not suited for protons of so low an energy, owing to lack of resolution and high background. The oxygen photoproton « lines », which are at higher energies were clearly visible in a previous oxygen experiment [3] performed with the same experimental arrangement.

On the other hand a characteristic result of the present investigation is the second broad maximum at $E_p \sim 10$ MeV in the proton spectrum at 23 MeV (Fig. 1). For energy conservation it cannot be attributed to the (γ, d) process while the (γ, np) process could give, at most, a negligible « tail ». If one assumes that the whole second maximum be due to processes leaving the ^{13}C nucleus in the fundamental state, then the cross-section curve which is marked *a*) in Fig. 1 is obtained. This somewhat arbitrary assumption is the only one which can give us in a simple way a cross-section curve. However, this curve with its low energy maximum, can hardly be reconciled with the yield data.

Indeed, if one starts from the cross-section curves of Fig. 2 (curve (*a*) for the (γ, p) and curves (*F*)-(*J*) for the (γ, np) process) one obtains, instead of (1), the protoproton yield ratio

$$(3) \qquad Y_{23}/Y_{30} = 1/1.65 ,$$

which is definitely different from (1), and indicates that the energy of the maximum of the cross-section curve is greater than shown by Fig. 2, curve (*a*).

The known nuclear levels of the residual nucleus $^{13}_{6}C$ which could contribute to the second maximum are at excitation energies of 3.09, 3.68 and 3.86 MeV [1,6]. At maximum γ energy of 23 MeV the following level at 6.87 MeV is interdicted. For $E_p > 12$ MeV, the only ^{13}C level energetically possible is the fundamental one. This energy region corresponds to the high energy continuous tail of the dotted curve (*a*).

We can conclude that the second maximum of the 23 MeV curve is partly due to processes leaving the residual nucleus in excited levels, so that we will have another cross-section curve, the maximum of which is located between the curves (*a*) and (*F*) of Fig. 2.

We can state with certainty that the second maximum is due to some sort of direct process excluding an intermediate compound nucleus state. However, it is difficult to decide, at the present state of knowledge, what type of process.

In fact the energy locations of the maximum in the (γ, p) cross-section curve, and in the (γ, n) cross-section

[6] F. AJZENBERG and T. LAURITSEN: *Rev. Mod. Phys.*, **27**, 77 (1955).

[7] D. H. WILKINSON: *Physica*, **22**, 1039 (1956).

curve (see curve (*J*), Fig. 2) do not fit naturally in the frame of the Wilkinson photoeffect model with the known or reasonably supposed energy locations of the single particle levels in ^{14}N. Therefore, the lack of more detailed experimental data, and particularly of angular distribution, makes it useless to try more elaborate speculations.

The greater part of the low energy protons, specially in the 30 MeV spectrum, must be attributed to (γ, np) processes, whose high contribution is explained by the structure of the ^{14}N nucleus with two « optic » nucleons. An accurate comparison between the integrated cross-sections for the (γ, p) and (γ, np) processes is not possible without making detailed (and arbitrary) assumptions on the correspondence of E_γ with E_p. A rough estimate can be made, which gives for the yield ratio $(\gamma, p)/(\gamma, np)$ a value somewhat less than unity.

* * *

Our grateful thanks are due to Prof. R. Ricamo and Prof. G. Wataghin who put at our disposal the means for making the present research.

We thank Prof. M. Cini and Dr. A. Agodi for many fruitful discussions and Dr. V. Emma for useful help in processing the plates.

2103

Associated Production of a K^- Meson and a Hyperfragment.

Tsai-Chü, B. Chemel and S. Desprez-Rebaud

Faculté des Sciences, Sorbonne - Paris

(ricevuto il 19 Maggio 1958)

Associated productions [1-4] of a K^+ meson and a hyperfragment were observed in nuclear emulsions exposed to cosmic rays. This report gives a clean-cut example of a similar event. The two strange particles are emitted from a small star (Fig. 1, Table I) of type 7+1n found in the Sardinia stack S36. Each prong of the star, except one at minimum ionization, comes to rest in the emulsion. The minimum ionizing prong can be identified as a K-meson; one slow prong is a hyperfragment showing neutral mesic decay. It seems probable that the interaction takes place between a photon of (1.37 ± 0.10) GeV and a proton of a heavy emulsion nucleus resulting in the production of a K^+-meson and a Λ^0 hyperon. The hyperon interacts with the nucleus and causes the hyperfragment.

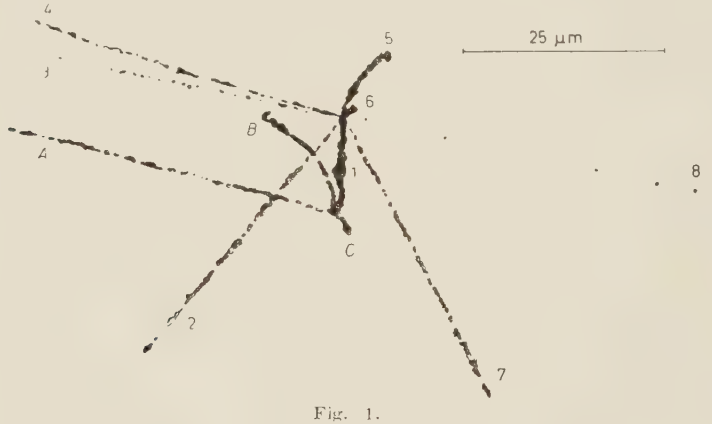

Fig. 1.

At minimum ionization, prong 8 has

[1] A. De Benedetti, C. M. Garelli, L. Tallone and M. Vigonne, *Nuovo Cimento* **12**, 466 (1954); *Suppl. Nuovo Cimento* **2**, 249 (1955).

[2] M. W. Friedlander, D. Keefe and M. G. M. Menon, *Nuovo Cimento* **2**, 663 (1955).

[3] P. Ciok, M. Danysz, J. Gierula, E. Skrzypczak and A. Wrobleski, *Suppl. Nuovo Cimento* **4**, 619 (1956).

[4] D. F. Falla, M. W. Friendlander, F. Anderson, W. D. B. Greening, S. Limentani, B. Sechi-Zorn, C. Cernigoi, G. Iernetti and G. Poiani, *Nuovo Cimento* **5**, 1203 (1957).

TABLE I. – *Prongs of the star* 7+1n.

Prong No.	Projection angle	Dip angle	Range in μm	Nature	Energy MeV	Momentum MeV/c	Gaps/25 μm at the end
1	+ 29.3°	+56° 30′	27	$^8Be_\Lambda$	20	558	2
2	— 7.4	— 2° 40′	146.5	^2H	6	149	17
3	— 69.6	— 30′	3452	^1H	29	239	23
4	— 73.4	—12° 10′	263.5	^1H	6.5	110.5	25.5
5	+171.2	+73° 10′	37	^1H	2	60	7
6	+169.3	+41°	3	^1H	0.3	24	9
7	+ 60.8	—17° 20′	148.5	^2H	6	150	24
8	+110	+ 1°	—	K	409	756	—
A	— 73.6	+32°	314	^1H	7.2	117	21
B	—131	—45° 20′	21	^1H	1.3	50	11
C	+56	+46° 30′	5	^4He	1.5	106	5

a flat trajectory of 4.8 cm in the same plate. It emerges from emulsion to air near the edge of the plate and has an ionization of (1.165±0.015) times the minimum. If prong 8 were a π meson, this ionization would correspond to a *pv* value of (179.0 ± 5.6) MeV; whilst multiple scattering, 0.0371° for a 100 μm cell, gives a *pv* value of (658±50) MeV. The particle has therefore a mass of (1005 ± 90) m_e, identifying it as a K meson. The K meson has an energy of (409 ± 30) MeV and a momentum of (756 ± 34) MeV/c respectively.

Prong 1, ending with a small star, has a short inclined trajectory. Both track width and gap density indicate the particle as having a charge higher than that of an α particle. Further, the track becomes slimmer as it approaches the secondary star. It is therefore evident that prong 1 represents the decay of a hyperfragment at rest. The three prongs of the secondary star can be identified by gap measurements [5]: prong *A* is a proton, prong *B* a particle of charge 1 and possibly also a proton, and prong *C* very probably an α particle. Their total kinetic energy is 10 MeV. It does not seem possible that such disproportionately high energy neutrons of 170 MeV may exist among the decay products. The hyperfragment must undergo a mesic decay. However, a π^- meson from the decay can only have a kinetic energy less than 25 MeV, and it will have a grain density more than 30 grains per 100 μm. No π^- meson can be found near the secondary star. If there is any present, it cannot possibly have escaped our observation. Then, a neutral meson must be emitted in place of the charged one. Momentum balance between the secondary prongs and the neutral meson will require a π^0 of 42 MeV, which is too high to satisfy the energy balance. So, slow neutrons must appear together with the charged prongs. The hyperfragment could be, *e.g.*

$$^8Be_\Lambda \rightarrow 2\,^1H + {}^4He + 2n + \pi^0 + Q\,.$$

The presence of neutral particles renders the *Q*-value, the mass number of the hyperfragment, etc., uncertain.

No heavy prong of the primary star has an energy exceeding 30 MeV. Prong 7 has a large deflection of 53° halfway towards the end. These prongs of evaporation are produced either simultaneously with the strange particles or through the latter's interaction with the heavy

[5] TSAI CHÜ, *Nuovo Cimento* **3**, 921 (1956).

TABLE II. – *Associated productions of* K^+ (0.41 GeV) *and* Λ^0 *by neutral primaries of* 1.37 GeV.

Production	Threshold GeV	Primary		Momentum (GeV/c)		Max. angle between secondaries
		energy	momentum	$\parallel$ to K^+	$\perp$ to K^+	
Photon nucleus	0.71	1.37 GeV	1.37 GeV/c	0.71	1.43	92°
Photon proton	0.91	1.37	1.37	1.14	0.76	63
Neutron nucleus	1.10	1.37	2.11	1.83	0.68	24
Observed	—	1.37	—	0.51	0.68	—

nucleus. The total kinetic energy of the heavy prongs, including that of the hyperfragment, is 69 MeV and their binding energy 72 MeV. Attributing an energy of (152 $\pm$ 80) MeV to the neutral prongs of evaporation, we have a good estimate of (1.37 $\pm$ 0.10) GeV for the total energy of the star or the energy of the neutral primary. About two thirds of the primary energy is taken by the K meson, less than one third by other prongs. So, we cannot possibly consider this star as an interaction caused by a K^- meson in flight, but rather as an associated production of strange particles. The primary energy is above the threshold for a photoproduction of K^+ and Λ^0, but below the threshold (1.6 GeV) for a neutron-proton production. It is close to 1.1 GeV for a neutron-nucleus production, if one assumes that the proton inside the nucleus moves with a Fermi energy of 25 MeV and in a direction opposite to the incident neutron. In the latter case, as the K^+, Λ^0, and the neutron have a small energy in the centre of mass system, they move forward within a small angle of 24° (Table II) in the laboratory system. So the resultant parallel component of momentum along the K^+ direction should be much larger than the perpendicular component. However, the observed parallel component (0.51 GeV) is much too small compared with 1.83 GeV. Further, the relative values of the two components observed vary in the same order as in the photon-nucleus production, but in reverse order in the neutron-nucleus production. Therefore, the photon-nucleus production can best satisfy our experimental data. The vertical cosmic rays fell on the stack from a projection angle of +14.8° to — 165.2°. The primary photon responsible for this event arriving near the horizontal direction may be produced locally somewhere around or inside the stack.

2106

LIBRI RICEVUTI E RECENSIONI

Proceedings of the Rehovoth Conference on Nuclear Structure, edited by H. J. LIPKIN; North-Holland Publishing Company, Amsterdam, 1958; pag. IX-613.

Questo volume contiene i resoconti della Conferenza sulla struttura dei nuclei tenuta a Rehovoth, in Israele, lo scorso settembre. Occorre veramente congratularsi con gli editori per la rapidità con cui, a relativamente breve distanza di tempo dalla Conferenza, è stato completato questo volume di rendiconti in magnifica ed accurata veste tipografica.

Oggetto della Conferenza era la discussione delle proprietà degli stati fondamentali dei nuclei e degli stati di bassa eccitazione. Nel volume sono riportati i testi delle comunicazioni presentate ed i punti salienti delle successive discussioni. Particolarmente utili sono i testi delle letture a carattere riassuntivo, presentate su invito, che nel loro insieme offrono un quadro completo ed aggiornato dei recenti sviluppi nella fisica nucleare di bassa energia. Diamo qui un breve cenno sul contenuto di queste letture. Sui modelli a shell EDEN dà un riassunto dei fondamenti teorici, TALMI discute l'interpretazione dei livelli, e KURATH espone i principi dell'intermediate coupling. Su modello unificato vi è una lettura di MOTTELSON, una di NEWTON, una di WILETS sulla fissione ed una di PEIERLS sui fondamenti teorici. Sui metodi matematici vi è una lettura di RACAH ed una di FLOWERS. Sulle transizioni elettromagnetiche vi sono tre letture, di WILKINSON, di DE SHALIT e di BERGSTRÖM. Sugli effetti dovuti alle dimensioni finite del nucleo le letture introduttive sono dovute a ROSE, WAPSTRA e ZWEIFEL. Sul decadimento beta vi sono due letture teoriche di KONOPINSKI e di LEE e tre sui lavori sperimentali di WU, STEFFEN e LANGER. Gli effetti extra nucleari sulle correlazioni sono trattati da ABRAGAM e da FRAUNFELDER. Nelle due ultime sessioni, a carattere tecnico, le comunicazioni introduttive furono date da GERHOLM, DUMOND, DEVONS, METZGER e COHEN, su problemi di spettroscopia e di misure di vite medie.

Particolare menzione, per la sua originalità, merita l'ultimo capitolo del volume che riproduce i bollettini giornalieri della conferenza e le comunicazioni presentate nella sessione sui risultati irreproducibili. Furono presentati lavori sperimentali, tra cui notevole un lavoro sull'annoso problema della vita media di Metusalemme e lavori teorici. Fra questi ultimi vanno segnalati un lavoro di ZIPKIN inteso ad una sistemazione teorica del complesso problema degli zipper (finiti o semifiniti), un lavoro di H. STRONG e di H. WEAK sulla teoria strong coupling delle interazioni deboli, nonchè una esposizione semplificata dei recenti progressi con la parità ad uso dei pedoni.

R. GATTO

PROPRIETÀ LETTERARIA RISERVATA

Direttore responsabile: G. POLVANI

Tipografia Compositori - Bologna

Questo fascicolo è stato licenziato dai torchi il 14-VII-1958

2108